Technical Report Documentation Page

1. Report No. FHWA/TX-13/0-6617-1	2. Government Accession No.	3. Recipient's Catalog No.
4. Title and Subtitle Revamping Aggregate Property Requirements for Portland Cement Concrete: Final Report		5. Report Date August 2013; Published November 2014
		6. Performing Organization Code
7. Author(s) J. Clement, Z. Stutts, A. Alqarni, D. Fowler, D. Whitney		8. Performing Organization Report No. 0-6617-1
9. Performing Organization Name and Address Center for Transportation Research The University of Texas at Austin 1616 Guadalupe Street, Suite 4.202 Austin, TX 78701		10. Work Unit No. (TRAIS)
		11. Contract or Grant No. 0-6617
12. Sponsoring Agency Name and Address Texas Department of Transportation Research and Technology Implementation Office P.O. Box 5080 Austin, TX 78763-5080		13. Type of Report and Period Covered Technical Report; 9/1/2010–8/31/2013
		14. Sponsoring Agency Code

15. Supplementary Notes
Project performed in cooperation with the Texas Department of Transportation and the Federal Highway Administration.

16. Abstract

Current Texas Department of Transportation (TxDOT) procedures for evaluating coarse aggregate for portland cement concrete (PCC) have been in place for over 39 years. Item 421 in the TxDOT "Standard Specifications for Construction and Maintenance of Highways, Streets, and Bridges" describes the tests and test limits that must be met by aggregates before they can be approved for use in portland cement concrete applications. The intention of Item 421 is to ensure that only strong, durable aggregates are used in concrete so that the life of concrete is not cut short by common distress mechanisms, which ultimately lead to costly repairs and replacements.

The two main tests currently used by TxDOT to evaluate aggregates are the magnesium sulfate soundness test and the Los Angeles abrasion and impact test. Unfortunately, past research has shown that the magnesium sulfate soundness test and the Los Angeles abrasion and impact test are not able to successfully predict the field performance of an aggregate in concrete. The requirements of Item 421 have thus far done a reasonably good job of ensuring long-lasting concrete; however, the current tests and test limits may be unnecessarily precluding the use of some local materials. As high quality aggregate sources are depleted and transportation costs increase, it will become more necessary to distinguish good performers from marginal and poor performers in the future.

If aggregate tests can be found that demonstrate better correlations with field performance, it may be possible to use more local aggregate sources and still provide the desired level of reliability for pavements, bridges, and other TxDOT concrete applications. Researchers will attempt to relate this test data to concrete behavior and ultimately recommend tests for improved TxDOT aggregate specifications.

17. Key Words Micro-Deval, aggregate, magnesium sulfate soundness, Los Angeles abrasion, AIV, ACV, AIMS 2.0	18. Distribution Statement No restrictions. This document is available to the public through the National Technical Information Service, Springfield, Virginia 22161; www.ntis.gov.		
19. Security Classif. (of report) Unclassified	20. Security Classif. (of this page) Unclassified	21. No. of pages 294	22. Price

Form DOT F 1700.7 (8-72) Reproduction of completed page authorized

THE UNIVERSITY OF TEXAS AT AUSTIN
CENTER FOR TRANSPORTATION RESEARCH

Revamping Aggregate Property Requirements for Portland Cement Concrete: Final Report

J. Christopher Clement
Zachary W. Stutts
Ali S. Alqarni
David W. Fowler
David Whitney

CTR Technical Report: 0-6617-1
Report Date: August 2013
Project: 0-6617
Project Title: Revamping Aggregate Property Requirements for Portland Cement Concrete
Sponsoring Agency: Texas Department of Transportation
Performing Agency: Center for Transportation Research at The University of Texas at Austin

Project performed in cooperation with the Texas Department of Transportation and the Federal Highway Administration.

Disclaimers

Author's Disclaimer: The contents of this report reflect the views of the authors, who are responsible for the facts and the accuracy of the data presented herein. The contents do not necessarily reflect the official view or policies of the Federal Highway Administration or the Texas Department of Transportation (TxDOT). This report does not constitute a standard, specification, or regulation.

Patent Disclaimer: There was no invention or discovery conceived or first actually reduced to practice in the course of or under this contract, including any art, method, process, machine manufacture, design or composition of matter, or any new useful improvement thereof, or any variety of plant, which is or may be patentable under the patent laws of the United States of America or any foreign country.

Notice: The United States Government and the State of Texas do not endorse products or manufacturers. If trade or manufacturers' names appear herein, it is solely because they are considered essential to the object of this report.

Engineering Disclaimer

NOT INTENDED FOR CONSTRUCTION, BIDDING, OR PERMIT PURPOSES.

Project Engineer: Dr. David W. Fowler
Professional Engineer License State and Number: Texas No. 27859
P. E. Designation: Researcher

Acknowledgments

Table of Contents

List of Tables

List of Figures

Chapter 1. Introduction

1.1 Need for Project

Current Texas Department of Transportation (TxDOT) procedures for evaluating coarse aggregate for portland cement concrete (PCC) have been in place for over 39 years. Item 421 in the TxDOT "Standard Specifications for Construction and Maintenance of Highways, Streets, and Bridges" describes the tests and test limits that must be met by aggregates before they can be approved for use in PCC applications. The intention of Item 421 is to ensure that only strong, durable aggregates are used in concrete so that the life of concrete is not cut short by common distress mechanisms, which ultimately lead to costly repairs and replacements.

The two main tests currently used by TxDOT to evaluate aggregates are the magnesium sulfate soundness test and the Los Angeles (LA) abrasion and impact test. These tests are meant to characterize the overall soundness and resistance to abrasion and impact of an aggregate respectively. However, these tests characterize intrinsic properties, and as such, the aggregates cannot be easily manipulated during production to ensure acceptance by these test criteria. Other tests are included in Item 421, such as gradation and decantation, but these tests can typically be accommodated for by aggregate producers through more stringent processing. It is imperative that the two most important tests in Item 421, the magnesium sulfate soundness and test and the LA abrasion and impact test, be able to successfully predict the field performance of an aggregate in concrete. Unfortunately, research conducted by many government transportation agencies and universities has shown that this is not necessarily the case. The requirements of Item 421 have thus far done a reasonably good job of ensuring long-lasting concrete; however, the current tests and test limits may be unnecessarily precluding the use of some local materials. A summary of the current concrete aggregate specifications in Item 421 can be found in Table 1.1. As high quality aggregate sources are depleted, and transportation costs increase, distinguishing between good performers from marginal and poor performers will become increasingly essential.

Table 1.1: Summary of Current TxDOT Concrete Aggregate Specifications in Item 421

Coarse Aggregate Test	Test Procedure	Test Limit
LA Abrasion	Tex-410-A	40%
Soundness (MgSO$_4$)	Tex-411-A	18%
Deleterious Substances	Tex-413-A	
clay lumps		0.25%
shale		1%
friable		5%
Decantation	Tex-406-A	1%
Gradation	Tex-401-A	
Fine Aggregate Tests	**Test Procedure**	**Test Limit**
Deleterious substances	Tex-413-A	
clay lumps		0.50%
Organic Impurities	Tex-408-A	Color
Acid Insoluble Residue	Tex-612-J	60%
Gradation	Tex-401-A	
Sand Equivalent Value	Tex-203-F	80
Fineness Modulus	Tex-402-A	2.6–2.8

A review of literature demonstrates that a variety of other potential aggregate tests are available to evaluate aggregates for PCC applications. If aggregate tests can be found that demonstrate better correlations with field performance, it may be possible to use more local aggregate sources and still provide the desired level of reliability for pavements, bridges, and other TxDOT concrete applications. Currently, TxDOT uses aggregates from not only Texas, but Mexico, Canada, Arkansas, Louisiana, New Mexico, Kentucky, Missouri, and Illinois (Texas Department of Transportation, 2012). Hauling materials long distances from out of state is not always a sustainable or economical solution if local materials area available. An improved specification for the qualification of aggregates will ideally allow for the use of more local aggregates, while still providing high quality, durable concrete.

1.2 Research Objectives

The ultimate aim of this research project was to examine how more coarse aggregate sources could be utilized in PCC without affecting the quality of the concrete produced. To achieve this goal several issues needed to be addressed, including the following:

- Investigating the history of aggregate testing to better understand why current specification limits are used.

- Understanding the way all state agencies manage aggregate qualification.

- Identifying common problems associated with aggregate distress.

- Investigating new aggregate qualification testing and comparing it with existing tests.

- Developing a laboratory testing procedure to evaluate aggregates in relation to current specifications and any potential new tests.

- Developing a procedure to determine the effects a specific aggregate has on a PCC mixture.

- Assessing field sections that are not performing as designed for possible signs of aggregate-related distress.

1.3 Scope of Project

In order to correlate performance with test results, the research team is in the process of collecting coarse aggregates from more than 50 sources and fine aggregates from more than 35 sources used by TxDOT. Aggregates tested represent a variety of mineralogies and geographic locations in Texas. Fine aggregates tested also include both natural sands and manufactured sands.

Coarse aggregate tests that were performed include the Micro-Deval test (Tex-461-A), LA abrasion and impact test (Tex-410-A), magnesium sulfate soundness test (Tex-411-A), British aggregate crushing value test (BS 812 Part 110), British aggregate impact value test (BS 812 Part 112), specific gravity and absorption test (Tex-403-A), flat and elongated particles test (Tex-280-F), Aggregate Imaging System (AIMS 2.0), and thermal conductivity test (using Mathis TCi equipment). Fine aggregate tests that were performed include the Micro-Deval test (ASTM D 7428), specific gravity and absorption test (Tex-403-A), Aggregate Imaging and System (AIMS 2.0), flakiness sieve (developed by Rogers and Gorman [2008]), acid insoluble residue test (Tex-612-J), Grace methylene blue test (developed by W.R. Grace Co.), organic impurities test (Tex-408-A), and sand equivalent test (Tex 203-F). Because the field performance history of an aggregate was not always readily available, researchers also performed a variety of concrete tests in an attempt to correlate results with aggregate tests. Concrete tests performed include compressive strength, flexural strength, modulus of elasticity, and coefficient of thermal expansion. Detailed procedures for coarse aggregate tests, fine aggregate tests, and concrete tests are located in Chapter 5.

1.4 Content

The total investigative scope of this project is summarized in two master's theses and one Ph.D. dissertation. The first published master's thesis, "Revamping Aggregate Property Requirements for Portland Cement Concrete," was written by Zachary Stutts and published in May of 2012. This document contained early research into literature and other sources, culminating in the design of the project test plan. Also reported in this document is an analysis of the historical trends of aggregates used in transportation infrastructure construction. This document sets the ground work for the testing of the coarse and fine aggregate. The next publication, "Quantifying the Characteristics of Fine Aggregate Using Direct and Indirect Test Methods," was written by Ali Alqarni and published in December of 2013. The final document "Recommendations for Coarse Aggregate Testing Requirements for use in Portland Cement Concrete," was written by Chris Clement and published in December of 2013.

This report is divided into 13 chapters:

- Chapter 2 contains a literature review for coarse and fine aggregate testing.

- In Chapter 3 a discussion of the development of the testing program is presented.

- Chapter 4 summarizes the materials acquisition that was required for the project.

- In Chapter 5 a discussion of the test methods used is presented.

- Chapter 6 summarizes the results from coarse aggregate testing.

- Chapter 7 provides an analysis of the results from coarse aggregate.

- Chapter 8 summarizes the results from laboratory concrete testing.

- Chapter 9 provides an analysis of the results from the laboratory concrete testing.

- Chapter 10 presents the investigation from field sites visited where aggregate problems were suspected.

- Chapter 11 presents an analysis of the fine aggregate test data generated.

- Chapter 12 presents the summary and conclusions from fine aggregate testing.

- Chapter 13 presents the summary and conclusions from coarse aggregate testing.

Chapter 2. Review of Literature

Researchers conducted a comprehensive literature search to obtain pertinent information on coarse and fine aggregate tests to predict the performance of concrete. The following is a synopsis of relevant literature which includes aggregate performance, properties, and test methods.

2.1 Relating Aggregate Performance, Properties, and Test Methods

Perhaps the most relevant piece of literature on the state of the knowledge of aggregate tests is the final report from the National Cooperative Highway Research Program (NCHRP) Project 4-20C, published in 2002. NCHRP 4-20C was a research study led by Folliard and Smith that reviewed literature and current practice to identify and recommend a suite of aggregate tests that relate to PCC pavement performance.

Folliard and Smith examined concrete pavement performance parameters affected by aggregate properties, determined which aggregate properties relate to concrete pavement performance, and then recommended the best test methods to evaluate those aggregate properties. According to the NCHRP 4-20C final report, the most important concrete pavement performance parameters are alkali-aggregate reactivity, blowups, d-cracking, roughness, spalling, surface friction, transverse cracking, corner breaks, faulting, punchouts, map cracking, scaling, and popouts (Folliard & Smith, 2002). Aggregate properties relating to these common distresses can be classified as physical properties, mechanical properties, chemical/petrographic properties, and durability properties. Physical properties include absorption, gradation, properties of microfines, shape, angularity, texture, and thermal expansion. Mechanical properties include abrasion resistance, elastic modulus, polish resistance, and strength. Chemical and petrographic properties are determined by mineralogy and durability properties are determined alkali-aggregate reactivity, and freeze-thaw resistance. Table 2.1, taken from the NCHRP 4-20C final report, provides a summary of the primary aggregate properties affecting key performance parameters.

Table 2.1: Summary of Primary Aggregate Properties Affecting Key Performance Parameters of Concrete Pavement (Folliard & Smith, 2002)

Aggregate Property	KEY PERFORMANCE PARAMETERS										
	AAR	Blowups	D-Cracking	Longitudinal Cracking	Roughness*	Spalling	Surface Friction**	Transverse Cracking	Corner Breaks	Joint Faulting	Punchouts
Absorption			X								
Abrasion Resistance				X			X	X	X	X	X
Angularity				X			X	X	X	X	X
Coefficient of Thermal Expansion		X		X		X		X	X	X	X
Elastic Modulus		X		X	X	X		X	X	X	X
Gradation				X	X	X		X	X	X	X
Hardness				X			X	X	X		
Mineralogy	X	X	X	X		X	X	X	X		
Porosity and Pore Structure	X		X								
Shape				X		X		X		X	X
Size	X		X	X		X		X		X	X
Strength				X		X		X	X		X
Texture				X		X	X	X	X	X	X

* Because roughness is affected by the presence of distresses, any aggregate properties that influence the development of those distresses will also influence the development of roughness.
** Surface friction is mainly affected by the polish resistance of fine aggregates because of the presence of the mortar-rich layer at the top surface of PCC pavements.

To recommend aggregate tests based on the primary aggregate properties of interest, researchers identified important test criteria. These criteria included current or potential ability of test method to predict PCC pavement performance, repeatability, and precision of test method, user-friendliness of test method, and availability and cost of test equipment. Tests that were recommended by researchers include both direct tests (performed directly on aggregate) and indicator tests (performed with mortar or concrete specimens containing the aggregate of interest).

Based on the aggregate properties of interest and the prioritized test criteria, the following test recommendations were made. Table 2.2, taken from the NCHRP 4-20C final report, summarizes these recommendations. For each aggregate property, the recommended tests are listed, along with sample type required and the significance of the test. Sample type is listed as "A" for aggregate, "C" for concrete, or "M" for mortar.

Table 2.2: Test Methods Recommended by NCHRP 4-20C for Various Aggregate Properties (Folliard & Smith, 2002)

Aggregate Property	Recommended Test Methods (from Folliard & Smith (2002))*	Sample Type**	Significance
PHYSICAL PROPERTIES			
Absorption	AASHTO T 84 - Specific Gravity and Absorption of Fine Aggregates	A	Specific gravity needed for mixture proportioning; absorption values needed for moisture corrections at batch plant. Absorption may influence workability.
	AASHTO T 85 - Specific Gravity and Absorption of Coarse Aggregates	A	Specific gravity needed for mixture proportioning; absorption values needed for moisture corrections at batch plant. Absorption may influence workability and possibly freezing and thawing resistance.
Gradation	AASHTO T 27 - Sieve Analysis of Fine and Coarse Aggregates	A	Standard test to determine particle size distribution. Data essential for mixture proportioning. Gradation strongly affects workability of concrete.
Properties of Microfines	AASHTO T 11 - Materials Fine Than No. 200 Sieve in Mineral Aggregates by Washing	A	Measures amount of material passing #200 sieve, which influences water demand, workability, shrinkage, etc.
	AASHTO T 176 - Plastic Fines in Graded Aggregates and Soils by the Use of the Sand Equivalent Test	A	Determines relative amount of clay like material. Quick and simple to perform.
	AASHTO TP 57 - Standard Test Method for Methylene Blue Value of Clays, Mineral Fillers, and Fines	A	Quick, semi-quantitative test to assess clays (and organic materials) in aggregates. Does not identify type of clay present.
	X-ray Diffraction Analysis (XRD)	A	Useful in identifying type of clay minerals present in aggregates
Shape, Angularity, and Texture	AASHTO T 304 - Uncompacted Void Content of Fine Aggregates	A	Provides index of fine aggregate angularity, sphericity, and surface texture. Higher void contents result in higher water demands.
	AASHTO TP 56 - Uncompacted Void Content of Coarse Aggregates (As influenced by Particle Shape, Surface Texture, and Grading)	A	Provides index of coarse aggregate angularity, sphericity, and surface texture. Higher void contents result in higher water demands.
	ASTM D 7491 - Test Method for Flat or Elongated Particles in Coarse Aggregates	A	Assesses coarse aggregate shape by identifying ratio of length to width (for different size fractions). Flat and elongated particles affect water demand, mixture consistency, and finishability.
Thermal Expansion	AASHTO TP 60-00 - Standard Test Method for the Coefficient of Thermal Expansion of Concrete (*indicator test*)	C	Measures coefficient of thermal expansion of concrete, which is a major function of aggregate thermal properties. Affects thermal cracking of pavements, especially for CRCP.
MECHANICAL PROPERTIES			
Abrasion Resistance	CSA A23.2-23A - Resistance of Fine Aggregate to Degradation by Abrasion in the Micro-Deval Apparatus	A	Wet attrition test to assess breakdown and slaking of concrete sand. Correlates well with Mg sulfate soundness test but has better precision. Max. loss of 20 percent recommended by CSA.
	AASHTO TP 58 - Resistance of Coarse Aggregate to Degradation by Abrasion in the Micro-Deval Apparatus	A	Wet attrition test to assess breakdown and slaking of concrete sand. Correlates well with Mg sulfate soundness test but has better precision. Max. loss of 14-17 percent recommended by CSA.
	AASHTO T 96 - Resistance to Degradation of Small-Size Coarse Aggregate by Abrasion and Impact in the Los Angeles Machine	A	Dry attrition test for coarse aggregates mainly used as a QC test. Can be used to assess breakdown during handling and may be related to abrasion from studded tires or chains.
Elastic Modulus	ASTM C 469 - Static Modulus of Elasticity and Poisson's Ration of Concrete in Compression (*indicator test*)	C	Indicator test to assess the impact of aggregate elastic modulus on concrete elastic modulus. Affects thermal and drying shrinkage cracking.
Polish Resistance	ASTM D 3042 - Insoluble Residue in Carbonates	A	Assesses the non-carbonate (usually siliceous) material intermixed with carbonate minerals in aggregates. Used as an index of polishing resistance of concrete sands.
Strength	British Standard 812 (Part 3) - Aggregate Crushing Value	A	Measures relative strength of graded coarse aggregate. Aggregate strength is most relevant for higher strength concrete.

	CHEMICAL/PETROGRAPHIC PROPERTIES		
Mineralogy	ASTM C 295 - Guide for Petrographic Examination of Aggregates for Concrete	A	Useful in identifying reactive (ASR or ACR) minerals and other deleterious materials. Mineralogy of aggregates affects many concrete properties including thermal and drying shrinkage.
	X-ray Diffraction Analysis (XRD)	A	Reported to be helpful in identifying non-durable carbonate aggregates. Useful tool in identifying types of clay present in aggregates.
	Thermogravimetric Analysis (TGA)	A	Reported to be helpful in identifying non-durable carbonate aggregates.
	X-ray Fluorescence Analysis (XRF)	A	Reported to be helpful in identifying non-durable carbonate aggregates.
	DURABILITY PROPERTIES		
Alkali-Aggregate Reactivity	ASTM C 295 - Guide for Petrographic Examination of Aggregates for Concrete	A	Identifies potentially reactive minerals and confirms findings from other tests (AASHTO T 303)
	AASHTO T 202 - Accelerated Detection of Potentially Deleterious Expansion of Mortar Bars Due to Alkali-Silica Reaction	M	Accelerated test suitable as screening test, but results should not be used independently to judge aggregate.
	ASTM C 1293 - Test Method for Concrete Aggregates by Determination of Length Change of Concrete due to Alkali-Silica Reaction	C	Long-term test (one year for aggregates, two years to assess pozzolans or slag) that relates well to field performance.
	CSA A23.2-26A - Determination of Potential Alkali-Carbonate Reactivity of Quarried Carbonate Rocks by Chemical Composition	A	Useful, rapid screening test to identify aggregates with potential for ACR.
Freezing and Thawing Resistance	AASHTO T 161 (modified Procedure C) - Resistance of Concrete to Rapid Freezing and Thawing	C	Effective means of assessing D-cracking potential of aggregates but is time consuming. Various modifications of procedure can be used, including pre-soaking aggregates in salt solution.
	CSA A23.2-24A - Unconfined Freezing and Thawing of Aggregates in NaCl	A	Rapid test with good ability to predict D-cracking. Use of NaCl improves correlation with field performance. Max. loss of four to six percent recommended by CSA.
	AASHTO T 104 - Soundness by Use of Mg or Na Sulfate (recommend Mg)	A	Common test conducted by most DOTs. Magnesium sulfate recommended over sodium sulfate.
	Iowa Pore Index Test	A	Assesses volume of micropores in aggregates, which is critical for D-cracking. Good correlation with field performance. Secondary loading limit of 27 mL specified by Iowa DOT.
	Modified Washington Hydraulic Fracture Test (after Embacher and Snyder, 2001)	A	Measures fracture of aggregates in pressurized vessel. Recent modifications have improved precision of test and correlation with AASHTO T 161.

*Tests are recommended to assess aggregate property unless otherwise noted - some are "indicator" tests that indirectly assess property
**Sample Type: A=Aggregate, C=Concrete, M=Mortar

As part of the NCHRP 4-20C final report, authors presented a flowchart to assist agencies in selecting aggregate tests. Decision blocks rely on the user's judgment as to whether or not certain parameters (i.e., "Is elastic modulus a concern?") are important in the decision making process. Certain aggregate properties may have a greater impact on certain PCC pavement types (for example, CoTE impact on continuously reinforced concrete pavements [CRCP]) but for the most part, the same aggregate properties influence the performance of all types of PCC pavement. Therefore, a single flowchart is logical for all pavement types. Figure 2.1 displays the flowchart for aggregate testing developed by Folliard and Smith (2002).
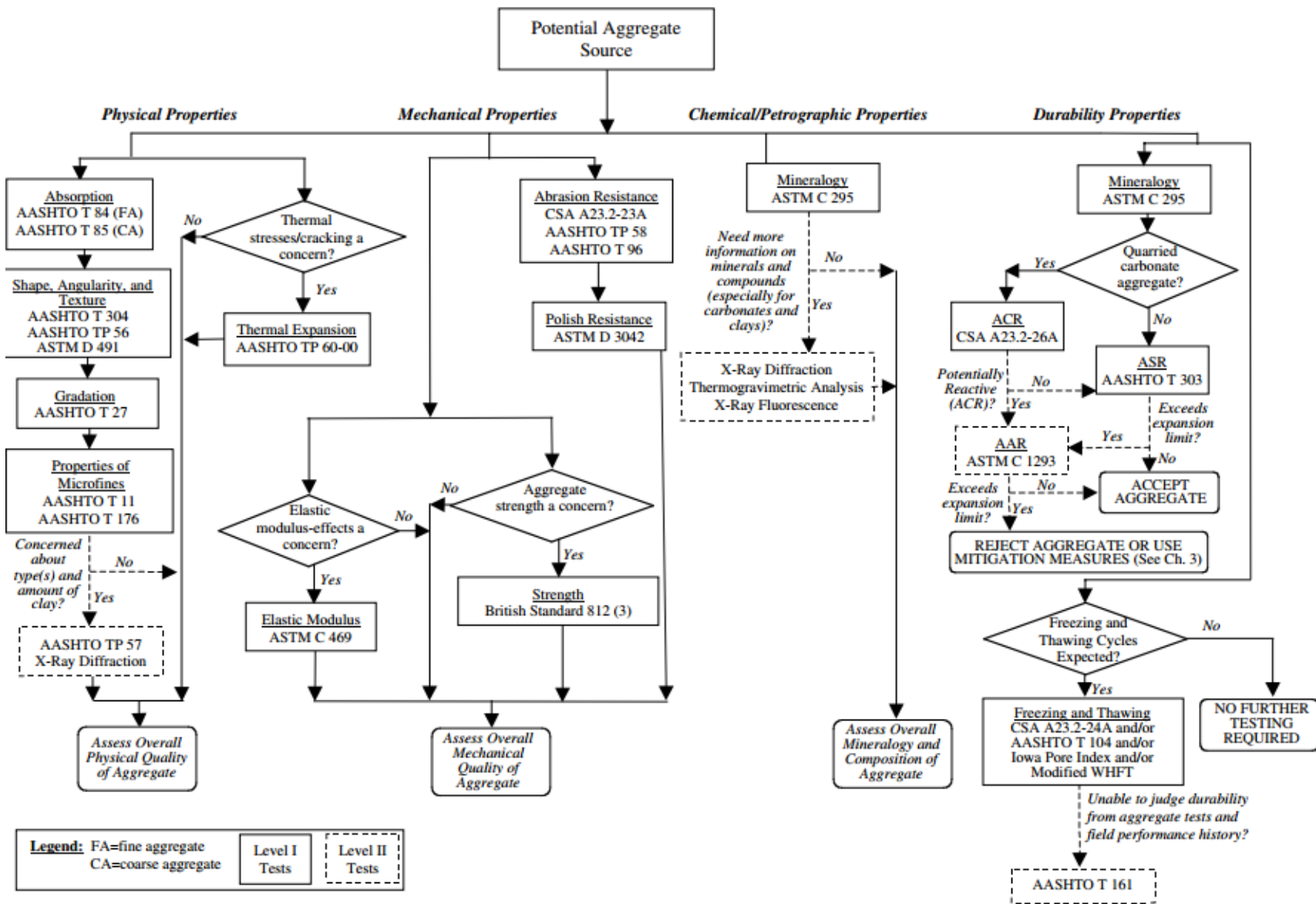
Figure 2.1: NCHRP 4-20C Recommendation for Aggregate Test Selection Process (Folliard & Smith, 2002)

When selecting test criteria for accepting or rejecting aggregates, engineers should first consider pavement type and design, climatic/environmental conditions, traffic loading, materials and mixture proportions, frequency of aggregate testing, and field performance histories of aggregates (Folliard & Smith, 2002). For example, freeze-thaw testing may not be as crucial in Texas as in Minnesota, or an aggregate may demonstrate good field performance history, despite not meeting a limit for a certain test.

2.2 Similar Research Projects

Research projects with similar scope and objective have been performed by various agencies in the past, although arguably none as comprehensive in size as the TxDOT research project ("Revamping Aggregate Property Requirements for Portland Cement Concrete") of which this report is a part. Other projects include ICAR 507-1F by Fowler, Allen, Lange, and Range (2006); WHRP 06-07 by Weyers, Williamson, Mokarem, Lane, and Cady (2005); FHWA-SC-05-01 by Rangaraju, Edlinski, and Amirkhanian (2005); NCAT 98-4 by Wu, Frazier, Parker, and Kandhal (1998); and studies by the Minnesota DOT by Koubaa and Snyder (1999) and Ministry of Transportation of Ontario by Senior and Rogers (1991). These research projects tested a variety of aggregates and attempted to relate test results with field performance. The findings of these research projects are presented in this section.

The International Center for Aggregates Research (ICAR) completed a study in 2006 (ICAR 507-1F) to determine the effectiveness of the Micro-Deval test in predicting performance of coarse aggregates for PCC, asphalt concrete, base course, and open-graded friction course (Fowler, Allen, Lange, & Range, 2006). Researchers collected coarse aggregates from 117 sources in Canada and the United States representing a diverse mix of mineralogies, geographies, and performance histories. Aggregates were subjected to a variety of tests including Micro-Deval, magnesium sulfate soundness, LA abrasion and impact, Canadian unconfined freeze-thaw, aggregate crushing value (ACV), ACV at saturated surface dry condition, specific gravity and absorption, particle shape factor determination, and percent fractured test. State DOTs that submitted aggregates for this study were surveyed for relevant information about the performance histories of the aggregates such as applications of use, years in service, average daily traffic, freeze-thaw exposure, failure characteristics, and time until failure. Researchers used this information to determine a rating for each aggregate. The rating criteria are presented in Table 2.3.

Table 2.3: Performance Criteria for ICAR 507 (Fowler, Allen, Lange, & Range, 2006)

Rating	Description from Fowler et al. (2006)
Good	used for 10 or more years with no reported non-chemical problems
Fair	used at least once where minor non-chemically related failures require minor repairs, but average service life extends beyond 10 years
Poor	used at least once where severe degradation or failure occurred within 2 years of service or during construction which severely inhibits and/or prevents the use of the application

After establishing performance rating for aggregates, the aggregates were subjected to the testing regimen and researchers examined the success rates for the Micro-Deval test and success

rates for the Micro-Deval test combined with other tests. The best single test indicator of field performance for all applications was the Micro-Deval test, but the best overall indicator of field performance was the Micro-Deval test used in combination with the Canadian unconfined freeze-thaw test. A Micro-Deval loss of 21%, combined with a Canadian unconfined freeze-thaw loss of 3.6% was able to bound 77% of good performers for PCC applications. Figure 2.1 graphically displays the bounding of performers by these criteria.
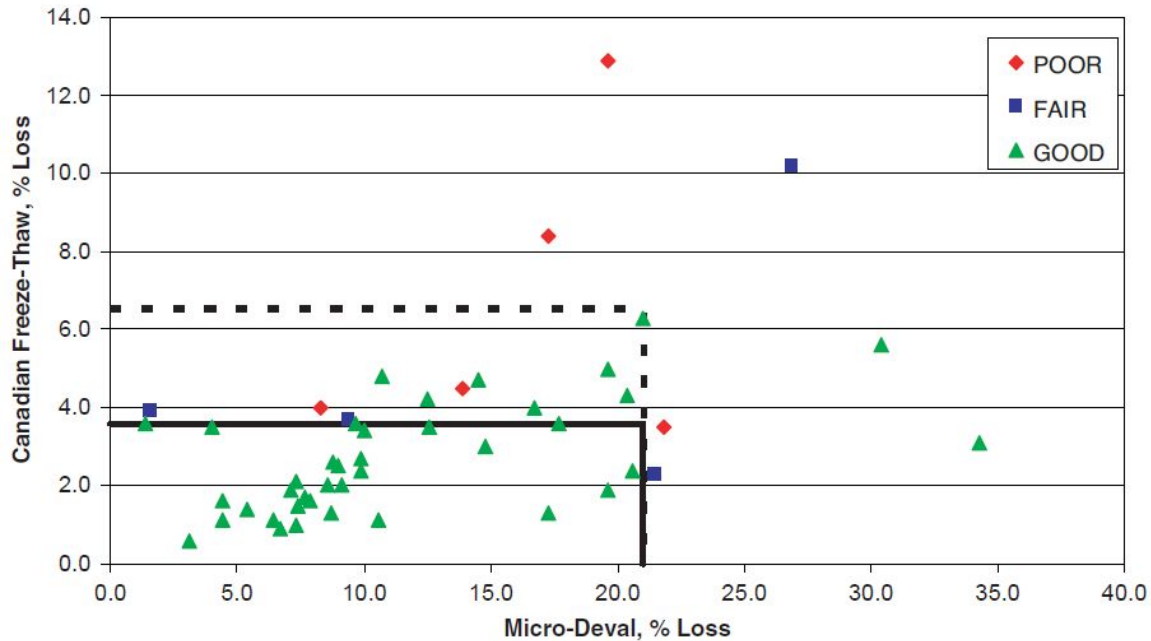
Figure 2.1: Canadian Freeze-Thaw vs. Micro-Deval (Fowler, Allen, Lange, & Range, 2006)

Figure 2.1 demonstrates that the limits of 21% for Micro-Deval and 3.6% for Canadian freeze-thaw were also able to exclude 100% of the fair performers and 100% of the poor performers. If the Canadian freeze-thaw limit is raised to 6.5% (dashed line), 95% of good performers are included, 50% of the fair performers are included, and 60% of the poor performers are included. However, it is important to note that only four fair performers and five poor performers were subjected to testing. These researchers acknowledged that further research of more marginal performers may be needed to refine these limits. Success rates of other tests are shown in Table 2.4.

**Table 2.4: Success Rate Summary of Tests in ICAR 507
(Fowler, Allen, Lange, & Range, 2006)**

Test	Test Alone (%)	Micro-Deval Combination (%)
Micro-Deval	83	N/A
Magnesium sulfate soundness	81	85
Canadian Freeze-Thaw	88	88
Absorption	83	83
Specific gravity (bulk)	85	87

*From Fowler et al. (2006)

ICAR 507 researchers also determined correlations between test methods to determine any trends that may exist. The most significant correlations were found to exist between LA abrasion and ACV (R^2 = 0.65) and between absorption and specific gravity (R^2 = 0.65). The particle shape factor test (ASTM D 4791) was not a good indicator of field performance and did not have significant correlation with any other test. Surprisingly, the magnesium sulfate soundness test and Canadian unconfined freeze-thaw test had a low correlation (R^2 = 0.39) when all data points were considered (Fowler, Allen, Lange, & Range, 2006).

A smaller study within ICAR 507 included the use of the Aggregate Imaging System (AIMS). Twenty aggregates of varying performance histories were tested and the researchers concluded that higher average angularity and texture indices generally corresponded to better field performance but particle shape factor and sphericity factor were not good indicators of performance. By using texture and angularity indices on the same plot, researchers were able to pick limits (220 and 2850 respectively) that successfully identified most good and poor performers. However, the ability of these limits to identify fair performers was not good. Overall, the ICAR 507 researchers believe that the AIMS shows promise for providing relevant information to predict field performance, pending more comprehensive studies.

In 1991, Rogers and Senior published results from an Ontario Ministry of Transportation research study that examined testing and performance of 100 coarse aggregates from Ontario. The research was initiated because the specifications at the time (LA abrasion, magnesium sulfate soundness, and 24-hour water absorption) were prohibiting the use of a few aggregate sources that were known to have satisfactory characteristics. The tests were also stated to have poor precision, poor correlation with field performance, and poor ability to distinguish between marginal aggregates (aggregates with test results falling near test limits). As a result, this study examined alternative tests and the selected aggregates were tested for Canadian unconfined freeze-thaw, Micro-Deval, aggregate impact value (AIV), polished stone value, and aggregate abrasion test. The aggregates were also rated as "good," "fair," or "poor" depending on pavement life and deterioration mechanisms.

Results of the Ontario study demonstrated that Canadian unconfined freeze-thaw and Micro-Deval were the best indicators of field performance and, when combined, were fairly successful at differentiating between "fair" and "poor" aggregates in PCC. Rogers and Senior also noted that water absorption can also be used as an indicator of poor performing aggregates. Other important conclusions included determining that the standard deviation for Micro-Deval

was less than the magnesium sulfate soundness, even for high loss aggregates, which is important for test precision. The two impact tests studied (LA abrasion and AIV) demonstrated relatively little relation to concrete field performance, yet had fairly high correlation to each other ($R^2 = 0.64$) (Rogers & Senior, 1991). The relationship between Micro-Deval abrasion loss and unconfined freeze-thaw loss is illustrated in Figure 2.2.
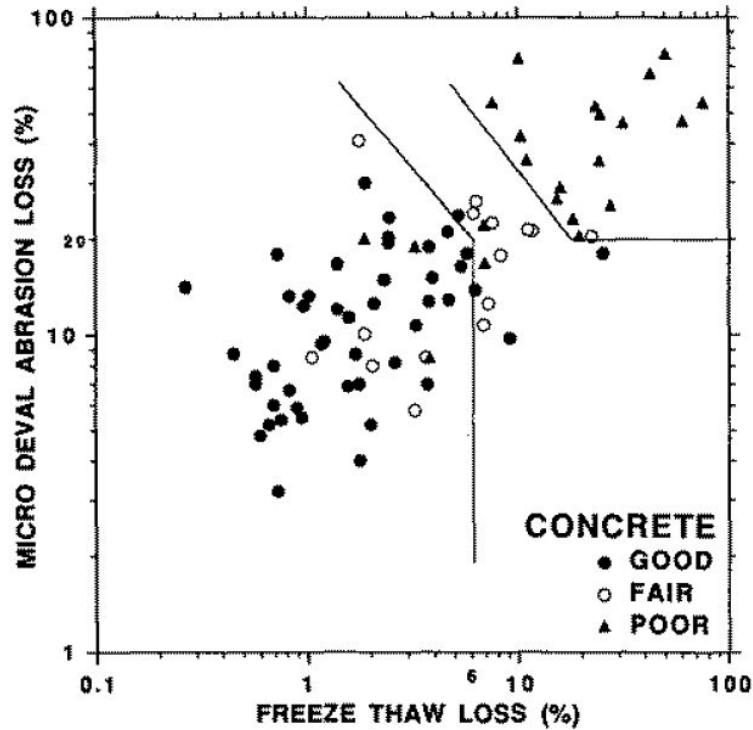
Figure 2.2: Relationship between Micro-Deval Loss and Canadian Unconfined Freeze-Thaw Loss with Performance Ratings for Ontario Aggregates (Rogers & Senior, 1991)

In 2005, researchers at the Virginia Transportation Research Council, in conjunction with the Wisconsin Department of Transportation (research project WHRP 06-07), evaluated 60 Wisconsin coarse aggregates on a variety of tests in an attempt to correlate results with field performance and recommend the most relevant tests. Tests in the study included sodium sulfate soundness, lightweight pieces in aggregate, frost resistance of aggregates in concrete, unconfined freeze-thaw, Micro-Deval, vacuum saturated specific gravity and absorption, and compressive strength of concrete. Wisconsin DOT officials classified each aggregate as "good" (20 total aggregates), "intermediate" (26 total aggregates), and "poor" (14 total aggregates).

Major conclusions of the WHRP 06-07 research project included finding a high correlation between Micro-Deval and vacuum saturated absorption ($R^2 = 0.86$) and the recommendation that absorption can be used as a primary indicator of durability (Weyers, Williamson, Mokarem, Lane, & Cady, 2005). The LA abrasion test was only able to identify the very worst aggregate sample as being poor but, although the LA abrasion test cannot directly predict the overall performance of an aggregate, it can be used to accurately estimate the strength. The sodium sulfate soundness test was determined to be highly variable. Although other literature has recommended an unconfined freeze-thaw limit of 10%, researchers determined that this limit would reject too many aggregates. As a result, they recommended a

14

limit of 15% for Wisconsin aggregates. A similar finding was noted regarding the Micro-Deval. Weyers et al. (2005) recommended adding the Micro-Deval to Wisconsin DOT test procedures but again, the recommended limit (18%) would reject too many aggregates. Weyers et al. (2005) concluded that a limit of 25–30% for Micro-Deval loss would be more reasonable for Wisconsin aggregates. Because the ACV and LA abrasion test were highly correlated and appear to measure the same property (aggregate strength), Weyers et al. (2005) saw no purpose in replacing the LA abrasion test. Based on these conclusions and additional recommendations made as part of this research project, a flow chart was created to assist DOT personnel in characterizing and qualifying coarse aggregates in the future. This flow chart is presented in Figure 2.3 (Weyers, Williamson, Mokarem, Lane, & Cady, 2005).
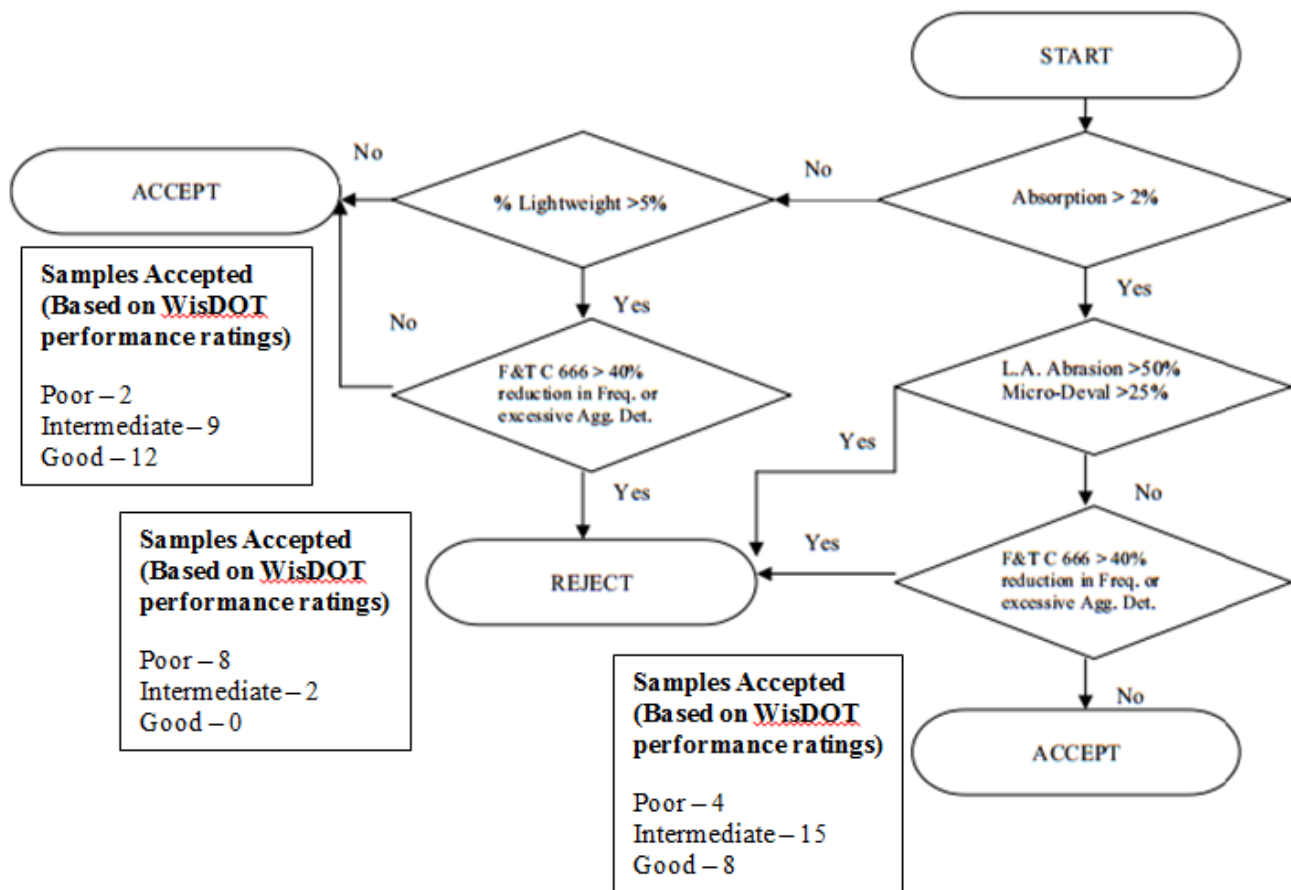
Figure 2.3: Aggregate Durability Testing Flowchart for Concrete Aggregates
(Weyers, Williamson, Mokarem, Lane, & Cady, 2005)

In 2005, Rangaraju, Edlinski, and Amirkhanian from Clemson University published a report (FHWA-SC-05-01) in conjunction with FHWA and South Carolina DOT that described the results of a study evaluating South Carolina aggregate durability properties of 23 coarse aggregates. The Micro-Deval and magnesium sulfate soundness test were examined and compared to the two tests historically used by South Carolina DOT: the LA abrasion test and the sodium sulfate soundness test. Field performance ratings of each aggregate were provided by South Carolina DOT officials in order to attempt to identify the tests that most accurately

distinguish performance. Results of this study demonstrated that no significant correlation between Micro-Deval and LA abrasion, or between Micro-Deval and either sulfate soundness test. However, Rangaraju, Edlinski, and Amirkhanian did find a strong correlation between magnesium sulfate soundness and sodium sulfate soundness. The LA abrasion limit of 55% did not do a good job in identifying marginal ("fair" and "poor") aggregates in field performance but a Micro-Deval limit of 17% was able to identify all marginal aggregates. As a result, Rangaraju, Edlinski, and Amirkhanian concluded that the Micro-Deval test does a better job of predicting aggregate durability and as such, should be implemented in South Carolina DOT specifications (Rangaraju, Edlinski, & Amirkhanian, 2005).

The National Center for Asphalt Technology (NCAT) published a report in 1998 (NCAT 98-4) that detailed a research project about aggregate toughness, abrasion resistance, and durability in asphalt concrete performance in pavements. Although this study was focused on asphalt concrete applications, general trends from test results are still applicable for aggregates used in PCC, as many sources provide aggregates for both applications. In this study, Wu, Parker, and Kandhal from Auburn University and Georgia DOT examined 16 aggregate sources (from all regions of the U.S. and varying in mineralogy) and subjected these aggregates to tests including LA abrasion, Micro-Deval, AIV, ACV, sulfate soundness, freeze-thaw soundness, Canadian unconfined freeze-thaw, and aggregate durability index. Aggregates included five carbonate sources, four gravels, two granites, one trap rock, one siltstone, one sandstone, and one steel slag. Surveys and discussions with DOT agencies allowed the researchers to provide a "worst case" characterization of aggregates as "good" (used for many years—no issues), "fair" (used for at least 8 years—some issues), and "poor" (problems occurred during first 2 years). Ratings were made independently for abrasion/toughness resistance and soundness/durability for each aggregate. The results of this study demonstrated that the Micro-Deval and magnesium sulfate soundness tests appear to be the best indicators of potential field performance of aggregates used in asphalt concrete. Limits of 18% for each test appear to separate good/fair performers from poor performers. Wu, Parker, and Kandhal concluded that the Micro-Deval test is the best choice for aggregate quality characterization (Wu, Parker, & Kandhal, 1998).

A study performed by Koubaa and Snyder at The University of Minnesota in the late 1990s examined test methods for better characterizing freeze-thaw durability of Minnesota aggregates for concrete applications. After completing concrete pavement condition surveys to document a variety of freeze-thaw performance, the researchers collected and tested aggregates from 13 sources (11 carbonates—mostly dolomites, 2 gravels). Tests performed include absorption and bulk specific gravity, PCA absorption, Iowa pore index, acid insoluble residue, X-ray diffraction analysis, X-ray fluorescence analysis, thermogravimetric analysis, Washington hydraulic fracture test, ASTM C 666, and the VPI single-cycle slow freeze test. Cores were also taken from the field for various tests and examinations. Results of this research project demonstrated that the tests with the best correlation to field performance were modified ASTM C 666 (procedure B), VPI single-cycle slow freeze test, and the hydraulic fracture test. Other tests with correlation to field performance, though not as strong, included absorption, specific gravity, Iowa pore index, and X-ray fluorescence. Field investigations demonstrated that fine-grained dolomites and aggregates with cracked shale particles caused poor freeze-thaw performance of the concrete. Due to discrepancies in otherwise strong patterns in test data, Koubaa and Snyder concluded that the best method for accepting or rejecting aggregates subject to freeze-thaw distress was to develop a flow chart, as no single test can accurately predict durability. The flow chart is not included in this literature review because, in the scope of this project, freeze-thaw

characterization is not a priority (only very northern parts of Texas experience more than a few yearly freeze-thaw cycles). However, the flow chart developed by Koubaa and Snyder can be found in conference proceedings from the Seventh Annual ICAR Symposium (Koubaa & Snyder, 1999).

2.3 Coarse Aggregate Tests

As coarse aggregate tests are the focus of this study, the research team conducted a comprehensive literature review to determine the most common and most effective coarse aggregate tests.

2.3.1 Abrasion Resistance

Abrasion resistance is an aggregate property that influences the breakdown of aggregate during production, handling, and mixing; the effect of studded tires on aggregates near exposed concrete surfaces; and the behavior of aggregates at concrete joints (Folliard & Smith, 2002). Breakdown of aggregate due to poor abrasion resistance can cause the production of microfines during mixing, which is not always desirable and can lead to workability and placement problems for the concrete. The two most popular tests to assess a coarse aggregate's abrasion resistance are the LA abrasion and impact Test (also known simply as the LA abrasion test) and the Micro-Deval test. A review of coarse aggregate specifications used by DOTs in the U.S. showed that the LA abrasion test is used to evaluate aggregates by 49 of 50 DOTs (see Section 3.2). The Micro-Deval test is currently used more in Canada than in the U.S. but there has been a significant interest in the potential of the Micro-Deval test by American researchers and DOTs alike during the past two decades.

2.3.1.1 Micro-Deval Test for Coarse Aggregates

The Micro-Deval test originated in the Deval test, which was developed in the 1900s to assess the quality of railroad ballast. French researchers wanted to modify this test to abrade, rather than fracture, aggregates after determining that running this test in a wet condition increased loss by friction and abrasion (Dar Hao, 2010). As a result, French researchers developed the Micro-Deval test, which subjects water, aggregate, and steel charge to 12,000 revolutions in a steel drum via a ball mill roller. Researchers in Canada further modified this test to allow for a larger aggregate sample size and slightly altered dimensions of the steel charge and drum (Rogers C., 1998). Today, most Micro-Deval specifications are based on the AASHTO standards similar to those documented by the Canadian researchers.

A significant amount of research in the past two decades has examined how to best use the Micro-Deval test to characterize and qualify aggregates. Several studies have focused on the potential of the Micro-Deval to replace other durability tests (such as sulfate soundness tests) due to its higher repeatability and lower variability. Although research has consistently demonstrated the high repeatability of the Micro-Deval test, its correlation with other tests has shown mixed results. For example, a study from 2005 showed that for the 23 aggregate sources studied (all from South Carolina), there appeared to be no significant correlation between Micro-Deval and either sulfate soundness test (Rangaraju, Edlinski, & Amirkhanian, 2005). Another study in 2003 showed similar results after testing 72 aggregates from the southeast United States, with Micro-Deval having a very low correlation ($R^2 = 0.11$) with sodium sulfate soundness (Cooley & James, 2003). However, a study in 2007 found that the Micro-Deval had a good correlation with

sodium sulfate soundness ($R^2 = 0.72$) for 32 Montana aggregates, and thus recommended the Micro-Deval test as a good candidate to replace the sodium sulfate test due its high correlation, repeatability, and quick test time (Cuelho, Mokwa, & Obert, 2007). An examination of the Micro-Deval test for Virginia sources yielded similar conclusions about the enhanced repeatability of the Micro-Deval test compared to sulfate soundness. For 20 aggregates tested, researchers found the average coefficient of variance (COV) for Micro-Deval to be 4.8% compared to 20–30% for magnesium sulfate soundness (Hossain, Lane, & Schmidt, 2008). Rogers and Senior also found the COV for Micro-Deval to be much lower than magnesium sulfate soundness (Rogers & Senior, 1991). Their results are displayed graphically in Figure 2.4.
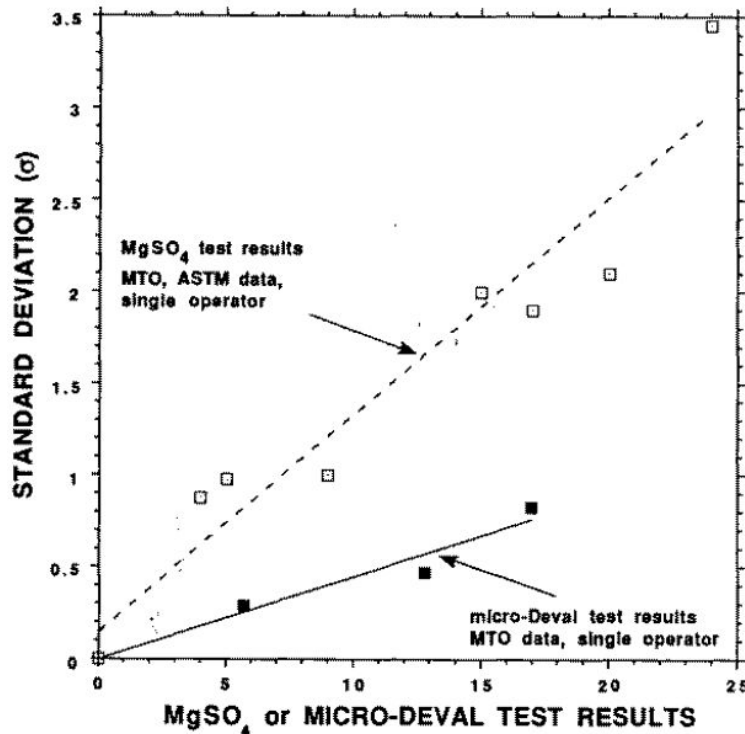
Figure 2.4: Standard Deviation against Loss in Magnesium Sulfate Soundness or Micro-Deval Abrasion Test (Rogers & Senior, 1991)

A 2007 study in Texas also showed that the Micro-Deval test had much better repeatability (within-lab precision) and reproducibility (between lab precision) than the magnesium sulfate soundness test. This study also attempted to alter the Micro-Deval test to improve its correlation with the magnesium sulfate soundness test, but no alterations were successful in improving the correlation beyond R^2 value of 0.80. Because of this finding, researchers concluded that the correlation was not strong enough to justify replacing the magnesium sulfate soundness test with the Micro-Deval test, but the Micro-Deval test should be implemented as a quality control tool (Jayawickrama, Hossain, & Hoare, 2007).

For predicting field performance, the Micro-Deval test appears to be very promising. In 1991, Senior and Rogers collected over 100 aggregates from Ontario and tested them for: Canadian unconfined freeze-thaw, Micro-Deval, AIV, polished stone value, and aggregate abrasion test. Unconfined freeze-thaw and Micro-Deval were the best indicators of field performance for concrete aggregates. It was also determined that standard deviation for Micro-

Deval was less than magnesium sulfate soundness, even for high loss aggregates (Rogers & Senior, 1991). A 2005 Wisconsin DOT study conducted by Weyers et al. recommended that the Micro-Deval test be added to Wisconsin DOT procedures after subjecting 60 aggregates of varying performance to a variety of tests. This study also found a high correlation ($R^2 = 0.86$) between Micro-Deval and vacuum saturated absorption (Weyers, Williamson, Mokarem, Lane, & Cady, 2005). A fairly comprehensive aggregate study in Texas (ICAR 507) examined 117 aggregate sources from North America and found the best correlation with field performance of concrete to be the Micro-Deval test when used in combination with the Canadian freeze-thaw test, as previously shown in Section 2.2 (Fowler, Allen, Lange, & Range, 2006).

Recommended limits vary for each study which is not necessarily surprising considering different studies examined different aggregates and correlated performance to different environmental regions. The FHWA study examining South Carolina aggregates noted that a Micro-Deval limit of 17% was sufficient in identifying all marginal performers (Rangaraju, Edlinski, & Amirkhanian, 2005). An FHWA study examining Montana aggregates concluded that if Micro-Deval loss is more than the recommended cutoff of 18–24%, then a second evaluation test should be performed before the aggregate is discredited for durability (Cuelho, Mokwa, & Obert, 2007). In a 1998 journal article summarizing the experience with the Micro-Deval test in Ontario, the author states that Micro-Deval limits in Ontario (as of 1998) were 13% for coarse aggregates used in concrete pavement and 17% for coarse aggregates used in structural concrete (Rogers C. , 1998).

2.3.1.2 LA Abrasion and Impact Test

The LA abrasion and impact test, also commonly referred to as simply the "LA abrasion test," is currently used by 49 of 50 state DOTs to evaluate aggregates (this is further discussed in Section 3.2). The NCHRP 4-20C final report recommends this test, but some researchers studies have shown that that although the LA abrasion test correlates well with some other aggregate tests, it does not correlate well with field performance.

Several studies have been conducted to examine which rock properties influence the results of the LA abrasion test. In 2007, Turkish researchers tested 35 different rock types (9 igneous, 11 metamorphic, 15 sedimentary) for LA abrasion and uniaxial compressive strength (UCS), and also classified rocks by porosity. For the UCS testing, rocks were collected and inspected to ensure they had no fractures or defects before being cored to dimensions of 38-mm (1.5-in.) diameter and 76-mm (3.0-in) length, trimmed, and subjected to UCS testing. Regression analysis demonstrated logarithmic relationships, which varied by type of rock and porosity class, between LA abrasion and UCS. Correlation coefficients were highest when grouped by porosity ($R^2 = 0.68$ for porosity <1%, $R^2 = 0.79$ for porosity between 1% and 5%, and $R^2 = 0.75$ for porosity >5%). For relationships based on rock type alone, correlation coefficients were $R^2 = 0.50$ for igneous rock, $R^2 = 0.81$ for metamorphic rocks, and $R^2 = 0.50$ for sedimentary rocks. For all rocks included in the study, the correlation coefficient was $R^2 = 0.63$ relating LA abrasion loss to unconfined compressive strength. Overall, this study demonstrated that the LA abrasion test is dependent upon the strength of the aggregate, porosity, and rock type (Kahraman & Fener, 2007).

Another group of Turkish researchers published the results of a similar project in 2009 that evaluated four limestones, three crystalline marbles, and one andesite to determine correlations between LA abrasion and physical properties such as bulk density, Schmidt hardness, shore hardness, P-wave velocity, and mechanical properties such as uniaxial

compressive strength, point load index, and indirect tensile strength of rocks. Results of the LA abrasion test were normalized by dividing by P-wave velocity to account for different porosities, densities, and presence of fractures. Researchers considered correlation coefficients of $R^2 > 0.50$ to be "statistically significant at a 99% confidence level with 10 degrees of freedom." The normalized LA abrasion loss showed highest correlations with compressive strength, tensile strength, Schmidt hardness, and point load index, and showed moderate correlations with bulk density and shore hardness. Thus, this research demonstrated that LA abrasion test results are not only influenced by aggregate strength and porosity, but by hardness and density as well (Ugur, Demirdag, & Yavuz, 2009).

A study with a more narrow scope in 1980 by researchers from Saudi Arabia examined igneous (particularly volcanic and plutonic) rocks and the influence of grain size and absorption capacity on LA abrasion loss. The study found that LA abrasion loss increased linearly with absorption capacity and that fine-grained (grain < 60-µm) igneous rocks were "tougher" (lower LA abrasion loss) than coarse-grained (grain > 2-mm) rocks of the same porosity (Kazi & Al-Mansour, 1980). These three studies suggest that the results of the LA abrasion test depend on, and thus indirectly characterize, absorption, porosity, strength (both tensile and compressive), density, and hardness.

When researchers have attempted to correlate LA abrasion with field performance, they have found little correlation between the two. In his paper explaining the Canadian experience with Micro-Deval testing, Rogers states anecdotally that in Ontario, researchers have noticed that LA abrasion results do not correlate well with field performance, although the test does have the capacity to identify aggregates prone to breakdown during handling (Rogers C. , 1998). The 2005 Wisconsin DOT study found that in their study of 60 aggregates, the LA abrasion test was only able to identify the very worst aggregate sample as being "poor." However, this study did confirm findings of the Turkish researchers that the LA abrasion test can accurately estimate aggregate strength (Weyers, Williamson, Mokarem, Lane, & Cady, 2005). The 2005 study conducted in South Carolina also found that the LA abrasion test was not a good predictor of field performance when they determined that the state specified 55% limit did not do a good of identifying marginal ("fair" and "poor") aggregates in field performance (Rangaraju, Edlinski, & Amirkhanian, 2005).

Although research shows that the LA abrasion test does not correlate well with field performance, it does correlate well with a few other common aggregate tests. The ICAR 507 study determined that LA abrasion had good correlation with ACV ($R^2 = 0.65$) (Fowler, Allen, Lange, & Range, 2006). The Ontario study which explored a variety of aggregate tests found a similar correlation between LA abrasion and AIV ($R^2 = 0.64$) (Rogers & Senior, 1991). At least three studies (ICAR 507, FHWA-SC-05-01, and a Southeastern Superpave Center project) have demonstrated that although LA abrasion and Micro-Deval both attempt to characterize abrasion resistance of aggregates, the two tests do not correlate well at all (Rangaraju, Edlinski, & Amirkhanian, 2005), (Fowler, Allen, Lange, & Range, 2006), (Cooley & James, 2003). However, a study conducted on Montana aggregates found that Micro-Deval and LA abrasion actually had good correlation for low loss materials, but discontinuities existed for higher loss materials, causing a lower overall correlation coefficient ($R^2 = 0.46$) (Cuelho, Mokwa, & Obert, 2007).

Alternative methods to the LA abrasion test have been explored by at least one research study. In 2008, researchers published a report detailing the results of a study that examined the relationships between aggregate type and compressive strength, flexural strength, and abrasion

resistance of high strength concrete. Researchers prepared 50-mm x 50-mm x 100-mm (1.97-in. x 1.97-in. x 3.94-in.) prismatic high strength concrete specimens which were saw-cut and placed in the LA abrasion machine without the traditional steel shot. After 28 days of curing, the specimens were subjected to 100 revolutions and 500 revolutions and a loss was measured at each stage. Other tests performed in this study include the traditional LA abrasion test, uniaxial compressive strength of rock, Bohme apparatus abrasion, and compressive and flexural strength of concrete. Results demonstrated that both aggregate strength and texture influenced the compressive strength, flexural strength, and abrasion resistance of high strength concrete. The traditional LA abrasion test had very high correlation (R^2 = 0.95) with uniaxial compressive strength of the aggregate, but interestingly the traditional LA abrasion test had a lower correlation (R^2 = 0.67) with the alternative LA abrasion method using prismatic concrete specimens (Kiliç, et al., 2008).

2.3.2 Soundness and Freeze-Thaw Resistance

Tests recommended by NCHRP 4-20C to characterize soundness and freeze-thaw resistance of aggregates include the magnesium sulfate soundness test, the Canadian unconfined freeze-thaw test, and the Iowa pore index test (Folliard & Smith, 2002).

2.3.2.1 Sulfate Soundness Test

The sulfate soundness of aggregates can be measured by using a magnesium sulfate solution or a sodium sulfate solution. This test involves cycles (typically five) soaking an aggregate in a sulfate solution and then drying the aggregate. This test was originally developed in 1828 to simulate freezing of water in stone before refrigeration was controllable and widely available (Rogers, Bailey, & Price, 1991). The idea was to simulate crystallization pressures of ice formation during freezing and thawing events by causing salt crystals to form during the heating stage of this test (Folliard & Smith, 2002). Of the state DOTs that do use the sulfate soundness test, 28 states specify the use the use of sodium sulfate, 9 states specify the use of magnesium sulfate, and 2 states allow the use of either magnesium sulfate or sodium sulfate. Eleven states do not use sulfate soundness testing. State specifications are further discussed in Section 3.2.

The most common complaints about the sulfate soundness test are its lack of correlation to field performance, its time of testing (7–10 days), and its high variability (Jayawickrama, Hossain, & Hoare, 2007). Several research studies have confirmed the assertion that the sulfate soundness tests have high variability compared to tests like the Micro-Deval and LA abrasion (Weyers, Williamson, Mokarem, Lane, & Cady, 2005), (Cuelho, Mokwa, & Obert, 2007), (Hossain, Lane, & Schmidt, 2008). Although Rangaraju et al. determined that the two sulfate soundness tests are highly correlated to each other, NCHRP 4-20 only recommends use of the magnesium sulfate soundness test due to the higher variability of the sodium sulfate soundness test (Folliard & Smith, 2002).

Several studies have examined the correlation between the Micro-Deval test and the sulfate soundness tests with mixed results. Rangaraju et al. found no correlation between Micro-Deval and either sulfate soundness test after testing 23 South Carolina aggregates (Rangaraju, Edlinski, & Amirkhanian, 2005). Cooley and James found a very low correlation (R^2 = 0.11) between Micro-Deval and sodium sulfate soundness after testing 72 aggregates in the southeast United States (Cooley & James, 2003). However, Cuelho et al. found that the sodium sulfate test had a good correlation (R^2 = 0.72) with Micro-Deval after testing 32 Montana aggregates

(Cuelho, Mokwa, & Obert, 2007). Jayawickrama et al. found a high correlation ($R^2 = 0.7$) between Micro-Deval and magnesium sulfate soundness for Texas aggregates but said that the correlation wasn't high enough to justify replacing the magnesium sulfate soundness test (Jayawickrama, Hossain, & Hoare, 2007).

2.3.2.2 Canadian Unconfined Freeze-Thaw Test

Although less common than the sulfate soundness test, the Canadian unconfined freeze-thaw test has shown success in its correlation to freeze-thaw damage in PCC pavements and in its high precision (Folliard & Smith, 2002). This test was developed during the 1980s by researchers in Canada as a means to simulate realistic freezing and thawing cycles while the aggregate is exposed to moisture and salts (Rogers, Bailey, & Price, 1991). In the Canadian unconfined freeze-thaw test, three sizes of coarse aggregate are soaked in a 3% sodium chloride solution for 24 hours, then drained and subjected to five cycles of freezing (for 16 hours) and thawing (8 hours), and then re-sieved afterwards. A mass loss is calculated from the final material. Canadian specifications require a mass loss of 6% or less for severe exposure conditions and a mass loss of 10% or less for moderate conditions (Folliard & Smith, 2002).

Several research projects have examined the Canadian unconfined freeze-thaw test. In 1991, researchers from Ontario collected over 100 aggregates from Ontario and subjected them to a variety of tests (this research project is also discussed in Section 2.2). They concluded that applying limits based on the Canadian unconfined freeze-thaw test and the 24-hour water absorption test was one way of identifying good, fair, and poor performers. Aggregates that had good field performance histories were mostly bounded by a Canadian unconfined freeze-thaw loss of 6% and an absorption capacity of 1.5%. Another boundary of 13% Canadian unconfined freeze-thaw loss and an absorption capacity of 2% was able to identify most aggregates with good or fair performance histories. It should be noted that although these limits captured most good and fair performers, several good and fair performers fell outside these limits as demonstrated by Figure 2.5, from the final report of this study.
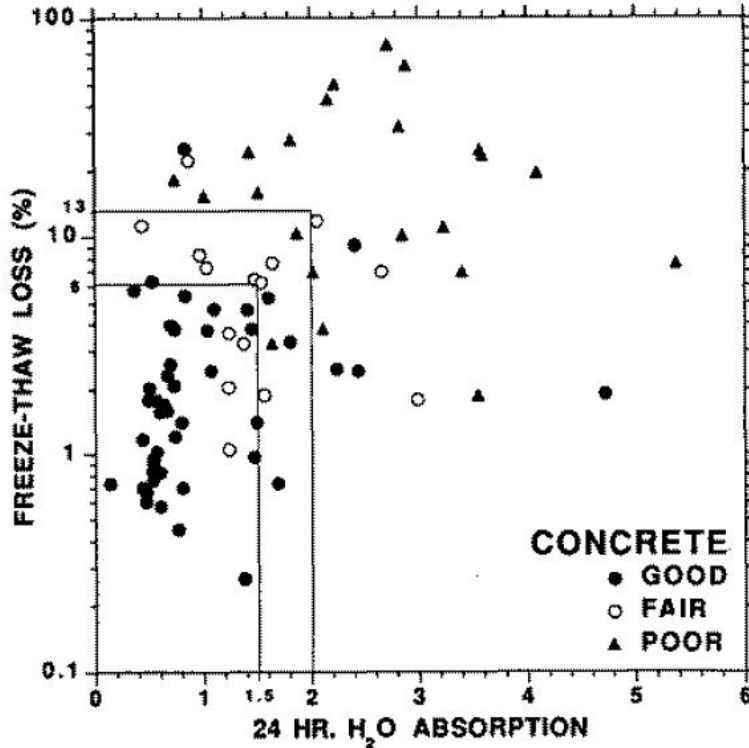
Figure 2.5: Canadian Unconfined Freeze-Thaw versus Absorption Capacity
(Rogers & Senior, 1991)

ICAR 507 was another research study that had similar conclusions to Rogers & Senior's study in Ontario. ICAR 507 collected over 100 aggregate sources from the United States and Canada and subjected these samples to a variety of tests. This study found that the best single test indicator of field performance for all applications was the Micro-Deval test, but the best overall indicator of field performance was the Micro-Deval test used in combination with the Canadian unconfined freeze-thaw test. A Micro-Deval loss of 21%, combined with a Canadian unconfined freeze-thaw loss of 3.6%, was able to bound 77% of good performers for PCC applications. Figure 2.1 graphically displays the bounding of performers by these criteria. The limits of 21% for Micro-Deval and 3.6% for Canadian freeze-thaw were also able to exclude 100% of the fair performers and 100% of the poor performers. If the Canadian freeze-thaw limit is raised to 6.5% (dashed line), 95% of good performers are included, 50% of the fair performers are included, and 60% of the poor performers are included. However, it is important to note that only four fair performers and five poor performers were subjected to testing. The researchers acknowledged that further research of more marginal performers may be needed to refine these limits. This study found little correlation ($R^2 = 0.39$) between the Canadian unconfined freeze-thaw test and the magnesium sulfate soundness test (Fowler, Allen, Lange, & Range, 2006).

The Wisconsin DOT study, also discussed in Section 2.2, examined 60 Wisconsin aggregates and determined that the recommended limit of 10% for Canadian unconfined freeze-thaw rejected too many aggregates. They instead proposed a 15% limit, which would ensure that only very non-durable aggregates were rejected by the limit. They also found that the Canadian unconfined freeze-thaw test had no correlation with the sodium sulfate soundness test (Weyers, Williamson, Mokarem, Lane, & Cady, 2005).

2.3.2.3 Iowa Pore Index

The Iowa pore index test was developed as means of identifying aggregates susceptible to freeze-thaw damage, particularly D-cracking behavior. This test uses a pressurized vessel to quantify the amount of macropores and micropores in an aggregate. Theoretically, a higher volume of micropores indicates that an aggregate will be more susceptible to D-cracking. When running the Iowa pore index test, a 9-kg (19.8-lb) sample of dried aggregate is placed in a pressure vessel along with water and then a 241-kPa (35.0-psi) pressure is applied. The amount of water absorbed by the aggregate under this pressure in the first minute is the primary load, an attempt at quantifying macropore volume. The amount of water absorbed by the aggregate at this pressure for the next 14 minutes is the secondary load, which is indicative of micropore volume. Iowa DOT places a 27-mL limit on the secondary load to avoid aggregates prone to D-cracking (Folliard & Smith, 2002). Figure 2.6, from a Michigan DOT report, demonstrates sample water uptake rates for various aggregates from a river gravel sample during the Iowa pore index test.
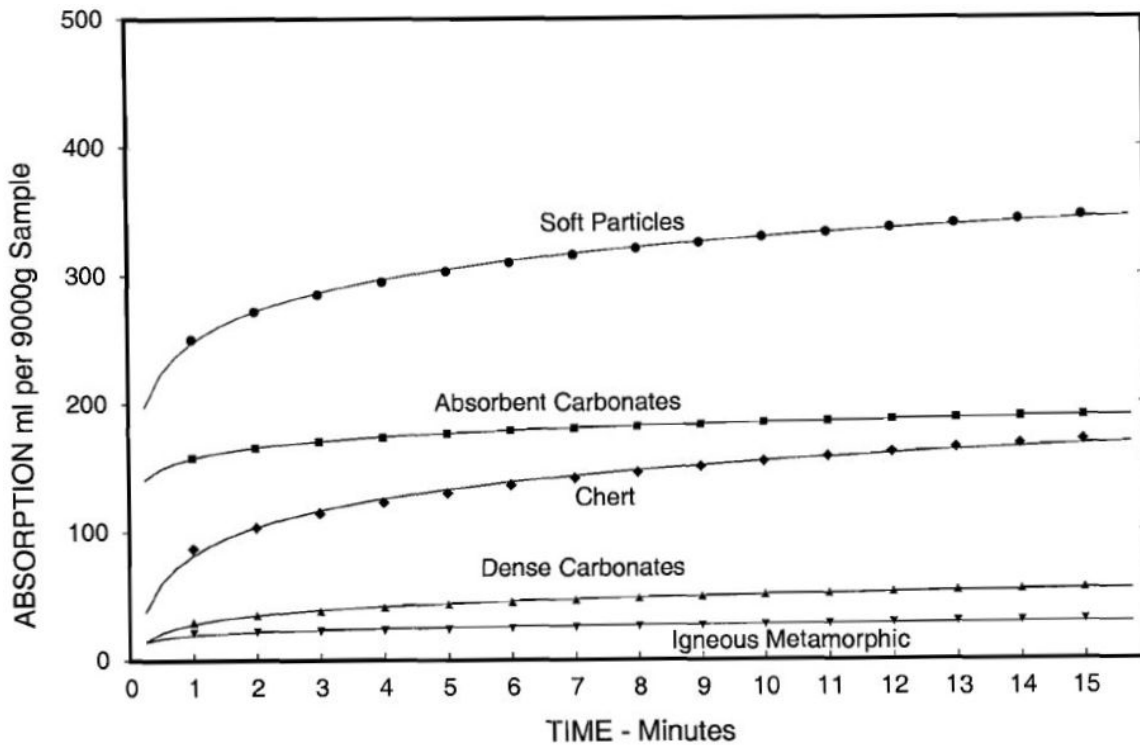
Figure 2.6: Water Uptake Rates for Various Aggregates in Iowa Pore Index Test
(Muethel, 2007)

A study performed by researchers at The University of Minnesota in the late 1990s examined test methods for better characterizing freeze-thaw durability of Minnesota aggregates for concrete applications. Results of this research project demonstrated that the Iowa pore index test was correlated with field performance, though not as well as other tests such as modified ASTM C 666 (procedure B), VPI single-cycle slow freeze test, and the hydraulic fracture test (Koubaa & Snyder, 1999).

2.3.3 Strength and Impact Resistance

Strength and impact resistance of aggregates is important for not only high strength concrete applications, when compression failure occurs due to aggregate fracture, but also for handling and transportation of aggregate as well. Perhaps the only realistic way to directly measure aggregate strength is through the unconfined compressive strength testing of rock. However, this method often yields highly variable results and is not always possible for river gravels, which can have small maximum particle sizes unfriendly for coring devices (Folliard & Smith, 2002). The LA abrasion and impact test, British ACV, and the British AIV are all tests that indirectly measure aggregate strength and/or impact resistance. It is important to note that while some minimal level of integrity and strength is important for aggregates, concrete strength may not be highly important to all PCC applications. A TxDOT research project demonstrated that concrete strength had negligible correlation with performance of CRCPs (Won, 2001).

2.3.3.1 LA Abrasion and Impact Test

The LA Abrasion and Impact Test, also commonly referred to as simply the "LA abrasion test," is currently used by 49 of 50 state DOTs to evaluate aggregates (this is further discussed in Section 3.2). The NCHRP 4-20 final report recommends this test as an abrasion test, but some research studies have shown the LA abrasion test correlates well with aggregate tests that measure strength and impact resistance. ASTM International added "impact" to the test's title, acknowledging the role of steel shot and aggregate impact in the test's results. However, research has also shown that this does not correlate well with field performance.

Several studies have been conducted to examine which rock properties influence the results of the LA abrasion test. In 2007, Turkish researchers tested 35 different rock types (9 igneous, 11 metamorphic, and 15 sedimentary) for LA abrasion and UCS, and also classified rocks by porosity. For the UCS testing, rocks were collected and inspected to ensure they had no fractures or defects before being cored to dimensions of 38-mm (1.5-in.) diameter and 76-mm (3.0-in) length, trimmed, and subjected to UCS testing. Regression analysis demonstrated logarithmic relationships, which varied by type of rock and porosity class, between LA abrasion and UCS. Correlation coefficients were highest when grouped by porosity ($R^2 = 0.68$ for porosity <1%, $R^2 = 0.79$ for porosity between 1% and 5%, and $R^2 = 0.75$ for porosity >5%). For relationships based on rock type alone, correlation coefficients were $R^2 = 0.50$ for igneous rock, $R^2 = 0.81$ for metamorphic rocks, and $R^2 = 0.50$ for sedimentary rocks. For all rocks included in the study, the correlation coefficient was $R^2 = 0.63$ relating LA abrasion loss to unconfined compressive strength. Overall, this study demonstrates that the LA abrasion test is dependent upon the strength of the aggregate, porosity, and rock type (Kahraman & Fener, 2007).

Another group of Turkish researchers published the results of a similar project in 2009 that evaluated four limestones, three crystalline marbles, and one andesite to determine correlations between LA abrasion and physical properties such as bulk density, Schmidt hardness, shore hardness, P-wave velocity, and mechanical properties such as uniaxial compressive strength, point load index, and indirect tensile strength of rocks. Results of the LA abrasion test were normalized by dividing by P-wave velocity to account for different porosities, densities, and presence of fractures. Researchers considered correlation coefficients of $R^2 > 0.50$ to be "statistically significant at a 99% confidence level with 10 degrees of freedom." The normalized LA abrasion loss showed highest correlations with compressive strength, tensile strength, Schmidt hardness, and point load index, and showed moderate correlations with bulk density and shore hardness. Thus, this research demonstrated that LA abrasion test results are not

only influenced by aggregate strength and porosity, but by hardness and density as well (Ugur, Demirdag, & Yavuz, 2009).

A study with a more narrow scope in 1980 by researchers from Saudi Arabia examined igneous (particularly volcanic and plutonic) rocks and the influence of grain size and absorption capacity on LA abrasion loss. The study found that LA abrasion loss increased linearly with absorption capacity and that fine-grained (grain < 60-μm) igneous rocks were "tougher" (lower LA abrasion loss) than coarse-grained (grain > 2-mm) rocks of the same porosity (Kazi & Al-Mansour, 1980). These three studies suggest that the results of the LA abrasion test depend on and thus indirectly characterize absorption, porosity, strength (both tensile and compressive), density, and hardness.

When researchers have attempted to correlate LA abrasion with field performance, they have found little correlation between the two. In his paper explaining the Canadian experience with Micro-Deval testing, Rogers states anecdotally that in Ontario, researchers have noticed that LA abrasion results do not correlate well with field performance, although the test does have the capacity to identify aggregates prone to breakdown during handling (Rogers C., 1998). The 2005 Wisconsin DOT study found that in their study of 60 aggregates, the LA abrasion test was only able to identify the very worst aggregate sample as being "poor." However, this study did confirm findings of the Turkish researchers that the LA abrasion test can accurately estimate aggregate strength (Weyers, Williamson, Mokarem, Lane, & Cady, 2005). The 2005 study conducted in South Carolina also found that the LA abrasion test was not a good predictor of field performance when they determined that the state-specified 55% limit did not do a good of identifying marginal ("fair" and "poor") aggregates in field performance (Rangaraju, Edlinski, & Amirkhanian, 2005).

Despite research showing that the LA abrasion test does not correlate well with field performance, it does correlate well with a few other common aggregate tests. The ICAR 507 study determined that LA abrasion had good correlation with ACV (R^2 = 0.65) (Fowler, Allen, Lange, & Range, 2006). The Ontario study, which explored a variety of aggregate tests, found a similar correlation between LA abrasion and AIV (R^2 = 0.64) (Rogers & Senior, 1991). At least three studies (ICAR 507, FHWA-SC-05-01, and a Southeastern Superpave Center project) have demonstrated that although LA abrasion and Micro-Deval both attempt to characterize abrasion resistance of aggregates, the two tests do not correlate well at all (Rangaraju, Edlinski, & Amirkhanian, 2005), (Fowler, Allen, Lange, & Range, 2006), (Cooley & James, 2003). However, a study conducted on Montana aggregates found that Micro-Deval and LA abrasion actually had good correlation for low loss materials, but discontinuities existed for higher loss materials, causing a lower overall correlation coefficient (R^2 = 0.46) (Cuelho, Mokwa, & Obert, 2007).

Alternative methods to the LA abrasion test have been explored by at least one research study. In 2008, researchers published a report detailing the results of a study that examined the relationships between aggregate type and compressive strength, flexural strength, and abrasion resistance of high strength concrete. Researchers prepared 50-mm x 50-mm x 100-mm (1.97-in. x 1.97-in. x 3.94-in.) prismatic high strength concrete specimens which were saw-cut and placed in the LA abrasion machine without the traditional steel shot. After 28 days of curing, the specimens were subjected to 100 revolutions and 500 revolutions and a loss was measured at each stage. Other tests performed in this study include the traditional LA abrasion test, uniaxial compressive strength of rock, Bohme apparatus abrasion, and compressive and flexural strength of concrete. Results demonstrated that both aggregate strength and texture influenced the

compressive strength, flexural strength, and abrasion resistance of high strength concrete. The traditional LA abrasion test had very high correlation ($R^2 = 0.95$) with uniaxial compressive strength of the aggregate, but interestingly the traditional LA abrasion test had a lower correlation ($R^2 = 0.67$) with the alternative LA abrasion method using prismatic concrete specimens (Kiliç, et al., 2008).

2.3.3.2 Aggregate Crushing Value (ACV)

The ACV test is a British standard that subjects an aggregate sample to confined compression using a machine typically used for compression testing of concrete cylinders. Approximately 2500 g (5.5 lb) of aggregate passing the ½-in. (12.5-mm) sieve and retained on the 3/8-in. (9.5-mm) sieve is placed in a cylindrical containment apparatus consisting of steel plates and a steel ring. The aggregate is compressed for approximately 10 minutes at a constant load rate, until the force has reached 400 kN (90,000 lb). This test procedure is described further in Chapter 5.

Of the reviewed literature that discussed the use of the ACV, none have ultimately recommended the ACV as a means of predicting or identifying field performance of aggregates. Perhaps the strength of aggregate is less crucial for typical DOT applications (pavements, bridges, etc.) than the integrity of the overall concrete mixture. Regardless, at least one study found that the ACV test correlated well ($R^2 = 0.65$) with the LA abrasion test (Fowler, Allen, Lange, & Range, 2006). However, the LA abrasion test has itself been criticized for lack of correlation with field performance. The Wisconsin DOT study (discussed in Section 2.2) concluded that there was no reason to change the LA abrasion requirement to an ACV requirement since they are highly correlated and appear to measure the same property (Weyers, Williamson, Mokarem, Lane, & Cady, 2005).

2.3.3.3 Aggregate Impact Value (AIV)

The AIV is a British standard that subjects a confined aggregate sample to a falling impact load. A sample of aggregate, passing the ½-in. (12.5-mm) sieve and retained on the 3/8-in. (9.5-mm) sieve, of approximately 500 g (1.1 lb) in mass (depending on the density) is placed in a steel cup 38 cm (15 in.) below a steel hammer the same diameter as the inside of the cup. The user drops the steel hammer, guided by vertical rods, and raises it 15 times and the sample is sieved over a No. 8 (2.36-mm) sieve. The mass loss is recorded and the final result of the test is mass loss by percentage of original mass. The test procedure is further described in Chapter 5.

Researchers in Ontario studied this test in the early 1990s but concluded that it had little correlation to field performance. They did determine that the AIV test had a good correlation ($R^2 = 0.64$) with the LA abrasion test (Rogers & Senior, 1991).

2.3.4 Absorption

Absorption capacity of aggregate is an important physical property as aggregates with more absorptive potential tend to be more porous and are thus typically weaker, less durable, and more prone to freeze-thaw damage. At least one state DOT, Minnesota, limits absorption capacity for aggregates used in PCC applications (Folliard & Smith, 2002).

2.3.4.1 Specific Gravity and Absorption of Coarse Aggregate

The most common procedure for testing coarse aggregate absorption is AASHTO T 85 (*Specific Gravity and Absorption of Coarse Aggregate*). In this test procedure, the user submerges a sample of aggregate in water for at least 15 hours and then removes it from water and dries all water from the surface of all the particles with a cloth or towel. When no free water can be observed on the particles' surface, it is considered to be at a "saturated surface dry" state, meaning internal pores are still occupied with water, but no water remains at the surface of the aggregate. The user records the saturated surface dry weight of the aggregate and places the sample in the oven to dry. When the sample has a consistent mass (completely dry), the user records the dry mass of the sample; the percentage change in mass represents the aggregate's absorption capacity.

Many studies have determined that absorption capacity is an important parameter, but is often too variable to justify prescriptive limits. Rogers shows in Section 2.2 that lower absorption capacities and lower Canadian unconfined freeze-thaw values tend to signify aggregates with better performance histories. A Minnesota DOT study also found that absorption capacity of aggregates correlated to field performance, though the correlation was not as significant as other tests such as ASTM C 666 (Procedure B), VPI single-cycle slow freeze test, and the Washington hydraulic fracture test. The Wisconsin DOT study discussed in Section 2.2 also includes absorption capacity as a decision parameter in its recommended aggregate selection flowchart shown in Figure 2.1.

2.3.5 Shape Characteristics—Shape, Angularity, and Texture

Shape characteristics of aggregates can influence workability, water demand, shrinkage, and strength of concrete mixtures. Literature has also shown that aggregate shape properties influence yield stress and modulus of elasticity of early age concrete, particularly when the aggregate elastic/viscous properties differ significantly from the cement (Mahmoud, Gates, Masad, Erdoğan, & Garboczi, 2010). Aggregates that are more cubical or angular in shape tend to require more water to achieve the same slump or workability. Aggregates with a rougher texture can improve bond strength at the aggregate-mortar interface leading to stronger concrete due to macroscopic mechanical adhesion (Folliard & Smith, 2002). There are traditional methods to determine shape characteristics, such as proportional calipers, which may warn of aggregates with flat and elongated particles. Newer methods, such as AIMS, are evolving to take advantage of current technologies to provide more data regarding these important shape characteristics.

2.3.5.1 Proportional Caliper for Determining Flat & Elongated Particles

Many state DOTs use a proportional caliper to manually measure particles in an aggregate sample and compare the maximum dimensions of a particle to its minimum dimension. An aggregate possessing an excess of particles above a 4:1 dimension ratio may lead to workability issues during concrete placement (Folliard & Smith, 2002). Some states incorporate this testing as a means of finding aggregates susceptible to breakage during compaction of HMA mixes. The most common standard of this test is ASTM D 4791 and the Texas DOT version of this test, Tex-280-F is described in Section 5.18. A picture of the proportional caliper device is presented in Figure 5.7.

2.3.5.2 Aggregate Imaging System (AIMS 2.0)

AIMS is a machine consisting of a camera, lights, computer software, and movable trays, designed to capture and analyze the shape, angularity, and texture of coarse aggregates and the form and angularity of fine aggregates. The camera captures images of the aggregate particles, either lit directly or backlit, and the software analyzes these images and provides the user with data summarizing the shape characteristics. For coarse aggregates, the user places a set of aggregate particles on a transparent tray and places this tray into the machine. The AIMS machine rotates the tray three times to capture images of each particle. The first image captured is backlit such that only the aggregate's two-dimensional shape is captured and this image is analyzed by the fundamental gradient method. The second image captured requires the camera to focus on the particle, thus allowing a particle height (as a function of focal length) to be determined, and three-dimensional analysis to be realized. The third image captures a close-up surface texture of the aggregate particles that is analyzed by the wavelet method. The data are output in a spreadsheet file that includes a distribution of shape characteristics. Specific algorithms and analysis techniques used by the machine and software are described by the developer, Eyad Masad, and are available through the Texas Transportation Institute (Masad, 2005).

In order to determine the repeatability and accuracy of the AIMS machine, researchers from Texas A&M (including the developer himself) conducted a study examining 500 particles and the effects of multiple operators and machines, as well as comparing AIMS results to results obtained from X-ray computed tomography and a digital caliper. In this study, AIMS was found to have a COV of 11% for any given source (single operator) and a COV of 5% for the same set of aggregates (single operator). Mahmoud et al. concluded that the effects of random placement of the same aggregate particles in different orientations had minimal effects on the angularity. In experiments with two AIMS machines (single operator) and multiple operators (single AIMS machine), the angularity measurements were found to be highly correlated ($R^2 = 0.97$ and $R^2 = 0.98$ respectively) as were texture measurements ($R^2 = 0.97$ and $R^2 = 0.92$). However, slope and intercept for texture was not 1 and 0 (Mahmoud, Gates, Masad, Erdoğan, & Garboczi, 2010). Thus, it seems that the texture measurement is not as repeatable as the angularity measurement.

In the same study, Mahmoud et al. (2009) determined that length, thickness, and width dimensions as measured by AIMS correlated very well with both the X-ray computed tomography ($R^2 = 0.96, 0.84, 0.91$) and digital caliper ($R^2 = 0.96, 0.81, N/A$). However, AIMS underestimated those dimensions by about 10% compared to X-ray computed tomography. This effect was mostly cancelled out when overall ratios were computed (Mahmoud, Gates, Masad, Erdoğan, & Garboczi, 2010).

2.3.6 Thermal Properties

Thermal properties are important in understanding and predicting concrete behavior for applications such as CRCP or mass pours. If thermal properties are not thoroughly understood or accounted for, thermal cracking may occur. Thermal properties are also input parameters for some computer programs such as *ConcreteWorks*.

2.3.6.1 Thermal Conductivity

The current method to measure thermal conductivity is ASTM C 177-04. However, it requires a specimen in the shape of a large rectangular prism so the preparation of a field or lab

sample is time-intensive. This method is also not recommended for highly heterogeneous materials and the varying mix designs of pavements means that ASTM C 177 may not be applicable or reliable (Carlson, Bhardwaj, Phelan, Kaloush, & Golden, 2010).

Acknowledging this problem, researchers from Arizona State University developed a new test method for thermal conductivity using cylindrical specimen geometry. Researchers sought to take advantage of the fact that concrete cylinders are either casted or cored on a regular basis as a means of quality control for mechanical properties. In their experimental setup, researchers drilled a 3/8-in. (9.5-mm) hole through a 4-in. (102-mm) by 6-in. (152-mm) concrete cylinder and placed a 3/8-in (9.5-mm). by 6-in. (152-mm) heating element in the hole. The top and bottom of the concrete cylinder was insulated as shown in Figure 2.7. Thermocouples placed on the inner and outer walls of the concrete cylinder allowed for measurement of temperature as heat diffused through the specimen (Carlson, Bhardwaj, Phelan, Kaloush, & Golden, 2010).
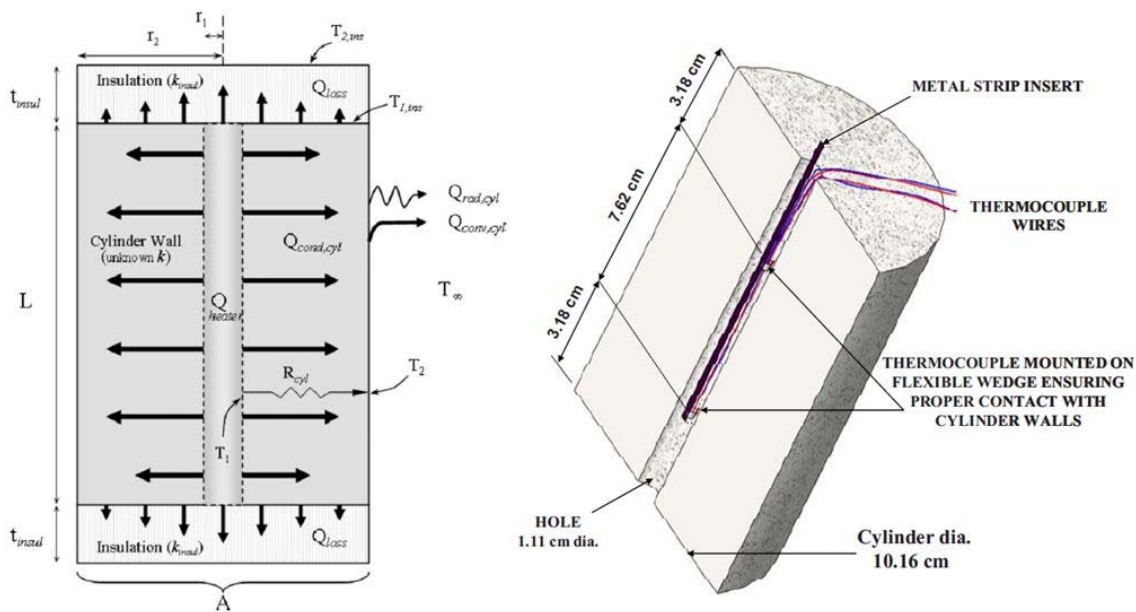
Figure 2.7: Test Setup for Thermal Conductivity Testing of a Cylindrical Specimen (Carlson, Bhardwaj, Phelan, Kaloush, & Golden, 2010)

After acquiring necessary data, fundamental heat transfer theory was used to determine the thermal conductivity of the specimen. The use of a sample with thickness larger than twice the maximum aggregate size prevents thermal bridging, which would skew results. Thus, this method is able to more accurately characterize the composite nature of concrete.

Carlson et al. (2010) validated the accuracy of this test setup by using an ultrahigh molecular weight polyethylene with known thermal conductivity. Researchers also prepared a hot-mix asphalt (HMA) cylindrical specimen and extracted a concrete core from an interstate in Arizona to test. Results compared favorably with values for HMA and concrete in the literature. The PCC cylinder test had higher variation than the HMA specimen, possibly due to the larger aggregate size. Overall, this test method shows potential for future use of determining thermal conductivity using cylindrical concrete specimens (Carlson, Bhardwaj, Phelan, Kaloush, & Golden, 2010).

2.3.6.2 Coefficient of Thermal Expansion (CoTE)

CoTE is a very difficult variable to measure for coarse aggregates. Linear displacement methods are not applicable due to the wide variety of shapes and sizes of aggregates, and volumetric measurements such as the dilatometer often have unacceptably high noise compared to the precision required to measure aggregate expansion under temperature change. At least one TxDOT research project attempted to back-calculate CoTE values of aggregate from concrete CoTE tests (Du & Lukefahr, 2007), and another research project attempted to use dilatometry to measure CoTE of aggregate (Mukhopadhyay & Zollinger, 2009). The current standard for measuring CoTE of a concrete specimen is AASHTO TP 60-00, which requires a core or cylinder 7 in. (178 mm) long and 4 in. (102 mm) in diameter, and it does not directly account for the aggregate CoTE.

Current AASHTO pavement design procedures ignore type of coarse aggregate selected. TxDOT researchers have found that coarse aggregates can significantly impact pavement performance and service life when other variables are held constant (Won, 2001). Spalling and wide/irregular cracks cause the most problems in Texas concrete pavements, particularly in CRCP. The AASHTO Road Test design procedures do not consider these modes of failure but rather emphasize fatigue cracking as the main failure mode of concern. According to at least one TxDOT researcher, thermal expansion of concrete (along with modulus of elasticity, drying shrinkage, and bond strength between aggregate and mortar) is a property that should be considered in pavement design and is significantly influenced by type of coarse aggregate used. Significantly different performance levels have been observed in Texas on the same roadways (thus same traffic loads and same environmental conditions) when different coarse aggregate is used in different sections. For example, the frontage road of Beltway 8 in Houston used a crushed limestone aggregate in one section and siliceous river gravel in another section and the latter section has experienced major spalling. Another example is the frontage road of IH-610, also in Houston. This road used a lightweight aggregate in one section and siliceous river gravel in another section and again severe spalling has been observed in the latter case (Won, 2001).

Research continued at TxDOT to evaluate the CoTE of 94 concrete mixtures where the coarse aggregate was the only variable parameter (41 siliceous gravels, 44 limestone, 3 dolomite, 1 mixed limestone and dolomite, 1 siliceous rhyolite, 1 blended limestone and siliceous gravel, 1 siliceous/limestone gravel, 1 siliceous sandstone, and 1 lightweight aggregate). The mix design was a TxDOT class P pavement mixture with Type I cement, no supplementary cementitious materials, no admixtures, aggregate resieved to a TxDOT grade 5, and a control fine aggregate sieved to a TxDOT grade 1. CoTE values were back-calculated using a formula proposed by Emanuel and Hulsey. TxDOT used Tx-428-A as their testing standard (modified version of AASHTO TP 60) and compared results to a Federal Highway Administration (FHWA) Long Term Pavement Performance (LTPP) program, which used AASHTO TP 60-00 on concrete cores from Texas highways. TxDOT researchers determined that concrete made with siliceous river gravel as coarse aggregate had, on average, 30% higher CoTE than did concrete made with limestone coarse aggregate. However, some overlap was observed as not all siliceous gravel had higher CoTE than limestone (Du & Lukefahr, 2007). Figure 2.8 displays the results of this testing.
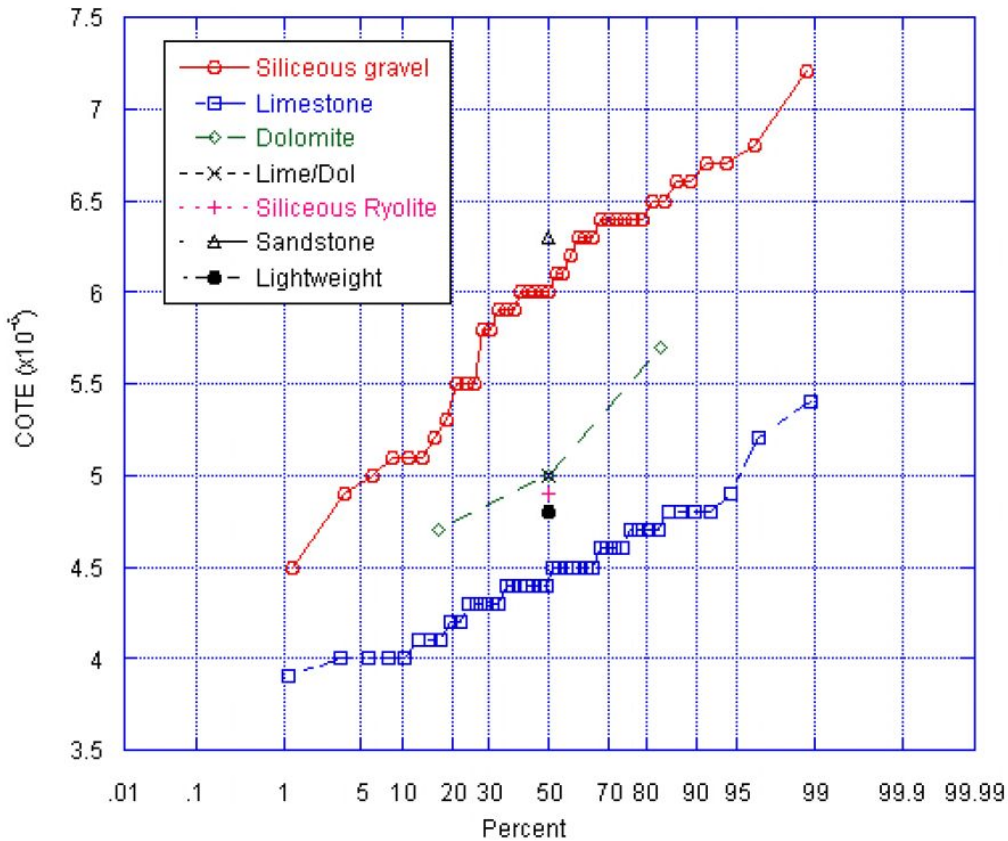
Figure 2.8: Probability Plot of CoTE Sorted by Aggregate Type (Du & Lukefahr, 2007)

As part of the same study, researchers found no significant correlation between CoTE and specific gravity, or between CoTE and dynamic modulus (3, 7, 14, 28 days), or between CoTE and compressive strength (3, 7, 14, 28 days). Comparisons between TxDOT CoTE values and FHWA CoTE values showed some discrepancies. However, it is important to note that TxDOT tested 94 specimens at known ages using a controlled mix design, whereas FHWA tested 182 specimens that were cores of unknown age and unknown mix proportions. For the limestone concrete specimens and siliceous river gravel specimens, TxDOT results showed smaller CoTE values and less variation than did the FHWA tests results. Although both TxDOT and FHWA samples were saturated during CoTE testing so that age should not play a significant role (demonstrated by previous research conducted by Emanuel and Hulsey [1977]), it is possible that different aggregate sources and varying paste volumes were the primary causes between the discrepancies in TxDOT and FHWA data. The ultimate conclusion of this research study was that back-calculating a CoTE value for coarse aggregates may be helpful for state agencies to identify aggregates prone to early-age cracking (Du & Lukefahr, 2007).

Mukhopadhyay and Zollinger (2009) believe they have developed a test method to measure CoTE of aggregate using dilatometry. The dilatometry method is advantageous because it can measure CoTE of aggregates as-received and thus is significantly quicker (can be finished within 24 hours) than other methods and it may even be possible to use this as a quality control monitoring tool to monitor aggregate source variability (similar to Jayawickrama's proposal for use of the Micro-Deval as a project level quality control too). The new dilatometer test method developed by these researchers uses a stainless steel container, a brass lid, a glass float (to which

an LVDT calibrated to 1/100 mm or 0.0004 in. is attached), a thermocouple, and a data acquisition system. Change in temperature of a water bath from 10°C (50°F) to 50°C (122°F) causes a change in water level due to thermal expansion of the tested material, water, and dilatometer container. Simple physics equations can be used to back-calculate the CoTE of the material tested, in this case aggregate.

Researchers validated results of this dilatometry testing by measuring CoTE for known materials such as steel alloys and comparing results to CoTE obtained from strain gauge based measurements and to literature. Researchers also compared tested aggregate CoTE values to literature for validation (two gravels, two limestones, two sandstones, and a granite). Researchers recommend that for homogenous aggregates, the average CoTE value from four heating and cooling cycles be taken to yield an acceptably low COV (≤10%). For heterogeneous aggregates such as river gravel, researchers recommend running at least two runs (each with four heating and cooling cycles) with different samples to achieve the same low level of variance (Mukhopadhyay & Zollinger, 2009).

2.3.7 Mineralogical and Chemical Composition

Knowing the mineralogical and chemical composition of an aggregate can help engineers and scientists identify potential problems in concrete aggregates, such as alkali-aggregate reaction, presence of detrimental clays and mica, shrinkage and thermal issues, and overly weathered material (Folliard & Smith, 2002). Keeping track of aggregate mineralogical composition can also help DOTs track and identify trends with good-performing and poor-performing aggregates. The two most common methods of identifying mineralogical and chemical composition are petrographic analysis and X-ray diffraction.

2.3.7.1 Petrographic Examination

Petrographic examination is typically performed by a trained and experienced petrographer, knowledgeable of local geology, following ASTM C 295 (*A Guide for Petrographic Examination of Aggregates for Concrete*). As part of the petrographic examination, petrographers identify key constituents and proportions of an aggregate sample using a variety of tools including microscopes, cameras, polishing/grinding wheels, and a variety of hand tools. Table 2.5, taken from the NCHRP 4-20C final report, displays the potential benefits of performing petrographic analysis on concrete aggregates. In addition to the benefits listed in Table 2.5, researchers from Ontario also determined that petrographic examination would be useful in identifying weak and weathered material (Rogers & Senior, 1991).

Table 2.5: Potential Benefits of Petrographic Analysis (Folliard & Smith, 2002)

Some Potential Benefits of Petrographic Analysis—from Folliard & Smith (2002)
Identification of minerals with potential for **ASR** or **ACR**
Estimation of **mica** content (from point count) in given size fraction of fine aggregate, especially relevant when analyzing material retained on the #200 Sieve (Rogers, 2002). Excessive mica contents (> 10% in specific size fraction) may lead to workability problems in fresh concrete, including increased water demand, segregation, and bleeding. Other materials that may adversely affect workability, such as muscovite, can also be identified.
Assessment of minerals and structure of **carbonate aggregates**, which may provide index of durability and soundness. A petrographic technique has been proposed to generate a petrographic number (PN), which has been reportedly linked to the **durability** of carbonate aggregates (Oyen et al., 1998)
Assessment of **thermal** and **shrinkage** potential, based on identifying the type and amount of minerals present in a given aggregate (Meininger, 1998)
Assessment of aggregates **surface texture** and **mineralogy**, which can be related to **bonding** with mortar
Development of petrographic database for aggregate sources by state DOTs to allow for correlation with aggregate type, source, and mineralogy to PCC pavement performance. This is essential in developing and maintaining field service records linking aggregate sources to PCC pavement performance (Meininger, 1998).

2.3.7.2 X-Ray Diffraction (XRD)

XRD is an advanced analysis technique that sometimes requires the material of interest to be ground to a fine powder (depending on the exact analysis method). A diffractometer, which fires an incident X-ray beam at the sample and receives the scattered beam, is used to gather data. Output from XRD appears as a plot of scattering intensity versus scattering angle. From this plot, peaks can be identified that correspond to individual material components of the sample.

XRD can be particularly useful for identifying deleterious clays as demonstrated by one study at the University of Wisconsin. Munoz et al. (2005) explored the impact of clay-coatings on concrete. Past research has shown that when an excess amount of clay is present in a concrete mixture (due to "dirty" coarse or fine aggregates), the water demand may be increased and the pozzolanic hydration products may be altered. These researchers were interested in exploring this topic further in this project. Aggregates were cleaned and the then recoated with three known clay types. Concrete was mixed and researchers performed XRD and scanning electron microscopic analysis to examine hydration products. Munoz et al. (2005) concluded that when aggregates that have clay-coatings are used in concrete mixtures, some of the clay will be dissolved by the water in the mixture but some of the clay will remain adhered to the coarse aggregate. The amount of clay that is dissolved in water or remains adhered to the aggregate depends on the type of clay. They also found that clays do have an impact on rate of hydration. Whether the rate of hydration is increased or decreased also depends on the type of clay: "The clay with macroscopic swelling (Na-montmorillonite) is the most difficult to detach and decreases the rate of hydration. Clays with crystalline swelling (Ca-montmorillonite) and no swelling (Kaolin) are easier to detach and increase the hydration reaction of cement pastes" (Munoz, Tejedor, Anderson, & Cramer, 2005). These researchers also used XRD analysis to examine the influence of microfines on concrete properties as discussed in the next section.

2.3.8 Presence of Microfines

Microfines are typically considered material finer than the No. 200 sieve (75-µm) and are usually classified as very fine particles of a parent rock, as opposed to clay. An excess of microfines can lead to decreased finishabiltiy of fresh concrete, air entrainment problems, and an increase in water demand, which can cause in increase in water-to-cement ratio, which can lead to reduced strength and increased drying shrinkage (Folliard & Smith, 2002). Microfines can either be found attached to the aggregate (due to handling, dust of fracture, etc.) or can be generated during mixing. Although excess microfines can be detrimental to concrete performance, calculated replacement of cement with microfines can be beneficial.

In the past few years, researchers at the University of Wisconsin explored the effects of microfines on fresh and hardened concrete properties. Munoz et al. identified 10 aggregates from the state of Wisconsin that were suspected to have microfine coatings. After XRD analysis, three aggregates were selected (as representative) to be studied more in depth. Ten concrete mixes were created: "original coated aggregate series," "washed aggregate series," and "artificial coated aggregate series." The P200 (ASTM C 117) test, California cleanness value, methylene blue value (MBV), and modified MBV (product of P200 and MBV) were compared and correlated to concrete tests. Researchers concluded that even when microfines are present in amount under 1.5%, they influence fresh and hardened concrete properties, the extent of influence depending on nature and amount of microfines. For carbonate microfines, a small difference (< 0.2%) in cleaned and as-received aggregate did not influence slump or shrinkage, but did slightly improve tensile strength of the concrete. Coatings classified as "clay/carbonate" did not influence shrinkage or freeze-thaw durability, but did decrease slump and increase tensile strength. Coatings classified as "dust" or "clay/dust" both decreased slump and increased shrinkage, but did not influence concrete strength or freeze-thaw durability. Due to its absorptive nature, "clay" coatings had the most dramatic influence on concrete properties. These coatings decreased slump and increased shrinkage dramatically. The addition of water to maintain workability also caused a decrease in tensile strength and freeze-thaw durability. Perhaps the most important conclusion from this study is that quantifying the amount microfines alone (as currently quantified through ASTM C 117) is not a good enough measure for deleterious material. This study showed that the type of microfines is just as important as the quantity. Researchers also determined that because it identifies quantity of clay, the modified MBV had the best correlation (out of the other microfine tests) with compressive strength and durability tests (Munoz, Gullerud, Cramer, Tejedor, & Anderson, 2010).

Rached et al. (2009) also examined the effects of microfines (specifically from limestone and granite sources) on concrete properties, with the objective of reducing cement content through replacement with microfines. Mortar mixes of three fine aggregates demonstrated that workability depends on paste volume, paste composition, and type of aggregate used. Shape and gradation of the fine aggregates affected workability of the mortar mixes. As expected, aggregates with higher angularity resulted in "increased paste volume and [high-range water reducing admixture (HRWRA)] demand. Aggregates with coarser grading generally required lower HRWRA demand but required higher paste volume to ensure adequate cohesiveness." (Rached, De Moya, & Fowler, 2009) Overall, Rached, De Moya, and Fowler determined that replacement of cement with microfines (up to 30%) was able to improve compressive strength, shrinkage, permeability, and abrasion resistance (Rached, De Moya, & Fowler, 2009).

2.4 Fine Aggregate Tests

2.4.1 Abrasion Resistance

Abrasion resistance of aggregates is an important property of aggregates, particularly for fine aggregates. Fine aggregates are more susceptible to mechanical breakdown during handling and mixing, which can lead to production of excess fines. Fine aggregates also provide surface texture for concrete, which is critical for applications where friction is necessary, such as area subject to direct traffic. Fine aggregates must be resistant to abrasion to provide the necessary friction.

2.4.1.1 Micro-Deval Test for Fine Aggregates

The Micro-Deval test for fine aggregates is very similar to the Micro-Deval test for coarse aggregates. A standard gradation of sand, ranging from No. 8 (2.36-mm) to No. 200 (75-μm), is placed in the Micro-Deval container along with steel charge and soaked for one hour prior to testing. The Micro-Deval container is then rotated for 15 minutes at approximately 100 revolutions per minute. The sample material is then removed and washed over a No. 200 (75-μm) sieve. The remaining material is oven-dried and weighed and the relative amount of material lost, as a percentage, signifies the final Micro-Deval loss.

The Ministry of Transportation in Ontario (MTO) has studied Micro-Deval abrasion of fine aggregates in addition to Micro-Deval abrasion of coarse aggregates. In 1991, researchers in Ontario collected 86 natural sands and 21 quarry screenings from Ontario, all of which had satisfactory performance in PCC and/or asphaltic concrete. These researchers examined several tests for evaluating the quality of fine aggregate in concrete and asphalt. These tests included the Micro-Deval test, the ASTM attrition test, and the MTO attrition test, and the magnesium sulfate soundness test for fine aggregates. They found that the sulfate soundness test for fine aggregates suffers from poor multi-laboratory precision (COV of about 10.5%). The Micro-Deval was identified as a suitable replacement for the magnesium sulfate soundness test because it has good correlation with this test ($R^2 = 0.88$), is quicker (2 days vs. 10 days), and has a much better multi-laboratory precision (COV of 1.9%). Both ASTM attrition and MTO attrition tests had fairly high variance (COV of 11.0% of 14.1% respectively). The Micro-Deval loss also correlated well with absorption ($R^2 = 0.81$), which is logical considering more absorptive materials are typically more porous, and thus more susceptible to breakdown during wet abrasion (Rogers, Bailey, & Price, 1991).

In the years following, the Ontario researchers also determined that the Micro-Deval test for fine aggregates was useful in identifying weak and soft material such as shale. They also found a high correlation with Micro-Deval loss of fine aggregates and drying shrinkage of paste. A Micro-Deval loss of approximately 25% was the limit for negligible shrinkage. Sands with Micro-Deval loss higher than 25% loss showed much greater mortar shrinkage. Ontario specifications (as of 1998) dictate a maximum Micro-Deval loss of 20% for fine aggregate used in PCC (Rogers C., 1998).

Researchers from the Virginia Transportation Research Council also explored the use of the Micro-Deval test for assessing fine aggregate durability. Ten fine aggregates were evaluated by Micro-Deval, petrographic examination, magnesium sulfate soundness test for fine aggregates, and freeze-thaw soundness. District materials engineers subjectively rated each source as "good," "borderline," or "poor." However, ratings were not always based on

performance but sometimes related to compliance with specifications. The Micro-Deval loss was measured by three methods: 1) traditional method of loss of No. 200 (75-μm) sieve, 2) weighted average based on test gradation, and 3) change in area under gradation curves before and after the test. Researchers concluded that the weighted average Micro-Deval loss differentiated between good and poor-performing aggregates 80% of the time (8 of 10 sources). The area between the curves loss calculation was also able to have the same success rate. As a result, modifying the loss calculation for Micro-Deval improved its ability to identify poor performers. A rated loss of less than 20% should provide good performance. For aggregates with less than 1.5% absorption, the MTO standard of 24 hours soaking can be reduced to one hour soaking without significantly affecting Micro-Deval loss results (note that the current ASTM D 7428 specification dictates one hour soaking time). This project also reached that same conclusion as Rogers et al. (1991): that the Micro-Deval test also had lower variability than the other soundness tests, and is thus more repeatable and reproducible. In this study, Micro-Deval COV was 2.3%, compared to 16.9% for magnesium sulfate soundness, and 28.7% for freeze-thaw soundness. Finally, researchers also concluded that the Micro-Deval test can be used as a quality control check to determine if material from a source has changed significantly (Hossain, Lane, & Schmidt, 2008).

One research project by Rached (2011) at The University of Texas examined the Micro-Deval test, among others, as an evaluative tool measuring potential friction loss. The scope of this project was to examine the use of manufactured sands in pavement concrete, since manufactured sands are becoming more necessary and are known to affect skid resistance, workability, and finishability. Rached examined the Micro-Deval test, acid insoluble residue (AIR) test, absorption, and the DFT60 test (coefficient of friction at 60 km/hr), among others, and determined that the Micro-Deval loss correlates well (R^2 = 0.87) with the DFT60 test in a polynomial relationship. AIR had a weaker correlation (R^2 = 0.44) with DFT60. Absorption had a reasonably high correlation (R^2 = 0.62) with DFT60, but the author would not recommend the ASTM C 128 absorption test due to its subjectivity and lack of repeatability. As a result, Rached concluded that the Micro-Deval test is more suitable than the AIR test for evaluating polish resistance of fine aggregates due to its higher correlation with DFT60 and the fact that it is a mechanical test and polishing is a mechanical behavior. As a final recommendation, Rached commented that the AIR and Micro-Deval tests can be used in combination to indicate the presence of carbonates and determine the hardness of fine aggregates. The author also proposed blending guidelines for manufactured sands based on AIR and Micro-Deval results (Rached M. M., 2011).

2.4.2 Absorption

As with coarse aggregates, absorption is an important property of fine aggregates. Aggregates with higher absorption capacity are typically more porous, and therefore weaker and more susceptible to breakdown and abrasion.

2.4.2.1 Specific Gravity and Absorption of Fine Aggregates

A variety of methods for measuring bulk density and absorption were developed by researchers in the 1920s and 1930s but the ASTM standard for measuring these properties (ASTM C 128) has remain relatively unchanged since 1948. The ASTM standard has been widely accepted but a few agencies and DOTs use slightly altered versions of this test (the test procedure is described further in Section 5.2.2). The Ontario MTO, Kentucky DOT, Kansas

DOT, and Mississippi DOT have historically washed sands over a No. 100 (150-µm) sieve prior to testing them for the saturated surface dry condition due to perceived inaccuracies in density calculations (Rogers & Dziedziejko, 2007).

Noting this discrepancy in test methods, researchers from Ontario conducted an investigation to determine the influence of microfines (<75 µm) on calculated absorption and density values of fine aggregates. The results of this investigation showed that stirring of the fine aggregate during testing can create artificial particles made up of conglomerated microfines. Because of this effect, sands with high microfines content (> 8% by mass) had higher absorption, lower density values, and higher variance compared to sands with microfines removed prior to testing. The presence of microfines in excess of 8% by mass caused relative density values to be off by as much as 0.13 and variance to be two times higher than a washed sand. When the microfines content is less than 4%, the error is negligible. Figure 2.9 demonstrates the severity of this problem. Researchers recommended that sands with high microfine content should be washed prior to ASTM C 128 testing to ensure more accurate specific gravity and absorption measurements (Rogers & Dziedziejko, 2007).
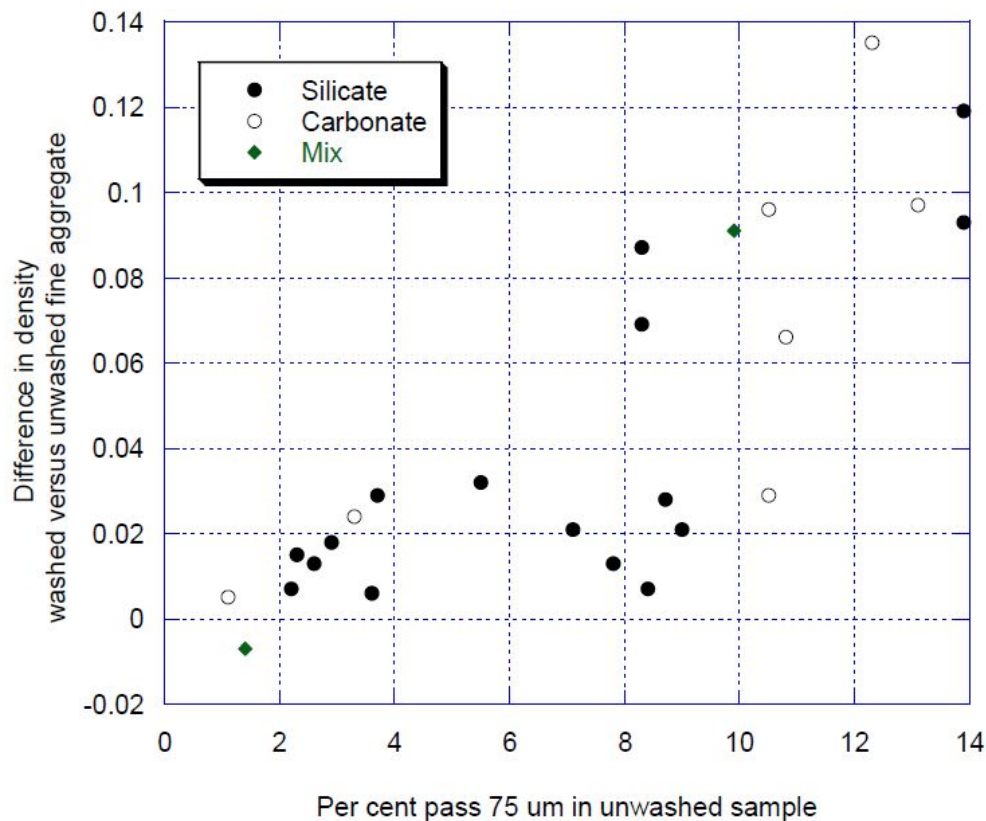
Figure 2.9: Difference in Density between Washed and Unwashed Samples of Fine Aggregate (Rogers & Dziedziejko, 2007)

2.4.3 Shape Characteristics

The shape characteristics of a fine aggregate are important particularly to fresh concrete properties such as workability and finishability. For example, manufactured sands tend to be more angular and therefore require a higher water demand to achieve the same slump as a natural

sand. Two promising tests have evolved over the last few years that either directly, in the case of AIMS, or indirectly, in the case of the flakiness sieve, quantify shape characteristics of fine aggregates.

2.4.3.1 AIMS 2.0

AIMS is also capable of determining shape characteristics of fine aggregates. AIMS is a machine consisting of a camera, lights, computer software, and movable trays, designed to capture and analyze the shape, angularity, and texture of coarse aggregates and the form and angularity of fine aggregates. The camera captures images of the aggregate particles, either lit directly or backlit, and the software analyzes these images and provides the user with data summarizing the shape characteristics. For fine aggregates, the user places a set of fine aggregate particles (separated by fraction size) on an opaque tray and places this tray into the machine. The camera in the AIMS apparatus is capable of capturing particles as small as 75-µm (retained on the No. 200 sieve). Output from the AIMS consists of quantified measurements of form and angularity for each particle, and a mean and standard deviation of each value as well. Aggregates typically follow a standard statistical distribution. Recent advances in this technology include a touching particle factor to eliminate inaccurate angularity analysis of fine aggregates where particles touch or overlap (Mahmoud, Gates, Masad, Erdoğan, & Garboczi, 2010).

2.4.3.2 Flakiness Sieve

After observing problems in field compact of HMA, Rogers and Gorman (2008) sought to develop an inexpensive and quick test to determine a measurement of flakey particles in a sand. Past research has demonstrated that sands in excess of 30% flakey particles may have issues during compaction of hot mix asphalt. Rogers and Gorman (2008) briefly considered a flat and elongated test using a hand-held set of proportional calipers, but variations in accuracy of calipers and poor multi-laboratory variation caused researchers to abandon this test. ASTM C 1252 (*Standard Test Methods for Uncompacted Void Content of Fine Aggregate*) was also considered but no realistic limit could be found to reject poorly compacting fine aggregate. Rogers and Gorman realized that slotted sieves, traditionally used for seeds and grains, could also be used to evaluate fine aggregate (Rogers & Gorman, 2008).

With this knowledge, Rogers and Gorman collected and tested 120 fine aggregates using Micro-Deval, specific gravity and absorption, uncompacted voids, the compacted aggregate resistance test developed by D. Jahn (2004), and the slotted sieve identified by this project. The flakiness sieve test, described by Rogers and Gorman (1998) in an appendix, uses two slotted sieves with slots of 1.8-mm and 1.0-mm respectively. The fine aggregate is sieved and broken down into separate size fractions. The sand retained on the No. 8 (2.36-mm) sieve is placed on the 1.8-mm slotted sieve and agitated. The same is done for the sand retained on the No. 16 (1.18-mm) sieve, except the 1.0-mm slotted sieve is used. The operator uses a set of tweezers to ensure that all flakey particles pass through the slots. All particles passing through the slotted sieves are considered flakey, and the final results are calculated by mass. The sieve is pictured in Figure 2.10 with sand particles retained.
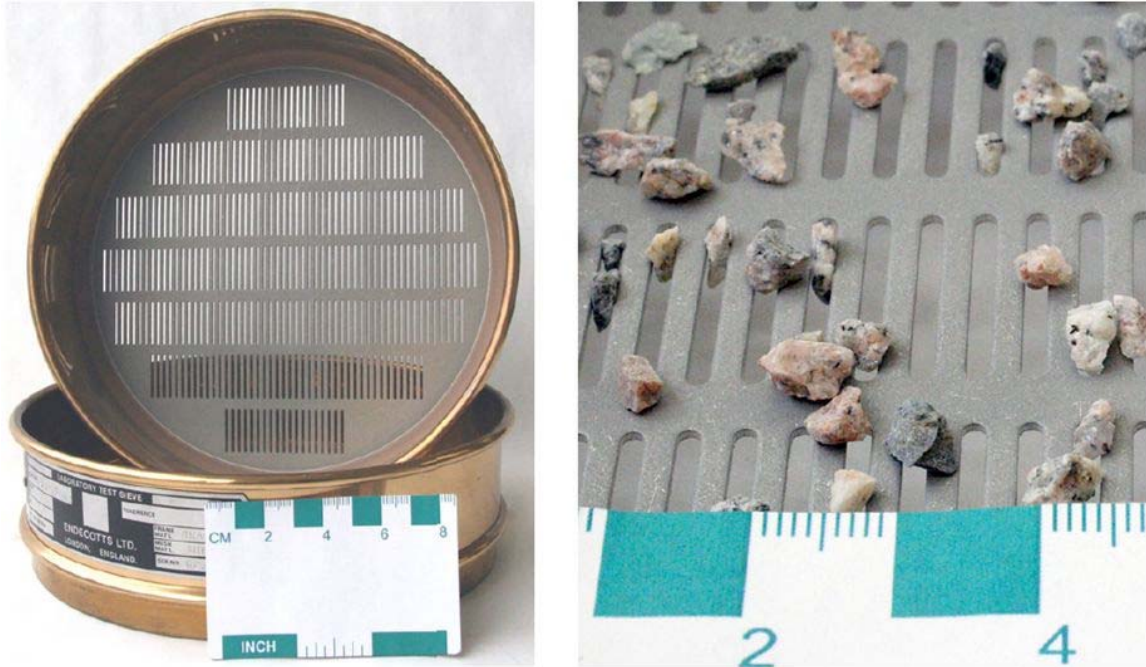
Figure 2.10: Slotted Sieve for Finding Flakey Particles in Fine Aggregate

After testing 120 fine aggregates, Rogers and Gorman concluded that natural sands tended to be less flakey than crusher screenings. No natural sands were found to have flakiness in excess of 25%. High flakiness on one sieve size tended to indicate high flakiness on the other sieve size, although regression coefficients were not strong. There was no obvious relationship between Micro-Deval loss and mean flakiness. Based on the two case studies in Ontario, contractors were unable to compact two sources that, when tested by the flakiness sieves, had flakiness in excess of 25% for No. 8 (2.36mm) and 30% for No. 16 (1.18mm). Rogers and Gorman recommend using the flakiness sieves as a means of detecting fine aggregate that is potentially difficult to compact (Rogers & Gorman, 2008). It is very possible that this test can also be applied towards workability and finishability of fresh PCC.

2.4.4 Mineralogical and Chemical Composition

Knowing the mineralogical and chemical composition of an aggregate can help engineers and scientists identify potential problems in concrete aggregates such as alkali-aggregate reaction, presence of detrimental clays and mica, shrinkage and thermal issues, and overly weathered material (Folliard & Smith, 2002). Keeping track of aggregate mineralogical composition can also help DOTs track and identify trends with good-performing and poor-performing aggregates. Some of the most common methods of identifying mineralogical and chemical composition of fine aggregate are petrographic analysis, XRD, and AIR.

2.4.4.1 Acid Insoluble Residue (AIR)

The AIR test is one way of determining carbonate content of fine aggregate. In this test, a fine aggregate sample is subjected to hydrochloric acid and carbonate aggregates are dissolved by the aggregate while siliceous aggregates remain. Carbonate aggregates polish more easily than siliceous aggregates which reduce skid resistance of friction-critical concrete applications.

Texas is one state that specifies use of this test (limit of 60% insoluble) due to the increased interest in using manufactured sands in concrete pavement applications. However, at least one research study by Rached has shown that the AIR test may not correlate well with the property that it is trying to measure.

The scope of Rached's project was examining the use of manufactured sands in pavement concrete, since manufactured sands are becoming more necessary and are known to affect skid resistance, workability, and finishability. Rached examined the Micro-Deval test, AIR test, absorption, and the DFT60 test (coefficient of friction at 60 km/hr), among others, and determined that the AIR test had a weaker correlation (R^2 = 0.44) with DFT60 than did the Micro-Deval test (R^2 = 0.87). As a result, Rached concluded that the Micro-Deval test is more suitable than the AIR test for evaluating polish resistance of fine aggregates due to its higher correlation with DFT60 and the fact that it is a mechanical test and polishing is a mechanical behavior. As a final recommendation, Rached commented that the AIR and Micro-Deval test can be used in combination to indicate the presence of carbonates and determine the hardness of fine aggregates. The author also proposed blending guidelines for manufactured sands based on AIR and Micro-Deval results (Rached M. M., 2011).

2.4.5 Deleterious Substances

Anecdotal evidence has long suggested that concrete mixtures containing clay content (from coarse or fine aggregate) will have a detrimental effect on the fresh and hardened properties of the concrete and reduce rheology. Norvell et al. (2007) explored this issue further by "doping" sand with clay minerals and (non-clay) microfines and examining the effects on concrete. Microfines replaced sand by 1–4% and mortar mixes were created to determine the impacts of water demand, compressive strength, and shrinkage. Norvell et al. (2007) found that all clays increased water demand and HRWRA demand to achieve a constant flow. Montmorillonite had the highest absorption of all clays studied. Figure 2.11, taken from a separate study by W.R. Grace & Co., displays the implications of this trend.
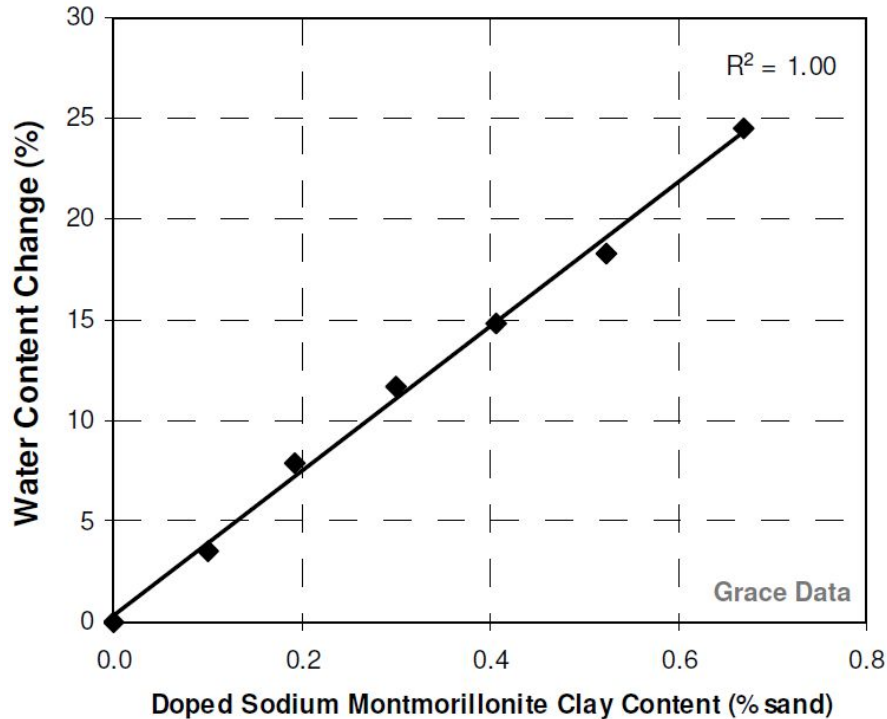
Figure 2.11: Effect of Sodium Montmorillonite on Concrete Water Demand for a 3 in. Slump (Koehler, Jeknavorian, Chun, & Zhou, 2009)

Surprisingly the microfines decreased the HRWRA demand and only increased the water demand slightly to achieve constant flow at a constant water-to-cement ratio. Interestingly, Norvell et al. (2007) also determined that the only reason clays caused lower compressive strengths of mortar was due to the necessary increase of water to achieve the same level of workability. When the water-to-cement content was held constant (and flow ignored), the impact of clay on compressive strength was negligible, except in the case of montmorillonite. Regarding drying shrinkage, microfines showed no effect, nor did kaolinite and illite clays. However, montomrillonite did have an adverse effect on drying shrinkage of the mortar mixes (Norvell, Stewart, Juenger, & Fowler, 2007).

Improved aggregate performance can be realized when polycarboxylate-based HRWRAs are dosed appropriately according to the clay content. However, this relies on accurate knowledge of the sand's clay content. Current methods to measure clay in aggregates include MBV, sand equivalent value and durability index, plasticity index, XRD, and thermo-gravimetric analysis.

2.4.5.1 Methylene Blue Test

Methylene blue is a dye that has a strong affinity for clay particles. As such, this test (note that there are several versions, the most common in the U.S. being AASHTO TP 57) subjects a fine aggregate sample to diluted methylene blue and the color of the mixed, filtered solution will depend on the clay content. Higher MBVs suggest higher clay content, which can indicate problematic aggregates.

In the past few years, researchers at the University of Wisconsin explored the effects of microfines on fresh and hardened concrete properties. Munoz et al. identified 10 aggregates from

the state of Wisconsin that were suspected to have microfine coatings. After XRD analysis, three aggregates were selected (as representative) to be studied more in depth. Ten concrete mixes were created: "original coated aggregate series," "washed aggregate series," and "artificial coated aggregate series." The P200 (ASTM C 117) test, California cleanness value, MBV, and modified MBV (product of P200 and MBV) were compared and correlated to concrete tests. Researchers concluded that even when microfines are present in amount under 1.5%, they influence fresh and hardened concrete properties, the extent of influence depending on nature and amount of microfines. For carbonate microfines, a small difference (< 0.2%) in cleaned and as-received aggregate did not influence slump or shrinkage, but did slightly improve tensile strength of the concrete. Coatings classified as "clay/carbonate" did not influence shrinkage or freeze-thaw durability, but did decrease slump and increase tensile strength. Coatings classified as "dust" or "clay/dust" both decreased slump and increased shrinkage, but did not influence concrete strength or freeze-thaw durability. Due to its absorptive nature, "clay" coatings had the most dramatic influence on concrete properties. These coatings decreased slump and increased shrinkage dramatically. The addition of water to maintain workability also caused a decrease in tensile strength and freeze-thaw durability. Perhaps the most important conclusion from this study is that quantifying the amount microfines alone (as currently quantified through ASTM C 117) is not a good enough measure for deleterious material. This study showed that the type of microfines is just as important as the quantity. Munoz et al. (2010) also determined that because it identifies quantity of clay, the modified MBV had the best correlation (out of the other microfine tests) with compressive strength and durability tests (Munoz, Gullerud, Cramer, Tejedor, & Anderson, 2010).

Because there is an inherent level of subjectivity to the methylene blue test, researchers at W.R. Grace & Co. sought to improve this test method by removing subjectivity and enhancing repeatability and reproducibility. The test developed by Grace is similar to the traditional AASHTO test, but the test is performed on an entire sample of sand (not just the microfines) and uses a UV colorimeter to analyze color of the final filtered solution sample. The new methylene blue test allows the entire sample to be measured, which is important because all clay in the sand in measured which ensures more representative results. The reproducibility and repeatability were comparable to the traditional AASHTO method. Researchers at Grace demonstrated that inadequate sieving can cause the traditional methylene blue test to produce inaccurate results, as shown in Figure 2.12 (Koehler, Jeknavorian, Chun, & Zhou, 2009).
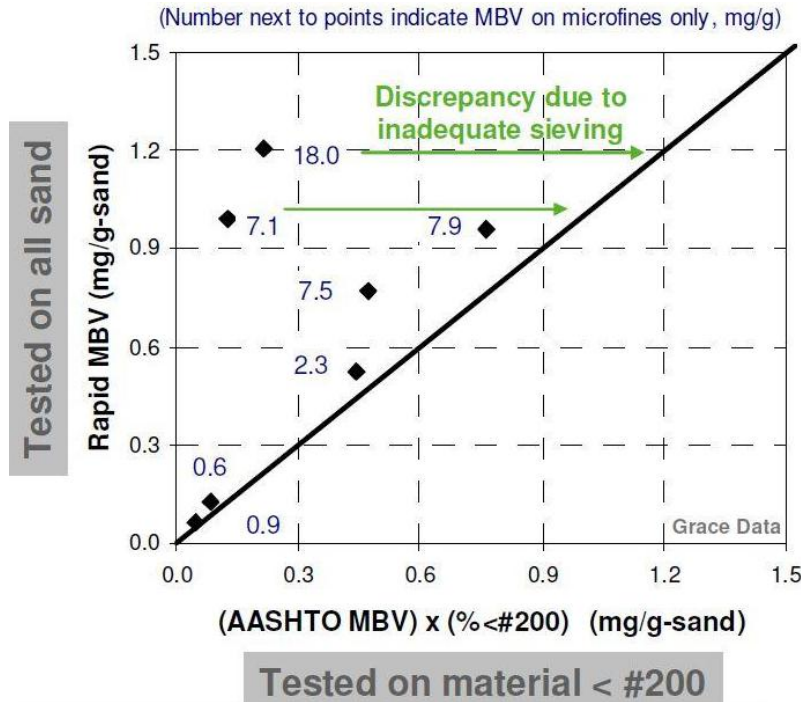
Figure 2.12: Methylene Blue Testing of Full Sand versus Microfines (Koehler, Jeknavorian, Chun, & Zhou, 2009)

2.4.5.2 Organic Impurities

Investigations by early concrete researchers at the Lewis Institute showed that even small amount of tannic acid or surface loam (from decomposing organic materials) can significantly reduce concrete strength due to interference with the hydration process (Lewis Institute, 1921). As a result, most state DOTs specify use of the AASHTO test for organic impurities. In this test, a fine aggregate sample is subjected to a sodium hydroxide solution and allowed to remain undisturbed to react for 24 hours. Any organic material in the sample will react with the sodium hydroxide solution to produce a dark liquid. The operator examines the color of the supernatant liquid and if it is darker than a standardized color, the fine aggregate is subjected to a 7-day mortar cube strength test. The fine aggregate is typically deemed to have an unacceptable amount of organic content if the compressive strength of the mortar cube is less than 90–95% of a control sample.

2.4.5.3 Sand Equivalent Test

The sand equivalent test is a test method that is used to determine the proportion of "detrimental fine dust of clay-like particles in soils or fine aggregates" (Texas Department of Transportation, 2009). This test subjects a fine aggregate sample to a flocculating solution (calcium chloride) in order to separate fine particles from the coarser sand. The higher the sand equivalent value, the cleaner the sand is perceived to be. From the survey of other DOT specifications (discussed further in Section 3.2), the research team determined that only 11 state DOTs specify this test for aggregate quality control. Of these 11 states, Texas has the highest (most restrictive) limit at 80.

44

Alhozaimy (1998) examined 100 natural sands and 100 crushed manufactured sands in Saudi Arabia to compare the sand equivalent test (ASTM D 2419) with another test that measures fine particles in a sand: the ASTM C 117 test (*Materials Finer than No. 200 Sieve by Washing*). This study determined that, for the natural sand, the sand equivalent test was strongly correlated to the materials finer than No. 200 test. However, no correlation existed between the two tests for crushed manufactured sands, leading the author to call the sand equivalent test "misleading" for these types of fine aggregates. Furthermore, investigations between the two tests and water demand of mortar, showed a correlation between sand equivalent and water demand for only the natural sands (Alhozaimy, 1998). Although this was only one research study, it strongly suggests that the sand equivalent test for manufactured sands may not sufficiently serve its purpose.

Chapter 3. Development of Testing Program

3.1 Survey of TxDOT

The research team surveyed TxDOT District Members and Construction Division personnel to obtain more information about aggregates used in Texas, as well as concrete conditions and recurring problems.

3.1.1 Development of District Surveys

The research team developed a standardized survey for TxDOT district personnel to glean information from the tremendous amount of knowledge and experience of area engineers and laboratory personnel. The focus of the district surveys was to identify fine and coarse aggregate types that have been used in concrete over the years, particularly those that performed poorly so that they could be obtained for testing in order to determine limits for test procedures. The survey also focused on identifying specific field problems related to aggregates.

It was important that the survey be standardized and performed by only one or two researchers to ensure consistency and to eliminate bias. The standardized survey included a statement of purpose to brief the interviewee on the goals and methods of the project and continued with specific questions regarding aggregate performance in that district. Topics of questions included aggregate performance, aggregate testing procedures, and aggregate sources that are commonly used in the district as well as sources that are no longer used.

Prior to implementation, the standardized survey was sent to the project committee members for feedback and approval. After including feedback in the final revision of the surveys, the surveys were sent via email to district engineers and lab personnel to allow district personnel time to evaluate the questions and provide the most appropriate responses. Researchers followed up the emails with phone interviews.

3.1.2 Results of District Surveys

Researchers were able to communicate with TxDOT personnel in all 25 districts across the state and get information from 22 of those districts. The interviewees range from lab supervisors to materials engineers to traffic engineers. In most cases, the interviewee was the district lab supervisor as these personnel seemed to have the most information about aggregate sources and testing in their district. In some cases, district personnel polled area engineers to obtain other relevant information. Observations and knowledge of area engineers are an important piece of the district surveys, particularly for the larger districts.

One of the questions addressed by the surveys involved district laboratory testing procedures and equipment. Not surprisingly, all districts perform quality monitoring tests on aggregates when necessary. However, most district labs do not have equipment for LA abrasion, magnesium sulfate soundness, or acid insoluble residue (AIR) testing so aggregates are typically sent to the TxDOT Construction Materials and Testing Laboratory in Cedar Park, Texas for these tests. A few districts (Waco and Odessa) did possess equipment for LA abrasion and/or magnesium sulfate soundness but typically sent aggregates to the TxDOT materials lab anyway. Despite the fact that there is no Micro-Deval requirement for Item 421, all districts reported possessing the equipment to run this test. Results varied by district as to how frequently the Micro-Deval test is performed. Many districts run and record Micro-Deval loss values for

bituminous aggregates on a regular basis (as recommended by Jayawickrama [2007]) but do not perform the Micro-Deval test for concrete aggregates as frequently.

When asked about their opinions regarding the usefulness of the current Item 421 test methods, interviewee responses varied. Some interviewees felt that they did not possess the expertise to comment on these tests, while others freely gave their opinion. One popular response was that the current sand equivalent limit of 80 may be slightly higher than necessary. Several district personnel felt that this limit may be precluding the use of sands that could still make strong, durable concrete. Interestingly, one district raised the limit on the sand equivalent test to 90 after reporting problems with a sand possessing sand equivalent values in the 80s. One laboratory supervisor felt that the decantation limit may be too high in addition to the sand equivalent limit being too high. Another laboratory supervisor felt that the fineness modulus limit may cause some aggregates to be rejected that would perform well otherwise. Other personnel felt that the Micro-Deval test, sieve analysis, and the sand equivalent test are useful, and the organic contents test and decantation test are relevant. The research team also contacted aggregate producers for collection of aggregates (see Chapter 4) and several producers have suggested if gradation limits were slight adjusted, more aggregates could be used locally to make good-performing concrete. However, gradation requirements of concrete aggregates are not in the scope of this project.

Most districts have no trouble with aggregates meeting specification limits so they do not allow deviations to these limits, or they do allow deviations but only on an as-needed basis. Some districts do allow deviations due to recurring issues in their district (i.e., sand equivalent limit of 90 as previously discussed). The Beaumont district relies on aggregates being shipped in due to poor local geology and as a result, the decantation limit for these aggregates is raised. The Laredo district has trouble with coarse and fine aggregates not meeting gradation so they have altered the fine aggregate gradation to allow the No. 8 (2.36-mm) sieve to pass with 75–100%. Although the Fort Worth district does not allow deviations to specification limits, they noticed severe problems with aggregate quality in the fall of 2010 when 9 of 15 producers failed quality monitoring (QM) tests for gradation and/or decantation in September and 5 of 15 producers failed QM tests for gradation and/or decantation the following month. The cause of this widespread drop in quality was unknown.

As far as evaluation of the aggregate sources, it seems that sources in the Aggregate Quality Monitoring Program (AQMP) have been used very successfully in districts throughout the state (the AQMP is discussed further in Section 4.1.1). A survey of TxDOT district personnel revealed that most districts have access to at least a few aggregate sources within their district, with the exception of a few districts in eastern Texas. Most districts are able to use somewhat local resources, though some districts are forced to ship aggregates in from other districts or states. Survey results showed that districts use anywhere from one to more than a dozen aggregate sources on a regular basis for TxDOT projects. Many districts have also used local non-AQMP sources with success and there are several of these producers in the process of being approved and added to the current AQMP list. Survey results also showed that TxDOT projects used local aggregates where possible but local geology conditions, particularly in the eastern districts, prevented local sources from being utilized. In the Atlanta, Beaumont, Bryan, and Lufkin districts, coarse aggregates are shipped in from elsewhere (from other districts in Texas or Arkansas, Louisiana, Oklahoma, Canada, and Mexico). There are also non-AQMP sources in several districts that have been used successfully for non-TxDOT concrete applications but due

to specification limits (particularly magnesium sulfate soundness and sand equivalent) are not used in TxDOT projects.

It was somewhat difficult to discern the common concrete aggregate problems in Texas because not all interviewees were aware of specific problems in their district or did not know the nature or causes of distress. District surveys showed reports of alkali-silica reaction (ASR) in at least six districts (Beaumont, Bryan, Dallas, Houston, San Angelo, and Waco), although specific locations had already been investigated in all of these districts. Minor to moderate spalling and non-ASR cracking were also reported in at least five districts (Atlanta, Beaumont, Fort Worth, Paris, Tyler), although interviewees did not necessarily know the cause of distress due to the widespread nature of the problem, age of the concrete, or lack of information. Atlanta TxDOT personnel believe that the cause of most cracking in that district is due to siliceous aggregates with high CoTE values. The problem is prevalent in pavement applications (but not structural applications) due to the use of continuously reinforced concrete pavements (CRCP). There is currently no CoTE limit in the district and brining in aggregates with low CoTE values would be cost prohibitive. The Lufkin district also experienced a thermal expansion problem that was investigated within the last 2 years. The same expansion problem has been observed in Houston in CRCP pavements, so aggregates with high CoTE values (particularly siliceous river gravel) are now avoided when possible. This trend was documented by Won (2001) and Du & Lukefahr (2007). Another common response to the question of aggregate issues was the occasional problem of "dirty" or rounded aggregates causing low compressive strengths. Other concrete issues were typically attributed to age.

3.1.3 Survey of TxDOT Construction Pavement and Materials Division

The goal of the survey of the TxDOT Construction (CST) Division was to obtain the results of aggregate tests for frequently run sources, aggregate test methods, an aggregate data base, and performance data.

The results of the aggregate tests for frequently run sources were provided by CST for all aggregates meeting the AQMP requirements for concrete and bituminous applications. Results include values for rated source LA abrasion, magnesium sulfate soundness, Micro-Deval, coefficient of thermal expansion (where applicable), ASR (where applicable), and AIR.

Aggregate test methods, as described in Item 421, were also provided by TxDOT personnel. These test methods include LA abrasion (Tex-410-A), magnesium sulfate soundness (Tex-411-A), organic impurities (Tex-408-A), and sand equivalent (Tex-203-F). A more detailed description of these test methods can be found in Chapter 5.

A recommendation of aggregates to test for the project was made by TxDOT personnel to reflect a diversity of geographic locations (including river basins for gravel), mineralogies, and applications. Determining the final list of aggregates was an iterative process that involved several discussions on how to cost-efficiently transport and acquire those aggregates.

3.1.4 Summary

The most important results of the survey of TxDOT are the findings that districts do use local aggregate sources when possible, although this is very difficult to do in eastern Texas where local coarse aggregates are non-existent or poor quality. The most common problems reported that were known to be relate to aggregates were cracking due to ASR and thermal expansion. Neither of these issues is currently addressed directly with limits in Item 421. It is also important to note that in some cases, limits (particularly magnesium sulfate soundness and

sand equivalent) in Item 421 have caused local aggregates to be rejected even though they have been used successfully in other non-TxDOT concrete projects around the state.

3.2 Survey of Other States and Organizations

A review of testing and standards for aggregates in other states was conducted to understand the differences in the approach of how states qualify aggregate use in PCC. The most recent versions of DOT state construction specifications were reviewed for all 50 states to determine general trends in testing procedures and limits and to identify any significant deviations from how Texas approaches aggregate use.

3.2.1 Coarse Aggregate Specifications

The most common coarse aggregate qualification test is the LA abrasion test. Texas allows aggregates with up to 40% LA abrasion loss, which is close to the national average. Forty-nine states use the LA abrasion test to evaluate aggregates. The highest allowable limit is 60%, specified by both Georgia and Kentucky, while the lowest allowable limit is 30%, specified by Oregon, Illinois, Indiana, and Massachusetts. Maine is the only state to not specify use of the LA abrasion test. Kansas has different limits dependent on aggregate type and New Mexico uses an aggregate index value which combines LA abrasion, sulfate soundness, and absorption. Figure 3.1 displays LA abrasion limits for each state.
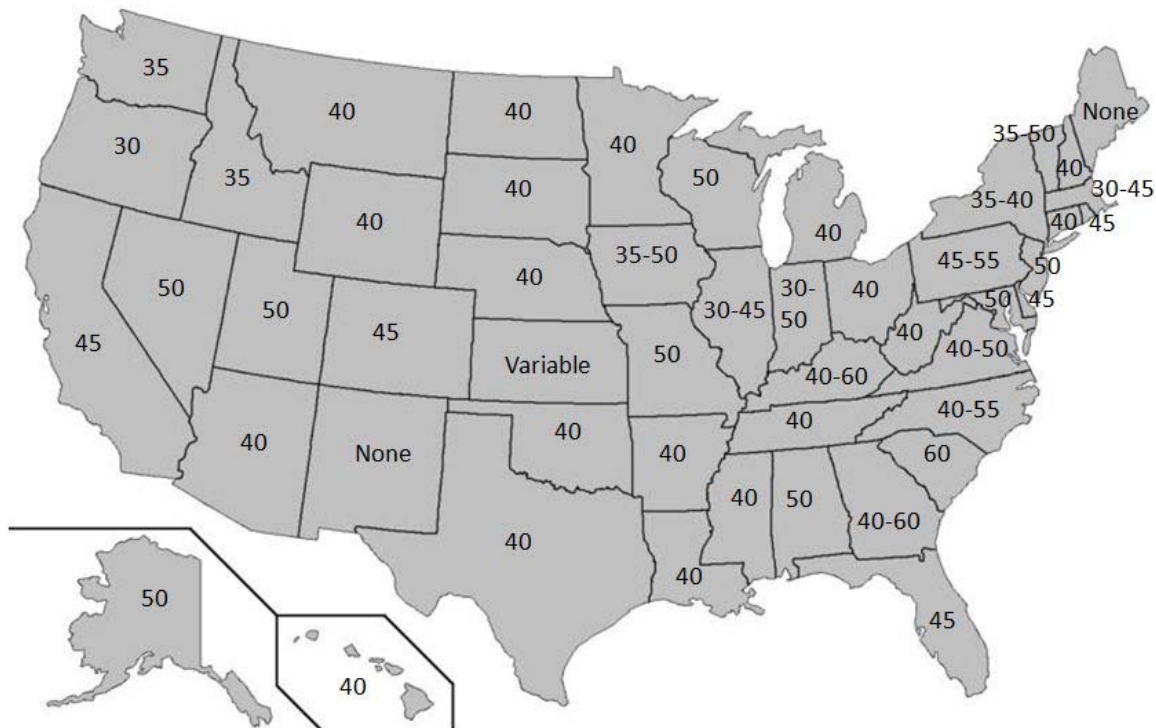
Figure 3.1: Limits for the LA Abrasion Test as Specified by State DOTs

The sulfate soundness test is also a very common test procedure used to evaluate aggregates. However, there appears to be no clear consensus with how to interpret and apply the results of this test. Twenty-eight states specify the use of sodium sulfate, nine states specify the

use of magnesium sulfate, two states allow the use of either magnesium sulfate or sodium sulfate, and eleven states do not use sulfate soundness testing. Ten states that do use the sulfate soundness test have an "opt out" clause for the test, allowing aggregate use with 5 years of field performance data and engineer approval. Arizona only requires this test for use above 4500-ft. elevation, while New York even specifies a 10-cycle sulfate soundness test, instead of the typical five-cycle version. The Texas limit of 18% for five-cycle magnesium sulfate soundness is somewhat high compared to other states, but is not the highest. Virginia has the highest limit and allows up to 30% for the five-cycle magnesium sulfate soundness test. Connecticut has the lowest limit for the five-cycle magnesium sulfate soundness test at 8%. The highest allowable limit for the five-cycle sodium sulfate soundness test was 25% (Illinois and Indiana), and the lowest allowable limit for the five-cycle sodium soundness test was 8% (Vermont). Figure 3.2 displays sulfate soundness limits for each state. Note that "Na" signifies the use of sodium sulfate soundness, while "Mg" signifies the use of magnesium sulfate soundness.
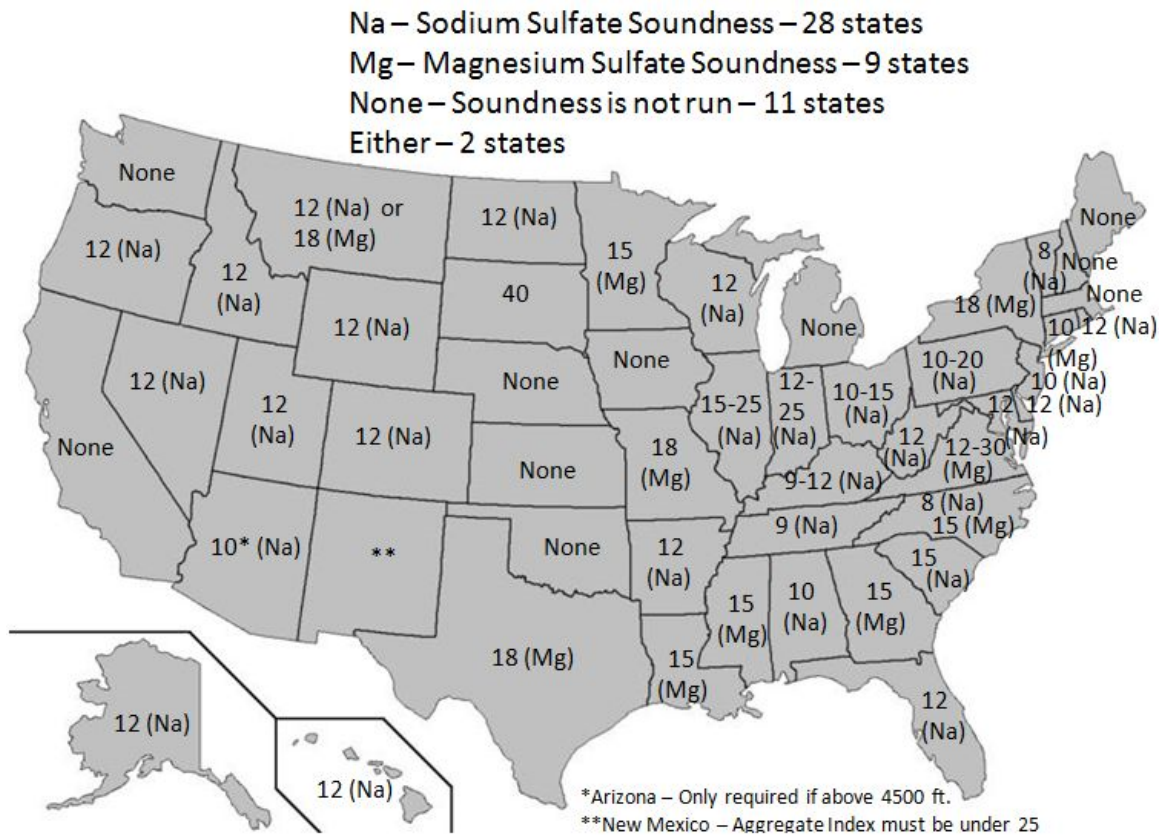
Figure 3.2: Limits for the Sodium Sulfate Test as Specified by State DOTs

Other important coarse aggregate tests include those used to measure the type and amount of deleterious material and microfines. Some states specify total limits for cumulative amount of deleterious materials based on clay lumps, shale, and friable particles, but states that do list limits for each type of deleterious materials are discussed as follows. Also, it is important to note that five states simply specify that the aggregate must be "free from deleterious material" and the state engineer of record is responsible for determining aggregate usage. For clay lump content, Texas has the most conservative limits in the country at 0.25% allowed. However, eight

51

other states match this limit for clay lump content. The highest allowable clay lump content is 2.5%, specified by New Mexico. For shale content, the Texas requirement of 1.0% is similar to most other states. The lowest allowable shale content is 0.4% (Minnesota) and the highest allowable is 10% (Pennsylvania). However, this limit only applies to curb and gutter applications; otherwise a 2.0% limit is specified. For friable particles, the limit in Texas of 5% is one of the highest in the country. The lowest allowable limit is 0.25% (West Virginia) and the highest allowable limit is 8% (Illinois). For decantation, the Texas limits of 1.0% to 3.0% (these limits depend on the aggregate type and composition of microfine material) are comparable to limits by other states (Texas Department of Transportation, 2004).

Other coarse aggregate specification limits included by state DOTs include an expansion limit for ASR-related expansion, a maximum content of flat and elongated particles (on either a 5:1 or 3:1 basis), a limit for coal and lignite content, and freeze-thaw limits that depend on the test. Several states use AASHTO T 103 for freeze-thaw testing while other states have state-specific unconfined freeze-thaw limits. As previously mentioned, New Mexico has a unique "Aggregate Index" to rate aggregates, which is based on a composite score from LA abrasion, sulfate soundness, and absorption. Alaska uses a machine that is smaller than the LA abrasion machine, but larger than the Micro-Deval apparatus, to simulate studded tire abrasion. This test uses small diameter steel charge and is conducted in the presence of water. A review of several Canadian specifications showed that Canadian provinces typically specify an absorption limit as well as Micro-Deval limits and unconfined freeze-thaw limits.

3.2.2 Fine Aggregate Specifications

Fine aggregate specifications in the state of Texas include tests for deleterious material, organic impurities, AIR, sand equivalent, and fineness modulus. For deleterious materials, Texas limits clay lump content to 0.5%, which is one of the most conservative limits in the country. Approximately 75% of states run this test and the highest allowable limit is 3% (eleven states) while the lowest allowable limit is 0.25% (Missouri and Virginia). Canadian provinces typically specify a total deleterious content.

For organic impurities, Texas requires that if the color of the sample supernatant liquid is darker than a standard color (Gardner No. 11), then the aggregate should be run for AASHTO T 71 mortar cube test and meet 95% compressive strength when compared to a control mixture. This test is run by 48 states with the same procedures. For samples failing the Gardner color test, states require from 90% (three states) to 100% (three states) mortar cube strength; however, most states specify a 95% mortar cube strength requirement.

The AIR test is run by only four states, including Texas. Texas, along with Oklahoma, has the strictest requirements at 60% insoluble by weight. The least restrictive requirements are specified by North Carolina and Ohio at 25%. In general, states require engineer approval for a fine aggregate depending on the application (friction surface or structural). Three states require natural sand on bridge decks and one state (Minnesota) requires all fine aggregates to be of natural origin.

The sand equivalent test is run by 11 states and the limit specified by Texas (80%) is the most conservative in the country but is also matched by two other states. The lowest allowable sand equivalent limit is Oregon at 68%. Most of the states that do not run sand equivalent specify a maximum loss by decantation.

Fineness modulus values are allowed to vary from 2.3 to 3.1 in the state of Texas, which is very similar to requirements by most other states. The value of 2.3 is the lowest allowable

fineness modulus by any state and the highest allowable fineness modulus is 3.5 (allowed by Connecticut and Michigan).

Other somewhat common fine aggregate specification limits included by state DOTs include an expansion limit for ASR-related expansion, sodium sulfate soundness limit (typically 10% over a five-cycle test), and absorption (typically 2.0–2.5%). Canadian provinces specify maximum total deleterious content as well as Micro-Deval limits. Indiana requires fine aggregates to be tested in a 3% brine freeze-thaw test. Hawaii specifies a limit of 40% for LA abrasion testing of fine aggregates.

3.2.3 Summary

For the majority of tests, Texas aggregate qualifications and limits are very similar to other states. For coarse aggregate tests, TxDOT standards represent an approximately average value for LA abrasion, loss by decantation, sulfate soundness, and shale content. TxDOT coarse aggregate standards are less conservative for friable particles but more conservative for clay lumps when compared to other state specifications. The most common tests performed by other states are content of flat and elongated particles, ASR testing, and aggregate freeze-thaw testing.

For fine aggregate tests, TxDOT standards represent an approximately average value for organic impurities and fineness modulus. TxDOT fine aggregate standards are more conservative for clay lump content, AIR, and sand equivalent value. The most common fine aggregate tests performed by other states are loss by decantation, ASR testing, and sulfate soundness testing.

3.3 Aggregate Workshop

An aggregate workshop was held on June 22, 2011, at the Pickle Research Campus in Austin, Texas, to provide the researchers the opportunity to gather information from the experience of TxDOT personnel, a retired representative from the Ministry of Transportation in Ontario (MTO), and representatives from major aggregate producers in Texas. A complete list of workshop attendees can be found in Appendix A. This meeting provided for a free and open discussion of (1) current problems in PCC related to aggregates; (2) most important aggregate properties and tests to measure those properties; (3) number and types of aggregates to be used in the study; (4) the appropriate methods for establishing performance test limits and criteria; and (5) determining the most appropriate test methods to establish the required performance of aggregates in concrete. During this meeting, attendees were able to discuss past failures observed in concrete pavements and structure as well as discuss the properties and tests that would be most useful in screening for quality materials. The research team was present during the discussion, but did not make comments in order to provide an unbiased discussion between the producers and TxDOT.

From a TxDOT perspective, a failure should be defined as a distress that causes money to be spent on repair or replacement earlier in the concrete life than anticipated. For example, even though minor pop-outs may be only a cosmetic issue, they must eventually be dealt with and would therefore be considered a failure. Few concrete failures in TxDOT projects can be directly attributed to aggregates. There are perhaps two main explanations for this. The first explanation is that it is very difficult to pinpoint the cause of a concrete failure because of the composite nature of the material. The second explanation may be that the AQMP has been successful in ensuring that good quality aggregates are used in TxDOT projects, and therefore failures are rare. Despite the general success of concrete aggregate usage by TxDOT, it is possible that current specifications are too conservative and preclude the use of good aggregates around the state. The

desire for differing specifications based on application was suggested. The main categories would be for structural needs and paving needs. Limits and testing would need to be established that would best predict and screen for materials to be used in these applications.

One aggregate issue in Texas includes excessive cracking in CRCP using siliceous river gravels, likely due to the high CoTE of this aggregate type. This issue has primarily occurred in the Houston District. Because of this problem, many districts have banned the use of river gravels in CRCP. However, the Fort Worth district has successfully used river gravels blended with 50% limestone in CRCP projects with no issues. Current research is investigating mitigation options for CRCP projects that use river gravels. TxDOT is currently in the process of introducing a statewide CoTE requirement for CRCP projects.

Other concrete issues around the state include freezing and thawing in the Panhandle and D-cracking, which has been identified at the Abilene Airport. However, these aggregate sources were later abandoned because of these problems. There have also been isolated incidents of polishing when carbonate fine aggregate was used, e.g., on IH 35 near San Antonio and in the Dallas and Fort Worth area, which was a 100% carbonate fine aggregate pavement. In areas where high volume paving was done and mass concrete was placed, issues with heat generation and management have been seen; this problem typically results in thermal cracking. Issues with aggregate thermal conductivity seem to have been a likely cause.

One specific example of a concrete failure due to an aggregate was in the Dallas District in Collin County where an aggregate from southern Oklahoma (Lattimore Stringtown) was used in a bridge deck. This aggregate had pyrite, shale, and asphaltic material, which made it perform very poorly in service. Aggregates with high contents of pyrites and other sulfides should be avoided. Aggregates with high shale content should be avoided as well. Producers can usually deal with shale during processing but this process can sometimes be tricky. If the shale is not handled correctly, an aggregate with a 0.4% decant at the quarry can result in a 1.0% or higher decant when the material reaches the ready mix plant.

The use of optimized gradation was highly supported by both producers and many of the TXDOT district personnel. It was commented that reductions of one sack of portland cement per cubic yard could be achieved by using optimized gradation. One comment made, however, suggested that the extra testing required for optimized gradations are often complicated and either not run or run incorrectly. One major problem concerning optimized gradation is the lack of storage bins at ready mix plants and hesitation of plants to have multiple aggregate piles.

Once the issue of common concrete distresses had been discussed, a list of the material properties and corresponding test methods was developed to provide a basis for selecting tests to be performed to screen aggregates. Properties that were given high priority by workshop attendees included combined gradation (more important for producer than buyer), resistance to degradation (can be measured by aggregate impact value, LA abrasion, and Micro-Deval), shape characteristics (can be measured by AIMS), texture (can be measured by AIMS), strength (important for structures—can be measured by compression point load index and concrete cylinder compression), modulus of elasticity (of concrete), CoTE, modulus of elasticity (of aggregate), freezing and thawing behavior (can be measured by modified ASTM C 666, Iowa pore index, Canadian freeze-thaw, and sodium or magnesium sulfate soundness), resistance to dimensional change (can be measured by wetting/drying cycles, Canadian unconfined freeze-thaw, CoTE, creep testing), resistance to abrasion (Micro-Deval with AIMS), lack of objectionable substances (e.g., chloride ions, sulfides, and clays), skid resistance (acid insoluble test), thermal conductivity, and petrography. Other properties and methods that were mentioned

54

by attendees were considered less important and thus given lower priority. These properties and methods included discrete measurements of decantation, the difference between TxDOT gradation and ASTM C33, strength (less important for pavements), absorption, and chemical resistance.

After the discussion of aggregate properties and relevant test methods, a discussion was held to determine the number and types of aggregates to collect for the study. The original aggregate list provided by TxDOT for the project was created to encompass a good representation of the Texas geology (Edwards formation, etc.). However, it was stated that more materials from the Edwards formation may be required due to the complex geologic formations found within. Additionally, there should be special interest taken in materials that are relatively new to use in Texas such as granites and dolomites. Attendees suggested that it may be possible to get bad sources from other states, such as D-cracking-susceptible aggregates from Michigan or Kansas.

Next, a discussion concerning the procedure for establishing the limits for use with the new tests was conducted. Chris Rogers, formerly with MTO, provided crucial insight on how Ontario established limits and also addressed some recurring problems encountered during the process. Several studies were conducted involving numerous tests that also determined known performance of existing concrete through surveys and field visits. One common problem was that if a source yields poorly performing aggregates, it tends not to be reused. Therefore, it is sometimes difficult to gather enough information about these sources. Rogers also emphasized that Ontario had different limits for different classes of concrete; however, it is important to remember that Ontario has very different environmental conditions than does Texas. Other ideas and advice provided by attendees during this discussion included correlating AIMS data (shape and texture) to concrete strength of volumetrically constant mixture designs, the need for cubical aggregates during testing to eliminate erroneous results due to flakey aggregates, and the necessity for petrographic examination.

At the end of the day, the workshop focused on selecting the best tests to be performed during this project. This discussion focused on identifying tests that would be valuable to run from an academic standpoint as well as tests that would be important to have for incorporating into a new test standard. During the discussion, an agreement was reached between the researchers and the project management committee that LA abrasion testing, and magnesium sulfate soundness testing would be conducted by TxDOT, since these two tests are not very good predictors of performance and will likely be excluded from future specifications. Additional testing by the research team will be selected to offset the work that would no longer be required (LA abrasion, magnesium sulfate soundness, and petrographic examination).

3.4 Finalizing Testing Plan

The research team met with TxDOT project committee members to discuss the testing plan in the context of the literature review and the suggestions provided by attendees of the aggregate workshop. For the most part, suggestions made at the aggregate workshop were supported by project committee members but a few changes and revisions were made with the goal of creating the most relevant and complete testing plan possible.

Although the Canadian unconfined freeze-thaw test has shown promise as a good indicator of field performance for coarse aggregates, project committee members felt that its only slight improvement in prediction of performance compared to magnesium sulfate soundness (according to results from ICAR 507) and its limited relevance to Texas, which has very little

freeze-thaw exposure, was not enough to justify its inclusion in the final testing plan. Similarly, the Iowa Pore Index test, which has been shown to potentially identify aggregates susceptible to D-cracking, was deemed too costly and not relevant enough to Texas environmental conditions to pursue further. Although LA abrasion and magnesium sulfate soundness tests have shown limited correlation to field performance, their inclusion was desired in the final testing plan since they are currently part of Item 421 specifications. Decantation was eliminated from the testing plan because TxDOT has already gathered a significant amount of relevant data in an internal study. Project committee members were somewhat skeptical of the value and importance of the aggregate impact value test and the aggregate crushing value test, but suggested that these tests be run on approximately 15 aggregates to determine potential of these tests before investing the time to test all coarse aggregates sources. The Micro-Deval, thermal conductivity, chemical composition (X-ray diffraction), AIMS 2.0, specific gravity, and absorption tests were all approved unanimously.

Fine aggregate tests supported for inclusion in the final testing plan include Micro-Deval, AIMS 2.0, chemical composition (X-ray diffraction), AIR, specific gravity, and absorption. The organic impurities and sand equivalent tests were added to the final testing plan because since they are currently part of Item 421 specifications. Test methods recently developed were also added to the final testing plan to determine their potential for future use. These tests are the flakiness test developed by Chris Rogers and the Grace Methylene Blue test which uses a colorimeter.

Concrete tests were included in the final testing plan due to the limited data gathered from district surveys about specific aggregate performance. These tests include compressive strength testing, flexural strength testing, CoTE, and modulus of elasticity.

The final testing plan is listed in Table 3.1. Descriptions of these test methods are provided in Chapter 5.

Table 3.1: Finalized Testing Plan

Coarse Aggregate Tests

LA Abrasion	*Tex-410-A*
Magnesium Sulfate Soundness	*Tex-411-A*
Micro-Deval	*Tex-461-A*
Thermal Conductivity	
X-ray Diffraction	
AIMS 2.0	
Specific Gravity and Absorption	*Tex-403-A*
Aggregate Crushing Value	*BS 812.110*
Aggregate Impact Value	*BS 812.112*

Fine Aggregate Tests

Micro-Deval	*ASTM D 7428*
AIMS 2.0	
X-ray Diffraction	
Grace Methylene Blue	
Organic Impurities	*Tex-408-A*
Acid Insoluble Residue	*Tex-612-J*
Specific Gravity and Absorption	*Tex-403-A*
Flakiness	*Rogers (2008)*
Sand Equivalent	*Tex-203-F*

Concrete Tests

Compressive Strength	*Tex-418-A*
Flexural Strength	*Tex-448-A*
CoTE	*Tex-428-A*
Modulus of Elasticity	*ASTM C 469*

Chapter 4. Materials Acquisition

4.1 Selection of Aggregates

A survey of TxDOT district personnel revealed that most districts have access to at least a few aggregate sources within their district, with the exception of a few districts in eastern Texas. Most districts are able to use somewhat local resources, though some districts are forced to ship aggregates in from other districts or other states.

As a large, geologically diverse state, Texas has a tremendous amount of aggregate resources, particularly of the carbonate variety. Limestones, dolomitic-limestones, and dolomites are common throughout much of Texas, as are river gravels on a regional level. Quality of limestones and dolomites varies by quarry and region, primarily due to geologic features of the Edwards formation (Fisher & Rodda, 1969). The composition of river gravels varies widely by region and river basin but may contain sedimentary, metamorphic, or igneous aggregates. Many river gravels are composed of predominantly carbonate and siliceous rocks, weathered by water. Although less common, there are also a few sandstone, granite, and rhyolite sources in Texas and nearby in Oklahoma.

A list of aggregates to test was suggested by TxDOT geologists and engineers to capture a representative sample of lithologies and geographies. The list was created with the understanding that the research team would be responsible for collecting aggregates close to Austin (the location of the laboratory testing) and TxDOT personnel would assist in the collection and delivery of aggregate sources far from Austin. The list went through several iterations to ease logistical transportation constraints and ensure that aggregates could be acquired or delivered in a timely manner. The final list of aggregates also took advantage of the fact that several aggregate samples were already present at the Construction Materials Research Lab at The University of Texas due to testing by other research projects.

Some of the selected aggregates will be used to make concrete for mechanical testing. The aggregate sources on the concrete list were rated as "good," "moderate," or "poor," depending on how consistently they meet specification requirements. As a result, some aggregates on the testing list are members of the TxDOT Aggregate Quality Monitoring Program (AQMP), as discussed in the following section, and some are not.

4.1.1 TxDOT Aggregate Quality Monitoring Program (AQMP)

The AQMP was created by TxDOT in 1977 to accelerate the acceptance of aggregate sources for use in TxDOT projects and to improve the overall efficiency of TxDOT operations. The AQMP involves quality monitoring (as the name implies), testing, and statistical analysis of aggregates to ensure consistency and compliance with specifications. TxDOT certifies personnel in both sampling and testing to ensure fair and representative data. To be accepted in the AQMP, producers must provide a test history of at least five TxDOT project samples produced 1 month apart within the last 2 years and allow periodic quarry/pit inspection and testing of materials by TxDOT personnel for each quarry or pit. Acceptance in the AQMP means that an aggregate source can bypass strenuous and time-consuming testing typically required at the beginning of TxDOT projects. Once accepted in the AQMP, the aggregate source is monitored frequently for material consistency, material quality, production trends, production rate, frequency of use in TxDOT projects, and test results (Texas Department of Transportation, 2007).

The AQMP lists are published semi-annually (one list for PCC-approved sources and one list for bituminous approved sources), and periodically include new data about the aggregate sources. Initially, only polish value ratings were available on the AQMP document, but in 1994, TxDOT began publishing data for LA abrasion and magnesium sulfate soundness (Jayawickrama, Hossain, & Hoare, 2007). Recent iterations of the AQMP document have added data for sources for Micro-Deval, coefficient of thermal expansion, alkali-silica reactivity for coarse aggregates, and acid insoluble residue, and alkali-silica reactivity for fine aggregates. However, not all data are available for every source and a disclaimer states that this information is only for reference. All sources are now also categorized by material type (i.e., partly crushed siliceous and limestone gravel).

4.2 Aggregate Collection

The list of aggregates to be tested as part of this research project was created with the understanding that the research team would be responsible for collecting aggregates close to Austin (the location of the laboratory testing) and TxDOT personnel would assist in the collection and delivery of aggregate sources far from Austin. Districts close to Austin included the Austin, Waco, Bryan, and San Antonio districts. A TxDOT district map is displayed in Figure 4.1.

For each aggregate source members of the research team asked employees a basic set of questions to obtain more information about the material. When possible, the research team spoke with quality control managers, who have a good idea of material availability and quality. Questions directed to these personnel fostered discussions about what types of materials are available on a regular basis, problems meeting TxDOT specifications, and history and use of the products. Specific collection strategies are discussed in the following sections.
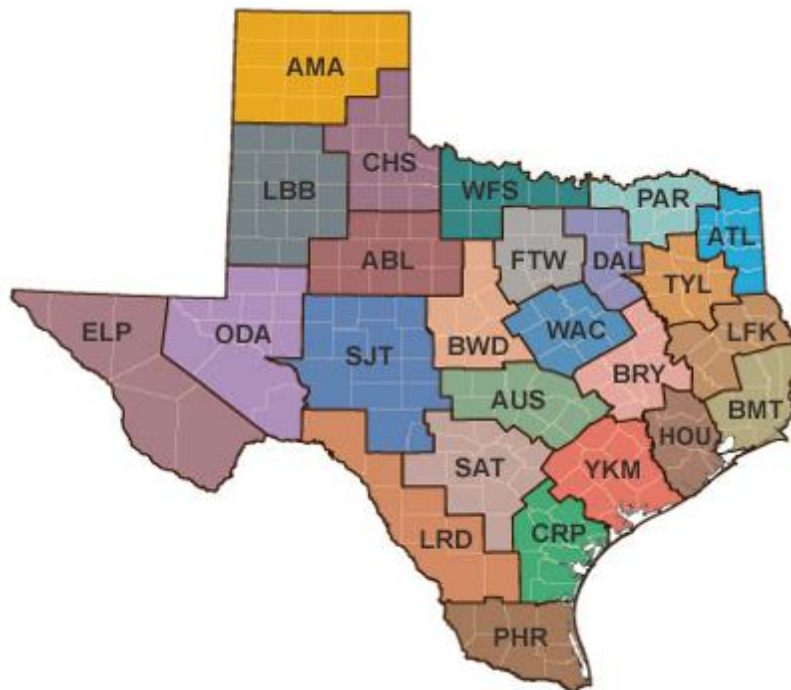
Figure 4.1: State Map of TxDOT Districts

4.2.1 Collection of Aggregate Sources Close to Austin

Aggregates located within a 3-hour drive of Austin were considered "close," and therefore the research team's responsibility to acquire. At least 10 sources on the final list of aggregates were located in the Austin district, 8 in the San Antonio district, and 5 more in the Waco district. For many of these sources, two or three members of the research team traveled to the quarry or pit to personally sample the material.

After arriving on location, the research team viewed and acknowledged safety procedures and then discussed which materials would be best to sample for the project with producer personnel. A producer employee, often the quality manager, then guided the research team to the material of interest. This material was often located in large stockpiles on site. Research members proceeded to obtain sample material, following sampling procedures outlined by TxDOT in the Tex-400-A (*Sampling Flexible Base, Stone, Gravel, Sand, and Mineral Aggregates*) specification. Understanding of and compliance with this sampling standard ensured that a representative sample of material was obtained for testing. If a front-end loader was available, the research team instructed the operator to approach the stockpile and cut into the stockpile from bottom to top in one continuous cut, exposing a clean, interior vertical face. The material from the first cut was discarded and the front-end loader operator then cut into the newly exposed face of the stockpile and lowered material from this cut to the ground. This process was repeated several times, until a large sample of material was available at ground level. The research team then took flat-nosed shovels and loaded the material of interest into 0.3-ft^3 (0.009-m^3) TxDOT-approved canvas bags or 8-ft^3 (0.23-m^3) *Super Sacks®*, pictured in Figure 4.2. If a front-end loader was not available, research team members used shovels and 5-gallon buckets to sample material at quarter points of the stockpile, with sample points at bottom, middle, and top of the stockpile for a total of 12 points. This material was then transferred to the TxDOT approved canvas bags or 8-ft^3 (0.23-m^3) Super Sacks. The canvas bags or Super Sacks were then loaded onto a trailer towed by the laboratory truck. Researchers proceeded to sample nearby stockpiles in the same manner if interested in additional material such as fine aggregate or crusher screenings. After sampling material at the first few sources, the research team decided that it would be more efficient to unload and handle material at the laboratory if it was in 8-ft^3 (0.23-m^3) Super Sacks. These Super Sacks were obtained from B.A.G. Corp. and are made of woven polypropylene fibers. Handles on the tops of the Super Sacks allow a forklift to easily lift and transport a full bag.

Figure 4.2: "Super Sack" Used to Collect and Transport Aggregates

To save time and reduce transportation costs, the research team contacted the Texas Aggregate and Concrete Association (TACA) in order to obtain assistance in gathering materials. The research team, with generous assistance from TACA and TxDOT employees, devised a plan in which the research team would ship Super Sacks to aggregate producers, who would then sample and transport material to a local TxDOT yard. A TxDOT truck would then travel to the local TxDOT yards and obtain the aggregates and transport them to Austin for testing. The research team is extremely grateful for everyone involved in this process (TACA, TxDOT, and producer personnel), which allowed the acquisition of material to be expedited and more cost-effective.

4.2.2 Collection of Aggregate Sources Far from Austin

Aggregates located farther than 3 hours away were acquired in a similar manner to aggregates located close to Austin that were collected with assistance from TACA and TxDOT. Again, the research team shipped Super Sacks to aggregate producers, who then sampled and transport material to a local TxDOT yard. A TxDOT truck would then travel to the local TxDOT yards and obtain the aggregates and transport them to Austin for testing. However, prior to shipping the Super Sacks, the research team contacted producers to ask employees the same basic set of questions to obtain more information about the material. When possible, the research team spoke with quality control managers who have a good idea of material availability and quality. Questions directed to these personnel fostered discussions about what types of materials are available on a regular basis, problems meeting TxDOT specifications, and history of use of the products.

4.2.3 Coarse Aggregate Distribution

A total of 58 coarse aggregates were collected for this study. The research sponsor and material suppliers asked that the exact names and locations of the aggregates not be presented. Therefore, an overview of the aggregates collected displaying the random sample identification number (1 through 58,) material lithology, and source district are presented in Table 4.1.

Table 4.1: Coarse Aggregate Distribution

Sample ID	Lithology	Source District	Sample ID	Lithology	Source District
1	Partly Crushed River Gravel	Yoakum	30	Limestone	San Antonio
2	Partly Crushed River Gravel	Yoakum	31	Limestone	Ft Worth
3	Partly Crushed River Gravel	Austin	32	Limestone	Lubbock
4	Partly Crushed River Gravel	Austin	33	Limestone	San Antonio
5	Partly Crushed River Gravel	Houston	34	Limestone	San Antonio
6	Partly Crushed River Gravel	Houston	35	Limestone	Austin
7	Partly Crushed River Gravel	Atlanta	36	Limestone	San Antonio
8	Partly Crushed River Gravel	Atlanta	37	Limestone	Abilene
9	Partly Crushed River Gravel	Atlanta	38	Limestone	Paris
10	Siliceous River Gravel	Austin	39	Limestone	Houston
11	Siliceous River Gravel	Austin	40	Limestone	San Antonio
12	Siliceous River Gravel	Dallas	41	Limestone	Austin
13	Siliceous River Gravel	Amarillo	42	Dolomite	Austin
14	Limestone River Gravel	El Paso	43	Dolomite	Austin
15	Limestone River Gravel	Lubbock	44	Dolomite	Paris
16	Limestone River Gravel	Waco	45	Dolomite	Paris
17	Limestone River Gravel	Waco	46	Dolomite	El Paso
18	Limestone River Gravel	Waco	47	Granite	El Paso
19	Limestone River Gravel	Waco	48	Granite	Paris
20	Limestone River Gravel	Amarillo	49	Granite	Childress
21	Limestone	Austin	50	Sand Stone	Austin
22	Limestone	Austin	51	Sand Stone	Paris
23	Limestone	Dallas	52	Sand Stone	Paris
24	Limestone	San Antonio	53	Sand Stone	Paris
25	Limestone	San Antonio	54	Trapp Rock	San Antonio
26	Limestone	Austin	55	Trapp Rock	San Antonio
27	Limestone	San Antonio	56	Rhyolite	Wichita Falls
28	Limestone	San Antonio	57	Rhyolite	Odessa
29	Limestone	Waco	58	Slate	Paris

Chapter 5. Laboratory Testing

5.1 Coarse Aggregate Tests

Coarse aggregate tests were selected based on a review of literature, a review of other state DOT specifications, and a discussion with personnel in industry and academia. Chapters 2 and 3 contain more information about the selection of aggregate tests. Because this research project is funded by TxDOT, TxDOT standards were used when possible. Otherwise, ASTM standards or other widely accepted test methods were used to ensure repeatable and consistent results. Members of the research team were certified on several tests by TxDOT to ensure that standard procedures were followed correctly. See Table 3.1 to view the complete list of coarse aggregate tests performed.

In the following sections, the test methods are listed and followed by a general background, description of procedures, documentation of precision, and comments regarding the approach of the research team for each test.

5.1.1 Micro-Deval Test for Coarse Aggregates

French researchers developed the Micro-Deval test, which subjects water, coarse aggregate, and steel charge to approximately 12,000 revolutions in a steel drum via a ball mill roller. Researchers in Canada further modified this test to allow for a larger aggregate sample size and slightly altered dimensions of the steel charge and drum (Rogers C., 1998). Today, most Micro-Deval specifications are based on the standards documented by the Canadian researchers. The standard used by this research project was Tex-461-A (*Degradation of Coarse Aggregate by Micro-Deval Abrasion*).

The Micro-Deval test requires that the aggregate sample be washed and dried prior to testing. A standard gradation is specified for concrete aggregate for this test and provided in Table 5.1. The total mass of the sample should be 1500 ± 5-g.

Table 5.1: Coarse Aggregate Gradation Required for Micro-Deval Test (Tex-461-A)

Sieve Size	Target Mass
3/4" - 1/2"	660 ± 5 g
1/2" - 3/8"	330 ± 5 g
3/8" - 1/4"	330 ± 5 g
1/4" - No. 4	180 ± 5 g

Once the sample has been weighed out, 5000 ± 5-g of stainless steel balls, of diameter 9.5 ± 0.5-mm, should be placed in the Micro-Deval container. The Micro-Deval container is a small stainless steel drum as shown in Figure 5.1. The aggregate sample can then be placed in the Micro-Deval container and soaked in 2000 ± 500-mL of tap water at 20 ± 5˚C (68 ± 9°F) for a minimum for one hour. After one hour, the Micro-Deval container is sealed and placed in the Micro-Deval machine. The Micro-Deval machine itself is a simple ball mill roller.

Figure 5.1: Micro-Deval Test Machine

The operator sets the appropriate time on the machine such that it will run for 120 ± 1 minute. The machine should be calibrated to revolve at 100 ± 5 revolutions per minute and the final revolution count should be 12,000 ± 600 revolutions. After 2 hours of revolutions, the Micro-Deval container is removed and the contents are washed over a No. 16 (1.18-mm) sieve (see Figure 5.2). Material passing the sieve is discarded. The retained material is oven-dried to a constant weight and weighed after drying. The oven-dried weight is recorded and compared to the original weight to get a percent loss calculation for the final Micro-Deval loss.

Figure 5.2: Sample Ready to Be Washed after Micro-Deval Test

The research team performed two Micro-Deval tests per source and recorded the mean loss unless the test results were different by more than 1.0%. In this case, a third Micro-Deval test was performed and the mean of the three tests was considered acceptable unless an outlier existed. Conditions of the inside surface of the steel drum should not affect results for testing of coarse aggregates, but the research team used a local limestone aggregate (Alamo Weir) as a control to monitor test conditions over time (Rogers C., 1998). Research has shown the Micro-Deval to be a very consistent test, but standard deviation increases with higher loss materials (Jayawickrama, Hossain, & Hoare, 2007). Figure 2.4 in Chapter 2 displays typical standard deviation results for this test based on average loss. The AASHTO standard of this test also provides information about the multi-laboratory precision of this test method, and is found in Table 5.2, taken from AASHTO T 327-09.

Table 5.2: Multi-Laboratory Precision Values for Micro-Deval Testing of Coarse Aggregate (AASHTO T 327-09)

Aggregate Abrasion Loss, Percent	Coefficient of Variation, Percent of Mean[a]	Acceptable Range of Two Results, Percent of Mean[a]
5	10.0	28
12	6.4	18
17	5.6	16
21	5.3	15

[a] These numbers represent, respectively, the (1s percent) and (d2s percent) limits as described in ASTM C 670.

5.1.2 Specific Gravity and Absorption Test for Coarse Aggregates

The specific gravity and absorption test requires that a representative sample of an aggregate be obtained and soaked for 15 to 24 hours, depending on the exact standard used. The aggregate is then dried to saturated surface dry (SSD) state, weighed in a calibrated pycnometer, and dried to an oven-dry state as described by the following procedures. The standard used by the research team was Tex-403-A (*Saturated Surface-Dry Specific Gravity and Absorption of the Aggregates*).

After a representative sample of aggregate is obtained, the aggregate is soaked (in a non-metal tub to avoid reaction) to ensure that all permeable pores of the aggregate become filled with water. The water should be at a temperature of 23 ± 2°C (73 ± 3°F). After the soaking period, the operator removes the aggregate and places it on a towel or cloth to absorb free moisture. The operator should dry the aggregate with the towel or cloth until no moisture is visible on the surface of the aggregate particles. At this point, the aggregate has reached the SSD condition where the outside surface of the aggregate has no free water but all internal pores remain filled with water. The aggregate is then placed in a container with a lid so that free evaporation does not remove additional moisture from the aggregate. This step should be repeated until approximately 1500 g (3.31 lb) of aggregate in the SSD state has been obtained and the weight of this sample recorded.

While the SSD aggregate is covered, the mass of a controlled volume of water must be measured. The controlled volume of water is obtained by filling a calibrated pycnometer with water at 23 ± 2°C (73 ± 3°F). The pycnometer is a 2000-mL mason jar with a metal pycnometer cap. A rubber bulb or syringe is used to fill the pycnometer with water until a rounded bead of water appears on top of the pycnometer cap. The outside of the pycnometer is dried and the pycnometer is weighed and this weight recorded. The pycnometer cap can be removed and the jar can be emptied until about ¼ of the water remains. At this point, the SSD aggregate is placed in the pycnometer. The operator should take extra care in placing aggregate in the pycnometer so that all material is accounted for. The jar is filled with water at 23 ± 2°C (73 ± 3°F) until it reaches the brim. The pycnometer should be agitated so that any entrapped air is freed. The pycnometer cap is again placed on the jar and a rubber bulb or syringe is used to fill the pycnometer until a rounded bead of water appears on top of the pycnometer cap. The outside of the pycnometer is dried and the pycnometer with aggregate is weighed and this weight recorded.

Finally, the aggregate is removed from the pycnometer, placed in a pan, and the pan placed in an oven where the aggregate is dried to constant mass. The weight of the aggregate at SSD, the weight of the pycnometer with water, and the weight of the pycnometer with aggregate are used to calculate the specific gravity and absorption capacity of the aggregate. Specific gravity is typically reported to the nearest 0.01 and absorption to the nearest 0.1% (Texas Department of Transportation, 1999).

According to the ASTM standard of this test (ASTM C 127), the standard deviation is 0.007 for SSD specific gravity for single-operator, and 0.011 for SSD specific gravity for multi-laboratory testing. The acceptable range of two results is 0.020 and 0.032 respectively (ASTM International, 2007).

Because this test is somewhat variable, the research team ran at least two tests per aggregate source. If the results of these two tests deviated more than the amount dictated by the ASTM C 127-07 standard, a third test was run and an average value taken of all three tests unless one test was determined to be an outlier.

5.1.3 LA Abrasion and Impact Test

The LA abrasion and impact test is performed on a sample of approximately 5000 g of aggregate. The aggregate sample, along with several large stainless steel balls, are loaded in the LA machine (pictured in Figure 5.3) and rotated approximately 500 times at about 33 rpm. The aggregate sample is then removed and sieved over a No. 12 (1.70-mm) sieve. The mass of material loss is determined as a percentage of the original sample mass to get the final LA abrasion results. The standard used by the research team was Tex-410-A (*Abrasion of Coarse Aggregate Using the Los Angeles Machine*), which simple refers to procedures described in ASTM C 131 (*Resistance to Degradation of Small-Sized Coarse Aggregate by Abrasion and Impact in the Los Angeles Machine*) and is described as follows.
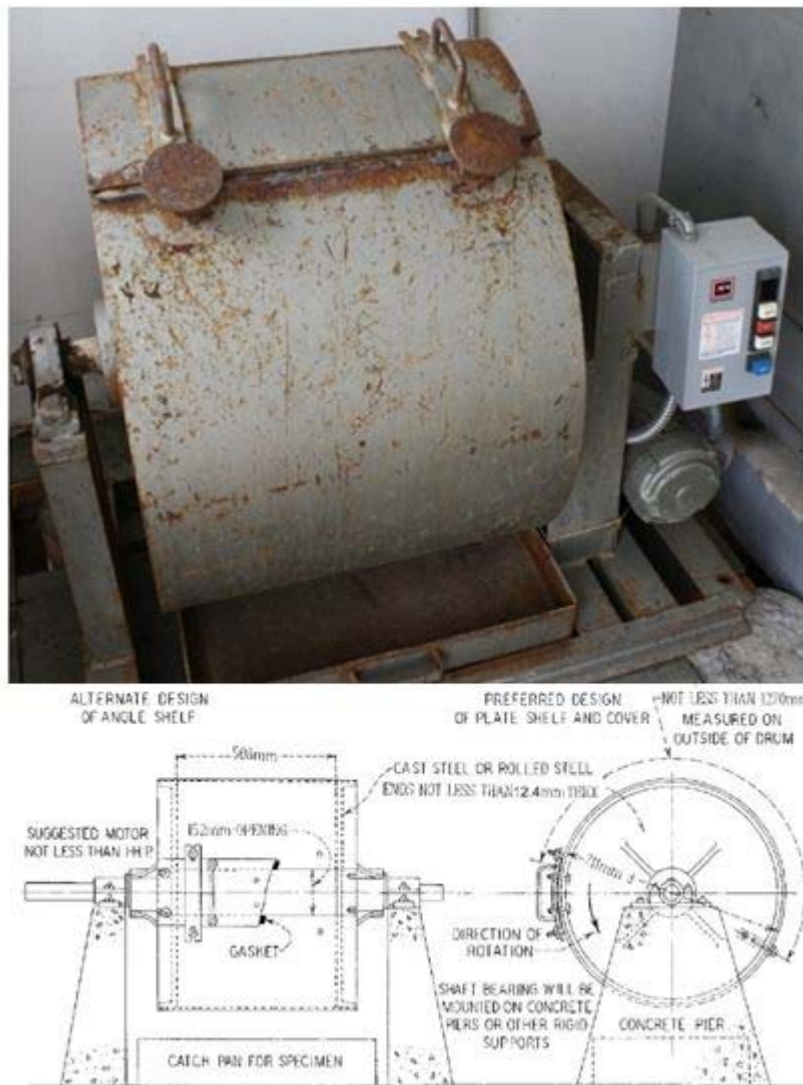
Figure 5.3: LA Abrasion Test Setup (Diagram from ASTM C 131)

The LA machine is a large, rotating steel drum with an inside diameter of 711 ± 5 mm (28 ± 0.2 in.) and inside width of 508 ± 5 mm (20 ± 0.2 in.). The steel walls of the machine are no less than 12.4 mm (0.49 in.) thick. A steel shelf is also located inside the drum and protrudes

89 mm (3.5 in.) into the drum. The function of the steel shelf is to cause the aggregate and steel shot to be lifted and dropped repeatedly as the drum rotates. A steel plate, with handles and a gasket seal, functions as the access point for the drum through which the aggregate and steel shot is placed. The LA machine should be calibrated to run at 30–33 revolutions per minute. The LA machine setup is displayed in Figure 5.3.

Prior to performing the LA abrasion test, a representative sample of aggregate must be obtained, washed, and oven-dried. The LA abrasion test can be performed on several sample gradations, so the amount of each size fraction necessary will depend on the gradation. This project used ASTM C 131 Grade B, which consists of 2500 ± 10 g of aggregate passing the 19.0-mm (¾-in.) sieve and retained on the 12.5-mm (1/2-in.) sieve, and 2500 ± 10 g of aggregate passing the 12.5-mm (1/2-in.) sieve and retained on the 9.5-mm (3/8-in.) sieve. This grading requires that 11 steel spheres be placed in the LA machine along with the aggregate. The steel spheres should be approximately 47 mm (1.9 in.) in diameter and weigh between 390 and 445 g. The total mass of the steel shot should thus be 4584 ± 25-g.

Once the correct mass of aggregate and steel shot is obtained, the operator places both materials in the LA machine. A counter is set at 500 revolutions and the machine is started. After the prescribed number of revolutions, the operator places a catch pan beneath the machine and removes the contents. The steel spheres are cleaned, removed, and placed aside for the next test. The aggregate sample is then sieved over a No. 12 (1.70-mm) sieve and the finer material is discarded. The remaining aggregate is weighed and this weight is recorded as the final mass. The operator may wet-sieve the material, but this is only necessary if dust remains adhered (and accounts for more than 0.2% of original mass) to the aggregate particles after initial sieving. The final LA abrasion loss is calculated as a percentage of mass lost compared to the original sample.

According to ASTM C 131-06, the single-operator coefficient of variance (COV) is approximately 2.0%, and thus two tests run by the same operator should not differ by more than 5.7%. The multi-laboratory COV is 4.5% and thus two tests should not differ by more than 12.7% (ASTM International, 2006).

To expedite testing, TxDOT construction materials laboratory volunteered to test aggregates for the LA abrasion test and provide results to the research team. Members of the research team prepared samples and delivered samples in batches to the TxDOT laboratory.

5.1.4 Magnesium Sulfate Soundness Test

The sulfate soundness of aggregates can be measured by using a magnesium sulfate solution or a sodium sulfate solution. This test involves cycles (typically five) of soaking an aggregate in a sulfate solution and then drying the aggregate. This test was originally developed in 1828 to simulate freezing of water in stone before refrigeration was controllable and widely available (Rogers, Bailey, & Price, 1991). The idea was to simulate crystallization pressures of ice formation during freezing and thawing events by causing salt crystals to form during the heating stage of this test (Folliard & Smith, 2002). Of the state DOTs that do use the sulfate soundness test, 28 states specify the use the use of sodium sulfate, 9 states specify the use of magnesium sulfate, and 2 states allow the use of either magnesium sulfate or sodium sulfate. Eleven states do not use sulfate soundness testing. The standard method used for this project was Tex-411-A (*Soundness of Aggregate Using Sodium Sulfate or Magnesium Sulfate*).

Prior to performing the magnesium sulfate soundness test, a representative sample of aggregate must be obtained, washed, and oven-dried. The gradation of the sample to be tested for concrete aggregates is listed in Table 5.3. The magnesium sulfate solution must also be prepared

in advance and allowed to sit for 48 hours prior to testing. The solution is prepared by adding magnesium sulfate in anhydrous or crystalline hydrate form to water at a temperature of at least 25˚C (75˚F) until the solution is beyond saturated (evident by presence of excess crystals). After allowing the solution to sit and cool to room temperature, the specific gravity of the magnesium sulfate solution should be between 1.295 and 1.308.

Table 5.3: Concrete Aggregate Size Fractions for Magnesium Sulfate Soundness Testing (Tex-411-A)

Sieve Size	Target Mass
¾-in. - ½-in.	670 ± 10 g
½-in. - 3/8-in.	330 ± 5 g
3/8-in. - ¼-in.	180 ± 5 g
¼-in. - No. 4	120 ± 5 g

After the solution and aggregate sample have been prepared, the operator places each fraction of aggregates in individual containers with holes (to allow for fluid circulation and draining) and submerges the container in the solution for 16 to 18 hours. The solution should be maintained at 20˚C to 24˚C (68˚F to 75˚F). After the submersion period, the sample is removed, drained for 15 min, and dried to constant mass in an oven. After drying, the sample is removed from the oven, allowed to cool to room temperature, and placed back in the magnesium sulfate solution. This process is repeated for a total of five cycles. After the fifth cycle, the sample is removed from the oven, allowed to cool to room temperature, and then washed by circulating hot water through the sample containers. After all salt is removed by washing, the aggregates are again dried in the oven. The aggregates are then sieved over their respective retained sieve sizes and a mass loss is calculated for each fraction size. This information is then used in combination with a normalized aggregate gradation (provided in Tex-411-A) to obtain the final magnesium sulfate loss.

As noted in the discussion of the literature review, both sulfate soundness tests have fairly low precision and repeatability. According to the ASTM standard for the sulfate soundness tests, the COV for a magnesium sulfate test (with total loss between 9% and 20%) is 25% (ASTM International, 2005).

To expedite testing, TxDOT construction materials laboratory volunteered to test aggregates for the magnesium sulfate soundness test and provide results to the research team. Members of the research team prepared samples and delivered samples in batches to the TxDOT laboratory.

5.1.5 Aggregate Impact Value (AIV)

The AIV is a British standard test method that subjects a confined aggregate sample to a falling impact load. A sample of aggregate, passing the ½-in. (12.5-mm) sieve and retained on the 3/8-in. (9.5-mm) sieve, of approximately 500 g in mass (depending on the density) is placed in a steel cup 38 cm (15 in.) below a steel hammer the same diameter as the inside of the cup. The user drops the steel hammer, guided by vertical rods, and raises it 15 times and the sample is sieved over a No. 8 (2.36-mm) sieve. The mass loss is recorded and the final result of the test is mass loss by percentage of original mass. The specific test method used by this research project

71

was British Standard 812 Part 112 (*Methods for Determination of Aggregate Impact Value*) and the procedures are described in this section.

The required apparatus to operate this test consists of a cylindrical metal base, a cylindrical steel cup, a metal hammer, and a means for raising and dropping the hammer in a controlled manner. The cylindrical metal base should be between 22 and 30 kg (48 and 66 lb) and should be affixed to a concrete block no less than 450 mm (17.7 in.) thick. The cylindrical steel cup should have an internal diameter of 102 ± 0.5-mm (4.0 ± 0.02-in.), a depth of 50 ± 0.25-mm (1.97-in ± 0.01-in.), and a thickness of at least 6 mm (0.24 in.) The metal hammer should have a mass between 13.5 and 14.0 kg (29.8 and 30.9 lb) and should fit snugly inside the metal cup. The hammer should be supported such that it may freely slide vertically and drop from a height of 380 ± 5-mm (15.0 ± 0.2-in.). The test setup used by this research project is shown in Figure 5.4.

To begin the test, an oven-dry sample of aggregate, passing the ½-in. (12.5-mm) sieve and retained on the 3/8-in. (9.5-mm) sieve, of at least 500-g in mass should be obtained and placed in the metal cup. The operator then uses a tamping rod to compact the aggregate by dropping the rod in a controlled manner 25 times at a height of 50-mm (1.97-in.) above the sample. Any aggregate that protrudes above the edge of the cup is removed. The mass should be recorded so that additional tests on the same aggregate source use the same mass. The user then places the cup in the testing apparatus below the hammer. The cup is secured to the testing apparatus and the operator raises and drops the hammer 15 times, waiting at least 1 second between drops. The cup is removed and then the aggregate sample is removed from the cup and sieved over the 2.36-mm (No. 8) sieve. The amount of material passing the 2.36-mm (No. 8) sieve divided by the original mass is the AIV (BSi, 1995).
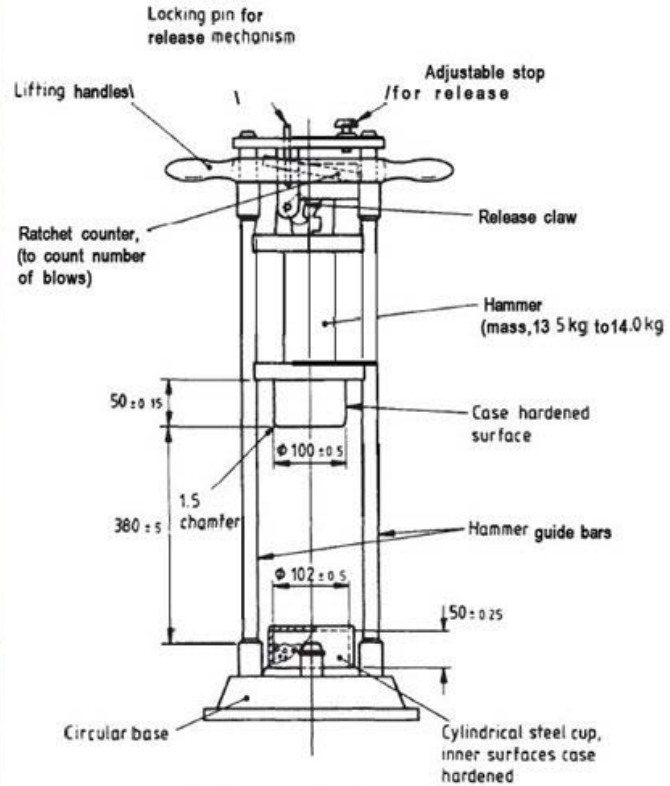
Figure 5.4: AIV Test Setup

The aggregate sample may be tested in a dry or SSD condition. The research team tested aggregates in the dry condition and ran the test four times per sample. The mean value of the four tests was recorded as the AIV. Repeatability and reproducibility of this test vary by lithology and can be found in British Standard 812 Part 112. A modification to this test was applied where the tested material was screened over the 4.75-mm (No. 4) sieve to compare with previously available data.

5.1.6 Aggregate Crushing Value (ACV)

The ACV test is a British standard that subjects an aggregate sample to confined compression using a machine typically used for compression testing of concrete cylinders. Approximately 2500 g of aggregate passing the ½-in. (12.5-mm) sieve and retained on the 3/8-in. (9.5-mm) sieve is placed in a cylindrical containment apparatus consisting of steel plates and a steel ring. The aggregate is compressed for approximately 10 minutes at a constant load rate, until the force has reached 400 kN (90,000 lb). The standard test method used by this research project was British Standard 812 Part 110 (*Methods for Determination of Aggregate Crushing Value*) and the procedures are described in the following section.

The testing components for the ACV include an open-ended steel cylinder, a plunger, and a base plate. The cylinder should have a diameter of 154 ± 0.5-mm (6.06 ± 0.02-in.), a depth of 125 to 140 mm (4.92 to 5.51 in.), and a wall thickness of at least 16.0 mm (0.63 in.). The plunger should have a diameter of 152 ± 0.5-mm (5.98 ± 0.02-in.) and an overall length of 100 to 115-mm (3.94-in. to 4.53-in.). The baseplate should be a square with side lengths of 200 to 230 mm

(7.87 to 9.06 in.) and a minimum thickness of 10 mm (0.39 in.). These components are pictured in Figure 5.5.

Figure 5.5: Equipment Used for ACV Test

To begin the test, an oven-dry sample of aggregate, passing the ½-in. (12.5-mm) sieve and retained on the 3/8-in. (9.5-mm) sieve, of at least 1500 g in mass should be obtained. The cylinder should be placed on the base plate and aggregate is placed in the cylinder in three layers, each layer subjected to 25 tamps from a tamping rod. The total depth of the aggregate sample in the cylinder should be about 100 mm (3.9 in.) after the three layers are added. The aggregate surface should be leveled and then the plunger is then placed on top of the aggregate. The entire apparatus is loaded into a compression testing machine and the aggregate is compressed for 10 ± 0.5 min. at a constant load rate, until the force has reached 400 kN (90,000 lb). The operator then releases the load and removes the testing apparatus. The testing apparatus is disassembled and the aggregate is removed by tapping a rubber mallet on the side of the cylinder. The aggregate sample should be sieved over the 2.36-mm (No. 8) sieve. The amount of material passing the 2.36-mm (No. 8) sieve divided by the original mass is the ACV. At least two tests should be performed and the mean recorded (BSi, 1990). A modification to this test was applied where the tested material was screened over the 4.75-mm (No. 4) sieve to compare with previously available data.

The research team performed this test three times per aggregate source and recorded the mean of the three tests as the ACV. Repeatability and reproducibility of this test vary by lithology and can be found in British Standard 812 Part 110.

5.1.7 Aggregate Imaging System (AIMS 2.0)

AIMS is a machine consisting of a camera, lights, computer software, and movable trays, designed to capture and analyze the shape, angularity, and texture of coarse aggregates and the form and angularity of fine aggregates. The camera captures images of the aggregate particles, either lit directly or backlit, and the software analyzes these images and provides the user with data summarizing the shape characteristics. For coarse aggregates, the user places a set of aggregate particles on a transparent tray and places this tray into the machine. There are four different trays for each size fraction of aggregate. Figure 5.6 displays the AIMS machine. The AIMS machine rotates the tray three times to capture images of each particle. The first image captured is backlit such that only the aggregates particle's two-dimensional shape is captured, and this image is analyzed by the fundamental gradient method. The second image captured requires the camera to focus on the particle, thus allowing a particle height (as a function of focal length) to be determined, and three-dimensional analysis to be realized. The third image captures a close-up surface texture of the aggregate particles that is analyzed by the wavelet method. The data are output in a spreadsheet file and includes a distribution of shape characteristics. Specific algorithms and analysis techniques used by the machine and software are described by the developer, Eyad Masad, and are available through the Texas Transportation Institute (Masad, 2005).

Figure 5.6: Setup of AIMS 2.0

For AIMS testing, the research team analyzed each aggregate source for all four size fractions before and after running the Micro-Deval test. The analysis before Micro-Deval testing provides general information about the aggregate and also provides a baseline to compare results to after Micro-Deval. The analysis after Micro-Deval testing provides data for change in shape, angularity, and texture. Some researchers have hypothesized that the change in shape, angularity, and texture will provide useful data for characterizing the abrasion resistance of an aggregate.

Mahmoud et al. (2010) found the AIMS to have a COV of 11% for any give source (single operator) and a COV of 5% for the same set of aggregates (single operator). Mahmoud et al. (2010) concluded that the effects of random placement of the same aggregate particles in different orientations had minimal effects on the angularity. In experiments with two AIMS machines (single operator) and multiple operators (single AIMS machine), the angularity measurements were found to be highly correlated ($R^2 = 0.97$ and $R^2 = 0.98$ respectively) as were texture measurements ($R^2 = 0.97$ and $R^2 = 0.92$). However, slope and intercept for texture was not 1 and 0. Thus, it seems that the texture measurement is not as repeatable as the angularity measurement.

5.1.8 Flat and Elongated Particles

Many state DOTs use a proportional caliper to manually measure particles in an aggregate sample and compare the maximum dimensions of a particle to its minimum dimension. An aggregate source possessing an excess of particles above a 4:1 dimension ratio may lead to workability issues during concrete placement (Folliard & Smith, 2002). Some states incorporate this testing as a means of finding aggregates susceptible to breakage during compaction of HMA mixes. The most common standard of this test is ASTM D 4791. Researchers used the Texas DOT version of this test, Tex-280-F (*Determining Flat and Elongated Particles*), which is described in the following section.

A proportional caliper is required to run this test. This device consists of a metal base plate, a fixed vertical post, and a swinging arm. Additional vertical posts are located such that their radial distance from the pivot point of the swinging arm is twice, three times, four times, and five times the distance from the pivot point to the farthest vertical post. The swinging arm allows the operator to adjust the proportional caliper for as necessary for each particle measured. A picture of the proportional caliper used by the research team is provided in Figure 5.7.
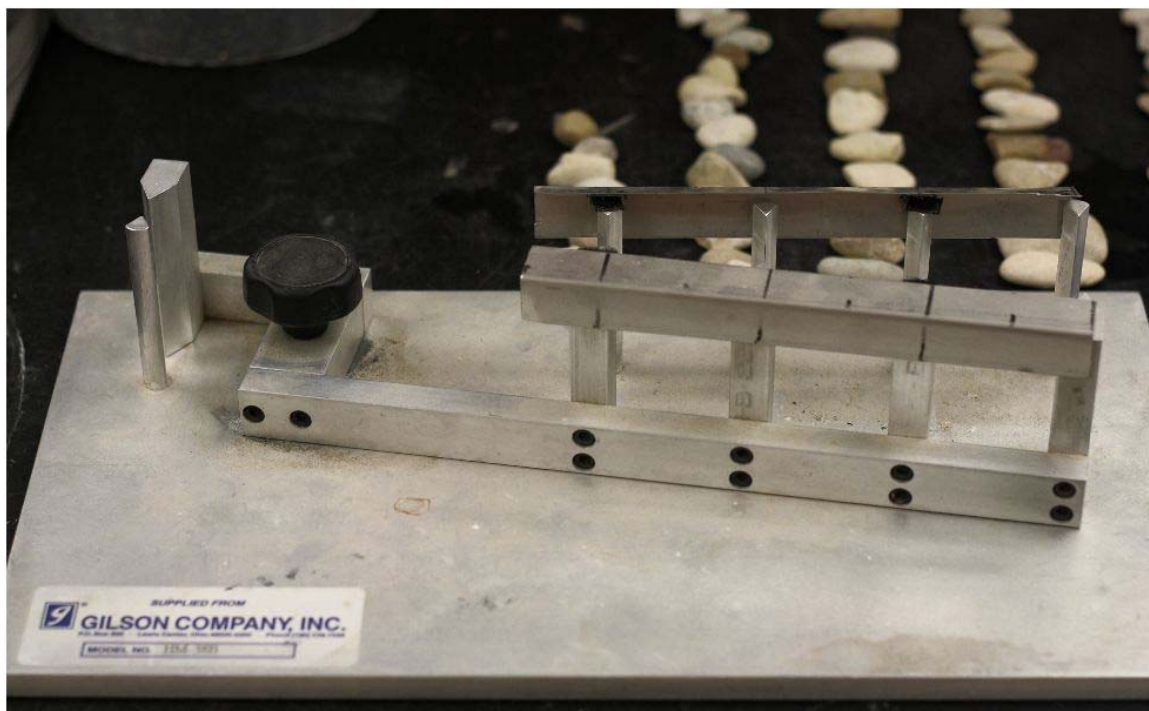
Figure 5.7: Proportional Caliper for Testing Flat & Elongated Particles

To begin the test, oven-dry samples of aggregate of each size fraction should be obtained. In this case, the research team measured aggregate particles retained on the ½-in. (12.5-mm), 3/8-in. (9.5-mm), ¼-in. (6.35-mm), and No. 4 (4.75-mm) sieves. Approximately 100 particles were tested for each size fraction; thus, a total of approximately 400 particles was tested for each aggregate source. For each aggregate particle, the operator sets the left-most opening to the minimum dimension, and then determines if the maximum dimension of the particle can pass through a critical opening on the right side of the proportional caliper. Typically, a critical ratio (e.g., 5:1) is selected and aggregate particles are considered "flat and elongated" if the maximum dimension perpendicular to the length and width cannot be placed through the opening matching the critical ratio. Once all particles are measured and classified as "flat and elongated" or "not flat and elongated," the flat and elongated percentage of each size fraction is multiplied by the percentage of each size fraction occurring in a sieve analysis of the original aggregate sample. This calculation provides a weighted average to obtain the final flat and elongated percentage for the aggregate source (Texas Department of Transportation, 2005).

For this research project, the operator placed each particle in a pile according to the dimension ratio it matched. For example, the most spherical particles would be classified as "2:1" and the most flat and elongated particles would be classified as "5:1" or "over." This method of recording ratios for every particle provides more data for analysis. Instead of getting a final flat and elongated percentage for one critical ratio, the researchers can manipulate the data to obtain a flat and elongated percentage for any ratio. The precision of this test is described in the ASTM standard of this test (ASTM D 4791) and is shown in Table 5.4 (ASTM International, 2010).

Table 5.4: Precision Values for Flat and Elongated Particles Test, from ASTM D 4791-10

19.0-mm to 12.5-mm Flat and Elongated (Percent)

Precision	Test Result (%)	(1S) %	(D2S) %
Single Operator	2.7	51.2	144.8
Multilaboratory		88.5	250.3

12.5-mm to 9.5-mm Flat and Elongated (Percent)

Precision	Test Result (%)	(1S) %	(D2S) %
Single Operator	34.9	22.9	64.7
Multilaboratory		43.0	121.8

9.5-mm to 4.75-mm Flat and Elongated (Percent)

Precision	Test Result (%)	(1S) %	(D2S) %
Single Operator	24.1	19.0	53.6
Multilaboratory		46.1	130.3†

5.1.9 Thermal Conductivity

Thermal properties, such as thermal conductivity, are important in understanding and predicting concrete behavior for applications such as continuously reinforced concrete pavements (CRCP) or mass pours. If thermal properties are not thoroughly understood or accounted for, thermal cracking may occur. Thermal properties are also input parameters for some computer programs such as *ConcreteWorks*.

There is currently no standard test method for measuring the thermal conductivity of aggregates. However, researchers have determined a method for evaluating the thermal conductivity of aggregate using a *Mathis TCi Thermal Conductivity Analyzer*. The *Mathis TCi Thermal Conductivity Analyzer* is a tool for rapid, non-destructive thermal conductivity and effusivity testing which can be used for solids, liquids, powders, and pastes. This machine operates based on the "modified transient place source technique. It uses a one-sided, interfacial, heat reflectance sensor that applies a momentary, constant heat source to the sample" (Mathis Instruments Ltd., 2012). A known current is applied to a heating element and the temperature rise at the sensor-material interface causes a change in voltage. The thermal conductivity of the material being tested is inversely proportional to the change in voltage. This test is completed in a matter of seconds and the thermal conductivity range that can be tested is 0 to 100 W/mK. Software provided with the machine creates output data in the form of a spreadsheet (Mathis Instruments Ltd., 2012).

The minimum sample size required for testing is 0.67-in. (17-mm). The research team plans to obtain large aggregate particles with a 3/4-in. (19-mm) minimum dimension and use a mechanical polisher to get a clean, polished, and even surface. The minimum sample thickness required for testing is 0.02-in. (0.5-mm) but because the calibration material is 3/8-in. (9.5-mm) thick, the research team attempted to polish aggregates to a thickness of 3/8-in. (9.5-mm). Because aggregates in concrete are effectively saturated, it will be more relevant to test aggregate samples in a saturated state rather than a dry state. Therefore, after polishing, aggregates will be soaked for 24 hours prior to testing.

According to the manufacturer, the accuracy of the Mathis TCi Thermal Conductivity Analyzer is better than 5% and the precision is better than 1% (Mathis Instruments Ltd., 2012). Because some aggregate sources, particularly river gravels, are composed of a wide range of minerals, the research team will prepare and test approximately 15 samples per source to ensure that the source is accurately represented.

5.1.10 Unconfined Freezing and Thawing

The unconfined coarse aggregate freezing and thawing test is a Canadian standard test method that subjects an unconfined aggregate sample to a series of freezing and thawing cycles. The specific method used by this research project was Canadian Standard (CSA) 23.2-24A (*Test method for the resistance of unconfined coarse aggregate to freezing and thawing*) and is described in this section.

A freezer capable of maintaining 0°F (-18°C) is used that has adequate air circulation to prevent a temperature variation of no more than ±1°F (2°C). Aggregate is to be separated into the size fractions listed in Table 5.5.

Table 5.5: Aggregate Size Fractions for Unconfined Freezing and Thawing Testing

Sieve Size	Target Mass	
¾-in. - ½-in.	1250	g
½-in. - 3/8-in.	1000	g
3/8-in. - ¼-in.	500	g
¼-in. - No. 4	350	g

The aggregate samples are then placed in autoclavable plastic containers and saturated with a sodium chloride solution of 3% by mass for 24 ± 2 hours. At the end of this saturation period the aggregate containers are rapidly drained by inverting them over a screen smaller than 5 mm, taking care that the aggregate remains in the container. The containers are then sealed to maintain the moisture level in the container and placed on their sides in the freezer. The samples are frozen for 16 ± 2 hours and then allowed to thaw at room temperature for 8 ± 1 hour. The jars are then rotated one quarter turn before being returned to the freezer. This process is repeated for five cycles of freezing and thawing. If the process of freezing and thawing must be interrupted, the samples are to remain in a frozen state until the cycles can continue.

At the end of the fifth cycle, once the aggregate has returned to room temperature, the containers are filled with tap water and rinsed over a screen smaller than 5 mm five times. The containers are then placed in an oven at 230°F ± 9 °F (110°C ± 5 °C) and dried to a constant mass. The aggregate is then re-sieved over the original sieve size for 3 minutes, as additional shaking is likely to cause mechanical breakdown of the sample. The sample loss is then calculated as a percent loss on each sieve size and is standardized to a normalized gradation.

Variability of the unconfined freezing and thawing test is dependent upon the value of the weighted average loss of the test. The highest single and multi-operator COV is 6% and 9%, respectively, for materials with an average weighted loss of 25%.

5.2 Fine Aggregate Tests

Fine aggregate tests were selected based on a review of literature, a review of other state DOT specifications, and a discussion with personnel in industry and academia. Chapters 2 and 3 contain more information about selection of aggregate tests. Because this research project is funded by TxDOT, TxDOT standards were used when possible. Otherwise, ASTM standards or other widely accepted test methods were used to ensure repeatable and consistent results.

5.2.1 Micro-Deval Test for Fine Aggregates

The Micro-Deval test for fine aggregates is very similar to the Micro-Deval test for coarse aggregates. A standard gradation of sand, ranging from No. 8 (2.36-mm) to No. 200 (75-µm), is placed in the Micro-Deval container along with steel charge and soaked for 1 hour prior to testing. The Micro-Deval container is then rotated for 15 minutes at approximately 100 revolutions per minute. The sample material is then removed and washed over a No. 200 (75-µm) sieve. The remaining material is oven-dried and weighed and the relative amount of material lost, as a percentage, signifies the final Micro-Deval loss. The standard test method used by the research team was ASTM D 7428 (*Resistance of Fine Aggregate to Degradation by Abrasion in the Micro-Deval Apparatus*) and is described in the following section.

The Micro-Deval test requires that the sample aggregate be washed over the No. 200 (75-µm) sieve and dried prior to testing. A standard gradation is specified for concrete aggregate for this test and provided in Table 5.6. The total mass of the sample should be 500 ± 5-g.

Table 5.6: Fine Aggregate Gradation Required for Micro-Deval Test (ASTM D 7428)

Sieve Size	Target Mass
No. 4 – No. 8	50 g
No. 8 – No. 16	125 g
No. 16 – No. 30	125 g
No. 30 – No. 50	100 g
No. 50 – No. 100	75 g
No. 100 – No. 200	25 g
Total	500 ± 5 g

Once the sample has been weighed out, 1250 ± 5-g of stainless steel balls, of diameter 9.5 ± 0.5-mm, should be placed in the Micro-Deval container. The Micro-Deval container is a small stainless steel drum. The aggregate sample can then be placed in the Micro-Deval container and soaked in 750 ± 50-mL of tap water a temperature of 20 ± 5˚C (68 ± 9°F) for a minimum for one hour. After 1 hour, the Micro-Deval container is sealed and placed in the Micro-Deval machine.

The operator sets the appropriate time on the machine such that it will run for 15 minutes. The machine should be calibrated to revolve at 100 ± 5 revolutions per minute and the final revolution count should be 1500 ± 10 revolutions. After 15 minutes of revolutions, the Micro-Deval container is removed and the contents are washed over a No. 200 (75-µm) sieve. Material passing the sieve is discarded. The retained material is oven-dried to a constant weight and weighed after drying. The oven-dried weight is recorded and compared to the original weight to get a percent loss calculation for the final Micro-Deval loss.

The research team performed two Micro-Deval tests per source and recorded the mean loss, unless the test results were different by more than 1.0%. In this case, a third Micro-Deval test was performed and the mean of the three tests was considered acceptable unless an outlier existed. The inside surface of the stainless steel drum can affect the results of the Micro-Deval test for fine aggregates, so it is recommended that a reference sand be run periodically. Testing of carbonate sands can lead to "polishing" of the steel drum surface which has been shown to affect test results (Rogers C. , 1998).

According to the ASTM standard, the single-operator COV is approximately 3.4% and the multi-laboratory COV in approximately 8.7% (ASTM International, 2008).

5.2.2 Specific Gravity and Absorption Test for Fine Aggregates

The specific gravity and absorption test for fine aggregate requires that a representative sample of an aggregate approximately 3000 g in mass and passing the No. 4 (4.75-mm) sieve be obtained and soaked for at least 24 hours. The aggregate is then dried to SSD state, weighed in a calibrated pycnometer, and dried to an oven-dry state as described by the following procedures. The standard used by the research team was Tex-403-A (*Saturated Surface-Dry Specific Gravity and Absorption of the Aggregates*).

After a representative sample of aggregate is obtained, the aggregate is soaked (in a non-metal tub to avoid reaction) to ensure that all permeable pores of the aggregate become filled with water. The water should be at a temperature of 23 ± 2˚C (73 ± 3˚F). After the soaking period, the operator removes a sample of the fine aggregate and places it a clean, smooth surface such as a metal pan. The sample is spread out and allowed to air dry for several hours. While drying, the operator should stir the sand periodically to ensure that none of the sample gets drier than the SSD state. Some standards allow the use of external heat, but the TxDOT test method does not. Drying may take several hours or several days depending on the aggregate sample. A fan may be used to accelerate convection and thus speed the drying time. To determine if the sample is at SSD, the operator places a metal cone (wide end down) on a metal base plate and fills the cone with sand until slightly overflowing. The operator then lightly tamps the sand in the cone 25 times by dropping the tamper about 5-mm (0.2-in.) above the surface of the fine aggregate. The moisture condition of the fine aggregate sample will be evident upon lifting the cone. If the material slumps completely, then it is too dry. If the material maintains its shape completely, then it is too wet. A sample in the SSD condition should slump slightly. Test materials are pictured in Figure 5.8.

Figure 5.8: Testing a Sand for Specific Gravity and Absorption

At this point, the aggregate has reached the SSD condition. The operator should obtain and immediately weigh approximately 1200 g of aggregate in the SSD. Next, the SSD aggregate is placed in the pycnometer, which should be calibrated by the same methods described in Section 5.1. The operator should take extra care in placing aggregate in the pycnometer so that all material is accounted for. The jar is filled with water at 23 ± 2˚C (73 ± 3˚F) until it reaches the brim. The pycnometer should be agitated so that any entrapped air is freed. The pycnometer cap is again placed on the jar and a rubber bulb or syringe is used to fill the pycnometer until a

rounded bead of water appears on top of the pycnometer cap. The outside of the pycnometer is dried and the pycnometer with aggregate is weighed and this weight recorded.

Finally, the aggregate is removed from the pycnometer, placed in a pan, and the pan placed in an oven where the aggregate is dried to constant mass. The weight of the aggregate at SSD, the weight of the pycnometer with water, and the weight of the pycnometer with aggregate are used to calculate the specific gravity and absorption capacity of the aggregate. Specific gravity is typically reported to the nearest 0.01 and absorption to the nearest 0.1% (Texas Department of Transportation, 1999).

The research team noticed that allowing the sand to cool to room temperature also allowed an uptake of moisture from the air. A pan of oven-dry sand could easily gain a few tenths of a percent of mass from moisture in the air alone in a matter of minutes, thereby skewing absorption values. Therefore, it is recommended that the sand be weighed immediately after removal from the drying oven.

5.2.3 AIMS 2.0

AIMS is a machine consisting of a camera, lights, computer software, and movable trays, designed to capture and analyze the shape, angularity, and texture of coarse aggregates and the form and angularity of fine aggregates. The camera captures images of the aggregate particles, either lit directly or backlit, and the software analyzes these images and provides the user with data summarizing the shape characteristics. The camera in the AIMS apparatus is capable of capturing particles as small as 75-µm (retained on the No. 200 sieve).

For fine aggregates, the user places a set of fine aggregate particles (separated by fraction size) on an opaque tray and places this tray into the machine The AIMS machine analyzes at least 150 particles for analysis for each size fraction. After the AIMS machine has analyzed one size fraction, the user removes the tray, cleans it, and places the next size fraction of fine aggregate on the tray. This process is repeated until all size fractions have been analyzed. Because the fine aggregate particles are so small, many of them touch as they are distributed across the tray by the operator. Fortunately recent advances in the AIMS technology include a touching particle factor to eliminate inaccurate angularity analysis of fine aggregates where particles touch or overlap (Mahmoud, Gates, Masad, Erdoğan, & Garboczi, 2010). Output from the AIMS consists of quantified measurements of form and angularity for each particle, and a mean and standard deviation of each value as well. Aggregates typically follow a standard statistical distribution. The research team performed AIMS analysis of fine aggregate before Micro-Deval and after Micro-Deval to determine if a change in form and angularity would provide meaningful data.

5.2.4 Flakiness Sieve

After observing problems in field compact of HMA, Rogers and Gorman in Ontario sought to develop an inexpensive and quick test to determine a measurement of flakey particles in a sand. Past research has demonstrated that sands in excess of 30% flakey particles may have issues during compaction of hot mix asphalt. Rogers and Gorman realized that slotted sieves, traditionally used for seeds and grains, could also be used to evaluate fine aggregate (Rogers & Gorman, 2008). There is currently no accepted standard for this flakiness test for fine aggregate, but Rogers and Gorman have provided a description of this test and its procedures in the appendix of their 2008 paper entitled "A Flakiness Test for Fine Aggregates."

The flakiness sieve test, described by Rogers and Gorman, uses two slotted sieves with slots of 1.8 mm and 1.0 mm, respectively. The fine aggregate is sieved and broken down into separate size fractions. The sand retained on the No. 8 (2.36-mm) sieve is placed on the 1.8-mm slotted sieve and agitated. The same is done for the sand retained on the No. 16 (1.18-mm) sieve, except the 1.0-mm slotted sieve is used. The operator uses a set of tweezers to ensure that all flakey particles pass through the slots. All particles passing through the slotted sieves are considered flakey, and the final results are calculated by mass. Rogers and Gorman recommend testing at least 60 g of fine aggregate per fraction size to obtain a representative result. To calculate the final flakiness value, the results from the No. 8 and No. 16 can be averaged, or a weighted average can be calculated based on the gradation of the fine aggregate of interest.

Researchers tested each fine aggregate for flakiness using the test method described by Rogers and Gorman. Slotted grain sieves 200 mm (8 in.) in diameter meeting ISO 5223 were obtained from Endecott. Fine aggregate samples were obtained by first oven-drying and sieving a sample, and then using a mechanical splitter. At least three flakiness tests of 20.0 g each were run per fraction size, thus a total of at least 120.0 g was tested for each fine aggregate source.

5.2.5 Grace Methylene Blue Test

Because there is an inherent degree of subjectivity to the AASHTO methylene blue test (AASHTO TP 57), researchers at W.R. Grace & Co. sought to improve this test method by removing subjectivity and enhancing repeatability and reproducibility. The test developed by Grace is similar to the traditional AASHTO test, but the test is performed on an entire sample of sand (not just the microfines) and uses a UV colorimeter to analyze the color of the final filtered solution sample. The new methylene blue test allows the entire sample to be measured, which is important because all clay in the sand is measured which ensures more representative results.

W.R. Grace & Co. generously supplied the testing equipment and test procedures for their Grace methylene blue test. Testing materials needed for this test include a Hach DR 850 Colorimeter, a micropipette, a portable balance, several plastic and glass test tubes, a plastic weigh boat, a 3-mL syringe with luer-lok adapter, and a 0.2-μm syringe filter. Prior to testing a fine aggregate sample, the concentration of methylene blue solution should be calculated and a correction factor used if the solution concentration differs from 0.50% by weight.

Once the methylene blue solution concentration is confirmed, a slightly moist sample of fine aggregate weighing at least 20 g should be obtained. A sample of 20 g of sand should be weighed and added to a 45-mL plastic test tube with 30 g of methylene blue solution. The tube should be capped and agitated for one minute. A 3-minute rest period should follow and then the sample should be agitated for an additional minute. Approximately 2 mL of this test solution should be transferred to a 3-mL syringe with a luer-lok filter fitted. The syringe should be depressed such that 0.5–1.0-mL of solution is filtered and transferred to a new 1-mL plastic tube. Using the micro-pipette, 130 μL of solution is transferred from the 1-mL plastic tube to a new, empty 45-mL plastic test tube. The 130-μL sample is diluted by adding water to make the total diluted solution 45 g. The 45-mL plastic tube is then capped and mixed. Next, the diluted solution is transferred to a clean 16-mm glass tube and is ready to be measured by the colorimeter. Before measuring the diluted solution, the colorimeter should be zeroed by measuring a sample of water. Finally, the diluted solution can be measured by the colorimeter. The output of the colorimeter is a reading of milligrams of methylene blue per gram of sand. After using the correction factor, the methylene blue value can be divided by 1.60 to obtain an equivalent amount of sodium montmorillonite clay (W.R. Grace & Co., 2010).

The research team performed three Grace methylene blue tests per sample. Researchers at Grace determined that reproducibility and repeatability were comparable to the traditional AASHTO method (Koehler, Jeknavorian, Chun, & Zhou, 2009).

When performing this test, researchers noticed that when placing the sand in the initial weigh dish, the entire sample was not successfully transferred to the 45-mL test tube. A small amount of microfines remained adhered to the initial weigh dish or was fine enough to disperse into the air as the sample was being transferred. This error led to changes of up to 0.3% final clay content. As a result, researchers recommend placing the sand sample directly into the 45-mL test tube after tarring the scale appropriately.

5.2.6 Organic Impurities

In the organic impurities test, a fine aggregate sample is subjected to a sodium hydroxide solution and allowed to remain undisturbed to react for 24 hours. Any organic material in the sample will react with the sodium hydroxide solution to produce a dark liquid. The operator examines the color of the supernatant liquid and if it is darker than a standardized color, the fine aggregate is subjected to a 7-day mortar cube strength test. The fine aggregate is typically deemed to have an unacceptable amount of organic content if the compressive strength of the mortar cube is less than 90–95% of a control sample. The standard test method used by the research team was Tex-408-A (*Organic Impurities in Fine Aggregates for Concrete*) and is described in the following section.

Materials needed for this test include small glass bottles with volume of 12 to 16 oz (355 to 473 mL), a Gardner glass color standard, and 3% sodium hydroxide solution. An air-dried sample of approximately 300 g should be obtained prior to testing. The glass bottle should be filled with the air-dried sand up to the 4.5-oz (133-mL) mark. A small amount of sodium hydroxide (enough to cover the sample) should be added to the glass bottle. The bottle should be capped and shaken. More sodium hydroxide is then added to the 7-oz (207-mL) mark and the bottle is capped and shaken again. The bottle is then placed aside and allowed to sit undisturbed for 24 hours. After the 24-hour resting period, the operator should observe the color of the supernatant liquid and compare it to the Gardner color standard. If the color of the liquid is darker than the Gardner No. 11, the fine aggregate is subjected to a 7-day mortar cube strength test. The fine aggregate is typically deemed to have an unacceptable amount of organic content if the compressive strength of the mortar cube is less than 95% of a control sample (Texas Department of Transportation, 1999).

5.2.7 Sand Equivalent

The sand equivalent test is a test method that is used to determine the proportion of "detrimental fine dust of clay-like particles in soils or fine aggregates" (Texas Department of Transportation, 2009). This test subjects a fine aggregate sample to a flocculating solution (calcium chloride) in order to separate fine particles from the coarser sand. The higher the sand equivalent value, the cleaner the sand is perceived to be. The standard test method used by researchers for this test was Tex-203-F (*Sand Equivalent Test*) and it is described in the following section.

Materials needed for this test include calcium chloride solution, a transparent graduated plastic cylinder, rubber stopper, agitator tube, an 85-mL (3-oz.) measuring can, weighted foot assembly, 3.8-L glass bottle, and plastic or rubber tubing. The graduated plastic cylinder should have a 1.25-in. (31.8-mm) inside diameter and a height of approximately 17 in. (432 mm). To

prepare the calcium chloride solution, 577 g of ACS calcium chloride dehydrate should be dissolved in 1.9 L of distilled water. This solution should be further diluted by adding 88 cc of the solution to 3.8 L of distilled water. This final solution is the working calcium chloride solution. All mixing and dilution should be performed at 22 ± 3˚C (72 ± 5˚F). The workstation should be setup such that the calcium chloride solution is located 914 ± 25-mm (3-ft. ± 1-in.) above the work surface and can be siphoned into the graduated plastic cylinder.

   Prior to testing, a representative, oven-dried fine aggregate sample of at least 500 g should be obtained. This material should be sieved over the No. 4 (4.75-mm) sieve to remove any coarse material. After obtaining the sample material, the operator siphons calcium chloride solution into the graduated plastic cylinder such that the measurement reading is 101.6 ± 2.5-mm (4 ± 0.1-in.). The operator fills the 85-mL (3-oz.) measuring can with sample material and then slowly scrapes a scapula at a 45˚ angle over the measuring can to remove excess sand and ensure that 85 mL of bulk sand is obtained. The sample is then transferred to the graduated plastic cylinder. The cylinder is then agitated to remove air bubbles and allowed to sit for 10 ± 1 minutes (see Figure 5.9-A). The operator then stops the cylinder and places it in the mechanical sand equivalent shaker for 45 ± 1 seconds. The stopper is removed and the agitator is forced through the material with a gentle twisting and jabbing motion as the cylinder is rotated about its vertical axis (see Figure 5.9-B). This process should be continued so that all microfines and clay material are flushed from the coarse material until the level of the liquid reaches 381-mm (15-in.). The cylinder is allowed to sit for 20 ± 0.25-min and then the operator reads the level at the top of the clay layer. This value is recorded as the clay reading. Figure 5.9-C displays the sand equivalent test at this point for a sand with an unusually high clay reading. The operator then obtains the sand reading by gently dropping the weighted foot assembly into the cylinder until it comes to rest on the sand layer. The sand reading is calculated by subtracting 254 mm (10 in.) from the top indicator level. The final sand equivalent value is calculated by dividing the sand reading by the clay reading and multiplying by 100.
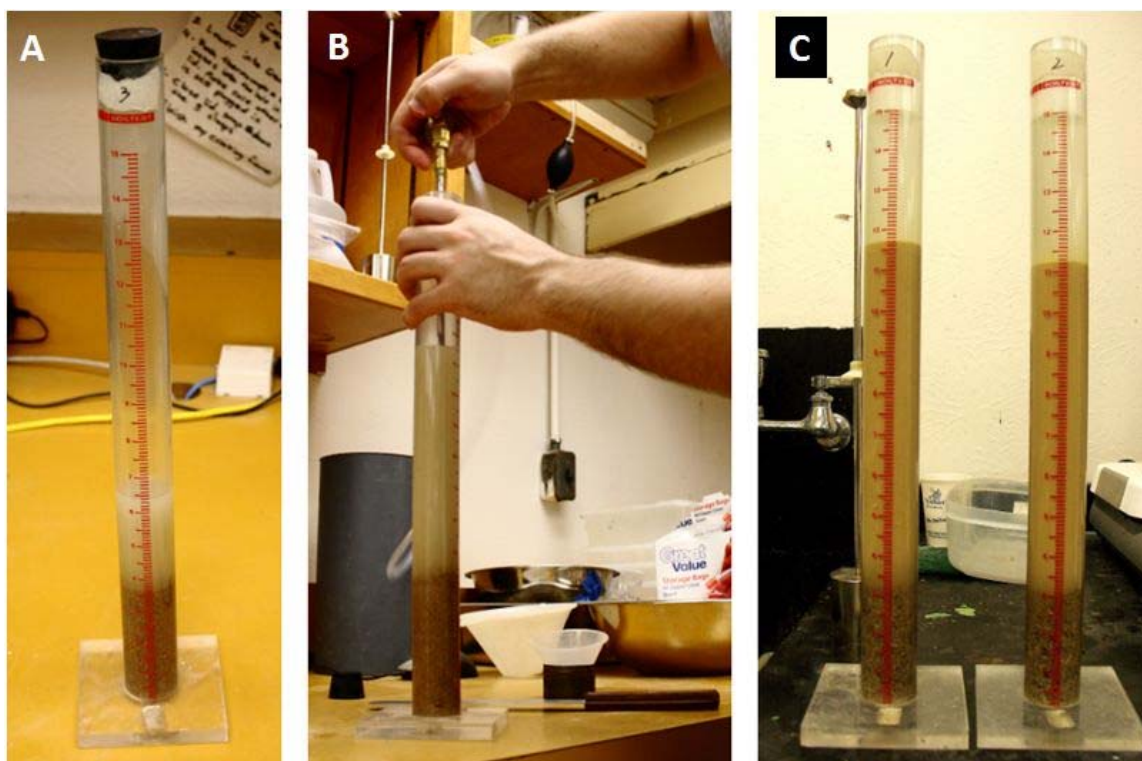
Figure 5.9: Sand Equivalent Testing

As per the Tex-203-F specification, the researchers performed this test twice per source and calculated the mean value. If the two tests differed by more than four points, a third test is performed and the mean of all three recorded. If the three tests differ by more than four points, the test results are discarded and the test must be performed again. The sand equivalent reading is typically reported to the nearest whole number.

According to the ASTM standard of this test (ASTM D 2419), the single-operator standard deviation is 1.5 for sand equivalent values greater than 80 and 2.9 for sand equivalent values less than 80. Therefore, two tests should not differ by more than 4.2 for sand equivalent values greater than 80 and 8.2 for sand equivalent values less than 80 (ASTM International, 2009). This precision is reflected by the Tex-203-F test standard, which requires discarding results differing by more than four points.

5.2.8 Acid Insoluble Residue

The acid insoluble residue test is one way of determining carbonate content of fine aggregate. In this test, a fine aggregate sample is subjected to hydrochloric acid and carbonate aggregates are dissolved by the acid while siliceous aggregates remain. The standard test method used by researchers for this project was Tex-612-J (*Acid Insoluble Residue for Fine Aggregate*) and the procedures for this test are described in the following section.

Materials needed for this test include a 2000-mL beaker, a stirring rod, a porcelain filtration apparatus, No. 2 filter paper, plastic tubing, a drying dish, and a hydrochloric acid solution. Prior to testing, a representative, oven-dried fine aggregate sample of at least 500 g should be obtained. From this sample, 25 g of fine aggregate is placed in the 2000-mL beaker. The operator places the beaker in a fume hood and slowly adds hydrochloric acid until reaction

ceases. An additional 25 mL of hydrochloric acid is added and stirred to ensure complete reaction. The remaining solution is decanted without loss of any sample material and then the remaining sample and solution is filtered over a No. 2-H filter paper. The filter paper is placed over the porcelain filtration apparatus such that distilled water can be washed over the sample to remove all acid without removing remaining aggregate. The filter paper, with remaining aggregate sample, is then oven-dried for 2 hours, and the final mass is recorded. The final mass of the sample is compared to the original mass to calculate the acid insoluble residue percentage by weight (Texas Department of Transportation, 2000).

The research team performed three tests per source and calculated a mean value to report as the acid insoluble residue for that source.

5.3 Concrete Tests

In order to relate aggregate tests to performance criteria, the research team decided to conduct mechanical concrete tests with the coarse aggregate as the only variable. Ideally, performance histories of aggregates would be available and could be used to rate an aggregate as "good," "fair," or "poor," but unfortunately this information is not always readily available. As a result, researchers will attempt to glean data and interpret results of mechanical concrete tests and their relation to the aggregate tests.

Researchers hope to begin mixing concrete samples soon and will cast ten 4-in. x 8-in. (100-mm x 200-mm) cylinders and three 4-in. x 4-in. x 14-in. (100-mm x 100-mm x 255-mm) beams per aggregate source. A total of 10 to 15 aggregate sources will be used for mixing and casting concrete.

The concrete mixture design has already been selected: a volume-controlled concrete mixture meeting requirements for TxDOT CoTE testing. As such, the concrete mixture will be a Class P pavement mixture with Type I cement from Alamo Cement. No supplementary cementitious materials or admixtures will be used. The fine aggregate, which will function as a control, is a clean, natural river sand obtained from TXI Webberville.

5.3.1 Compressive Strength

Compressive strength testing of concrete is a common quality control procedure to ensure that the concrete is hydrating properly and that strength is gained at the necessary rate. The research team will cast 4-in. x 8-in. (100-mm x 200-mm) concrete cylinders, and use Tex-418-A (*Compressive Strength of Cylindrical Concrete Specimens*) to determine the compressive strength of these concrete mixtures. The Tex-418-A standard simply refers users to the ASTM version of this test, which is ASTM C 39 (*Compressive Strength of Cylindrical Concrete Specimens*). The procedures of this test are discussed in the following section.

The compression testing machine available to the research team is a Forney FX-700, which is more than capable of performing this test within the prescribed constraints. Other necessary equipment such as steel caps and neoprene bearing pads were also available to the research team. After curing the cylindrical concrete specimens for 28 days (± 20 hours), the specimens are removed from the curing room and placed in a 5-gallon bucket full of water so that the specimen remains moist until immediately prior to testing. The operator then takes the steel caps and places the neoprene bearing pads inside the steel caps. After 100 tests, or the first visible sign of cracking, the neoprene pads should be discarded, and replaced with new pads. The operator then removes the concrete specimen from the water and places the caps on both ends of the specimen. The concrete specimen is then placed in the compression machine. The operator

should ensure that the surface of the bearing blocks in the machine is free from debris, and that the specimen is centrally placed on the blocks. At this point, the cage or screen on the testing machine is closed and locked for the safety of the test operator. The operator can then begin applying load to the specimen. The load should be applied at a rate of 0.25 ± 0.05 MPa/s (35 ± 7 psi/s), which means that the test may take several minutes, depending on the strength of the specimen. This load rate should be held as constant as possible for the duration of the test. The test is complete when the specimen displays a "well-defined fracture pattern" and supports no additional load. The operator then removes the load from the specimen, notes the fracture pattern, and records the final load. The final load divided by the average cross-sectional area of the specimen is the strength of the specimen (ASTM International, 2012).

For 4-in. x 8-in. (100-mm x 200-mm) specimens with strengths between 17 and 32 MPa (2500 and 4700 psi), the COV for single-operator use has been found to be 3.2%. Therefore, the acceptable range of individual cylinder strengths is 9.0% for two cylinders or 10.6% for three cylinders (ASTM International, 2012). The research team will test the compressive strength of three specimens per aggregate source, with testing to be performed at 28 days.

5.3.2 Modulus of Elasticity

The modulus of elasticity is an important property of concrete because it will dictate the stress imposed by a given strain. Strains, caused by thermal expansion for example, will cause higher stresses for concrete with higher elastic modulus of elasticity. Modulus of elasticity in the linear range can be calculated by obtaining two data points of stress and strain in the linear elastic range. The most common test method for measuring modulus of elasticity of concrete in compression is ASTM C 469 (*Static Modulus of Elasticity and Poisson's Ratio of Concrete in Compression*). The research team will use ASTM C 469 to determine the modulus of elasticity for several concrete mixtures.

The two main pieces of equipment necessary to perform this test are a compression testing machine and a compressometer. The compressometer is a device that fits around the concrete cylinder and is capable of measuring very precise changes in length between two gauge points. The gauge points should be separated by a distance at least three times the length of the maximum size aggregate. The deformation may be measured by a dial gauge, strain gauge, or by a linear variable transformer. Prior to the test, a matching cylinder should be tested in compression so that the ultimate load can be determined.

To begin the test, the operator removes a concrete cylinder from a curing room or bath, attaches the compressometer, and places the assembly in the compression testing machine. The specimen should be loaded twice, such that the first loading is used to correct any errors in the placement of the compressometer. During the second loading, the load rate should be 250 ± 50 kPa/s (35 ± 7 psi/s). The applied load and the longitudinal strain should be recorded when the longitudinal strain reaches 50 millionths and when the applied load reaches 40% of the ultimate load (as determined from the previous test). The modulus of elasticity can then be calculated by determining the slope of the stress-strain curve from a simple equation provided in ASTM C 469 (ASTM International, 2010).

Researchers plan on performing two modulus of elasticity tests per coarse aggregate for a total of 10 to 15 sources. Researchers will test one concrete cylinder in compression to obtain the ultimate strength, then test two cylinders for modulus of elasticity, and then test the same two cylinders for compressive strength.

According to ASTM C 469, the results of tests of two cylinders from the same batch should be no more than 5% different (ASTM International, 2010).

5.3.3 Flexural Strength

Flexural strength of concrete is important for resistance to tension and cracking. Flexural strength is typically determined by subjecting an unreinforced concrete beam to flexure by imposing one or two point loads in the middle of the span. The TxDOT method used by the research team is Tex-448-A (*Flexural Strength of Concrete Using Simple Beam Third-Point Loading*) and simply refers the user to ASTM C 78 (*Flexural Strength of Concrete*).

The flexural strength of concrete will be tested at third-point loadings as prescribed by the ASTM standard. The test setup should be similar to that shown in Figure 5.10. The bearing surfaces for the test specimen should be case-hardened steel and consist of partial cylinders with at least 0.80 radians of curved surface so that rotation is not restricted during loading.
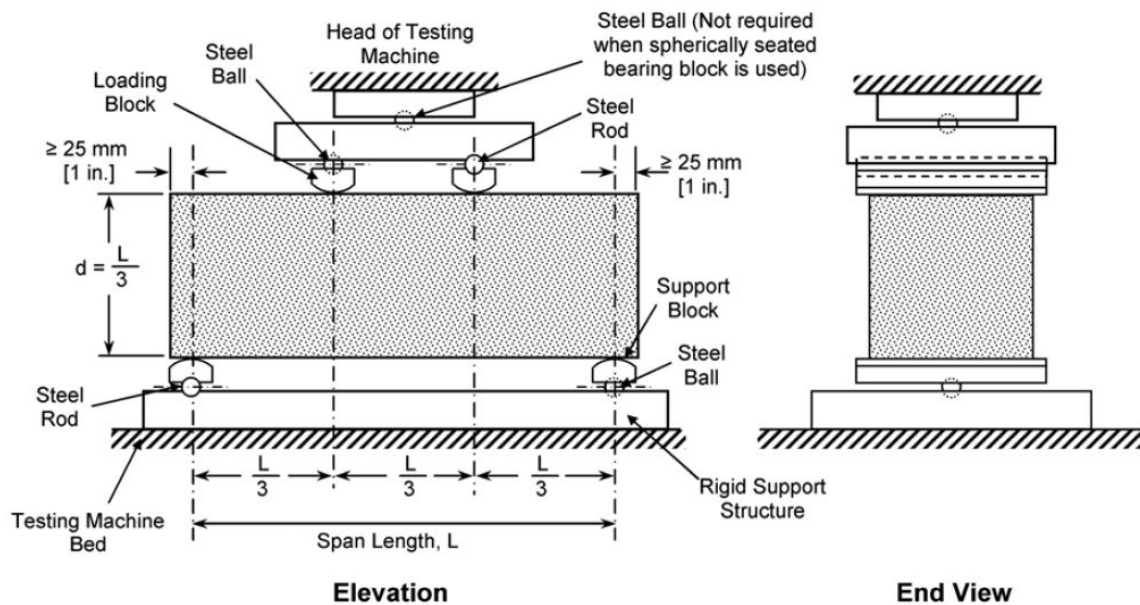
Figure 5.10: Setup of Concrete Flexure Test from ASTM C 78 (ASTM International, 2010)

Before placing the prismatic concrete specimen in the test apparatus, it should be placed on its side relative to its casting position. The operator should then center the concrete specimen in the test apparatus while conforming to the ASTM tolerances for position. The operator can then load the specimen up to 6% of ultimate load before again checking the position of the specimen and determining if there is any gap between the specimen and test blocks. Leather shims can be used to eliminate any gaps. The operator can then begin loading the specimen such that the tension face experiences a stress rate of 0.9 to 1.2 MPa/min (125 to 175 psi/min). The ASTM standard provides an equation for calculating the loading rate based on the geometry of the concrete specimen. The concrete specimen is loaded to failure and the operator should note the location of the fracture that initiated failure. If the fracture is located more than 5% outside the middle third of the beam, then the test results must be discarded. Otherwise, the modulus of rupture can be calculated based on simple equations located in ASTM C 78.

Strength of concrete will influence the precision of the test but the ASTM standard provides general information about precision. The single-operator COV has been found to be 5.7% and the multilaboratory COV has been found to be 7.0% for specimens from the same batch. Therefore, two tests using specimens from the same batch should not differ by more than 16% or 19% respectively (ASTM International, 2010).

The research team will create three 4-in. x 4-in. x 14-in. (100-mm x 100-mm x 255-mm) beams per aggregate source. A total of 10 to 15 aggregate sources will be used for mixing and casting concrete. The Tex-448-A standard provides an adjustment factor when beams are tested that are not 6-in. x 6-in. (150-mm x 150-mm) in cross section. However, the standard does not provide the adjustment factor for beams 4-in. x 4-in. in cross section so researchers will consult with TxDOT laboratory personnel to determine an appropriate adjustment factor.

5.3.4 Splitting Tensile Strength

Splitting tensile strength of concrete is an indirect test method used to determine the tensile strength of concrete. This test method is often used in lieu of flexure beam testing because of the reduced material needed per sample, as well as the more simplified test setup. Three 4-in. x 8-in. (100-mm x 200-mm) concrete cylinders were cast, and Tex-421-A (*Splitting Tensile Strength of Cylindrical Concrete Specimens*) was used to determine the strength of these concrete mixtures. The Tex-421-A standard simply refers users to the ASTM version of this test, which is ASTM C 496 (*Splitting Tensile Strength of Cylindrical Concrete Specimens*). The procedures of this test are discussed in the following section.

To begin the test, first the diameter and lengths of the specimen must be recorded at three locations. The sample is then placed in a jig to allow marking diametral lines on the ends of the sample. The lines are used to assist in centering the sample onto plywood bearing strips having dimensions of 1/8 in. thick, (3 mm) 1 in. wide (25 mm), and equal to or slightly longer than the specimen. Two strips are used in the test—one below and one above the sample—and are discarded at the end of the test. A loading rate of 100 to 200 psi/min (0.7-1.4 MPa/min) is applied continuously until failure of the specimen. The ultimate load at failure is recorded and the type of fracture surface is documented.

The COV for single-operator use has been found to be 5% for 6-in. x 12-in. (150-mm x 300-mm) specimens with an average strength of 405 psi (2.8 MPa). The acceptable range of individual cylinder strengths should not differ by more than 14% for two cylinders (ASTM International, 2012). The 28-day testing was performed on three specimens per concrete mixture.

5.3.5 Coefficient of Thermal Expansion (CoTE)

CoTE of concrete is a particularly relevant test considering the issues that TxDOT has seen from high CoTE concrete mixtures in CRCP pavements. Section 6.10 documents the observed and perceived problems further. Researchers will use Tex-428-A (*Determining the Coefficient of Thermal Expansion of Concrete*) to test for CoTE.

This test requires a water bath, support frame for the cylinder, a measuring device such as a linear variable differential transformer (LVDT), and a saw to cut cylinders down to size. The support frame should be made of stainless steel with the exception of the vertical members, which should be made of Invar, a material with low CoTE. The base plate should be 10 in. (254 mm) in diameter with three equally spaced support buttons to form circles of 2 in. (50 mm) and 3 in. (75 mm) diameter. A measuring device such as a spring-loaded submersible LVDT should be attached to the top of the frame to provide expansion measurements.

Prior to testing, the concrete cylinder should be saw-cut such that the length is 6 in. (150 mm) and both ends are plane to within 0.002 in. (0.050 mm). The specimens should be conditioned in a saturated limewater solution at 73 ± 4˚F (23 ± 2˚C) for at least 48 hours. After conditioning, the specimens are removed from the limewater, measured, and the original length recorded with a caliper within 0.004 in. (0.1 mm). The specimens are then placed in the support frame in the water bath with LVDT attached (note that a typical standard water bath can hold two or three support frames with specimens attached). The water bath is set to 50 ± 2˚F (10 ± 1˚C) for an hour. At this point the test has begun and the water temperature and displacement (as measured by the LVDT) should be recorded at 1-minute intervals for the remainder of the test. The water bath should be heated and cooled again in accordance with Figure 5.11. After the test cycle is complete, the operator performs a regression analysis on the temperature versus displacement plot for a heating or cooling phase. The slope of the linear regression line divided by the length of the specimen will provide the CoTE. A correction factor may be added based on the type of support frame used (Texas Department of Transportation, 2011). No precision information for this test is available in either the TxDOT or AASHTO standards.
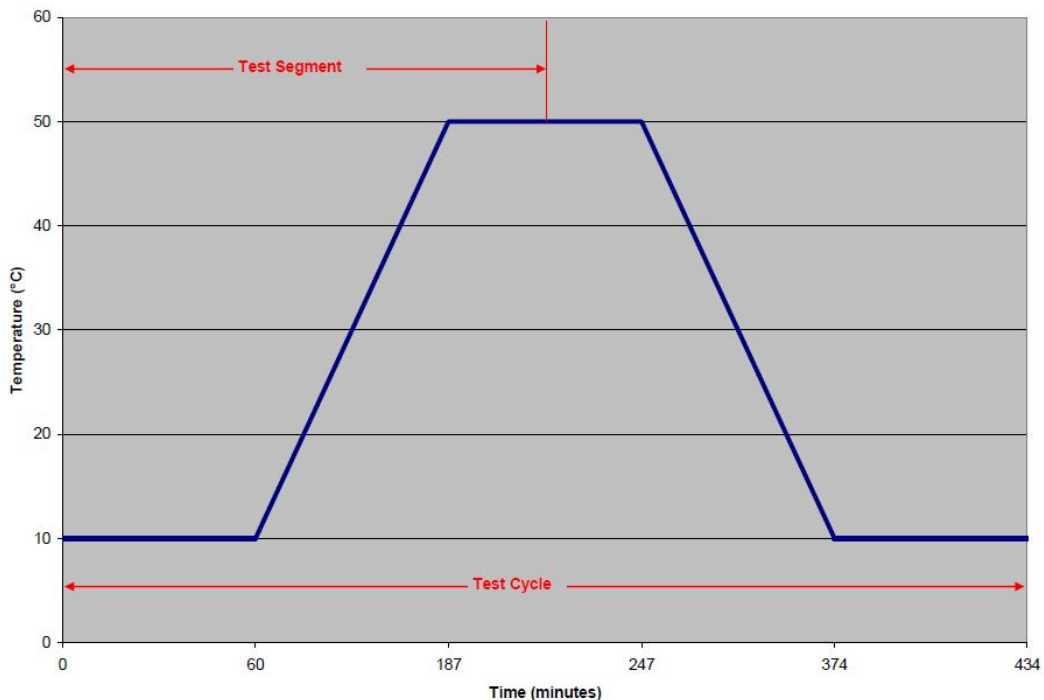
Figure 5.11: Temperature Cycle of Water Bath Required by Tex-428-A for CoTE Testing (Texas Department of Transportation, 2011)

The research team will perform CoTE tests on two concrete specimens per concrete mixture for a total of 10 to 15 aggregate sources. The cylinders will be tested at an age of no earlier than 28 days and no later than 90 days. When possible, the research team will also subject cores from aggregate sources to the same test and compare results.

Chapter 6. Coarse Aggregate Test Results

This chapter contains the results of coarse aggregate testing for the 58 aggregate sources collected. Data are presented graphically, with a primary graph showing all 58 aggregates. Discussion of the data will occur in Chapter 7. The data from this chapter will be presented in tabular form in Appendix B.

6.1 Micro-Deval

Micro-Deval testing was the preliminary test used to screen incoming aggregate samples. This test was used as the preliminary screener because of the quick completion time and low variability associated with the test. Two tests per aggregate sample were run to verify the published variability associated with the test. The results for all Micro-Deval tests are presented in Figure 6.1. Any aggregates with a loss of over 17%, the value typically regarded as the upper limit for acceptable performance under CSA A23.2-29A, were more closely scrutinized in the remaining testing properties, including searching for reported issues with field performance.
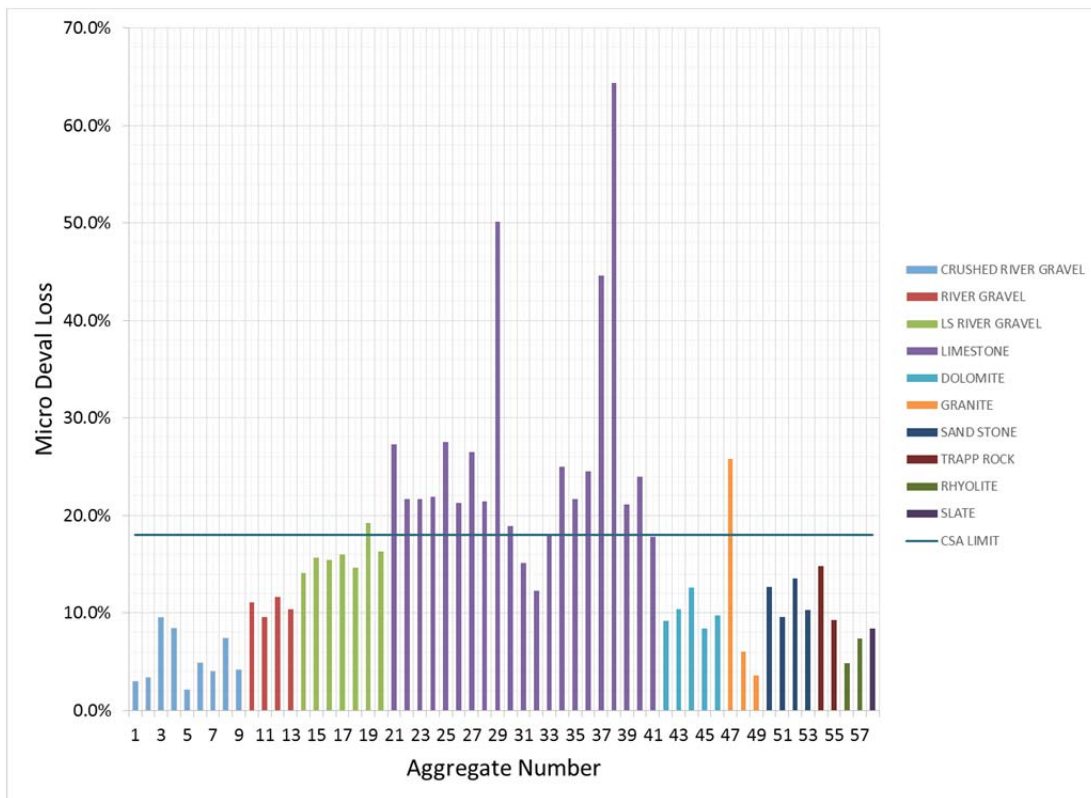
Figure 6.1: Micro-Deval Test Results

6.2 Specific Gravity and Absorption

A wide range of specific gravity and absorption values were observed for the aggregate set. Specific gravity values ranged from 2.40 to 3.08, absorption values ranged from 0.4% to 8.4%. The results for all specific gravity and absorption tests are presented in Figure 6.2. Gravels, aggregates 1 through 20, had a uniform specific gravity; however, the percent

93

absorption almost doubles when comparing siliceous gravels with limestone gravels. Limestones (aggregates 21–41) had a wider range in specific gravity; also, absorption is much more variable. Dolomites and trapp rock (aggregates 42–46 and 54–55) had higher specific gravity and lower absorption than the remaining lithologies (granite, sandstone, rhyolite, and slate).
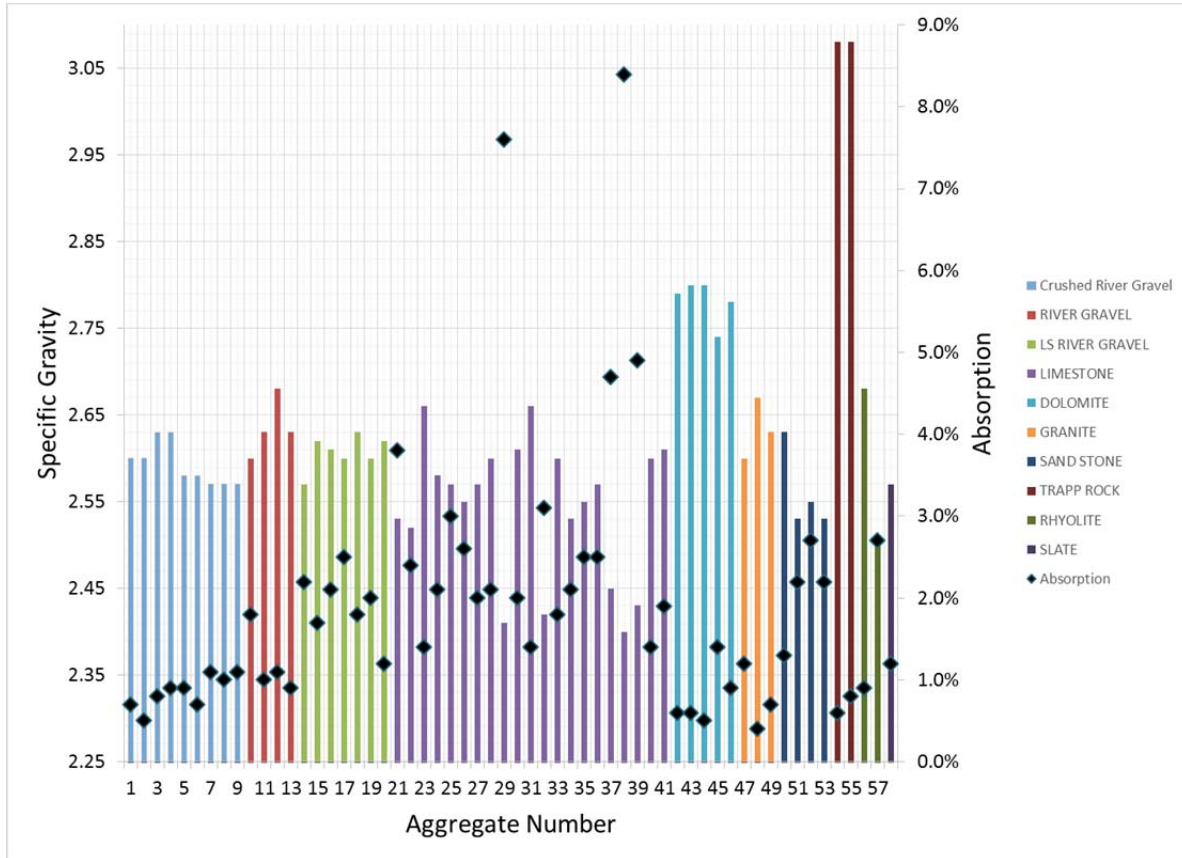
Figure 6.2: Specific Gravity and Absorption Results

94

6.3 LA Abrasion

LA abrasion testing is presented in Figure 6.3. This test is typically used to measure aggregate resistance to breakage. The typical loss limit specified for this test is 40%, and only three of the aggregate sources tested higher than this limit: two limestones (aggregates 29 and 38) and a granite (aggregate 47).
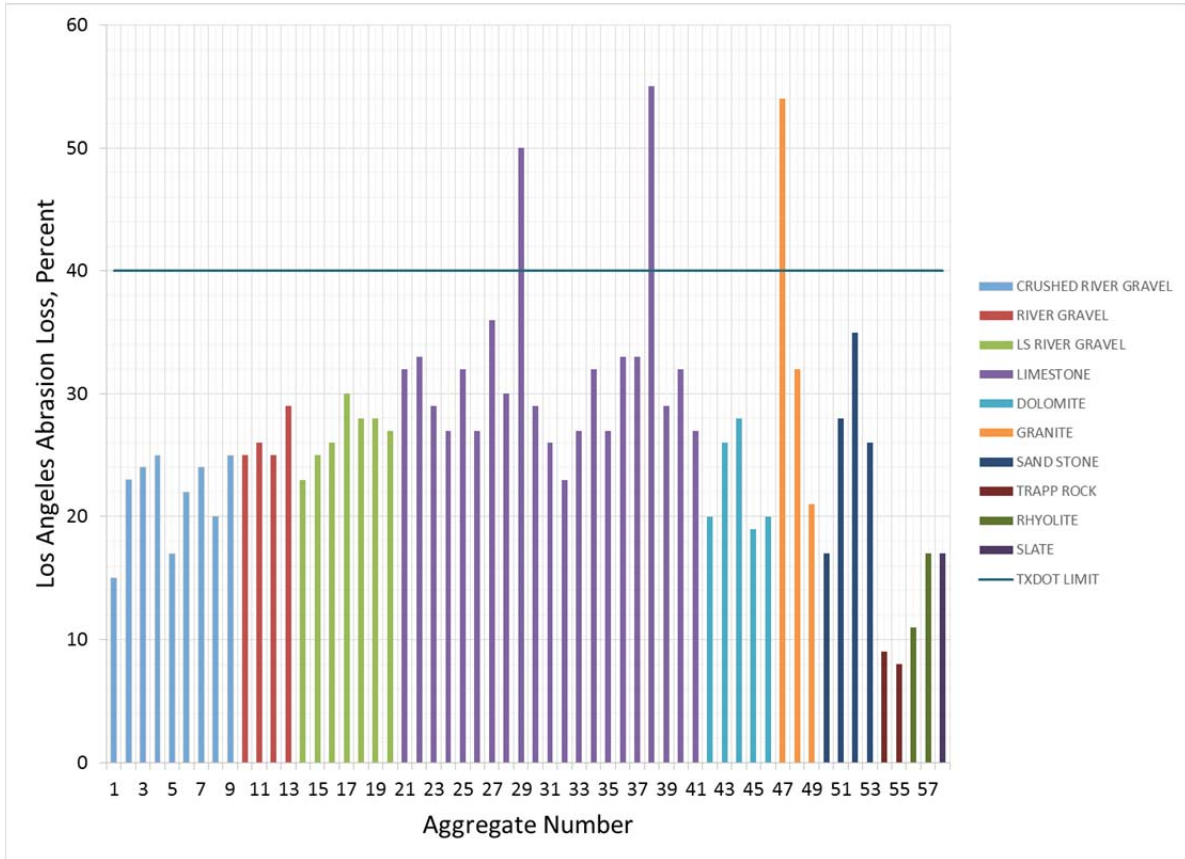
Figure 6.3: LA Abrasion Test Results

6.4 Magnesium Sulfate Soundness

Magnesium sulfate soundness testing has long been the standard test for indirectly determining the freezing and thawing durability of an aggregate. The results from the testing are presented in Figure 6.4.
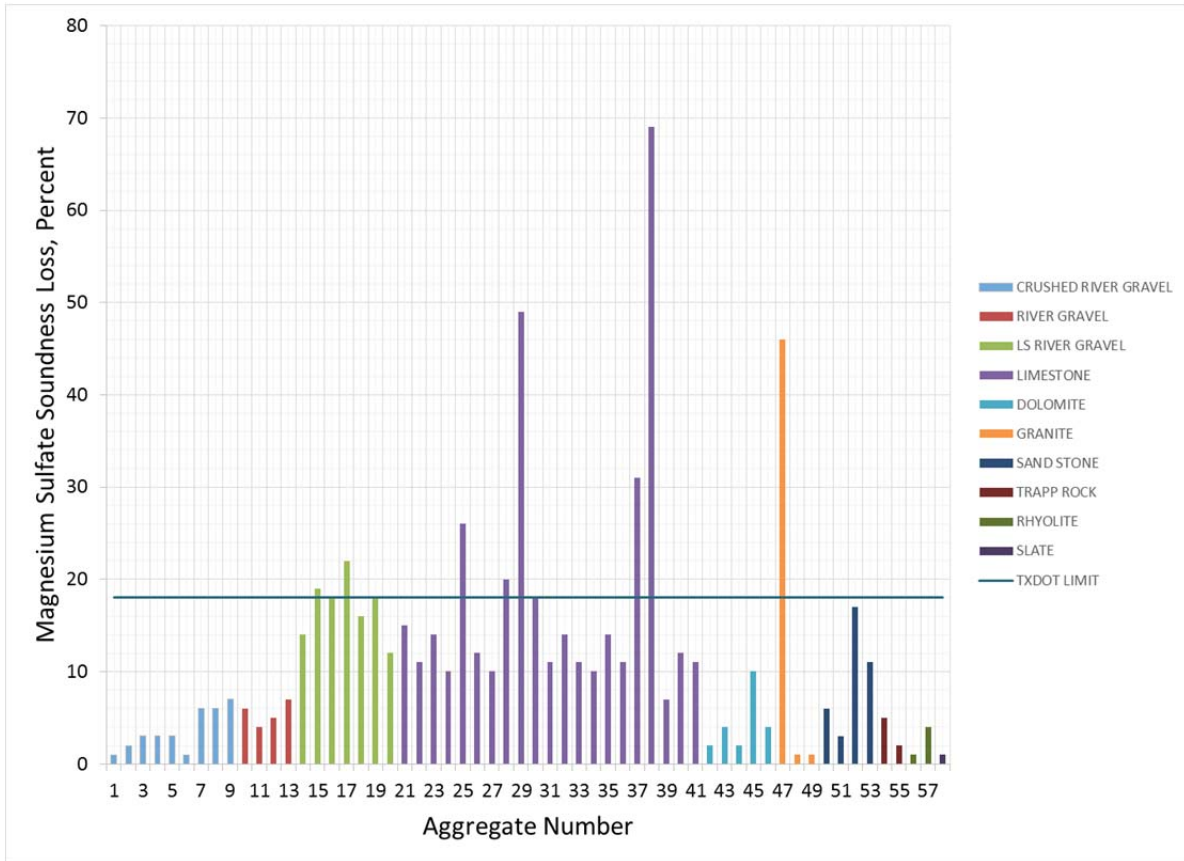
Figure 6.4: Magnesium Sulfate Soundness Test Results

The typical loss limit for magnesium sulfate soundness testing is 18%; eight aggregates had a loss of over 18%. These aggregates included two limestone river gravels (aggregates 15 and 19), five limestones (aggregates 25, 28, 29, 37, and 38), and a granite (aggregate 47).

6.5 Unconfined Freezing and Thawing

Unconfined freezing and thawing is not typically a test that is run in the United States. The Canadian version of the test has a specified loss limit of 6%. The results from unconfined freezing and thawing testing are presented in Figure 6.5. It is easily observed that over 60% of the aggregates collected have a loss greater than 6%; all lithologies collected had at least one sample that did not pass the testing requirements.
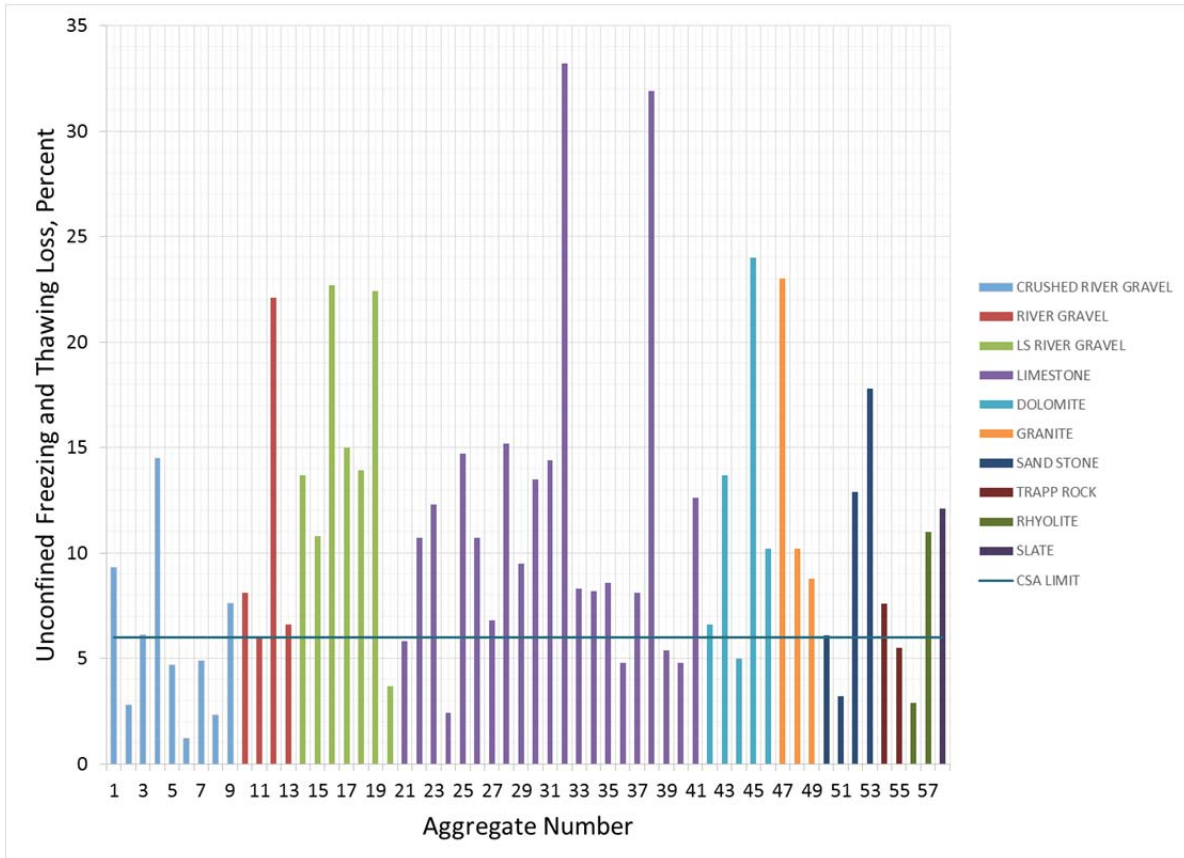
Figure 6.5: Unconfined Freeze Thaw Test Results

97

6.6 AIV

The results from AIV are presented in Figure 6.6. This test method was modified from the original British standard to correlate with unpublished testing previously performed by the project sponsor. As such, there is no published value typically used as a quantified loss. However, it is evident that three samples—two limestones (aggregates 29 and 38) and one granite (aggregate 47) —tested considerably higher than the other samples.
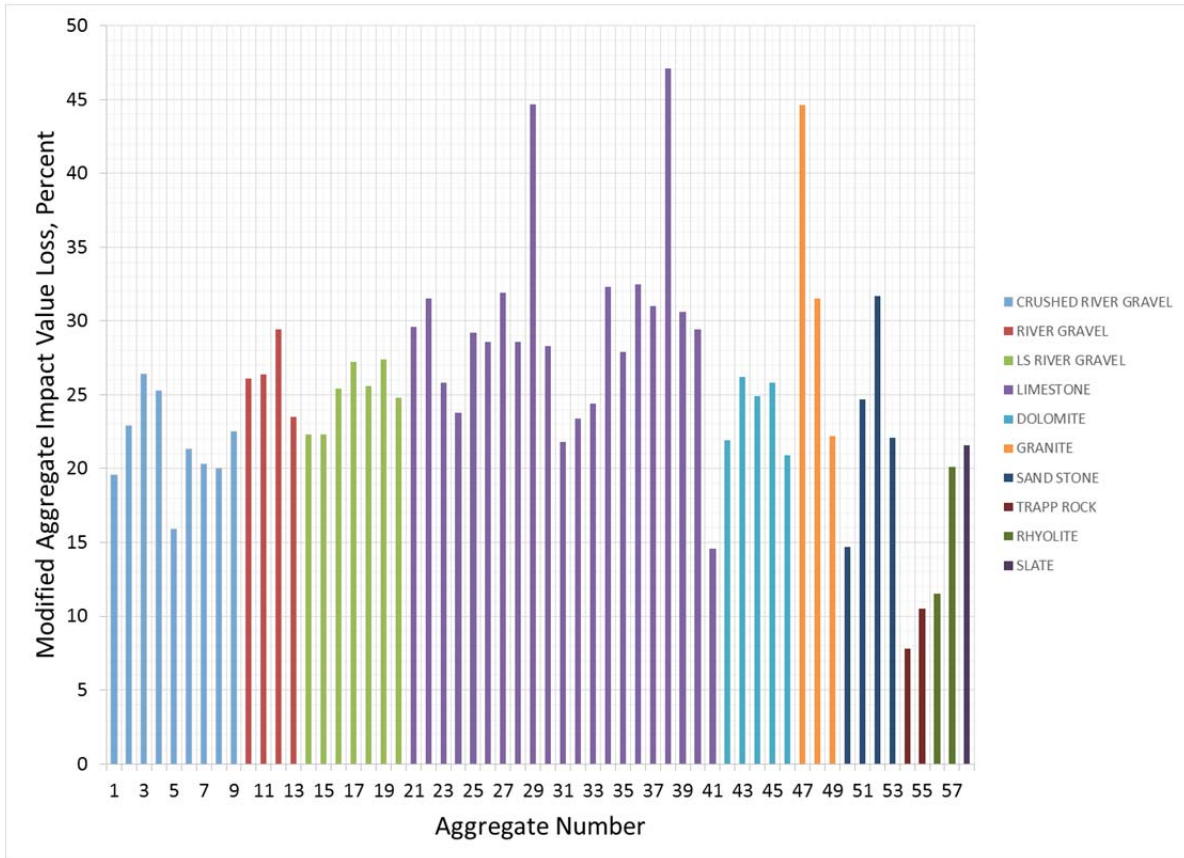
Figure 6.6: Modified Aggregate Impact Test Results

6.7 Modified ACV

The results from ACV are presented in Figure 6.7. This test method was also modified from the original British standard to correlate with unpublished testing previously performed by the project sponsor. As such, there is no published value typically used as a quantified loss. Material differences are less evident with this test method; however, the two highest loss samples were a limestone (aggregates 29) and a granite (aggregate 47).
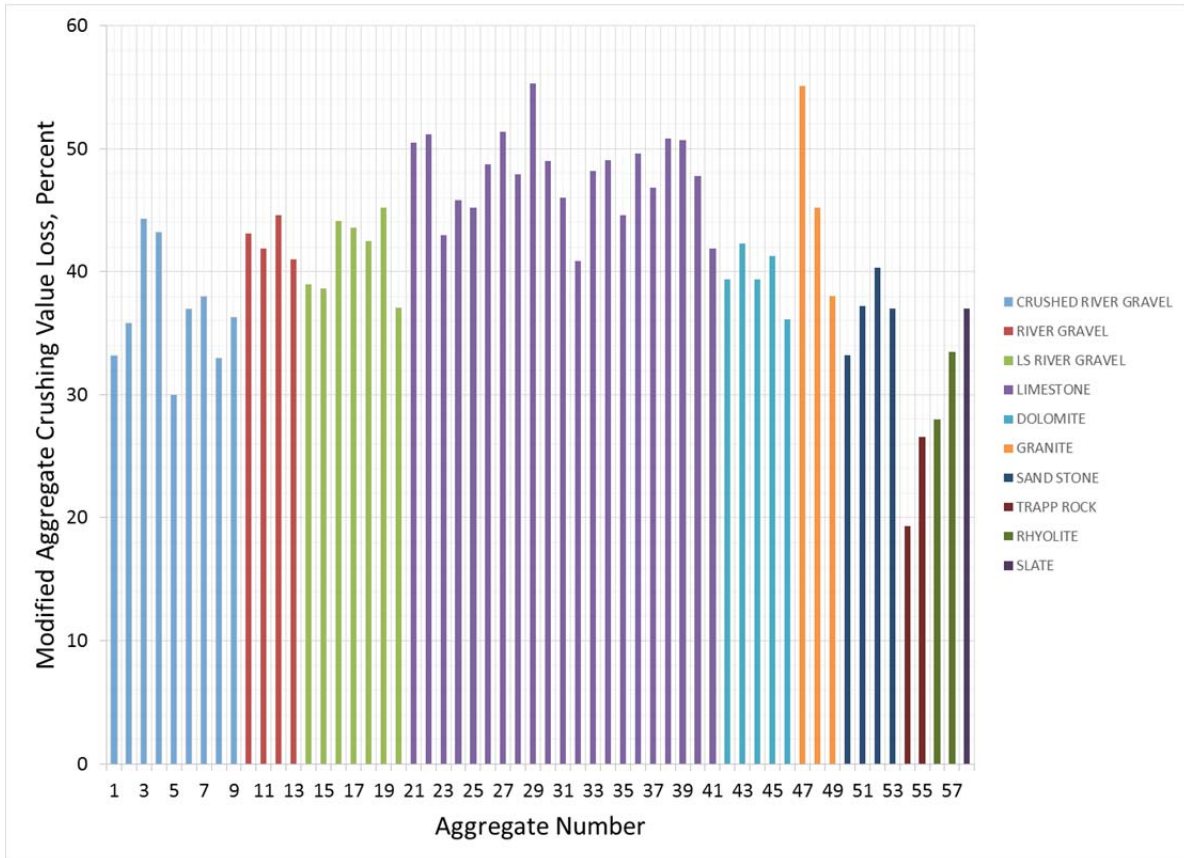
Figure 6.7: ACV Test Results

6.8 AIMS 2.0

Aggregates were also evaluated with the AIMS 2.0 system to determine the angularity, texture, and particles that are flat and elongated. This test method is used along with the Micro-Deval to determine how angularity and texture change when the sample is subjected to abrasion. However, this comparison will be discussed in Chapter 7. Angularity results are presented in Figure 6.8; results from texture are presented in Figure 6.9. Results from particles determined to be flat and elongated are shown in Figure 6.10.

Figure 6.8 shows that the non-crushed gravels have a lower angularity than the other materials, which are all crusher-produced. This trend is to be expected as the non-crushed gravels are subjected to years of erosion that reduce the angularity, a process simulated with the Micro-Deval. Figure 6.8 also shows that non-crushed gravels have much less reduction in angularity after being subjected to Micro-Deval testing.
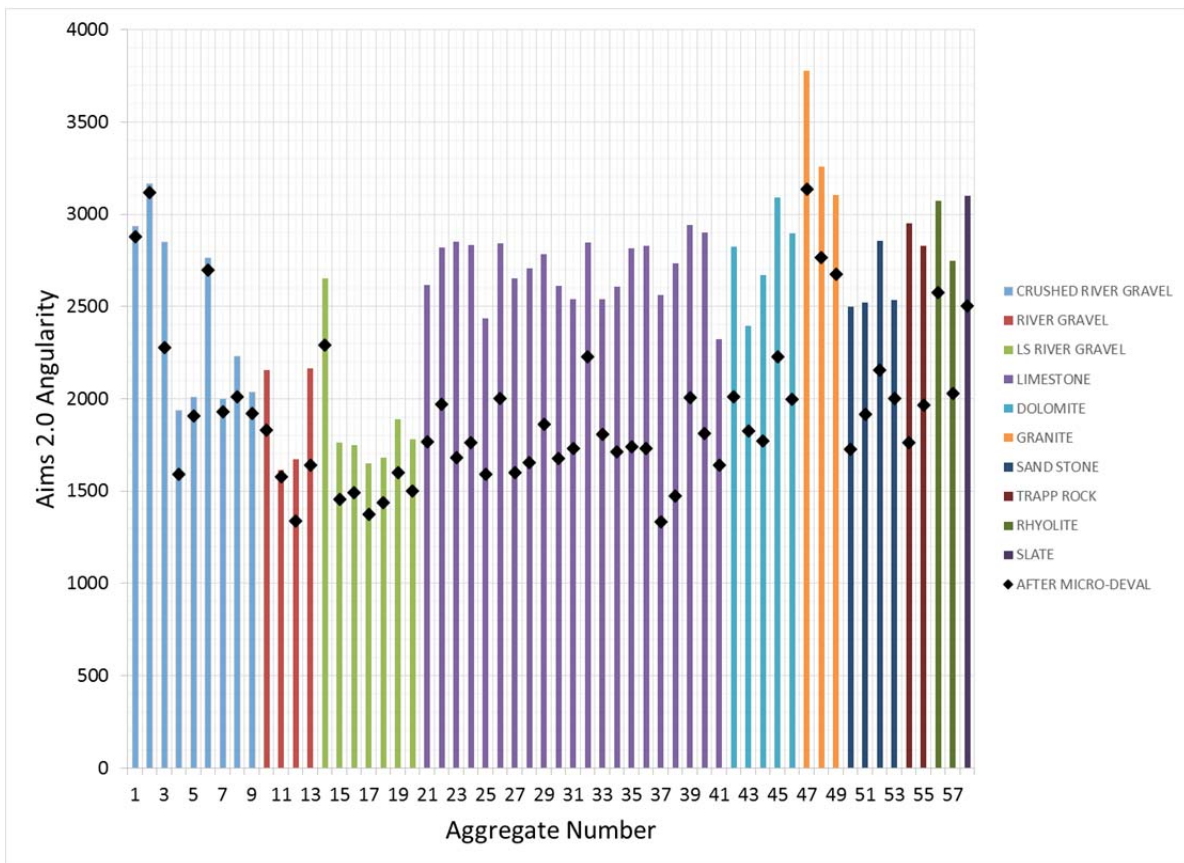
Figure 6.8: AIMS 2.0 Calculated Angularity

Figure 6.9 shows the results from texture determination of the aggregates. The only materials that show distinct differences from the data set are the granites (aggregates 46 to 49), which have a higher texture. Limestones (aggregates 21 to 41) also show a slightly lower texture than the gravels.
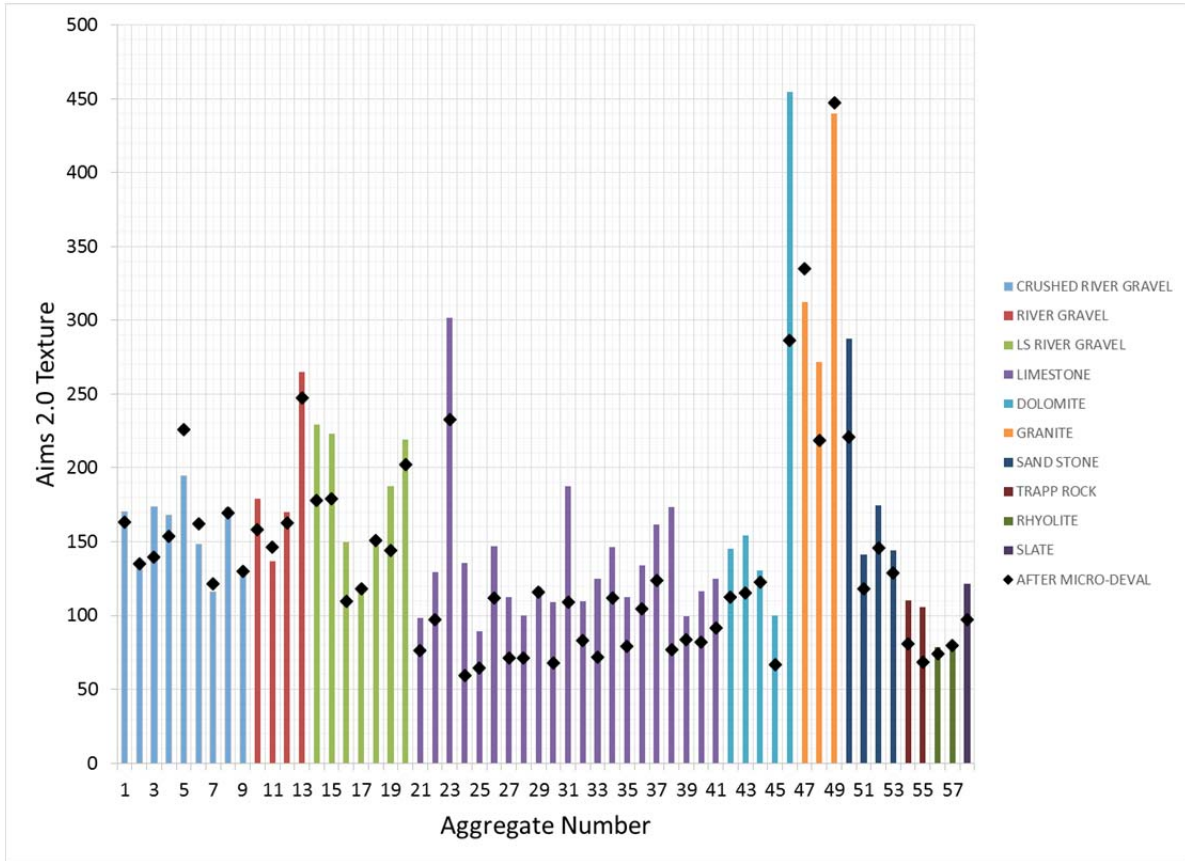
Figure 6.9: AIMS 2.0 Calculated Texture

Figure 6.10 shows the calculated percent of aggregate that is over predetermined aspect ratios, specifically those from 2:1 through 5:1. This figure shows that the gravels, aggregates 1 through 20, have much higher percentages of particles with higher aspect ratios (ratios of 3:1 or larger).
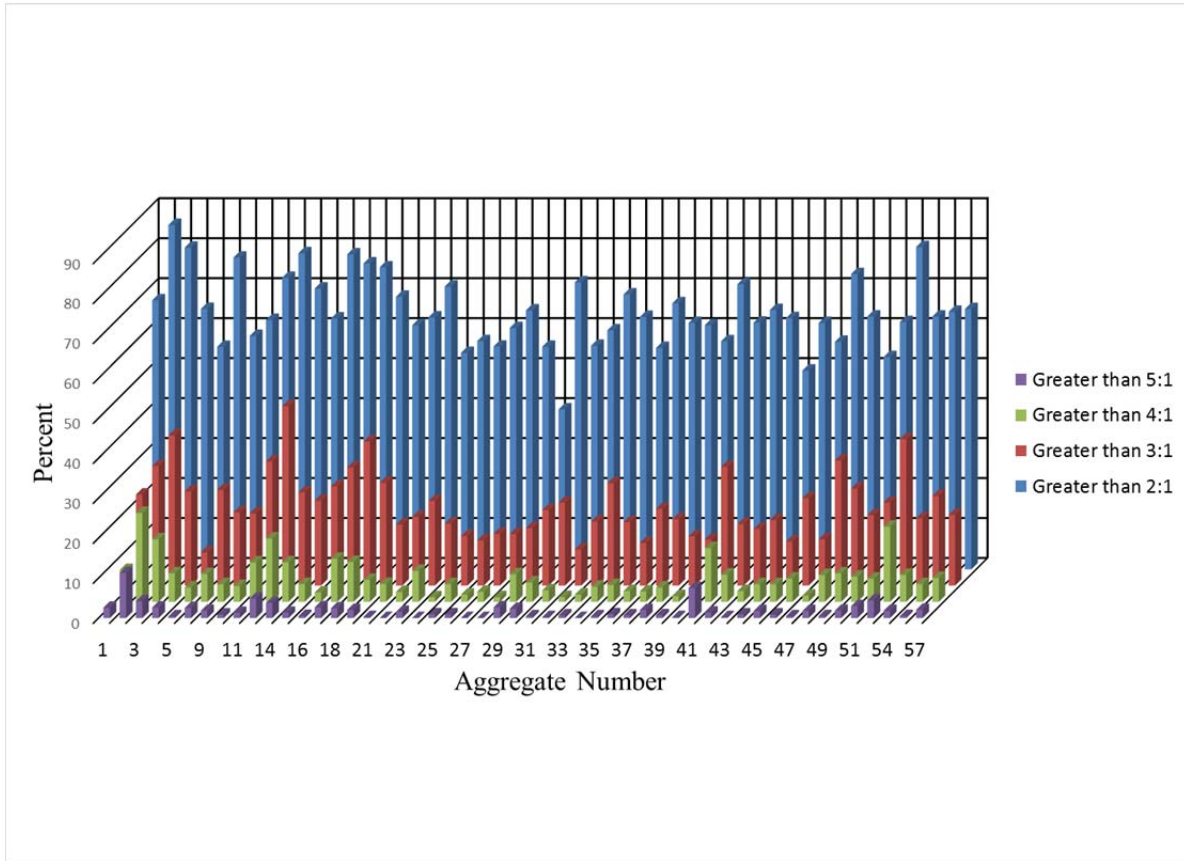
Figure 6.10: AIMS 2.0 Calculated Flat and Elongated Aggregate Content

6.9 Thermal Conductivity

Thermal conductivity was conducted using a Mathis Tci meter, provided by the project sponsor. The unit became inoperable during the research period, and analysis of the data collected until that date was performed to determine the value in expediting the repair of the unit. Analysis of the data did not return any strong correlations with concurrent research, and it was decided that no further testing would be conducted for this project. Table 6.1 presents the data that were collected before the sensor became inoperable.

Table 6.1: Thermal Conductivity Results

Aggregate Number	Lithology	Thermal Conductivity, w/(m*K)
1	Partly Crushed River Gravel	4.73
9	Partly Crushed River Gravel	5.56
10	Siliceous River Gravel	4.64
11	Siliceous River Gravel	4.36
14	Limestone River Gravel	3.13
15	Limestone River Gravel	5.38
16	Limestone River Gravel	3.14
19	Limestone River Gravel	3.79
23	Limestone	2.92
25	Limestone	3.4
27	Limestone	3.14
28	Limestone	3.25
29	Limestone	2.86
30	Limestone	3.24
31	Limestone	3.39
44	Dolomite	5.79
45	Dolomite	4.29
46	Dolomite	5.75
47	Granite	2.96
51	Sand Stone	5.66
54	Trapp Rock	3.14

6.10 CoTE

CoTE is not a test that is typically run on aggregate samples for construction purposes. However, the CoTE test used for concrete was used on aggregates obtained when the aggregate samples were sufficiently large.

The sample size used for the CoTE frame must be 7 inches (178 mm) high and at least 3 inches (76 mm) in diameter. Obtaining a sample of this size is very difficult considering material producers typically have no need for larger sized aggregate and crush it to more commonly sold sizes. Samples were collected from select sources to obtain a range of CoTE values. Blast-quarried material was collected before it was taken to the primary crusher at the producer. However, collecting the required size sample needed to extract a core from the siliceous gravel sources was much more difficult; only one source (aggregate number 4) had material large enough to extract the desired core size. Collected samples were then cast into a concrete base block, as shown in the left image of Figure 6.11, to correctly position the sample while the core was extracted using a modified core drill rig (shown in the right image of Figure 6.11).

Figure 6.11: Left: Large Aggregate Cast into Support Block for Drilling;
Right: Modified Core Drill Rig

Care was taken when selecting aggregates to ensure that a representative sample of the material was collected. This was accomplished by noting the exterior color of the aggregate pieces and selecting material accordingly. This approach was effective for the blast-quarried materials, but was less effective for the gravel source sampled. After the cores were taken the CoTE testing was conducted, and the data is presented in Table 6.2.

Table 6.2: CoTE Values of Pure Aggregate

Source #	Lithology	CoTE Microstrain per degree Fahrenheit	CoTE Microstrain per degree Centigrade
4	Sandstone	6.23	11.21
4	Limestone	3.20	5.76
4	Siliceous	6.40	11.52
4	Siliceous	6.42	11.56
29	Limestone	3.66	6.59
29	Limestone	2.39	4.30
29	Limestone	2.16	3.89
41	Limestone	2.24	4.03
41	Siliceous	5.94	10.69
44	Dolomite	4.56	8.21
44	Dolomite	4.69	8.44
44	Dolomite	4.14	7.45
44	Dolomite	4.51	8.12
50	Sandstone	4.28	7.70
50	Sandstone	4.20	7.56
55	Trapp rock	5.19	9.34
55	Trapp rock	4.70	8.46

A selection of the aggregate "shells" remaining once the core had been extracted was crushed and then cast into a concrete mixture design that was identical to those cast in Chapter 8. The selection of aggregates was made to give a range of CoTE values and was influenced heavily by the amount of material remaining in the "shell," as a minimum mass would be required to cast the cylinders. A comparison of these data will be presented in Chapter 9.

6.11 Direct Proportional Caliper

Originally, the direct proportional caliper was not going to be run for this project. The aspect ratio of aggregates was only going to be evaluated using the AIMS 2.0 device; however, early results with the AIMS device led the researchers to question the accuracy of the device. It was decided that the direct proportional caliper device would be used for comparison with the AIMS 2.0 device. The comparison is presented in Chapter 7 for the test results from the direct proportional caliper presented in Figure 6.12.
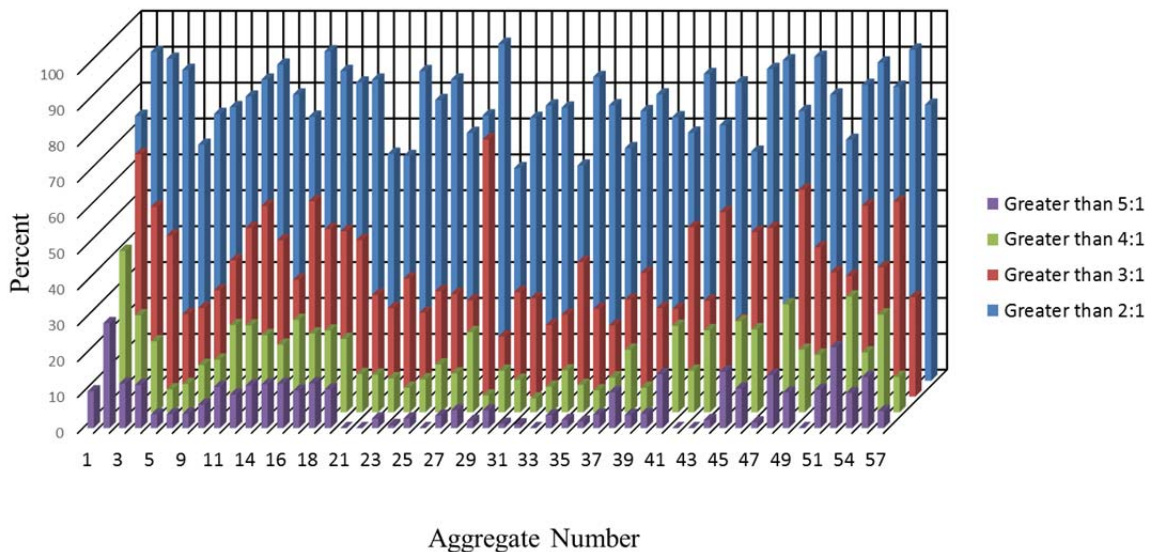
Figure 6.12: Flat and Elongated Aggregate Content Results from the Direct Proportional Caliper

Figure 6.12 shows that the gravels (aggregates 1 to 20) typically have a higher aspect ratio that the limestones (aggregates 21 to 41). This trend was also seen with the results from the AIMS 2.0. However, the direct proportional caliper also shows that the remaining lithologies also tend to have higher aspect ratio; this trend was more pronounced with this method than when using the AIMS 2.0.

6.12 Conclusions

The material properties presented in this chapter were used to select the best set of aggregates to perform concrete testing; this will be discussed in a later chapter. Aggregate properties were also tested with a number of different similar methods to allow for a comparison of test performance results; this will be discussed in the next chapter. Conclusions from the testing performed in this chapter include the following:

- A Micro-Deval loss of requirement of 17% excludes the majority of the limestone aggregates tested. Many of the limestones that test over a 17% loss have a successful history of field applications

- Three aggregates (29, 38, and 47) do not meet current TxDOT requirements for LA abrasion testing.

- Eight aggregates (15, 19, 25, 28, 29, 37, 38, and 47) do not meet current TxDOT requirements for magnesium sulfate soundness testing.

- 60% of materials tested would fail an unconfined freezing and thawing loss requirement of 6%. The majority of these materials do not show evidence of premature distress from freezing and thawing damage.

- Blast-quarried limestone aggregate showed a much higher change in angularity and texture when subjected to Micro-Deval testing than the other lithologies.

- Excavated gravel showed a higher content of flat and elongated particles than the blast-quarried materials.

Chapter 7. Analysis of Coarse Aggregate Test Results

This chapter contains an analysis of the coarse aggregate properties presented in Chapter 6. The focus of this chapter is to relate trends in data between test methods and to discuss any problems that were observed with the test results. Information presented in this chapter is included for determining the recommendations for coarse aggregate testing, presented in Chapter 13.

7.1 Resistance to Abrasion

7.1.1 Comparison of Methods

The two methods used to evaluate the abrasion resistance of aggregate were the LA abrasion test (Tex 410-A) and the Micro-Deval test (Tex 461-A). The basic theory behind these two tests is for an aggregate sample to be placed in a revolving metal drum for a period of time and to measure the resulting material loss. The two methods go about achieving the loss in completely different fashions. The LA method is a dry process that uses a large drum and large steel balls; the Micro-Deval is a wet process that uses a small drum and small steel balls. Figure 7.1 shows a comparison between the drums (front, Micro-Deval; rear, LA abrasion) and abrasion media (bottom, Micro-Deval; top, LA abrasion) for the two tests. The LA abrasion test container is also equipped with a ledge that forces the aggregates and charge to be lifted and then dropped, impacting the bottom of the drum. Because of this key difference, there is not a strong probability for correlation between the tests.
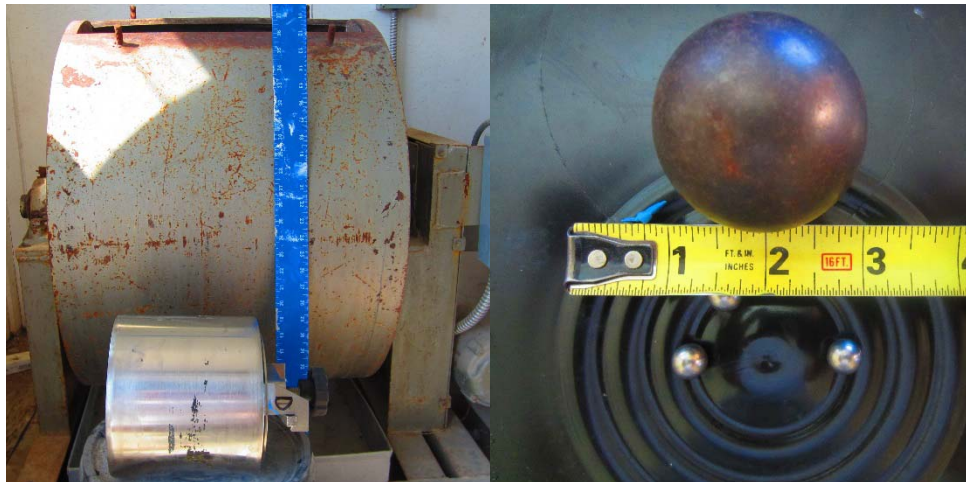
Figure 7.1: Size Comparison of Containers and Abrasive Charge Used

Figure 7.2 shows the relationship between the LA abrasion test and Micro-Deval. The correlation coefficient of 0.58 shows a moderate correlation between the tests, but is not indicative that the tests screen the same property. Considering only the limestone river gravels and blast-quarried limestone improves the correlation to 0.88. The lack of correlation is caused by the non-limestone lithologies, materials known to be harder and more abrasion resistant than the other materials. Considering these factors, the Micro-Deval is the better choice for evaluating

abrasion resistance. LA abrasion testing is more closely related to impact resistance, and will be discussed in the next section.
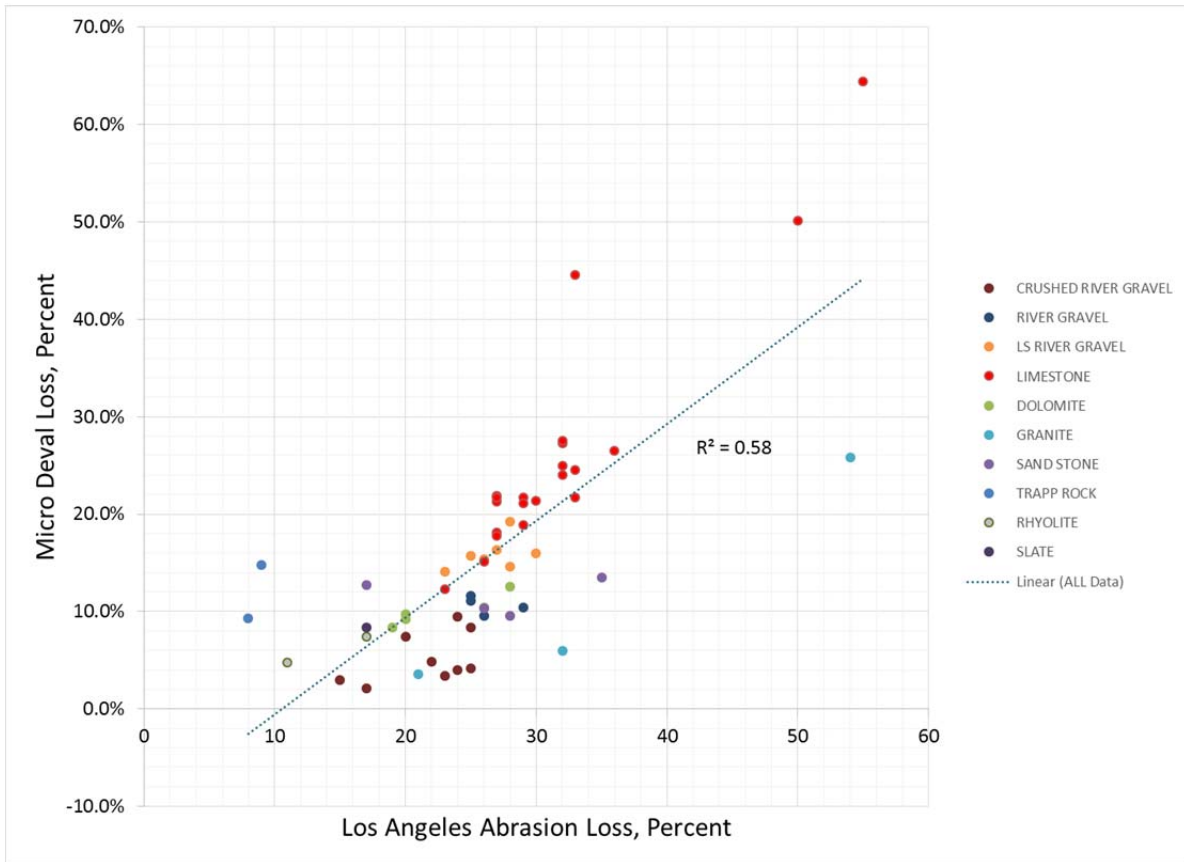
Figure 7.2: Comparison of LA Abrasion with Micro-Deval

7.1.2 Quantifying Abrasion Likelihood

The selection of Micro-Deval as the principal method to evaluate abrasion resistance resulted in the need to classify materials as either "hard" or "soft." One possible methodology behind this is comparing the Micro-Deval loss with the absorption capacity; this approach is based upon the assumption that hard materials are likely to be denser, having fewer internal air voids. A plot of this is presented in Figure 7.3.
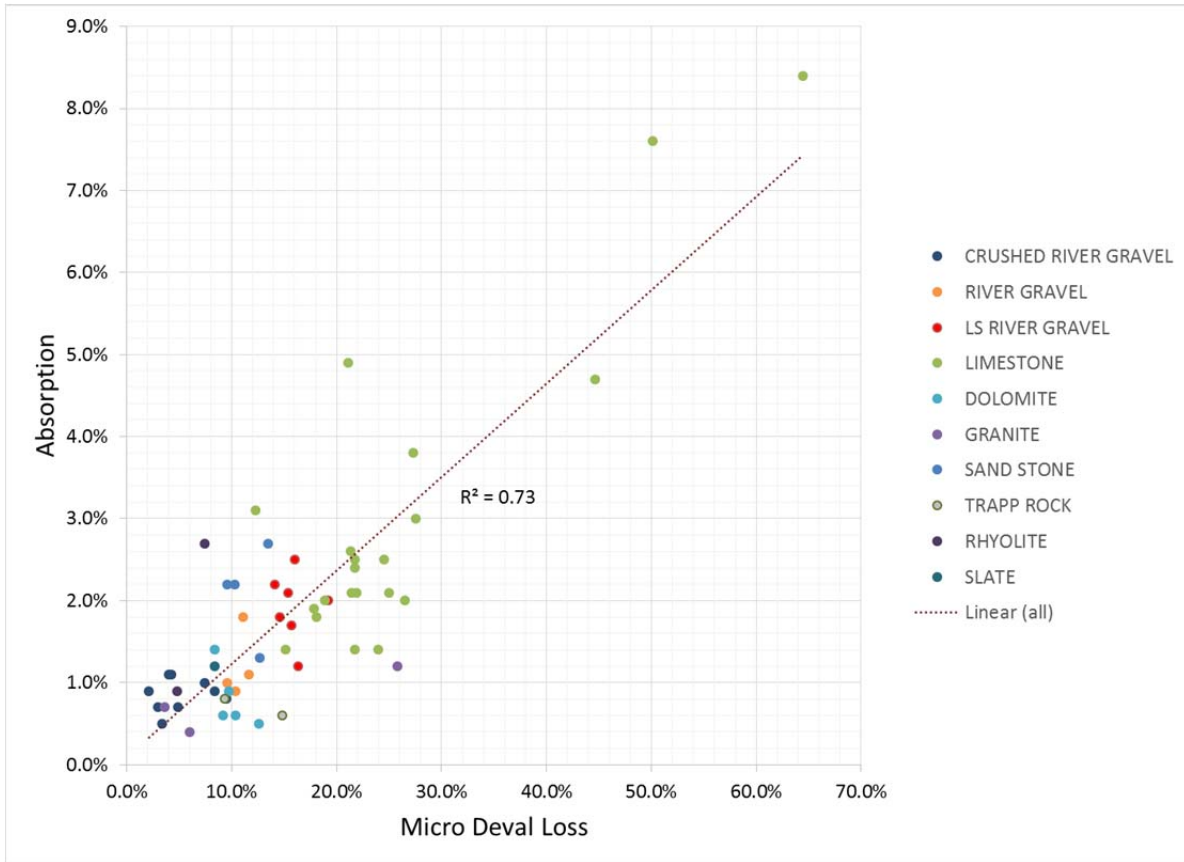
Figure 7.3: Comparison of Micro-Deval Loss with Absorption

Figure 7.3 shows a correlation coefficient of 0.73, indicating a probable relationship between these two values. However, it is evident that with some of the Micro-Deval loss values in the data set (values over 30%) that abrasion was not the only degradation mechanism occurring during testing.

Although the Micro-Deval was selected over the LA abrasion method for evaluating the abrasion resistance of an aggregate, there was still a need to differentiate between abrasion and breakage of material in the test. The AIMS 2.0 device was used to evaluate aggregates before and after the Micro-Deval test was run; this allowed for an analysis to be performed on the change in material shape characteristics. This approach compares an aggregate's change in angularity with respect to Micro-Deval loss, allowing for the material to be classified as having either high or low abrasion loss as well as high or low breakage loss (Mahmoud 2005). A plot of this approach is presented in Figure 7.4.
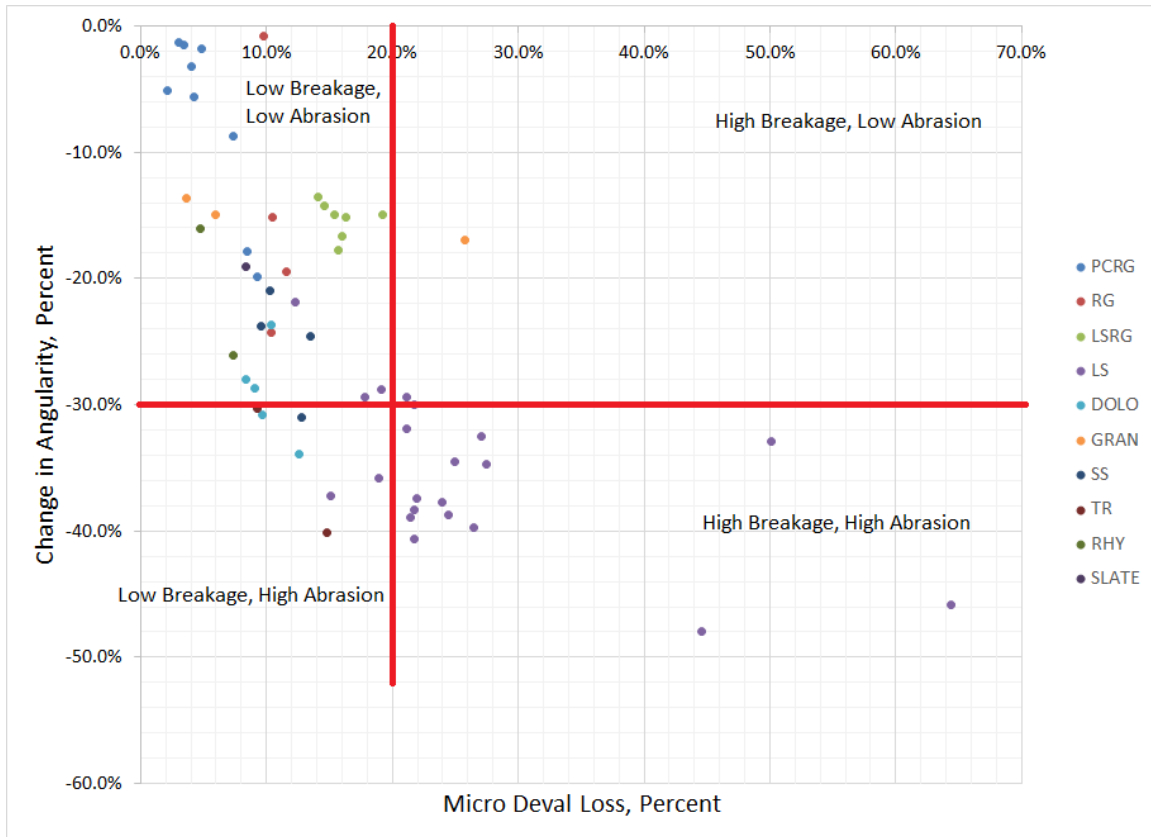
Figure 7.4: Aggregate Abrasion Characterization

Mahmoud suggested using a 20% limit for Micro-Deval loss as the dividing point between materials with high and low breakage. This point was combined with a 30% limit for angularity change to differentiate between materials with high and low abrasion loss.

Reviewing the data in Figure 7.4 shows that blast-quarried limestone is the principal lithology that is identified as having high abrasion loss; however, certain dolomites and sand stones were also classified in this region. Blast-quarried limestone was the only lithology to be classified with both high breakage and high loss; the dolomites and sand stones identified as having high abrasion loss were classified with low breakage likelihood. These observations are logical since dolomite and sandstone materials are typically stronger than limestones.

7.2 Resistance to Breakage

An aggregate that is resistant to breakage is an important property to consider; aggregate is transported by heavy machinery a number of times between initial production and final placement. Each breakage that occurs during this process results in a change in the total size distribution as well as the total fine material (material passing a #200 sieve); this can result in a material that may pose problems for use in concrete. The test methods used to evaluate the resistance to breakage of an aggregate were the LA abrasion test (Tex 410A), the aggregate crushing value (ACV) test (BS 812.110), and the aggregate impact value (AIV) test (BS 812.112)

7.2.1 Comparison of Methods

The LA abrasion test is typically the standard test used in the United States to evaluate the resistance to breakage of an aggregate. Many European countries use either the aggregate crushing or AIV test to evaluate resistance to breakage. The ACV test breaks aggregate by slowly loading a sample confined in a steel cylinder. The AIV test breaks aggregate by subjecting an aggregate sample to a series of blows from a hammer dropped from a prescribed height. The LA abrasion test breaks aggregate by rotating an aggregate sample with large steel balls in a steel drum equipped with a ledge; the ledge causes the sample to be lifted to the top of the drum where the material falls and impacts the bottom surface.

The LA abrasion test method results in a combination of abrasion and impact damage to the sample. Considering this, it would be expected that this test method would result in higher loss values for materials that would suffer both breakage and abrasion (materials that would be considered relatively soft and weak when compared to other lithologies) such as limestones. With this in mind, LA abrasion test results and AIV test results should have a moderate to strong correlation, as both methods damage aggregate through impact. Figure 7.5 presents a comparison between LA abrasion test results and AIV test results.
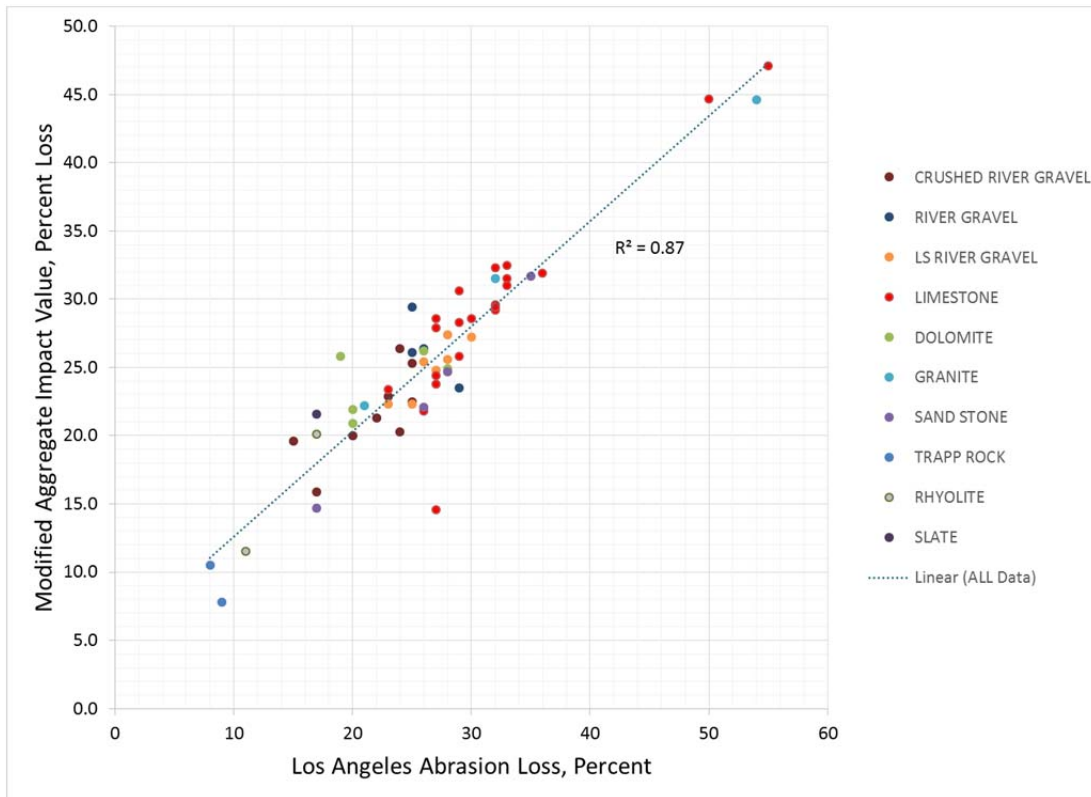
Figure 7.5: Comparison of LA Abrasion Loss with AIV Loss

Figure 7.5 shows a correlation coefficient of 0.87, indicating strong correlation between the two tests. As previously mentioned, the additional abrasion damage associated with the LA abrasion test method may be responsible for the slight differences in values.

Breakage of aggregate through crushing with the ACV method is less likely to correlate with the impact-based test methods, as impact resistance is often more related to a materials

toughness rather than just strength. A comparison of ACV and AIV test results is presented in Figure 7.6.
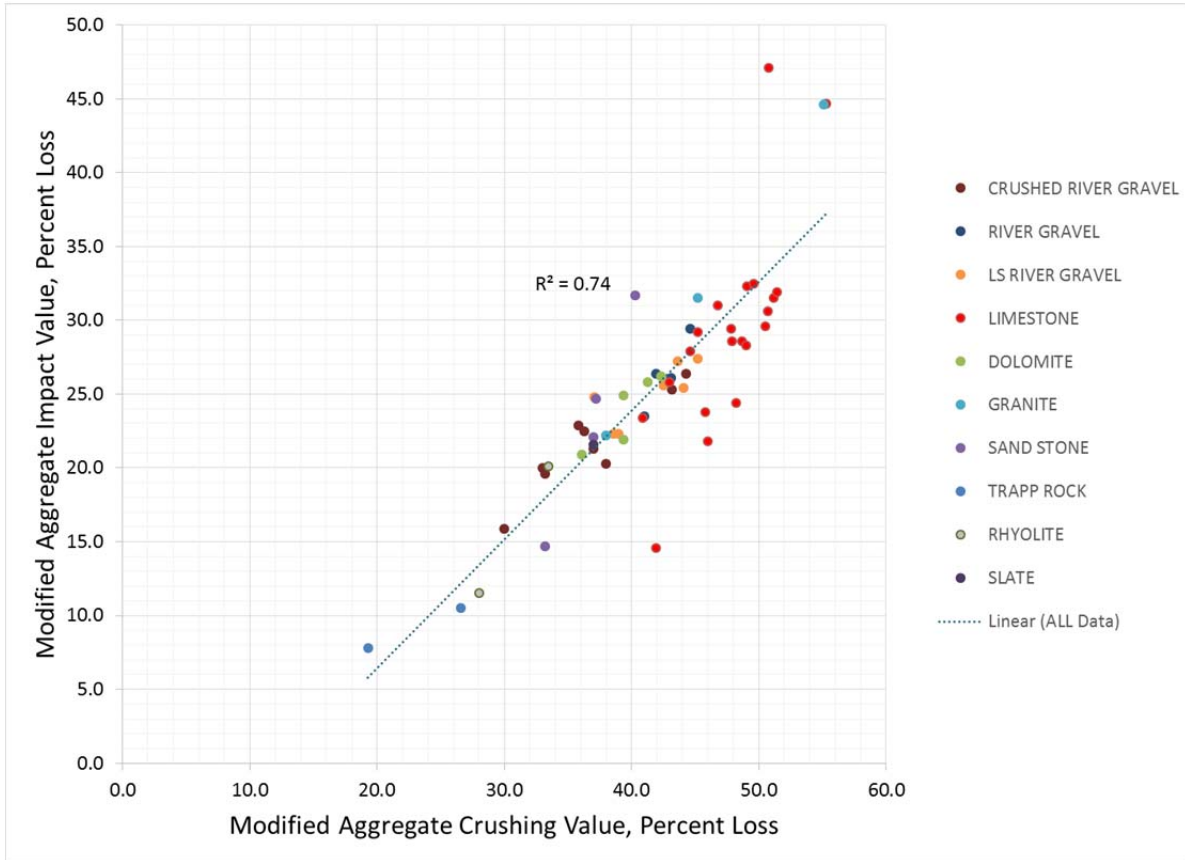
Figure 7.6: Comparison of ACV Loss with AIV Loss

Figure 7.6 shows a correlation coefficient of 0.74 between AIV and ACV test results. This trend was expected because of the difference in measuring breakage due to strength (ACV) and breakage due to toughness (AIV). Figure 7.7 shows a comparison of ACV test results with LA abrasion test results, which has a moderate correlation coefficient (0.68). The scatter in the data results from of the additional abrasion loss in LA abrasion that is not found in ACV testing.
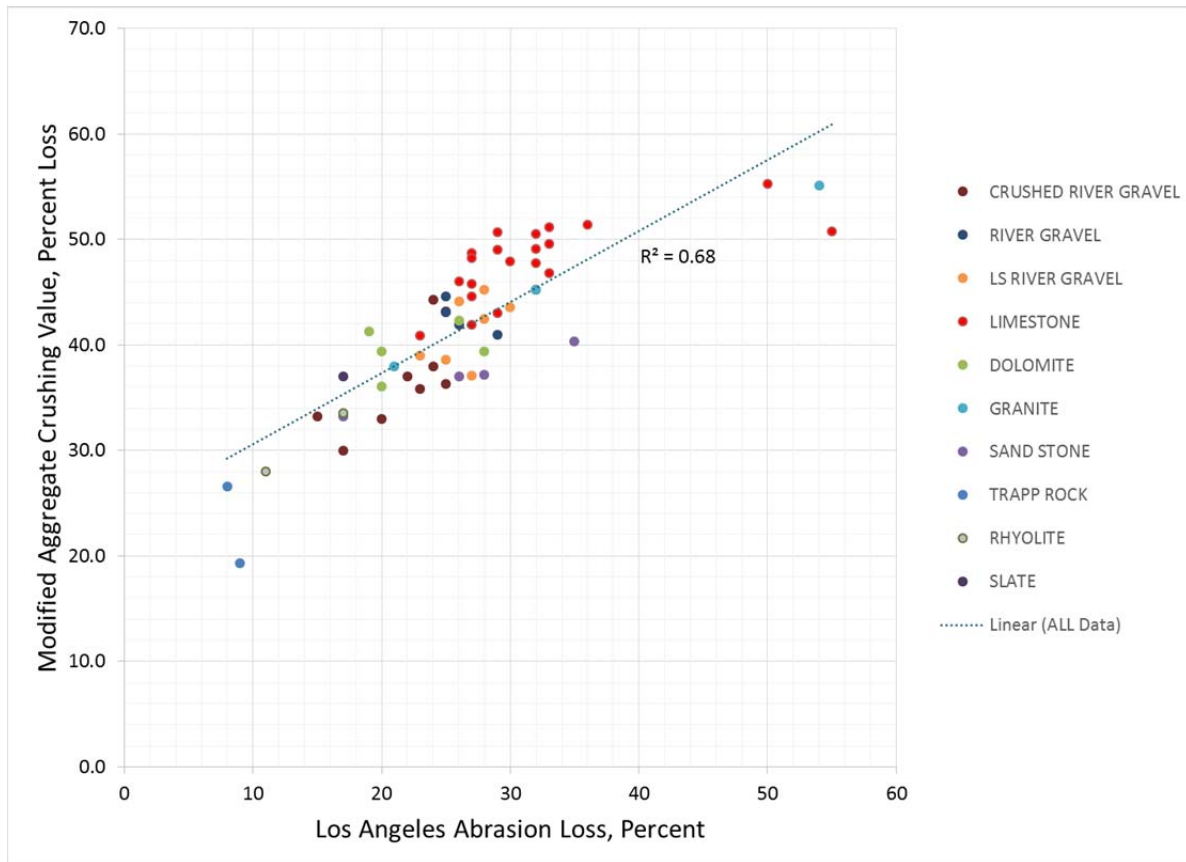
Figure 7.7: Comparison of LA Abrasion Loss with ACV Loss

7.2.2 Development of an Automated AIV Apparatus

Although results from the AIV test were very promising, one potential reason that the test method may have not become more widely used is the labor requirement of the test apparatus. The falling hammer section of the unit weighs approximately 35 pounds (15.9 kg) and the unit is typically attached directly to the floor. These factors mean that the operator of the unit must lean over to load the sample into the unit and this results in generally poor posture while lifting the hammer the required 15 times per test. These conditions result in a very high physical demand, reducing the total number of tests an operator can perform in a given day due to fatigue. Once fatigued, the operator is also more likely to err in performing the test methods, either from incompletely lifting the hammer to the drop height, or miscounting the total number of hammer falls performed.

As a result, it was decided to automate the AIV apparatus to reduce the possibility for incorrectly performing the test and to reduce the physical strain on the operator. This was accomplished through the following steps:

1. The test apparatus would be attached to an elevated concrete base, allowing the operator easier access to the device.

2. Raising the hammer on the device would be accomplished with assistance from an electric motor.

3. An electronic cycle counter with automatic stop feature would be incorporated into the device.

4. Repeated testing of materials would need to be performed to verify the performance of the modified device.

The conversion of the AIV apparatus to an automated system was simplified through the use of parts obtained from a Marshall compaction hammer (as used for ASTM D6926). The Marshall hammer is an asphalt mixture compaction hammer and is not used as frequently by many transportation agencies because of the shift to the Superpave design methodology. This trend creates great potential for other organizations to perform similar conversions at a substantially reduced cost.

A portable elevated concrete base was constructed to hold the automated AIV test frame and cycle controls. This base would allow for the operator to insert the test sample and operate the device without having to lean over the device. Next, the lifting handles were removed from the original AIV apparatus to allow for an automatic release trigger to be fashioned for the hammer. Once the release mechanism was attached, the total hammer weight was adjusted through the use of steel washers to maintain the required hammer weight. An adjustable release activator was installed on the hammer and the test cycle counter sensor was installed. The modified AIV apparatus is shown on the left of Figure 7.8, the right image of the same figure shows the release mechanism and cycle counter sensor.
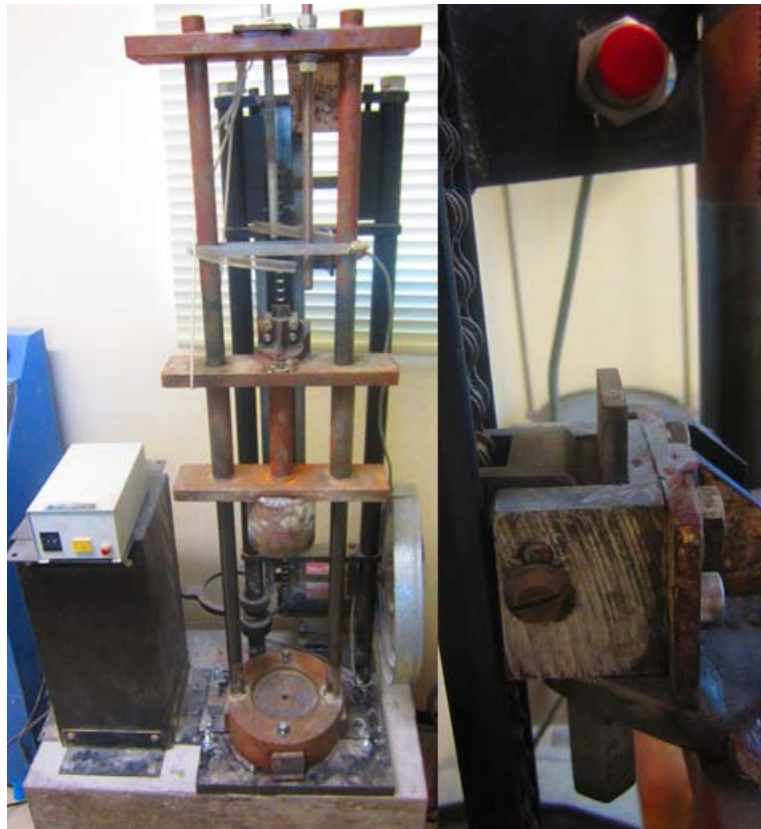
Figure 7.8: Modified AIV Apparatus

At this point, the machine was activated to observe the rate of hammer drops, since BS 812.112 requires a minimum 1-second delay between successive blows. The frequency of hammer blows was determined to be too rapid; an adjustment to the hammer lift chain system and drive pulleys was made to compensate and slow the rate. The modified apparatus was then reactivated to evaluate the ability of the machine to operate within all requirements of BS 812.112.

Once the machine was proven to operate in accordance with the test standard, a validation was performed to confirm that the automation did not affect the operation of the machine. Two aggregates were tested six times each to verify the single-test repeatability of the automated AIV hammer; data variance was within published values for the manual AIV hammer. Sixteen aggregate samples of various lithologies that had previously been tested with the manual system were re-tested with the automated test hammer. Results from these automated tests (when compared to manually run tests) were found to be within the published values of variance for the manual device.

Automation of the AIV device reduced the time needed to run the test when compared to the manual method. The device also allowed for more tests to be conducted in a given time period; this resulted from the combination of increased test completion speed and the reduction in operator fatigue when running successive tests. The modifications also reduce the possibility of physical injury to the operator from repeated lifting of the hammer.

7.3 Resistance to Volume Change

7.3.1 Comparison of Methods

Aggregates were evaluated for resistance to volume change using two test methods: magnesium sulfate soundness (Tex 411-A) and unconfined freezing and thawing (CSA 23.2-24A). These methods are intended to simulate potential distress that would be experienced due to wetting and drying or freezing and thawing volume changes. Figure 7.9 presents a comparison of the results of unconfined freezing and thawing testing and magnesium sulfate soundness testing. Ideally, these two test methods should have a high correlation, considering that both measure the resistance to volume change. Clearly, with a correlation coefficient of only 0.28, the two test methods are not testing materials with the same bias. The following sections will discuss trends seen in the data from both tests in an attempt to quantify the better testing method.
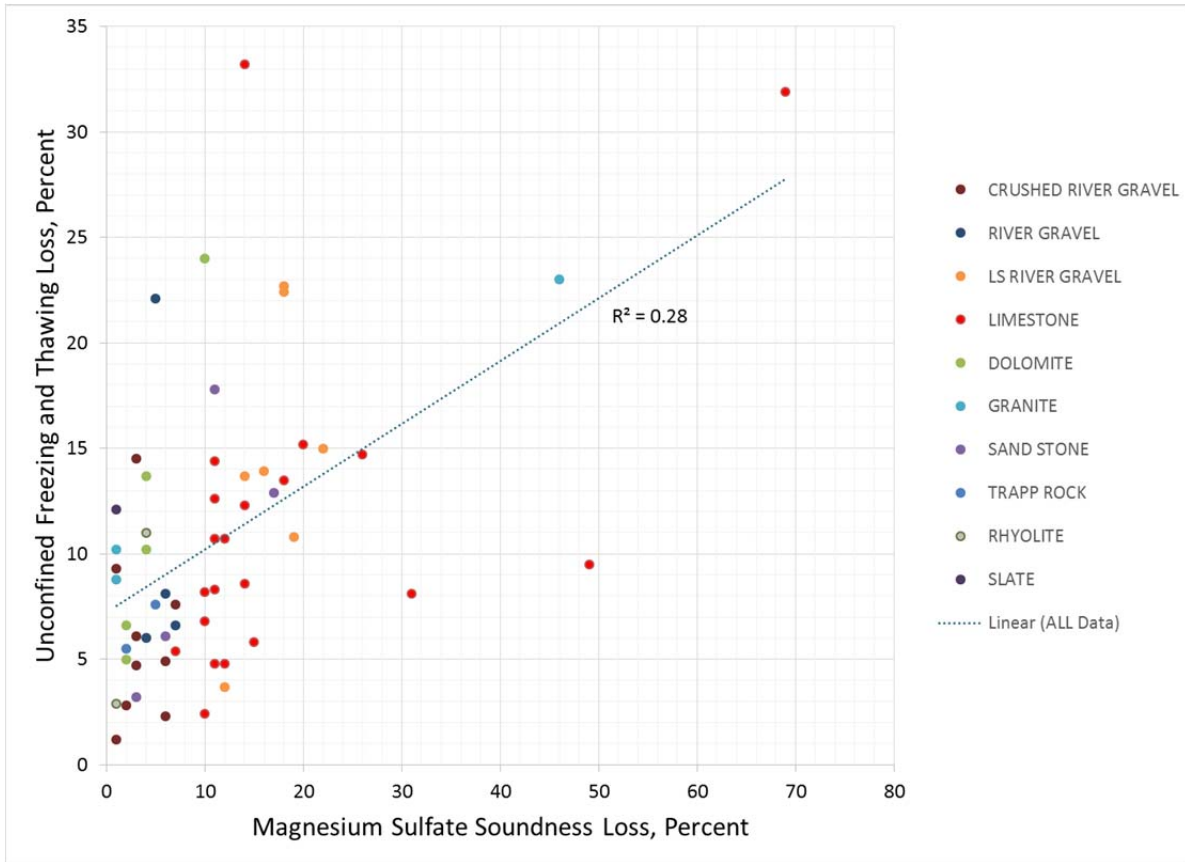
Figure 7.9: Comparison of Magnesium Sulfate Soundness Results with Unconfined Freezing and Thawing Results

7.3.2 Magnesium Sulfate Soundness

Distress from magnesium sulfate soundness testing results from the cyclic formation of crystalline solids in the void spaces of aggregates. These crystals form during the oven drying periods, at 230°F (110°C), when samples are between immersion cycles in a saturated magnesium sulfate solution (Folliard and Smith, 2002). It is assumed that an increase in void content should lead to a higher probability of distress due to magnesium sulfate soundness testing. Figure 7.10 presents the magnesium sulfate soundness test results in comparison with the percent absorption content of the aggregate.
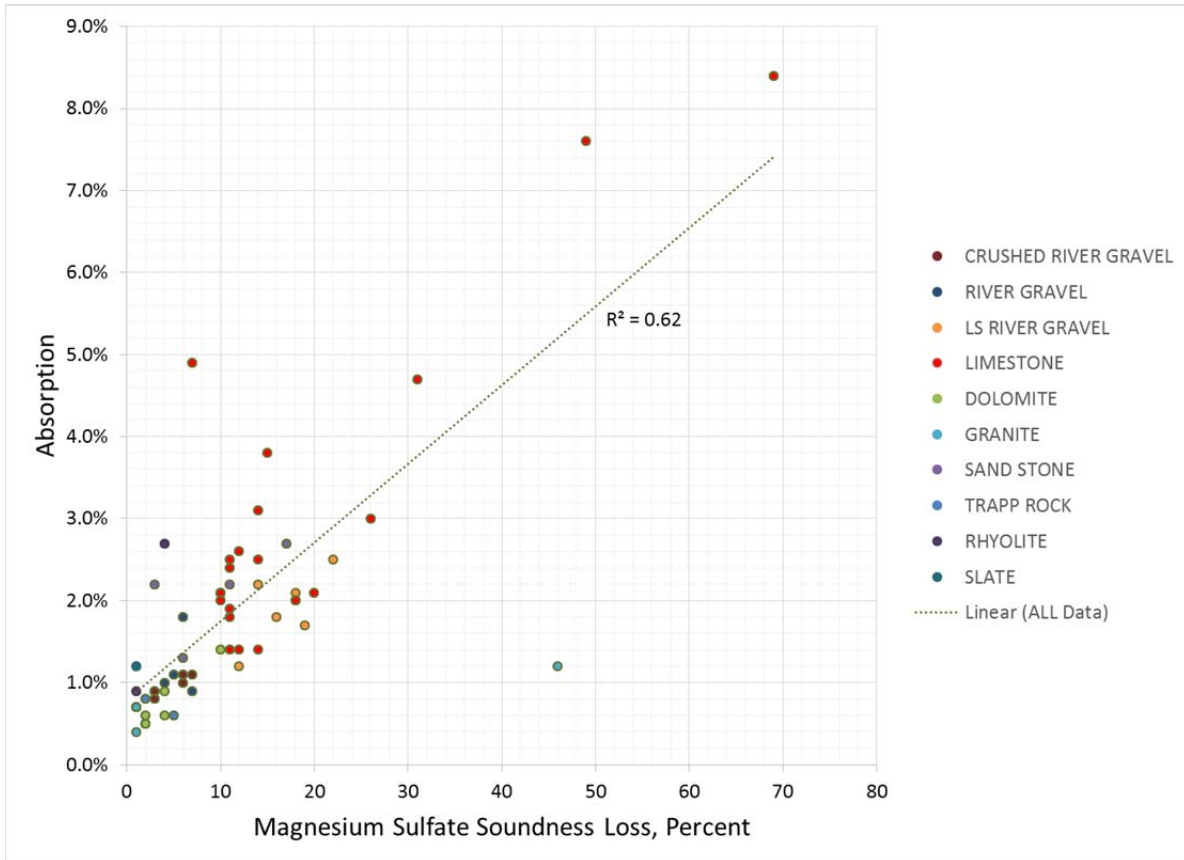
Figure 7.10: Comparison of Magnesium Sulfate Soundness Results with Absorption

Figure 7.10 shows a 0.62 correlation coefficient between the magnesium sulfate soundness loss and absorption capacity of an aggregate. This is a moderate correlation of the results and lends credit to theory of crystalline pressure resulting in distress. It also agrees with visual inspection of degradation as the test cycles progress; materials tend to become progressively more fractured with time. The comparison also shows that the materials most likely to perform poorly in testing are limestone based—either blast-quarried material or high limestone content river gravel.

7.3.3 Unconfined Freezing and Thawing

Distress from unconfined freezing and thawing testing differs from magnesium sulfate soundness testing in that the sample is saturated in a 3% sodium chloride solution before the test begins and is then subjected to freezing cycles (rather than oven drying) with the material at wetted surface conditions. Figure 7.11 presents the unconfined freezing and thawing loss with the percent absorption content of the aggregate.

117
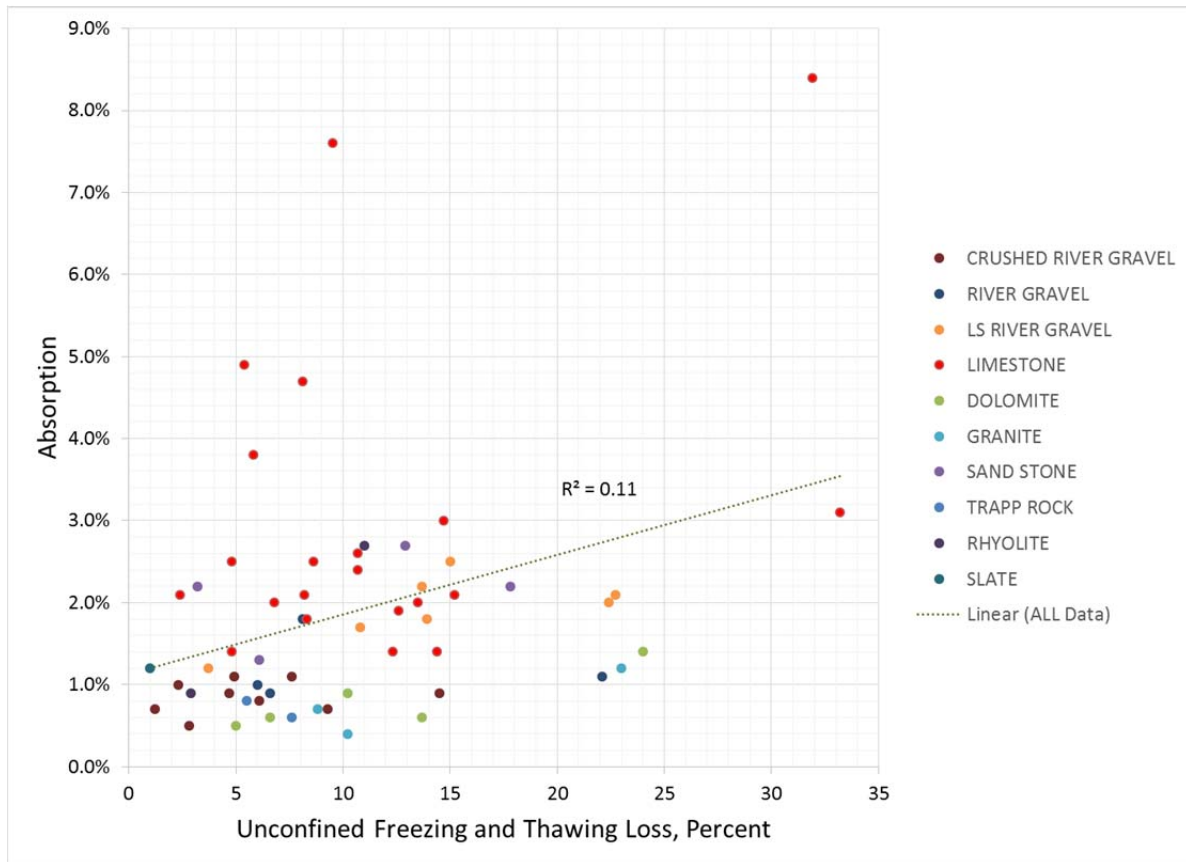
Figure 7.11: Comparison of Unconfined Freezing and Thawing Results with Absorption

Figure 7.11 shows a 0.11 correlation coefficient between the unconfined freezing and thawing loss and absorption capacity of an aggregate. This shows a very poor correlation between the bulk void content and distress resulting from freezing exposure in a salt solution. Materials with low and high air void contents are less likely than materials with moderate air void contents to suffer from this distress. Visible inspection of aggregates with the highest loss did not reveal the pure fracture failures seen in magnesium soundness testing, rather the surfaces of aggregates became pitted. The best possible explanation for this distress mechanism can be related to salt scaling distress in PCC. The maximum salt scaling distress in concrete occurs when using a 3% sodium chloride solution in mixtures that do not have an adequate air void content and in materials that do not have a strong exterior (Valenza, 2005). The freezing and thawing damage to concrete is similar to damage seen to the unconfined aggregates.

7.4 Shape Characterization

Shape characterization for this project was performed using an AIMS 2.0 device; these machines are not very common in laboratory settings, and as such, a need to evaluate the results from the unit was deemed necessary. This section will discuss the statistical error observed for the aggregates tested.

7.4.1 Angularity

The AIMS 2.0 device uses a backlit image (shown in Figure 7.12) to calculate an angularity index for the particle.

Figure 7.12: Sample Image Used for Angularity Calculation

This process is repeated over the size data set and is then compiled into mean and standard deviation for each evaluated size fraction. A plot of the mean angularity and standard deviations before and after Micro-Deval was run for ½-inch aggregate is presented in Figure 7.13; the other aggregate sizes show similar trends and are not presented.
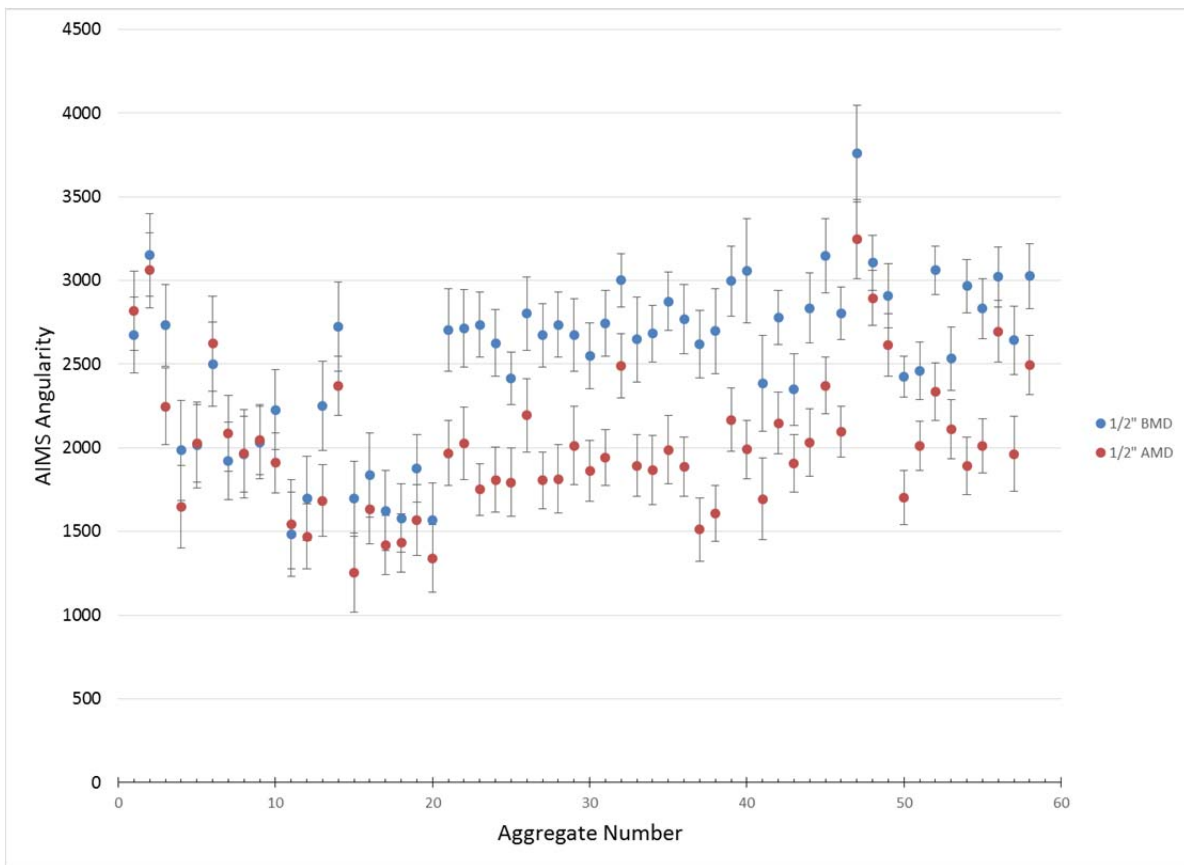
Figure 7.13: Mean and Standard Deviation for AIMS Calculated Angularity

This figure shows that the gravels—aggregates 1 to 20—have mean values, including standard deviations that overlap for analysis before and after Micro-Deval. This artifact could lead to possible erroneous interpretation of percent change in angularity before and after Micro-Deval. Considering this, an additional level of statistical analysis was performed to determine the confidence that the values measured indicated a change in angularity for the aggregate.

The procedure for performing the data analysis is presented in Section 9.1 of Devore, 2004. The results measured with the AIMS 2.0 had a standard normal distribution and a two-tailed test statistic value was used. The two calculated means for each aggregate (before and after Micro-Deval) were compared with the respective standard deviations and sample set sizes for analysis. The probability of a measurable change in angularity of an aggregate considering a 95% confidence interval is shown in Figure 7.14.
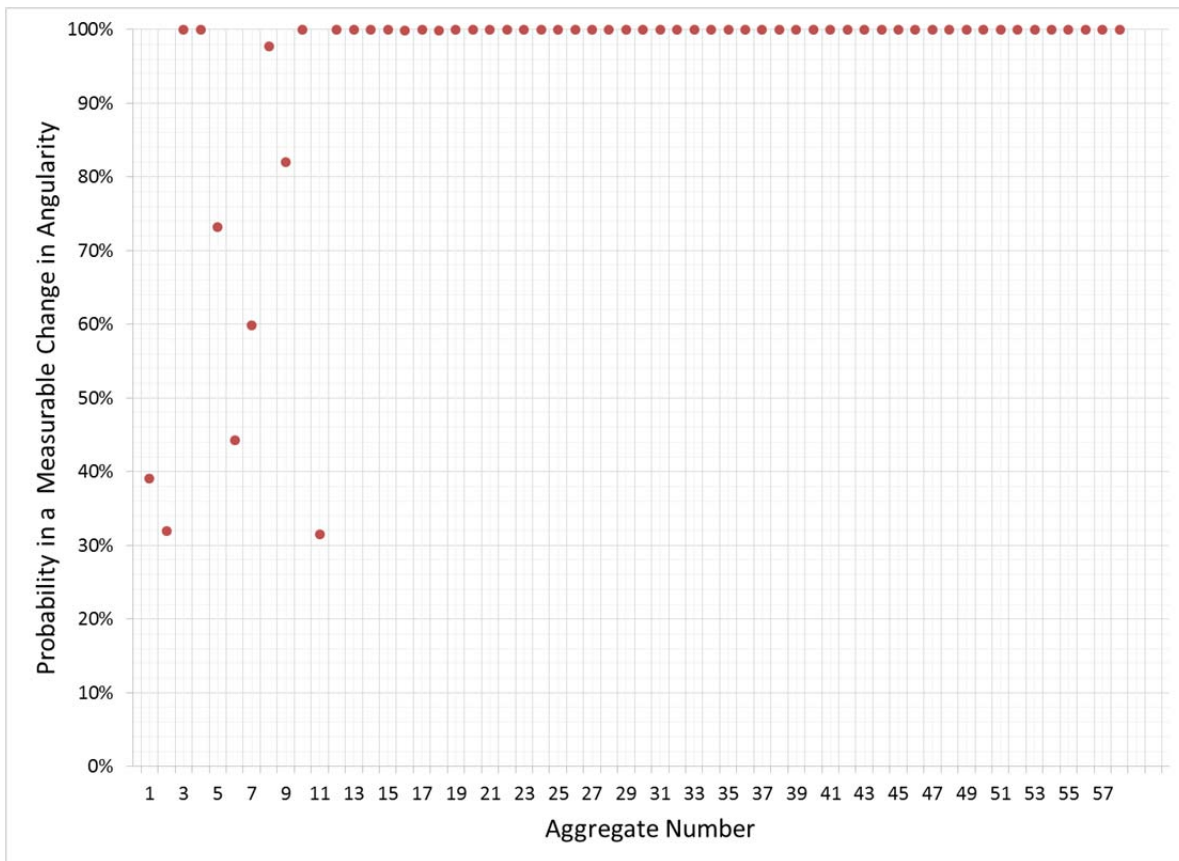
Figure 7.14: Probability of Measureable Angularity Change

Figure 7.14 shows that (for a 95% confidence interval) the only materials that do not show high probability of measurable change are high siliceous content gravels (aggregates 3 and 4) are crushed gravels with a moderate limestone content. This indicates that approximately 87% of the aggregate collected were accurately quantified for angularity change with the AIMS 2.0.

7.4.2 Texture

The AIMS 2.0 device uses a top-lit image (shown in Figure 7.15) to calculate a texture index for the particle; the texture is calculated based upon a wavelet analysis of the image.
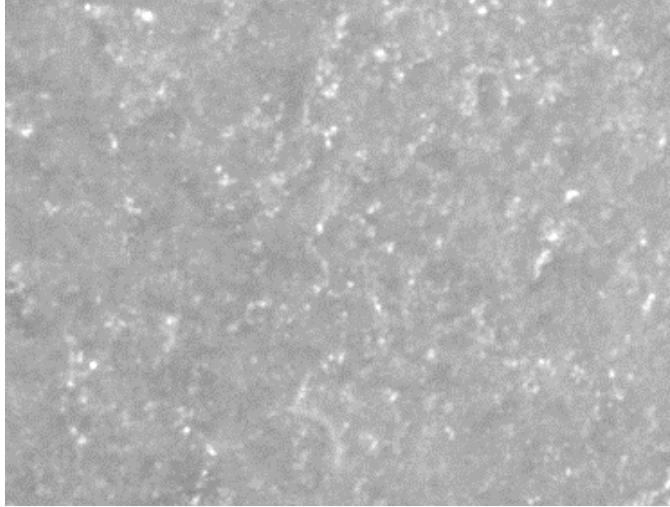
Figure 7.15: Sample Image Used for Texture Calculation

This process is repeated over the desired size data set and is then compiled into the mean and standard deviation for each evaluated size fraction. Figure 7.16 presents a plot of the mean texture and standard deviations before and after Micro-Deval was run for ½-inch aggregate; the other aggregate sizes show similar trends and are not presented.
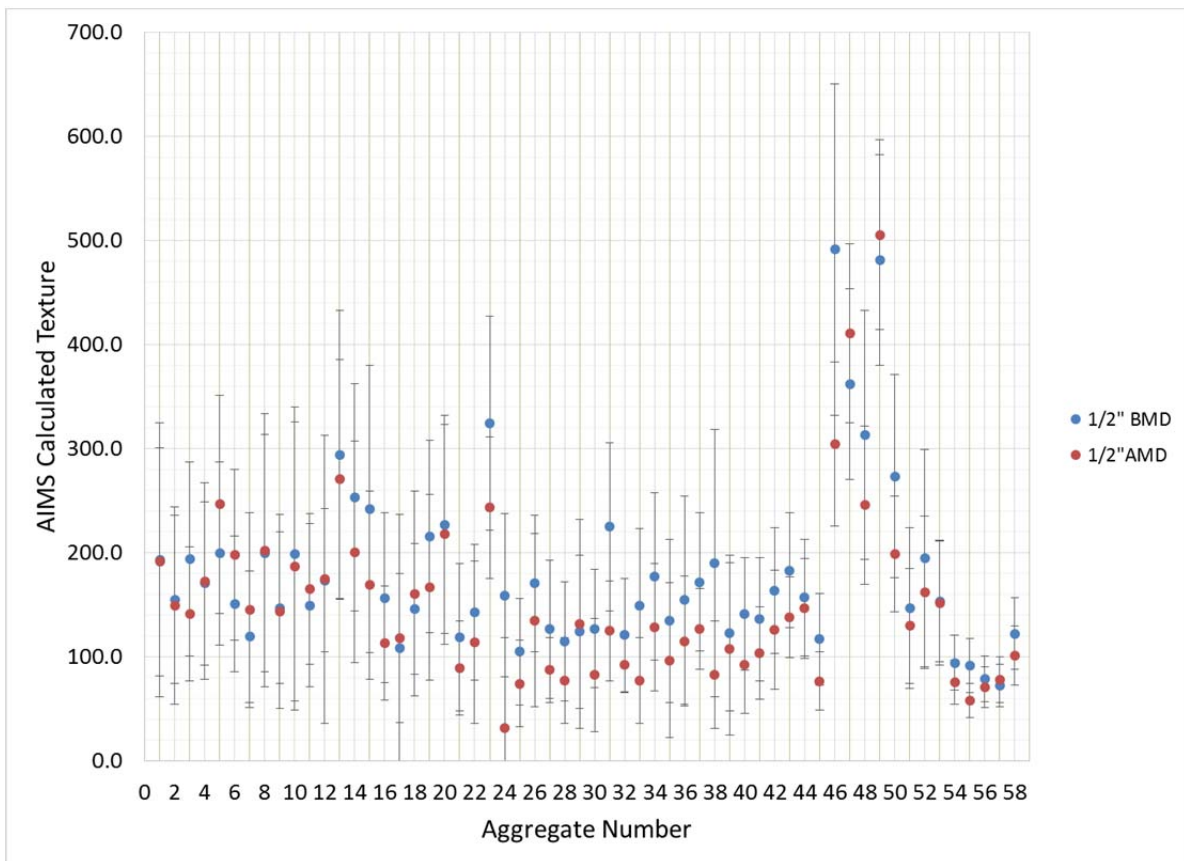
Figure 7.16: Mean and Standard Deviation for AIMS Calculated Texture

Figure 7.16 shows much more overlap of values than was seen in the data set from the AIMS calculated angularity. This trend was also seen and presented in Stutts (2012) in which an aggregate sample was colored between successive analysis runs, resulting in an apparent 163% increase in texture. Again, an additional level of statistical analysis was performed to determine the confidence that the values measured indicated a change in measured texture for the aggregate. The same analytical procedure outlined in Section 7.4.1 was performed. The probability of a measurable change in texture of an aggregate considering a 95% confidence interval is shown in Figure 7.17.
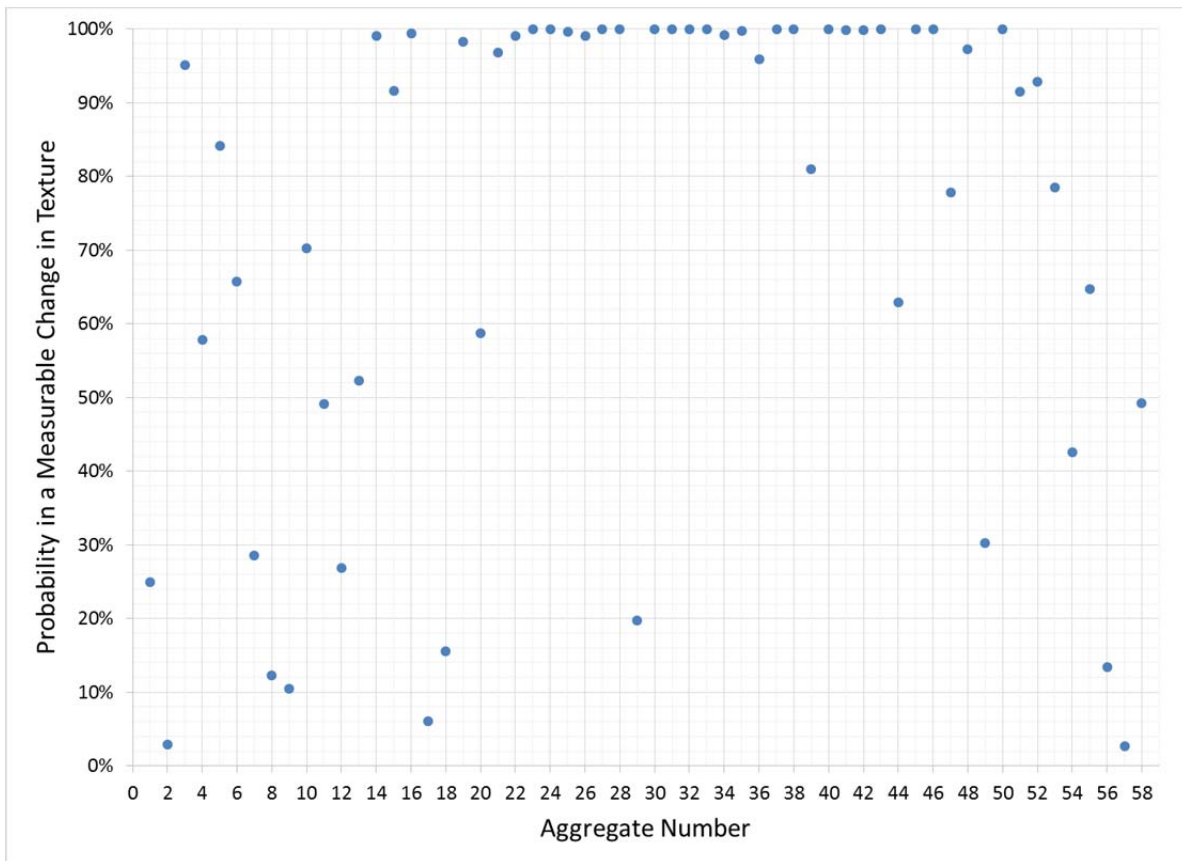
Figure 7.17: Probability of Measureable Texture Change

Figure 7.17 shows that (for a 95% confidence interval) the only materials that show high probability of measurable change are blast-quarried limestones and dolomites (aggregate numbers 20 to 48). These materials typically indicated at least a 20% decrease in texture; other lithologies, which typically had less than a reported 20% change in texture, had much lower probabilities for accurate measurable change. This indicates that approximately 50% of the aggregates collected were accurately quantified for texture change with the AIMS 2.0. Figure 7.18 presents the percent coverage of the data set and corresponding confidence interval for measurable texture change.
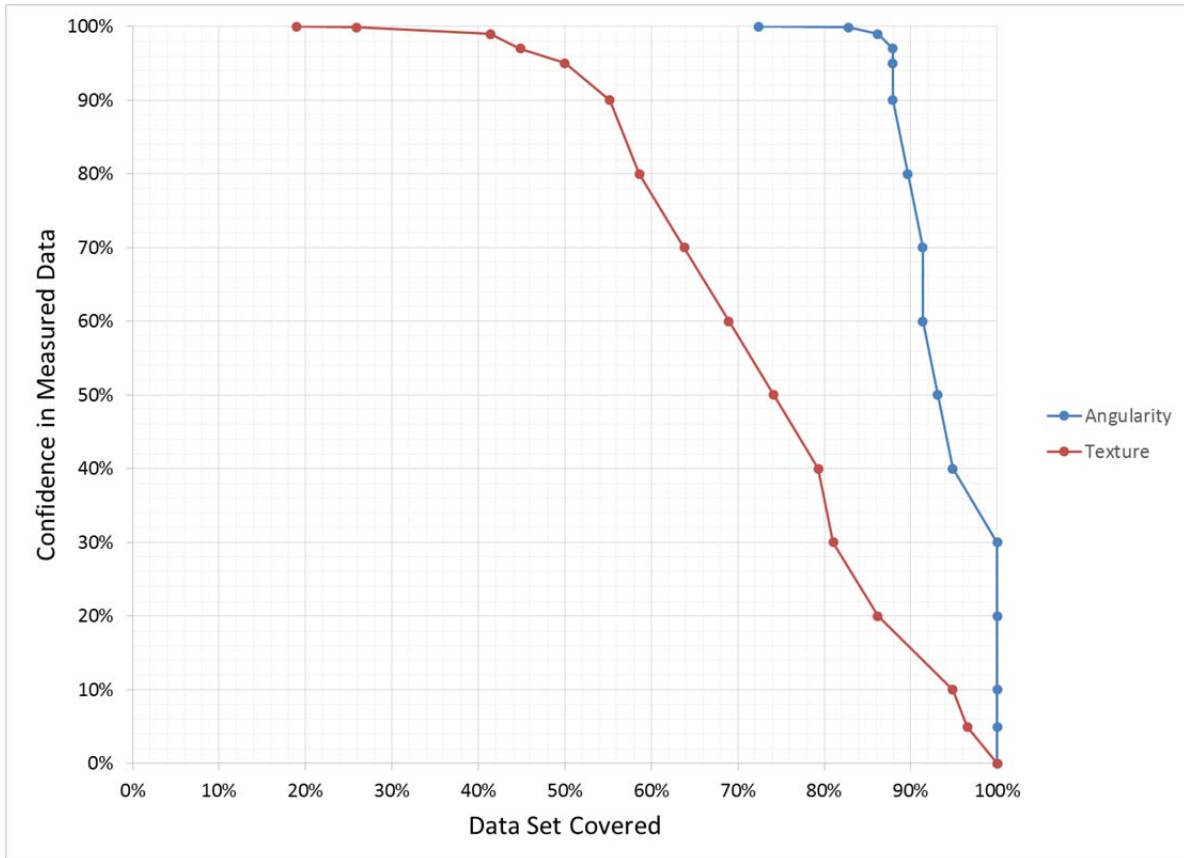
Figure 7.18: Data Confidence Interval Compared with Data Coverage

Figure 7.18 shows the differences between the confidence intervals between AIMS angularity and texture measurements. As mentioned previously, AIMS-calculated angularity changes have relatively high confidence for the data set tested; however, AIMS-calculated texture change is generally less reliable. The same percent coverage of data sets would require a confidence interval of only 20%.

7.4.3 Evaluation for Flat and Elongated Particles

An abundance of flat and elongated particles in a concrete mixture can negatively affect the workability and placement of a concrete mixture; there is also a possibility that concrete strength could be adversely affected. AIMS 2.0 also has the ability to measure particles for determination of flat and elongated pieces. This ability analyzes the profile dimensions from the two-dimensional image of an aggregate particle and then combines that with the focal height of the camera to determine particle height. While sound in theory, a validation of these calculations was deemed necessary; as such, materials were also evaluated with the direct proportional caliper (ASTM D4791). A comparison of the results from these methods is presented in Figure 7.19.
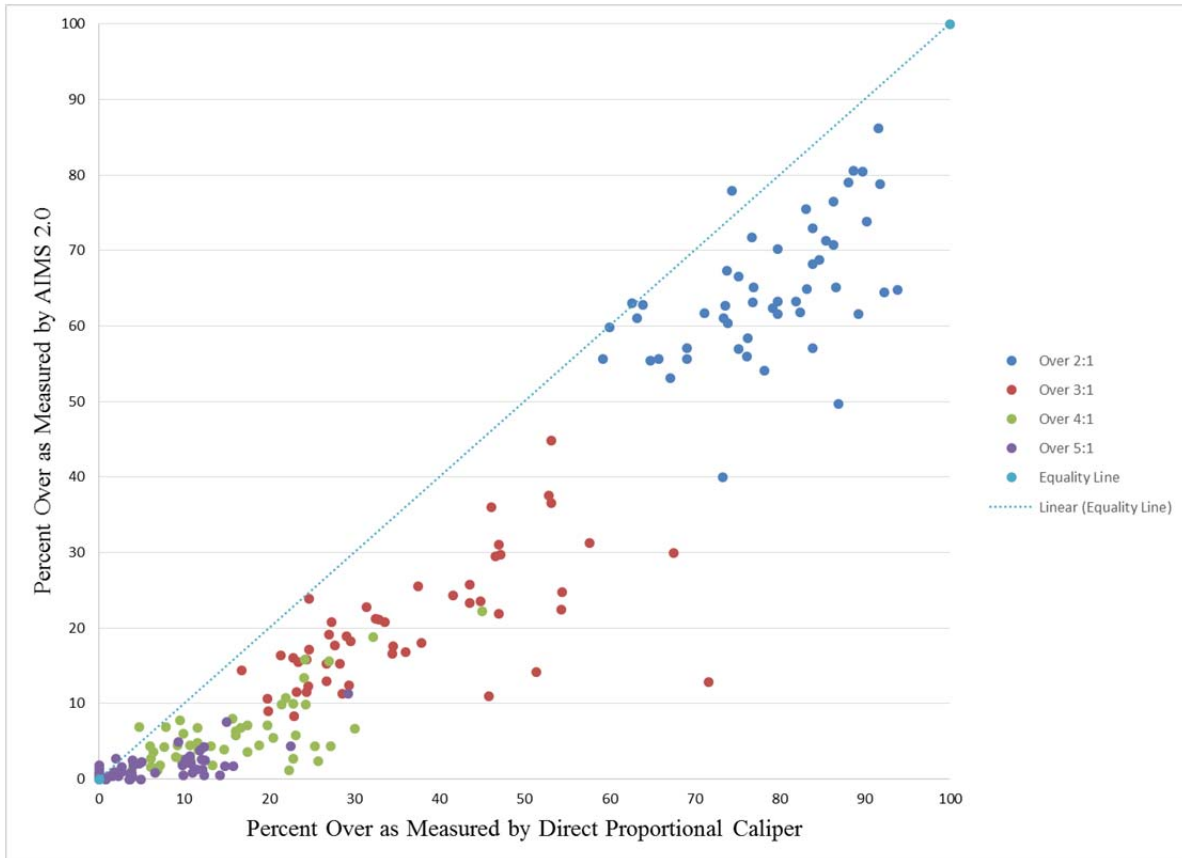
Figure 7.19: Comparison of Flat and Elongated Particle Evaluation

Figure 7.19 shows relatively poor correlation between the AIMS flat and elongated particle calculation and the methods from the direct proportional caliper. The AIMS evaluation underestimates flat and elongated particle content and becomes progressively worse with an increase in aspect ratio. The underestimation is a concern since the high aspect ratio particle content is the most important value property from the set.

7.5 Conclusions

This chapter presented an analysis of aggregate test data collected. Commentary of the trends seen for each aggregate property that was analyzed was included for the basis of selecting the best possible test methods for evaluating aggregate. The next chapter will discuss the results from concrete mixtures tested with a subset of the aggregates collected. Conclusions from the analysis performed in this chapter include the following:

- Considering the Micro-Deval loss in combination with angularity change from AIMS 2.0 provided a system for classifying materials in terms of likeliness to break and likeliness to abrade.

- AIV testing was modified to include an automated test apparatus.

- AIV testing had strong correlation to LA abrasion testing; however, AIV testing requires a smaller sample and can be performed more quickly.

- Very poor correlation exited between magnesium sulfate soundness testing and unconfined freezing and thawing testing.

- Confidence in results for the AIMS 2.0 determination of angularity was much higher than the results for texture determination and calculation of flat and elongated particles.

Chapter 8. Concrete Test Results

This chapter contains the results of concrete testing that was conducted on 24 of the 58 aggregate sources collected. A description of each test was provided in Chapter 5. Data will be presented graphically, with a primary graph showing all 24 concrete mixtures. The data from this chapter is included in tabular form in Appendix B.

8.1 Concrete Mixture Design Considerations

Many factors were considered for producing concrete mixtures from a selection of the aggregate that was collected. The data set needed to contain a representative variety of the lithologies collected and to emphasize aggregates not typically permitted in the production of PCC for TxDOT. These factors resulted in the selection of materials presented in Table 8.1.

Table 8.1: Aggregate Selection for Concrete Mixtures

Sample ID	Lithology	Sample ID	Lithology
1	Partly Crushed River Gravel	38	Limestone
4	Partly Crushed River Gravel	39	Limestone
9	Partly Crushed River Gravel	40	Limestone
11	Siliceous River Gravel	44	Dolomite
15	Limestone River Gravel	45	Dolomite
16	Limestone River Gravel	46	Dolomite
19	Limestone River Gravel	47	Granite
25	Limestone	51	Sand Stone
27	Limestone	52	Sand Stone
29	Limestone	54	Trapp Rock
30	Limestone	55	Trapp Rock
37	Limestone	57	Rhyolite

With the aggregate set selected for the mixtures, the next consideration was the concrete mixture design. The only desired variable in the concrete mixture design was the type of coarse aggregate that would be used. An additional consideration was for the targeted application type of the mixture design. Discussion with the project sponsor influenced the ultimate decision of the mixture design to allow for comparisons with previously generated unpublished data.

Ultimately, a concrete mixture design for a typical highway pavement with a 4400 psi (30 MPa) compressive strength was selected. Certain deviations to the standard mixture proportioning were included to allow for single variable analysis of results. Cement content, the water-to-cement ratio, and coarse aggregate volume remained constant for all mixtures; thus, the only variable would be the coarse aggregate used in the mixture.

However, one issue that had to be addressed was the highly variable gradations of the coarse aggregates. Several of the aggregates received were graded for use in asphalt concrete; others were coarse graded railway ballast, and two were even flexible base material gradations.

To solve this issue, all of the materials selected were crushed (where required), fractionated, washed, and regarded to a standardized proportioning. The proportioning percentages are presented in Table 8.2. This aggregate gradation was selected to maintain a uniform gradation of sizes and eliminate the possibility of large pockets of mortar in the concrete.

Table 8.2: Aggregate Gradation for All Mixtures

Size	Percent Retained
1 in.	0
3/4 in.	22
1/2 in.	46
3/8 in.	17
1/4 in.	12
#4	3

Once aggregate gradations had been standardized, concrete mixtures were cast. ASTM C 192 mixing procedures were followed for laboratory specimens. The slump of the fresh concrete was performed as described in ASTM C 143; the unit weight was determined as described in ASTM C 138. Temperature of concrete was measured in accordance with ASTM C 1064; air content was determined with a Type-B pressure meter using ASTM C 231. The fresh concrete properties are summarized in Table 8.3.

Table 8.3: Fresh Concrete Properties

Aggregate Number	Unit Weight, pcf	Slump, inches	Concrete Temperature, °F	Air Content, %
1	149	1	71.8	1.9
4	149	3.25	72.5	1
9	150	2	72.1	1.4
11	150	1.5	72.5	1.9
15	148	4.5	70.8	1.4
16	149	3.5	72.7	1.4
19	148	4	71.6	1.7
25	147	2.5	73.6	2.1
27	147	3	70	2
29	142	4.75	71.8	2.4
30	149	4	70.7	1.9
37	145	2	71.8	2.4
38	142	5.5	72.3	2.6
39	142	7	72.1	1.9
40	150	1	71.9	1.8
44	154	1.5	70.1	2.1
45	153	2	71.6	1.8
46	155	3	71.7	1.4
47	149	1	70.8	2
51	146	3.5	70.3	1.7
52	147	1.5	70.8	2.2
54	161	1	73.9	1.9
55	162	1.25	71.9	1.9
57	147	3	71.5	2.1

8.2 Compressive Strength

Compressive strength testing of concrete cylinders is the standard benchmark for evaluating mixtures. Three cylinders were tested per mixture cast. The results from 28-day compressive strength testing are presented in Figure 8.1. The average compressive strength for all mixtures was 6525 psi (45 MPa). Figure 8.1 shows that the use of aggregates 29 and 38 resulted in an approximately 30% lower than average compressive strength. However, only the mixture containing aggregate 38 did not meet the design compressive strength of 4400 psi (30 MPa).
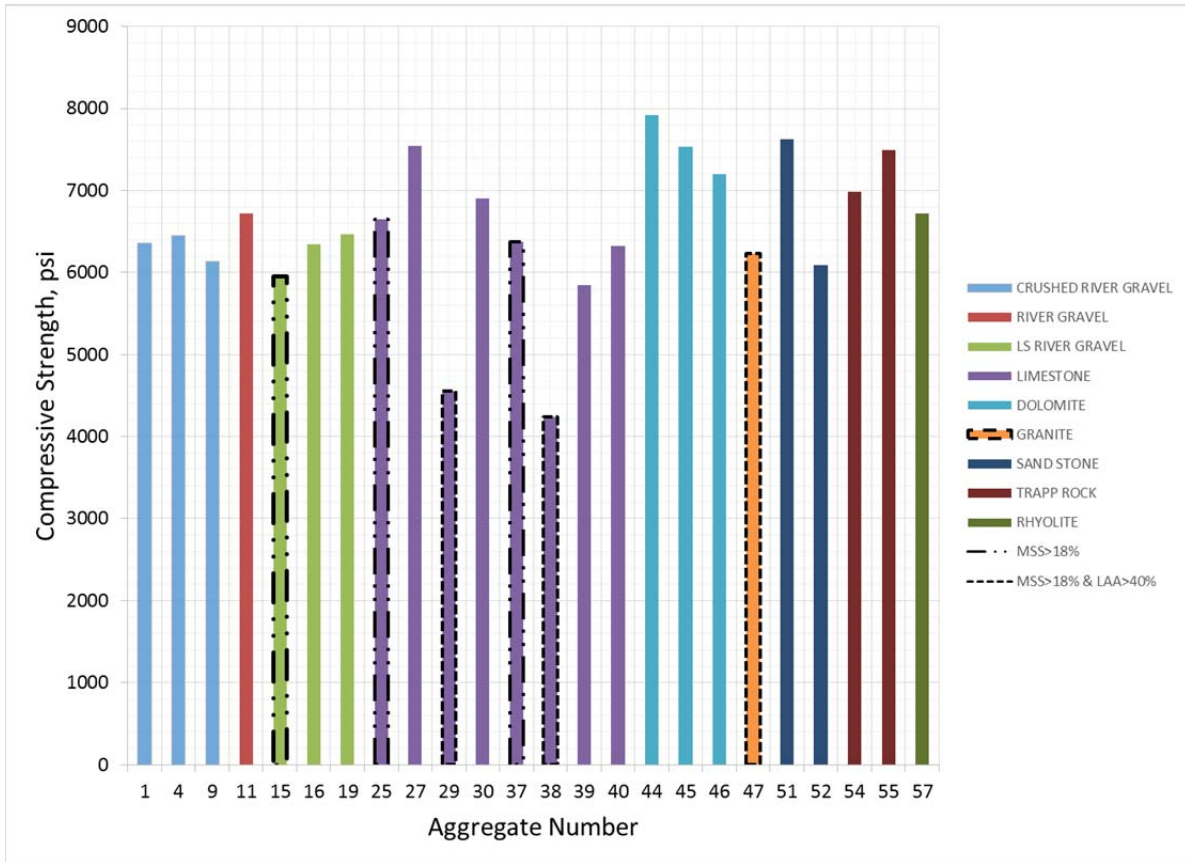
Figure 8.1: 28-Day Compressive Strength Results

8.3 Modulus of Elasticity

An important mechanical concrete property to be considered when there are concerns about deflections of a pavement or a structure or stresses produced due to restraint when temperature changes occur is the concrete modulus of elasticity. Results from modulus of elasticity testing are presented in Figure 8.2.
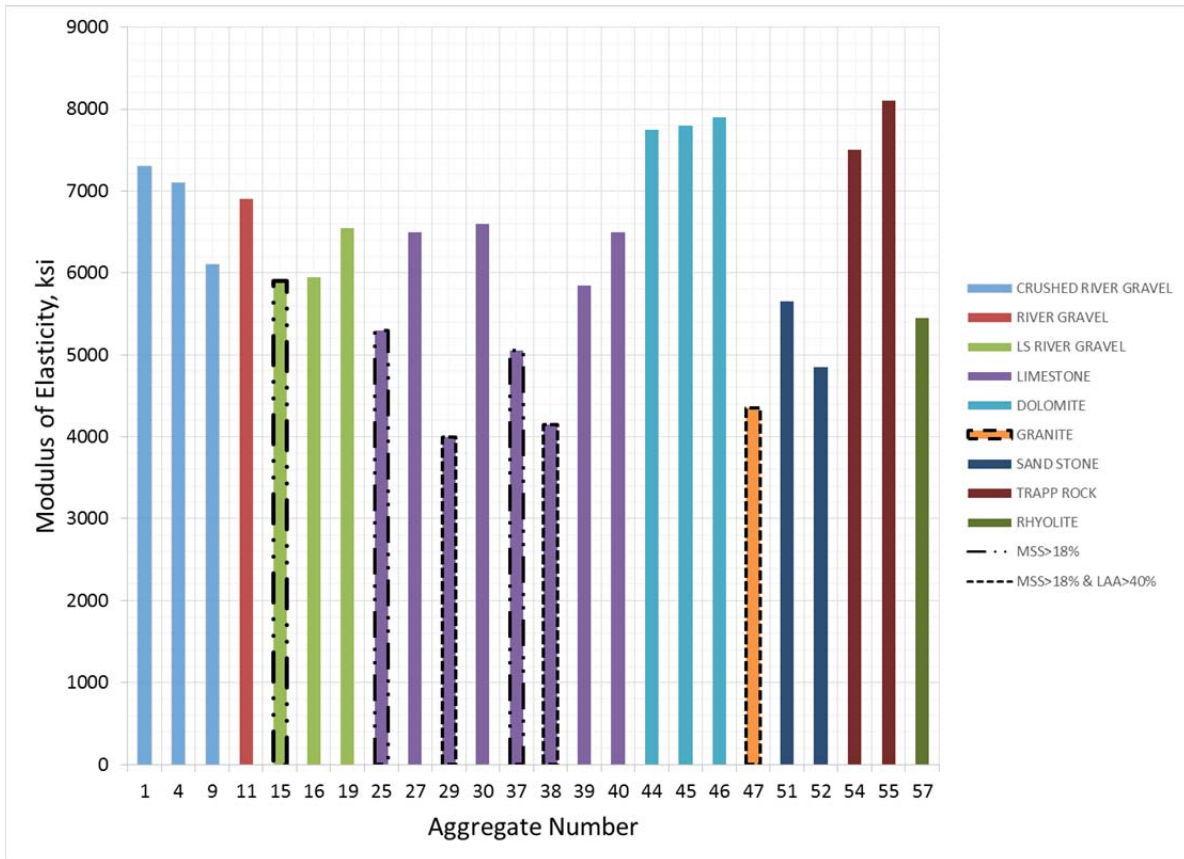
Figure 8.2: Modulus of Elasticity Results

The average modulus of elasticity for all mixtures is 6210 ksi (42.8 GPa). Mixtures containing aggregates 29, 38, and 47 had values that were at least 30% lower than the average; the mixture containing aggregate 55 was over 30% higher than average.

8.4 Flexural Strength

Flexural strength was determined using beams with third-point loading. Flexural beams were made for the preliminary concrete mixtures cast, but were discontinued due to the increased time and material volume needed for casting. Flexural beams are often not specified for construction projects, unless directly required for quality assurance testing in the field due to the increased cost associated with beam casting and testing. Results from the flexural testing are presented in Figure 8.3.
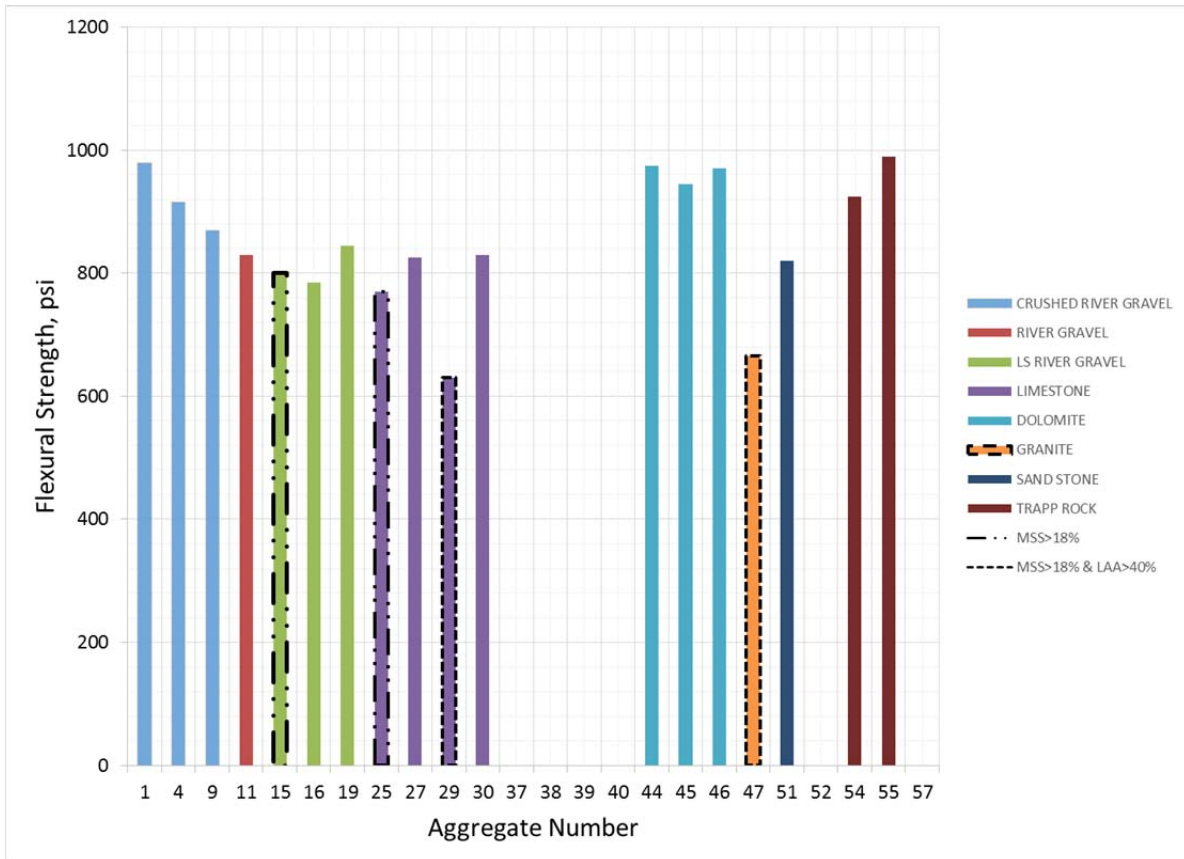
Figure 8.3: Flexure Beam Results

The average flexural strength of the mixtures cast was 850 psi (5.9 MPa); concrete made with aggregates 29 and 47 had approximately a 25% reduction in strength as compared to the average of mixtures cast.

8.5 Splitting Tensile Strength

An indirect method used to determine the tensile strength of a mixture is by using a splitting tensile test of a concrete cylinder. Originally, splitting tensile strength testing was not part of the testing program; however, once consideration was given to the most probable tests to be conducted in the field the test was added to the testing matrix. The results from splitting tensile testing are shown in Figure 8.4.
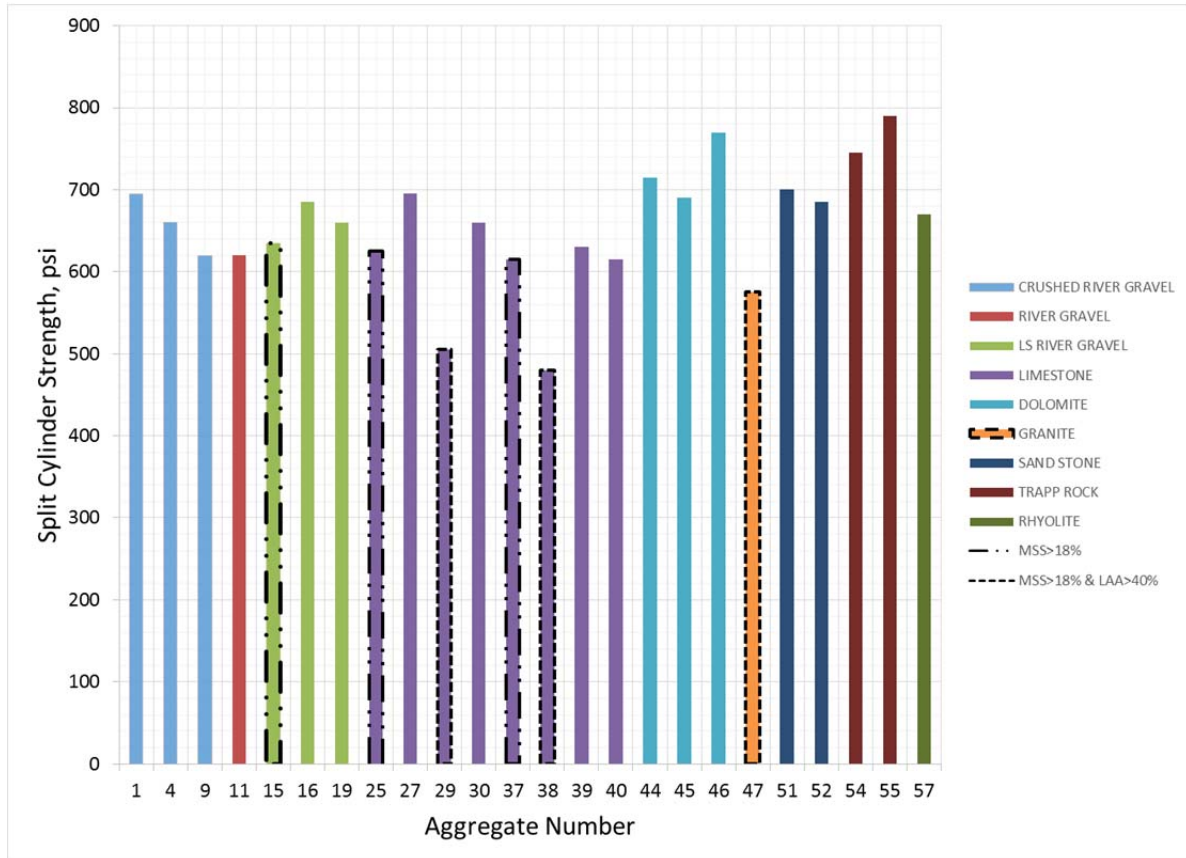
Figure 8.4: Splitting Tensile Strength Results

The average value from splitting tensile testing was 655 psi (4.5 MPa); using aggregates 29 and 38 resulted in strengths that were approximately 25% less than the average.

8.6 CoTE

CoTE testing is divided into two sections. The first section presents the results from the concrete cylinders that were made to evaluate the mechanical properties of aggregates used in concrete mixtures. The second section presents the results obtained from the concrete mixtures containing the crushed aggregate "shells" that resulted from removing cores from large samples discussed in Section 6.10.

8.6.1 CoTE of Standard Concrete Mixtures

The CoTE of a concrete mixture is an important mechanical property for determining the thermal stresses that will result in a structure due to temperature change. CoTE testing was performed by taking the average value from two samples each run three times. The CoTE values obtained are presented in Figure 8.5.
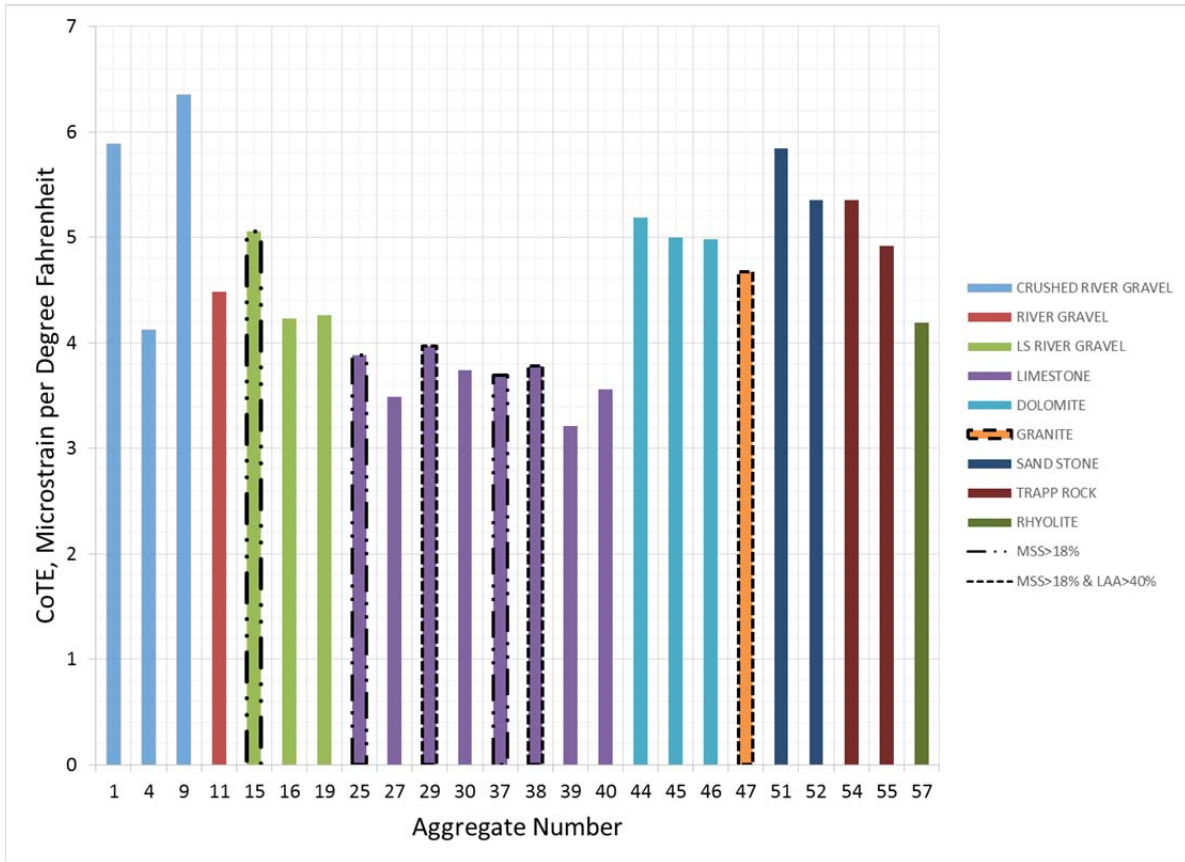
Figure 8.5: CoTE Testing of Standard Mixtures

8.6.2 CoTE of Crushed Aggregate Shell

CoTE testing was also performed on concrete that was made from selected crushed "shells" of aggregate that cores were extracted from (discussed in Section 6.10). The aggregate shells were first removed from the positioning bases and broken into intermediate pieces of approximately 3 in. (76 mm), before being crushed into a material that would have the same proportion of size fractions that were discussed in Section 8.1. These data were generated to determine the relationship between the CoTE of a particular aggregate and the corresponding concrete mixture and will be discussed in Chapter 9. The CoTE values obtained from testing are presented in Table 8.4.

Table 8.4: CoTE Testing of Crushed Aggregate Shells

Source #	Lithology	CoTE Microstrain per degree Fahrenheit	CoTE Microstrain per degree Centigrade
29	Limestone	2.39	4.30
4	Limestone	3.20	5.76
50	Sandstone	4.20	7.56
55	Trapp rock	5.19	9.34
4	Siliceous	6.40	11.52

8.7 Conclusions

The concrete properties presented in this chapter were a representation of the variety of material lithology that is found Texas. The data set also contained mixtures that have aggregate properties that would not typically be allowed for use in TxDOT concrete construction. Certain aggregates, namely numbers 28, 39, and 47, had a notable reduction in performance when compared the remaining 21 mixtures. The concrete properties presented above will be compared to the aggregate test results in the next chapter. Conclusions from the testing performed in this chapter include the following:

- A 30% reduction in compressive strength when compared to the average strength of all mixtures was observed with aggregates 29 and 38.

- A 30% reduction in modulus of elasticity when compared to the average strength of all mixtures was observed with aggregates 29, 38, and 47.

- A 25% reduction in split cylinder strength when compared to the average strength of all mixtures was observed with aggregates 29 and 38.

Chapter 9. Analysis of Concrete Test Results

This chapter contains an analysis of the concrete properties presented in Chapter 6. The focus of this chapter is to relate trends between aggregate test data and concrete test data. Special focus was given to materials that would not typically be allowed in concrete mixtures that do not meet TxDOT specification (aggregates 15, 25, 29, 37, 38, and 47).

9.1 Compressive Strength of Concrete

The compressive strength of a concrete mixture relies on the properties of the combination of materials used in the design. Although an aggregate's resistance to breakage is a crucial element in developing a concrete mixture with higher compressive strength, this property does not control the ultimate strength of a mixture. An additional concern about obtaining strength is the bond between the paste matrix and aggregate; this property can be influenced by the shape of an aggregate.

The strength of the paste matrix surrounding the aggregate is of equal importance in achieving high strengths. The concrete mixture design (discussed in Section 8.1) was based upon a 568 lb./yd^3 (337 kg/m^3) cement content and a 0.45 water-to-cement ratio; no supplementary cementitious materials or admixtures were used. The paste system was a control variable in the concrete mixture design and was designed for evaluation purposes to have adequate strength for general use. However, this mixture design was likely unable to provide ultimate concrete strength for many of the aggregates used; this made correlations between aggregate and concrete testing more difficult.

9.1.1 Effects of Aggregate Strength on Compressive Strength

Direct aggregate strength is a difficult property to measure; imperfections that may exist in a sample large enough for conventional testing often become the point of fracture when the sample is processed into smaller material. This project incorporated tests to determine the resistance to breakage of an aggregate (see discussion in Section 7.2); the results from these tests are compared with the compressive strengths of cylinders in Figure 9.1.
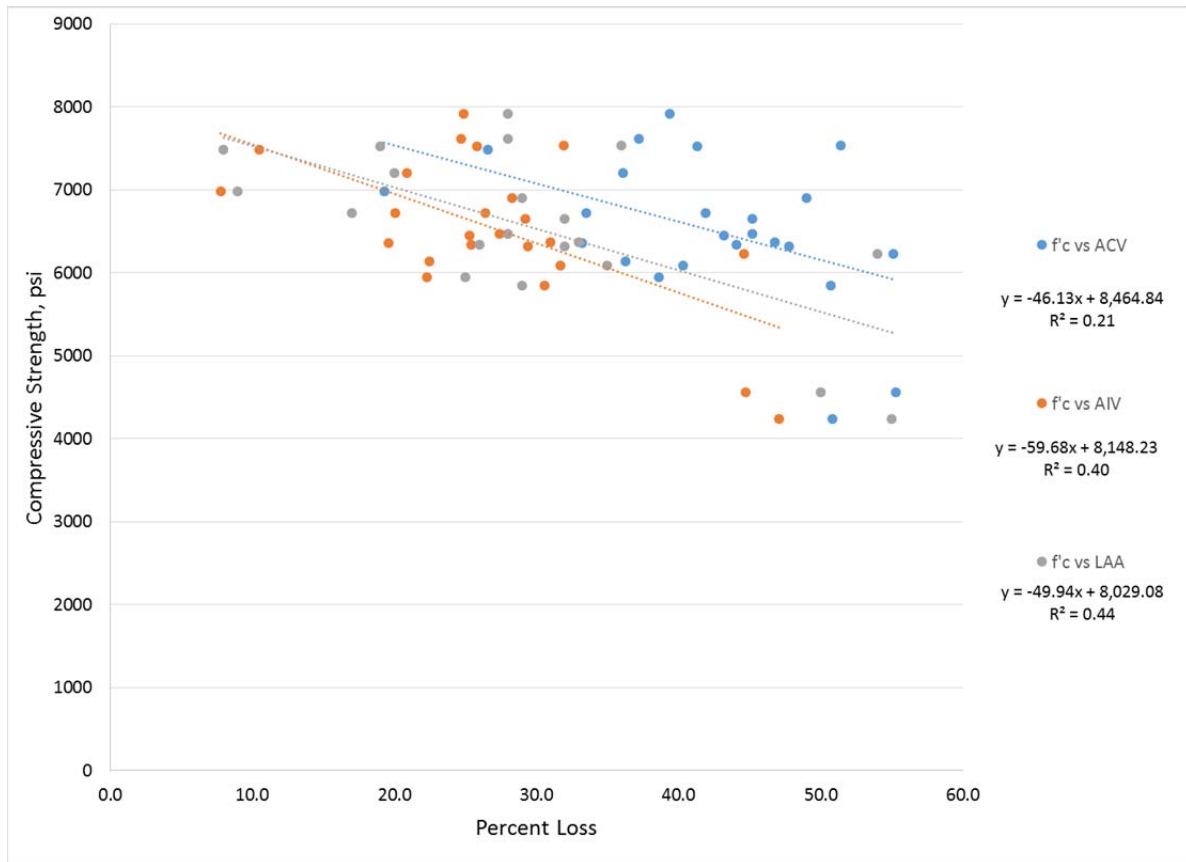
Figure 9.1: Aggregate Tests Results Compared with Concrete Compressive Strength

Figure 9.1 shows that the test with the highest correlation coefficient considering all aggregates tested is the LA abrasion test, with a coefficient of 0.44. Discussion in Chapter 7 favored results from the aggregate impact value (AIV) test because of the direct determination of breakage resistance, but this test only had a correlation coefficient of 0.40. The LA abrasion test loss is a combination of impact damage and abrasion damage; however, it should be noted that many of the aggregates that tested below a 30% loss in LA abrasion had very few fractured aggregates when examining the concrete cylinders after testing.

However, discussion in Section 7.1.2 considered the contribution of loss from abrasion as well as from breakage for classifying an aggregate. Aggregates with losses of over 20% when tested with the Micro-Deval were considered to have a high breakage component. Using this data point as a filter, the results presented in Figure 9.1 are reinterpreted considering only data sets that had over a 20% Micro-Deval loss, shown in Figure 9.2.
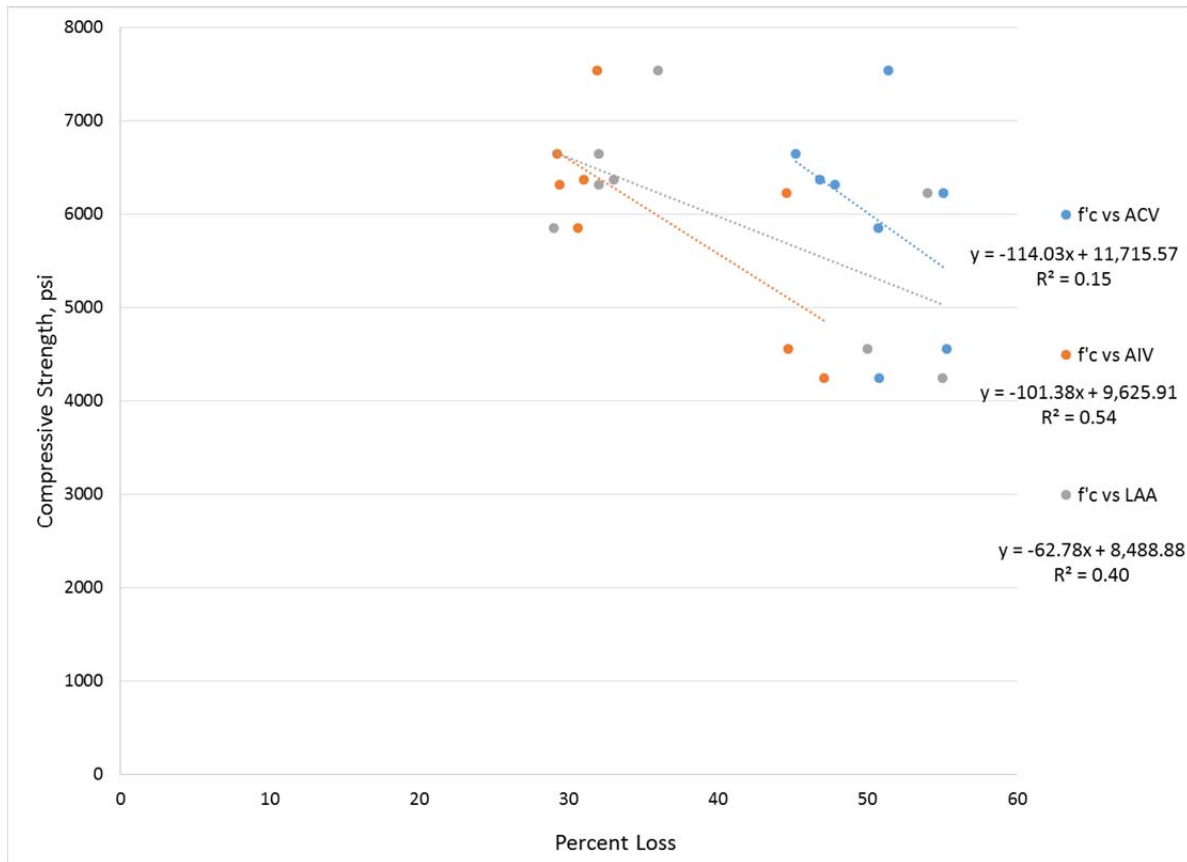
Figure 9.2: Aggregate Test Results Compared with Concrete Compressive Strength for Aggregates Over 20% Micro-Deval Loss

Figure 9.2 shows the highest correlation coefficient now belonging to the AIV test (0.54), while correlations from the LA abrasion test decreased to 0.40. AIV test results are therefore believed to have poor strength correlation for this particular concrete mixture design. However, neither analysis demonstrates that the resistance to breakage of an aggregate is a dominant factor for the compressive strength of a concrete mixture. Thus, it is very likely that these aggregates were not the cause of failure for these concrete mixtures; it is more likely that the paste matrix bond to the aggregate was the controlling factor.

9.1.2 Effect of Aggregate Shape on Compressive Strength

Aggregate shape can directly affect the resulting bond that a paste matrix has with an aggregate. Aggregate shape characteristics (angularity, texture, and flat and elongated particles) were determined with an AIMS 2.0 device and presented in Section 6.8; a discussion of these results, presented in Section 7.4, suggested that the only value that has the level of precision desired for analysis is the angularity determination. As such, only this value from the AIMS test will be considered for this discussion. Figure 9.3 presents the comparison between angularity values and compressive strength.
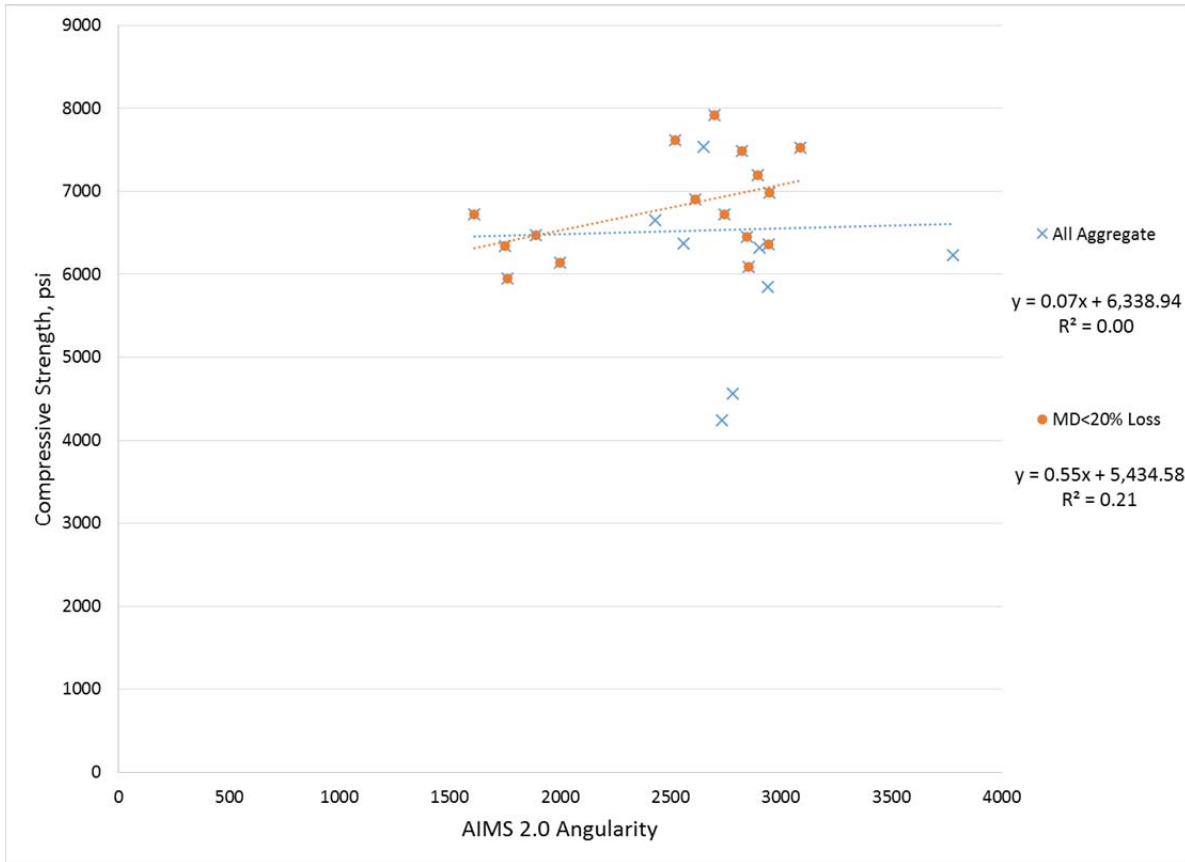
Figure 9.3: Comparison of AIMS 2.0 Angularity with Concrete Compressive Strength

Figure 9.3 presents the data considering two conditions. The first condition considers results from all data generated; this method returns almost nonexistent correlation, 0.002. The second condition again filters the data, but with values below a 20% Micro-Deval being shown. This approach improves the correlation to 0.21, assuming that materials with less than a 20% Micro-Deval loss are more likely to show abrasion loss than breakage loss (material is less likely to break). Once again, the poor correlation of data is likely due to the fact that the compressive strength of the concrete cylinders was not indicative of aggregate failure.

AIMS 2.0 flat and elongated calculations were compared to hand determination of flat and elongated particles (ASTM D 4791) and discussed in Section 7.4.3. The results indicated a pronounced drift between the results of the AIMS 2.0 and the hand method that increased with aspect ratio; as such the results from the hand determination are used for this discussion. Figure 9.4 presents the comparison of particle content with aspect ratios over four, a size ratio believed to cause problems in concrete.
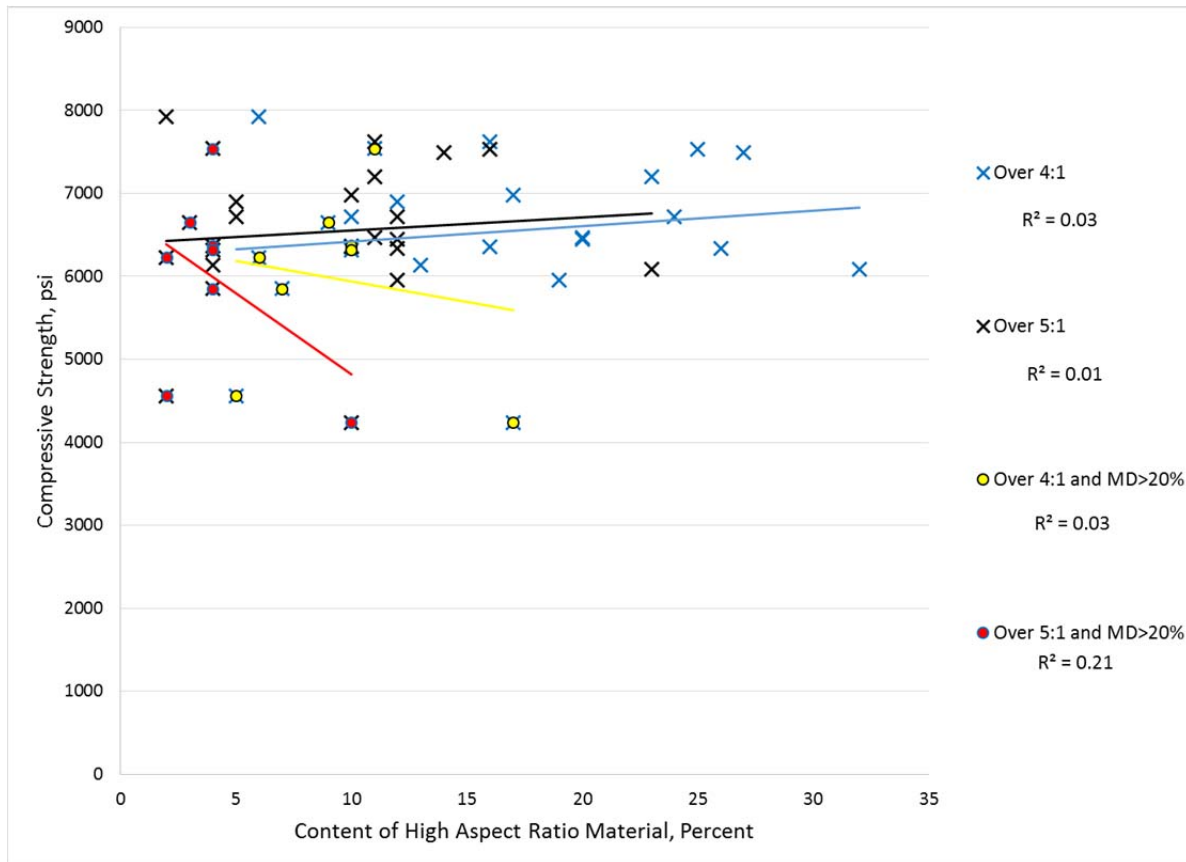
Figure 9.4: Comparison of Flat and Elongated Particle Content with
Compressive Strength of Concrete

Figure 9.4 presents the data again with two conditions. An analysis is performed for both aspect ratios (4:1 and 5:1) with and without considering a 20% Micro-Deval loss limit. The trend without considering the Micro-Deval loss limit (aggregate likely to have any combination of breakage and abrasion loss) show that for either aspect ratio, increase in particle percentage can cause a negligible to a slight increase in the compressive strength (correlation coefficients of 0.03 for 4:1 and 0.01 for 5:1). Discounting materials with under a 20% Micro-Deval loss (considering materials only likely to have high breakage) improves correlation for particles with a 9:1 aspect ratio (correlation coefficients of 0.03 for 4:1 and 0.21 for 5:1). This trend shows that a higher content of particles with a 5:1 aspect ratio can lead to a lower compressive strength.

9.2 Tensile Strength of Concrete

Tensile strength testing of concrete is rarely performed for many field applications. For most concrete construction, the tensile strength and resulting capacity of concrete is usually insignificant and therefore neglected when compared to the tensile capacity of reinforcing steel. However, concrete tensile strength is an important consideration when bonded overlays or tension anchorages are used. Two methods were used to evaluate the tensile strength of concrete: split cylinder testing (ASTM 496) and flexural beam testing (ASTM C78). Results from these test methods will be discussed in this section.

9.2.1 Discussion of Test Methods

Performing a direct pure tension test for a concrete specimen is difficult and only performed in rare situations. More common methods for determining the indirect tensile strength of a concrete specimen are the split cylinder test and flexure beam test. The split cylinder test applies a compressive force to the side of a cylindrical specimen, resulting in a tensile force being generated in the center of the specimen perpendicular to the applied load. Flexural beam testing typically involves loading a beam with third point loading to generate a constant moment region over the middle third of the beam until the beam fractures. For most applications, flexural beams require significant amount of concrete (which also results in the samples having a significant increase in mass compared to standard concrete samples), require substantial additional equipment for testing, and are more prone to breakage during handling prior to laboratory testing. In the beginning of the test program, concrete was tested for both flexure and splitting cylinder values. During the midway point of concrete batching, flexural beam testing was discontinued to allow for completion of more mixtures. Figure 9.5 presents a comparison between results from splitting cylinder testing and flexural beam testing.
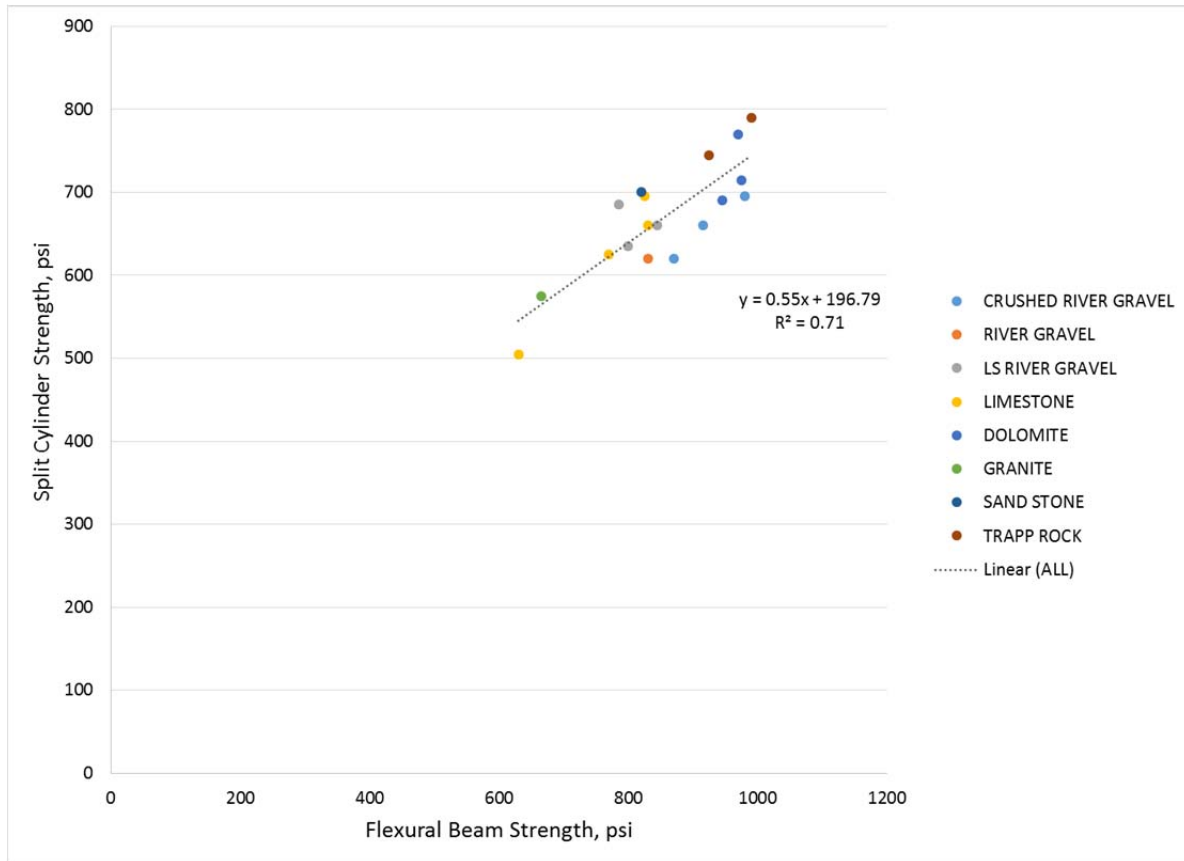
Figure 9.5: Comparison of Flexure Beam Strength with Split Cylinder Strength

Figure 9.5 shows a 0.71 correlation coefficient between the two test methods; this indicates a moderate relationship between flexural beam and split cylinder values. Considering this correlation and the fact that only split cylinder testing data are available for all concrete mixtures, flexural beam testing will be discussed no further.

142

9.2.2 Effect of Aggregate Strength on Tensile Strength

The tensile strength of a concrete mixture is approximately 10% of the compressive strength; this percentage is strongly influenced by the paste matrix bond to the aggregate. It is logical to assume that the aggregate shape factors will have a stronger correlation to concrete performance than aggregate strength. Similar to the compressive strength of an aggregate, the tensile strength of aggregate is once again a test procedure that is difficult to perform; most likely the test will be performed on an aggregate core, limiting the lithologies that can be tested with this method. The tests used to measure an aggregate's resistance to breakage will be used for comparison with concrete tensile strength (Figure 9.6).
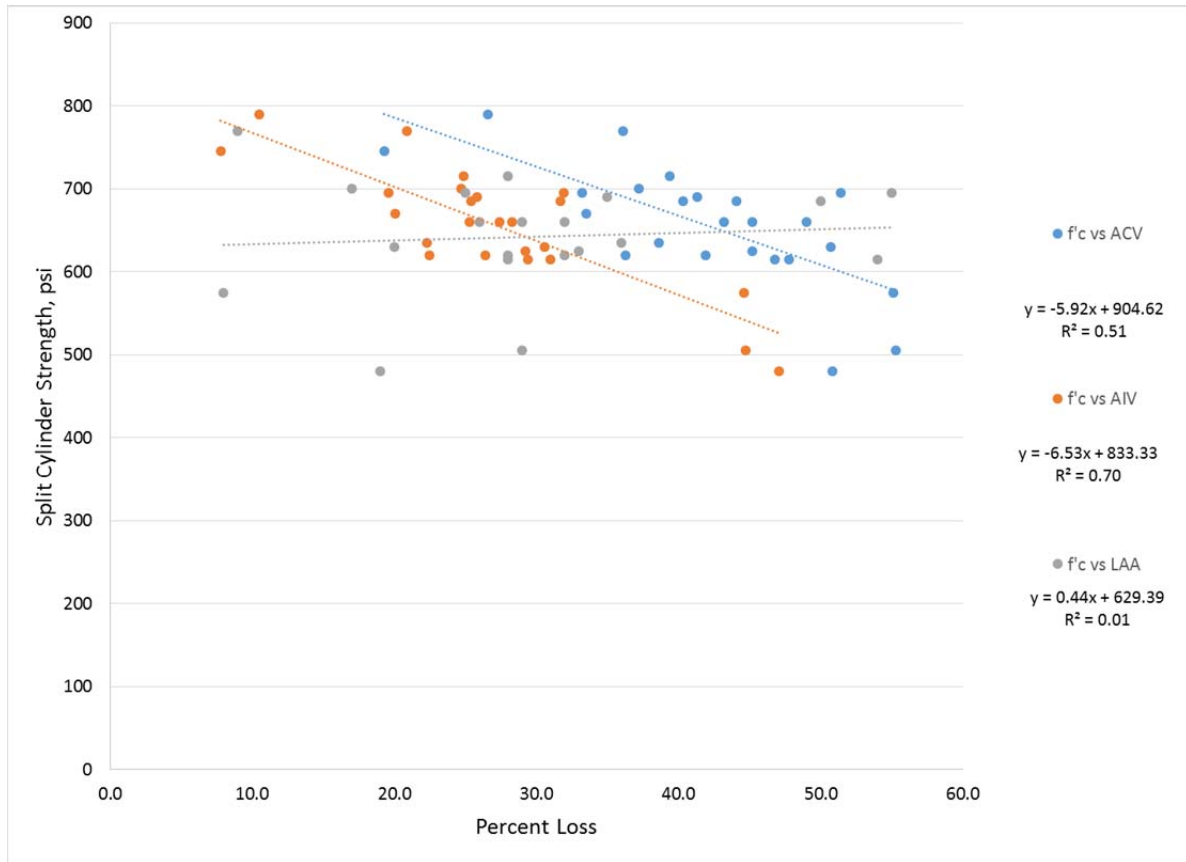
Figure 9.6: Aggregate Tests Results Compared with Concrete Split Cylinder Strength

Figure 9.6 shows that the test with the highest correlation coefficient considering all aggregates tested is the AIV test with a coefficient of 0.70; discussion in Chapter 7 favored results from the AIV test because of the direct determination of breakage resistance. The LA abrasion test has very poor correlation (0.01) considering all aggregates, a notable difference compared to correlations between the LA abrasion and concrete compressive strength. This trend may be related to the higher percentage of fractured aggregate resulting from split cylinder testing when compared to concrete compressive testing.

Recalling the discussion from Section 7.1.2 in which aggregate loss from abrasion was assumed the primary distress mechanism for aggregate with under a 20% loss, a comparison is made by considering aggregate with over a 20% Micro-Deval loss. Using this data point as a

filter, the results presented in Figure 9.6 are reinterpreted considering only data sets that had over a 20% Micro-Deval loss, shown in Figure 9.7.
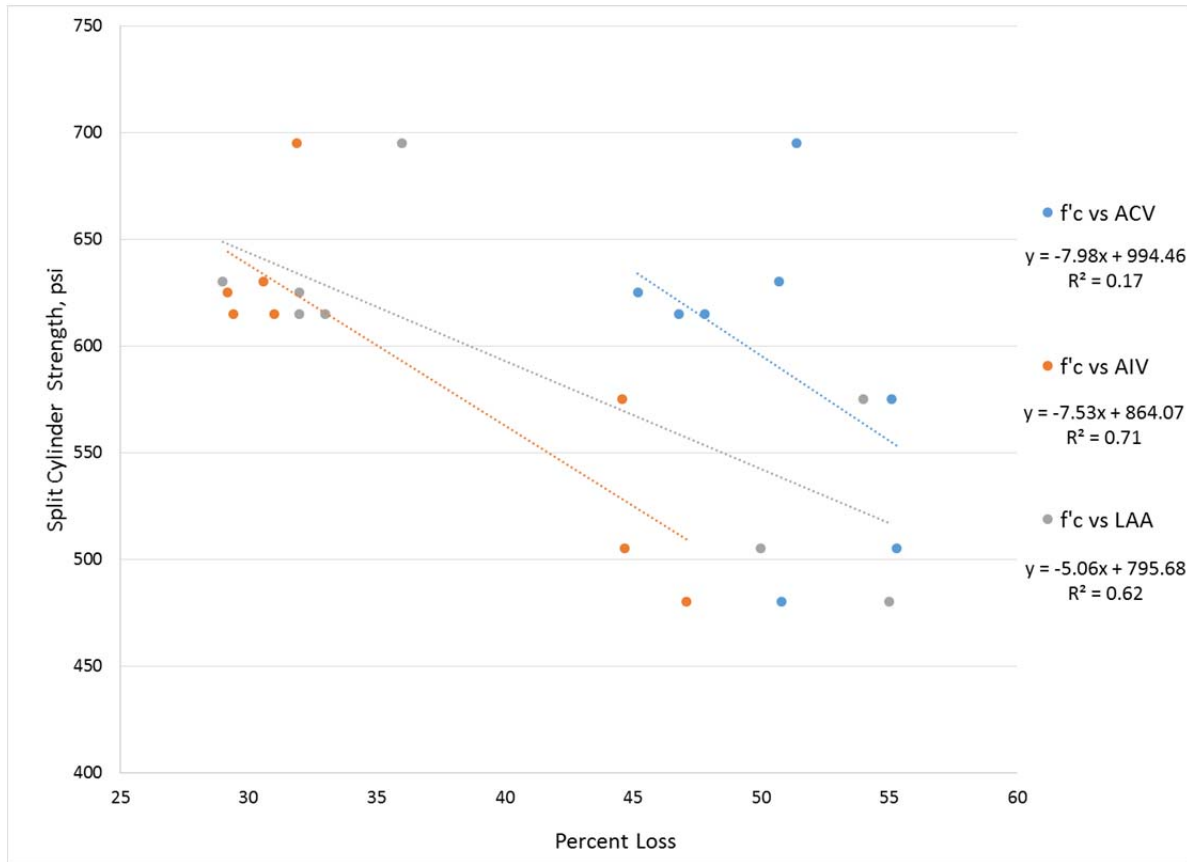
Figure 9.7: Aggregate Test Results Compared with Concrete Split Cylinder
Strength for Aggregates over 20% Micro-Deval Loss

Figure 9.7 shows the highest correlation coefficient again belonging to the AIV test (0.71); correlations from the LA abrasion test have also increased to 0.62 (from 0.01). AIV test results are considered to have moderate strength correlation for this particular concrete mixture design. This analysis indicates that the resistance to breakage has a prominent role in the split cylinder strength of a concrete mixture; contrary to the original assumption (suggested by Folliard and Smith, 2002) that aggregate shape characteristics would be of higher importance in determining tensile strength. Thus, it is more unlikely that the modification of paste matrix bond will provide substantial increases in split cylinder strength.

9.2.3 Effect of Aggregate Shape on Tensile Strength

For the reasons discussed in Section 9.1.2, only the AIMS 2.0 calculated angularity values will be discussed in relation to tensile strength. Figure 9.8 presents the comparison between angularity values and tensile strength.
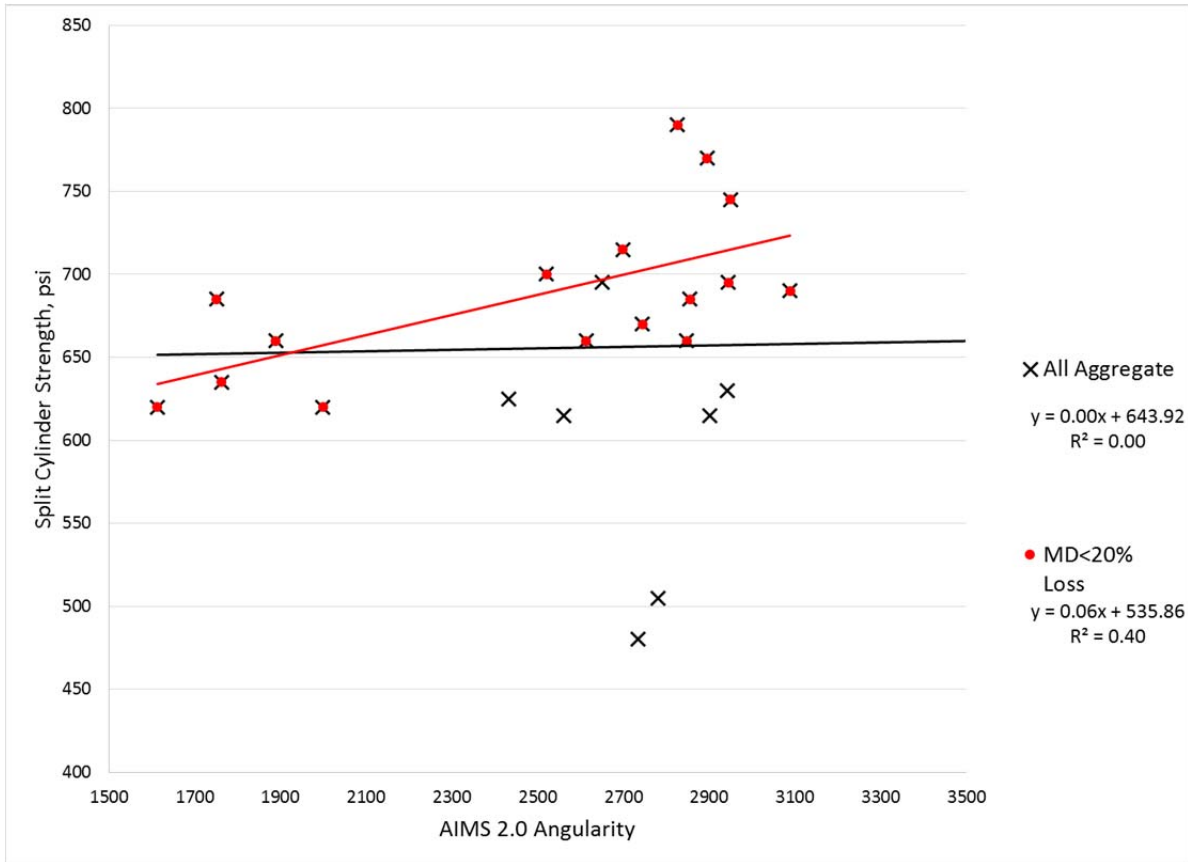
Figure 9.8: Comparison of AIMS 2.0 Angularity with Concrete Split Cylinder Strength

Figure 9.8 presents the data considering two conditions. The first condition considers results from all data generated; this method again returns almost nonexistent correlation between data, 0.001. The second condition again filters the data, but this time showing values below a 20% Micro-Deval. This approach improves the correlation to 0.40 (a notable improvement from the 0.21 correlation with compressive strength), with the assumption that materials with less than a 20% Micro-Deval loss are more likely to show abrasion loss than breakage loss (material is less likely to break). This trend shows that although tensile strength shows more correlation that compressive strength when compared with angularity, neither strength value seems to be strongly influenced by the property.

As previously discussed (Section 9.1.2), hand determination of flat and elongated particles was used instead of the results from AIMS 2.0. Figure 9.9 presents the comparison of particle content with aspect ratios over 4:1.
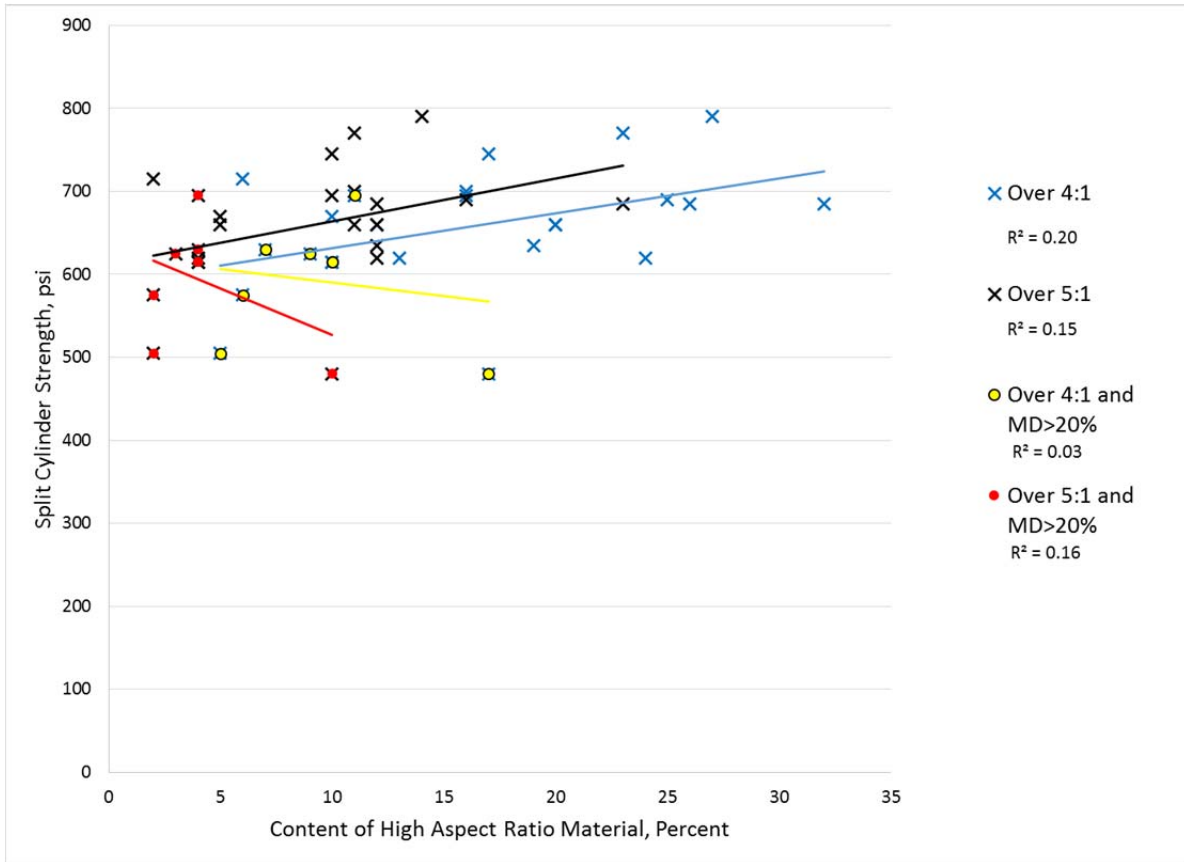
Figure 9.9: Comparison of Flat and Elongated Particle Content with Split Cylinder Strength of Concrete

Figure 9.9 presents the data with two conditions. An analysis is made for both aspect ratios (4:1 and 5:1) with and without considering a 20% Micro-Deval loss limit. The trend without considering the Micro-Deval loss limit (aggregate likely to have any combination of breakage and abrasion loss) shows that for either aspect ratio, an increase in particle percentage can cause a slight increase in the tensile strength (correlation coefficients of 0.20 for 4:1 and 0.15 for 5:1). Discounting materials with under a 20% Micro-Deval loss (considering materials only likely to have high breakage) drastically changes the slope of the trend line for particles with a 5:1 aspect ratio (correlation coefficients of 0.16 for 5:1). This trend indicates that a higher content of particles with a 5:1 aspect ratio can potentially lead to noticeably lower tensile strengths.

9.3 Modulus of Elasticity of Concrete

In most cases, the modulus of elasticity (MOE) of a concrete mixture is not a targeted design constraint; the property is typically only used to perform or verify calculations for resulting strains or deformations of a concrete structure. Considering this, no direct comparisons will be made for relating aggregate testing with the MOE of a concrete mixture. Rather, evaluations will be made concerning the relationships between measured MOE and calculated MOE from the formula presented in ACI 318-11 Section 8.5.1 (MOE= 33*{unit weight of

concrete$\}^{1.5}$ *{compressive strength$\}^{0.5}$). A comparison of these values is presented in Figure 9.10.
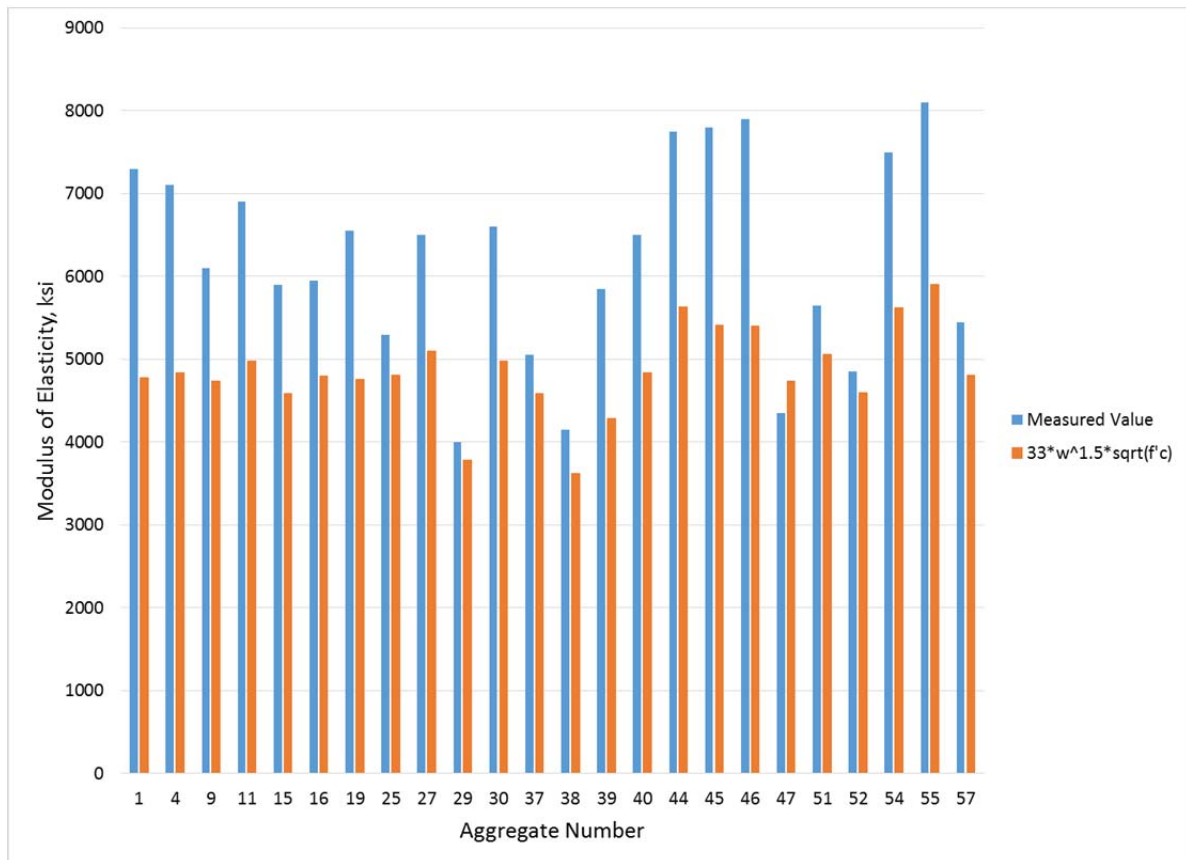
Figure 9.10: Comparison of Measured Modulus of Elasticity with ACI 318-11 Equation 8.5.1

Figure 9.10 shows that, for most aggregates tested, the ACI equation provides a highly conservative estimate of the modulus of elasticity. According to commentary provided in ACI 318-11 R8.5.1, "Measured values typically range from 120 to 80 percent of the specified value." A comparison of the measured values considering the range specified in ACI 318-11 is presented in Figure 9.11.
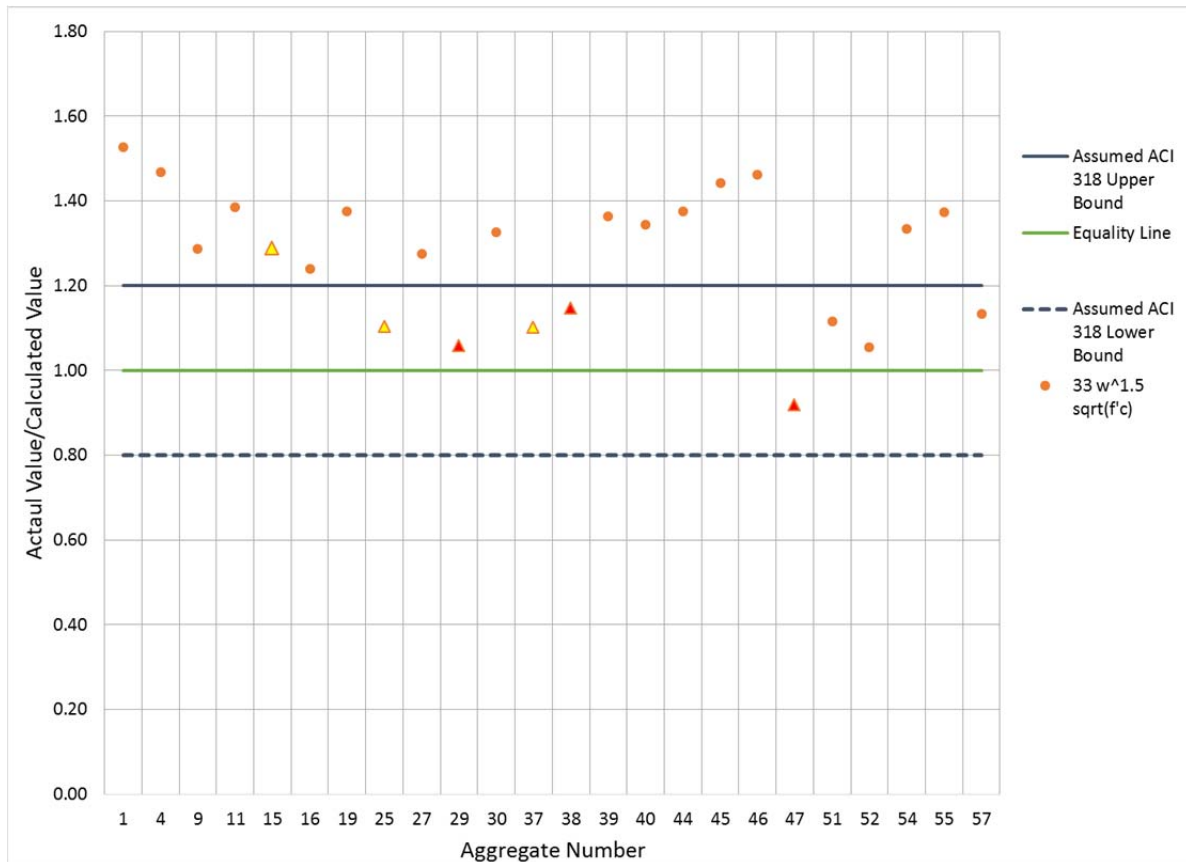
Figure 9.11: Comparison of Measured MOE with Stated Range in ACI Equation 8.5.1

Figure 9.11 shows the majority of the data set to be outside the stated normal range (on the conservative side) when compared to ACI Equation 8.5.1. Aggregate numbers 25, 29, 38, 39, and 47 fall within the bounds of the equation, but would typically not be allowed for use in concrete because of current aggregate specifications. Aggregates 51, 52, and 57 fall within the assumed bounds of the equation and are sand stones (51 and 52) and a rhyolite (57); these lithologies are much less commonly used in concrete as compared to the other groups.

9.4 CoTE of Concrete

CoTE of concrete is a concrete property believed to be responsible for distress in continuously reinforced concrete pavements in Texas, as discussed in Chapter 3. The primary lithologies in which this distress has manifested are siliceous river gravels and some dolomites. Considering this distress, an analysis of the most likely interacting concrete properties was performed.

9.4.1 CoTE for Regular Cylinders

Continuously reinforced concrete pavements (CRCP) constructed with dolomite and siliceous river gravel are more susceptible to CoTE-related damage (Du and Lukefahr, 2007). Section 3.1.2.2 discussed the relationship between the modulus of elasticity with the CoTE of a concrete mixture; this section commented on the higher resulting stresses experienced by concrete mixtures with a high modulus of elasticity. However, only considering the resultant

stress on a material is an incomplete analysis; this approach does not account for the strength of a material. Tensile strength failure is the controlling failure method for most concrete structures, including CoTE-related spalling in pavements. Figure 9.12 presents a comparison of calculated thermal change to induce cracking and the CoTE of concrete mixtures.
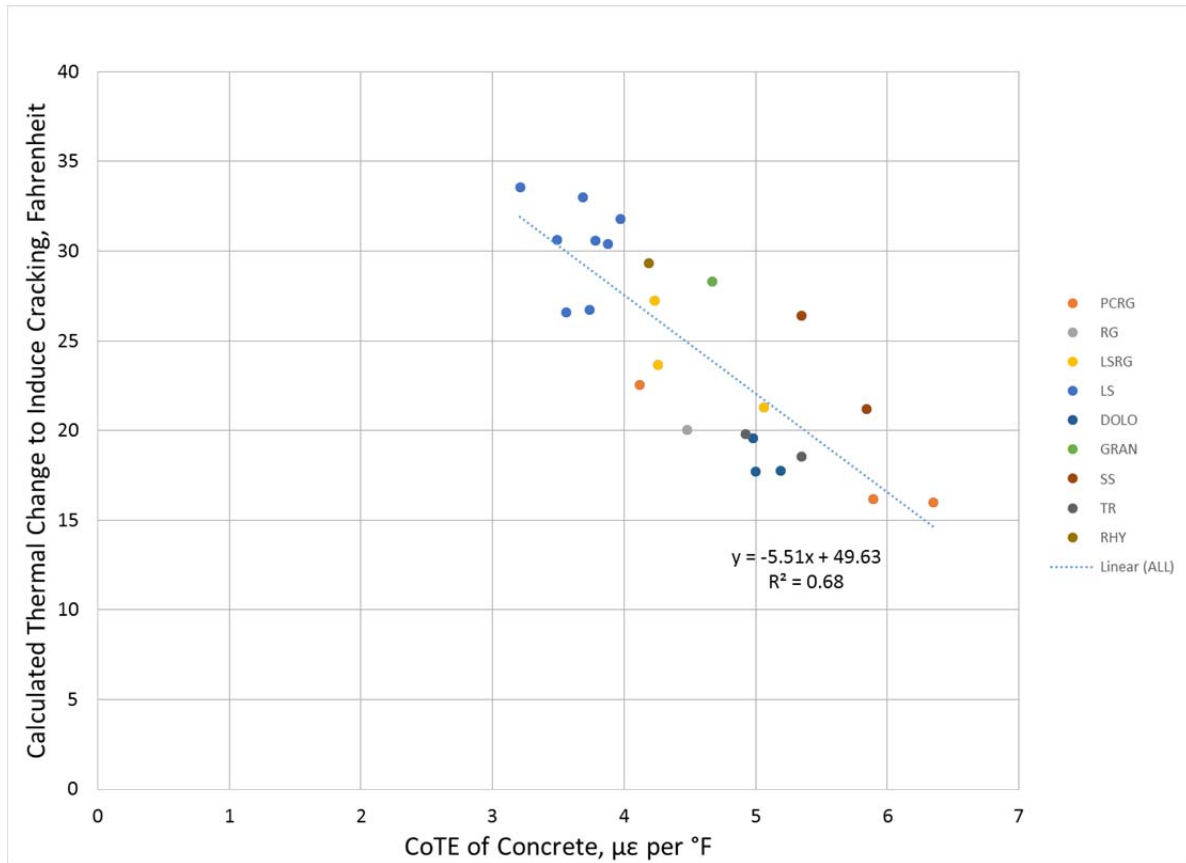
Figure 9.12: Calculated Thermal Change Resulting in Cracking Compared with Concrete CoTE

The thermal change to induce cracking shown in Figure 9.12 was calculated using the split cylinder strength, modulus of elasticity, and CoTE of a concrete mixture; this calculation complete restraint of a concrete element and is likely a conservative value. This figure shows that the materials most likely to experience pavement distress due to CoTE (dolomite and siliceous material) theoretically require less than a 20°F thermal change to induce cracking. Limestones— materials that are documented to perform well in CRCP (Du and Lukefahr, 2007)—theoretically could accommodate a 30°F thermal change, an increase of 150%. The data show that a maximum limitation of the CoTE for a concrete mixture should reduce cracking in CRCP but may possibly exclude material, such as sandstone, that could perform adequately.

9.4.2 CoTE for Cylinders made of Crushed Aggregate Shells

CoTE determination was also performed on pure aggregate cores, presented in Section 6.10. Extracting a core sample from a larger aggregate piece resulted in an aggregate "shell" of material of almost identical lithology to the original core, shown in Figure 9.13.

Figure 9.13: Left, Aggregate "Shell" Right, Pure Siliceous Aggregate Core

The hypothesis was then formed that a relationship would exist between the CoTE of a pure aggregate sample and a concrete mixture containing that aggregate. This hypothesis was tested on five of the aggregate samples presented in Chapter 6. The samples shown in Table 9.1 were used for this study.

Table 9.1: Aggregate Samples Used for Study

Source #	Lithology	CoTE Microstrain per degree Fahrenheit	CoTE Microstrain per degree Centigrade
29	Limestone	2.39	4.30
4	Limestone	3.20	5.76
50	Sandstone	4.20	7.56
55	Trapp rock	5.19	9.34
4	Siliceous	6.40	11.52
Mortar	Siliceous	5.28	9.50

The aggregate samples presented in Table 9.1 were specifically selected to provide discretely spaced data points (integer increments in cote from approximately 2 µε/°F to approximately 6 µε/°F) from the total number of samples aggregate samples presented in Section 6.10. Aggregate "shells" remaining for the materials listed were first removed from the positioning base that was cast around the aggregate to allow for core drilling and extraction. The "shells" were then broken into large pieces using a 10-lb (4.5-kg.) sledge hammer; the resulting pieces were broken with a 3-lb (1.4-kg.) hammer to allow for crushing in a Bico Chipmunk jaw crusher. The aggregate was progressively sieved and crushed to remove size fractions to allow for the same aggregate gradation discussed in Section 8.1 to be used in the concrete mixtures.

Concrete cylinders were then moist cured at 100% RH and 73°F (23 °C) for 28 days prior to CoTE determination. Figure 9.14 presents the comparison between the aggregate cores and concrete made with the crushed aggregate "shells."
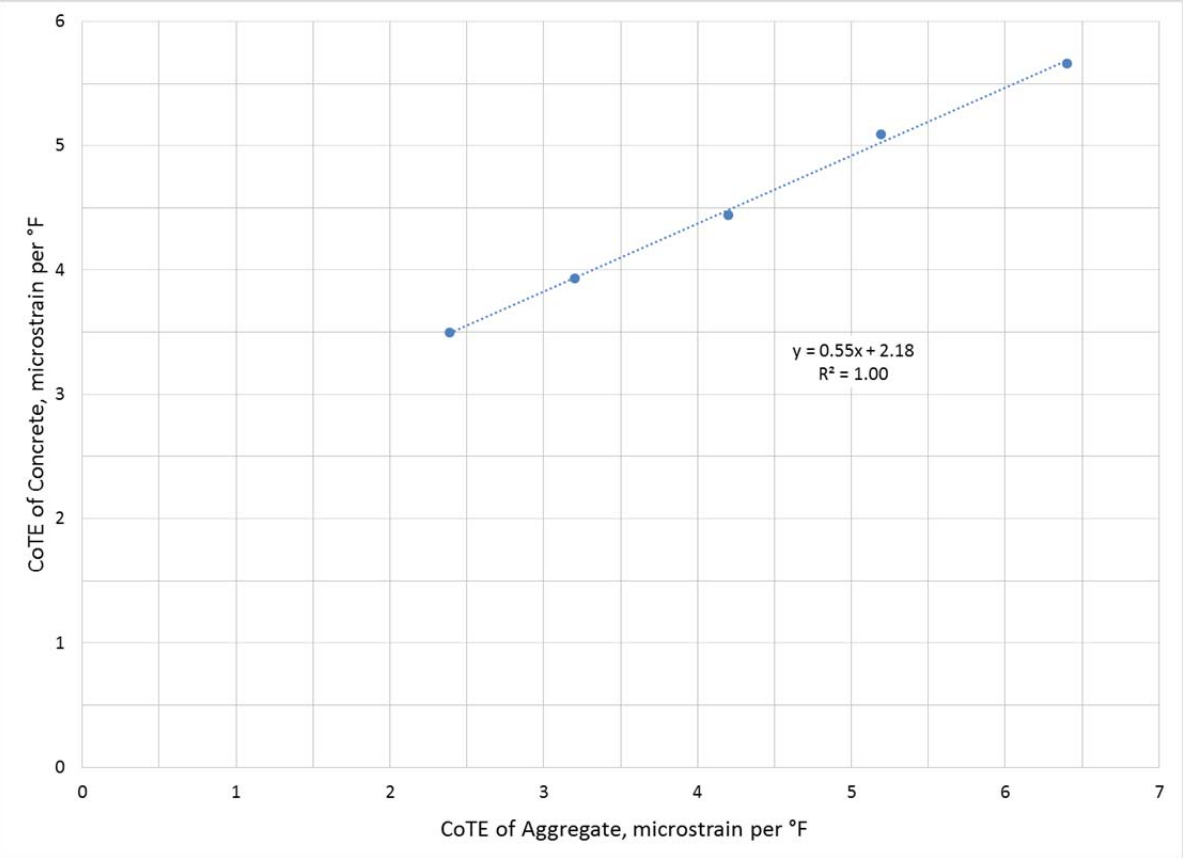
Figure 9.14: Comparison between CoTE of Aggregate Core and Concrete Made from Aggregate "Shell"

Figure 9.14 shows a very strong relationship between the CoTE of an aggregate core with the CoTE of a concrete mixture made with the crushed aggregate "shell" the core was removed from (correlation coefficient of 0.998). Analysis of the data will assume the relationship between the CoTE of aggregate and concrete is explained by the law of mixtures as suggested in the 1977 publication by Emanuel and Hulsey. The slope of the line (0.547) correlates to a 68.3% coarse aggregate contribution to the CoTE of concrete; interpolating from ACI 211 Table A1.5.3.6 for a nominal maximum aggregate size of 1-in (25-mm) and a fineness modulus of 2.75 for the sand returns a 68.5% volume of coarse aggregate (an error of 0.3% for the slope). Assuming the law of mixtures to be valid for this dataset would require the best fit line to pass through the point corresponding to equal CoTE between aggregate and concrete (5.28, 5.28), shown in Figure 9.15.
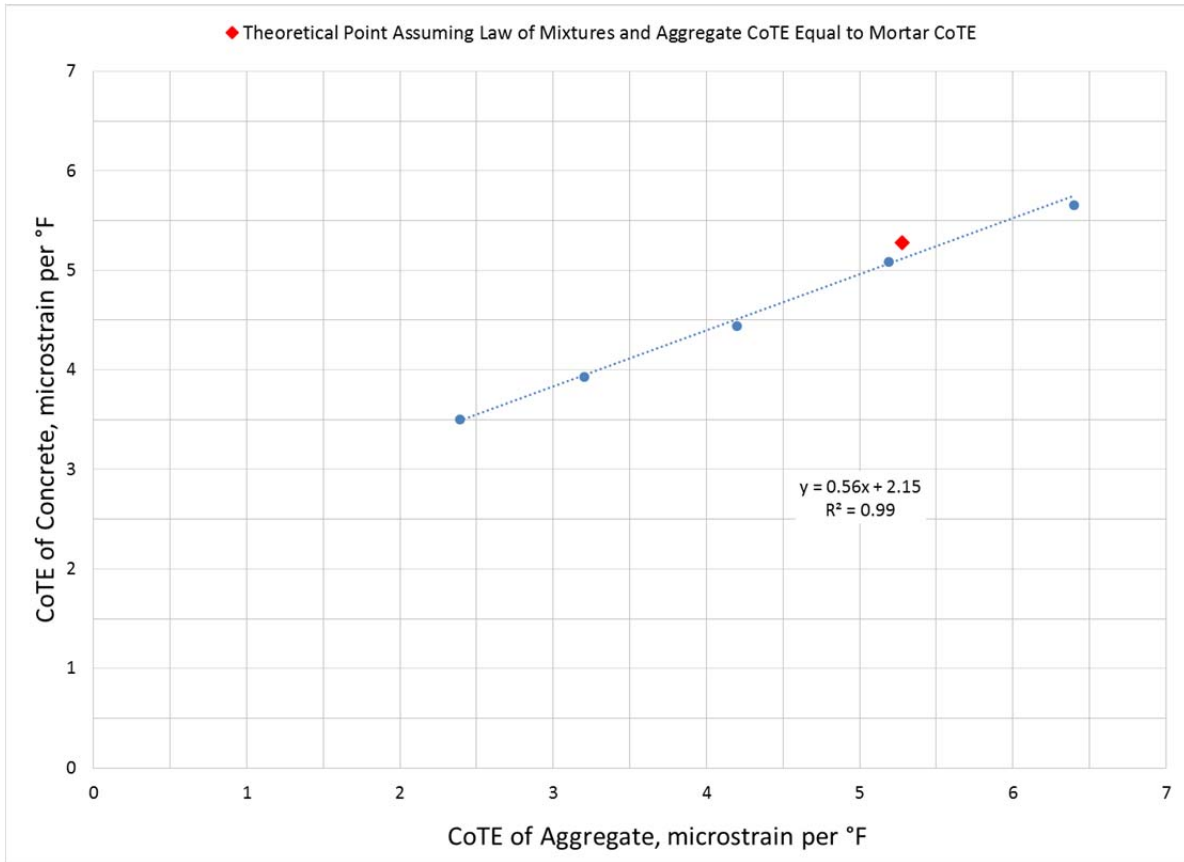
Figure 9.15: Comparison of CoTE Values Assuming a Law of Mixtures Relationship

Including the theoretical point for a concrete mixture made with an aggregate having the same CoTE as the mortar reduces the correlation coefficient slightly to 0.989. This indicates that a CoTE determination for a pure aggregate could potentially be used as a replacement for the standard CoTE determination using a concrete mixture. However, one major limitation to this approach requires that the aggregate in question have relatively uniform lithology; river gravel would not be an ideal material to use this approach for, as lithological variability in this material type would not allow for a practical sample size for estimating the CoTE of concrete (the number of required samples to provide an accurate representation of the material would offset the time and cost savings when compared to conventional testing.)

9.5 Conclusions

This chapter presented an analysis of the concrete test data. Commentary on the trends identified for each concrete test performed was included for the basis of establishing relationships between aggregate properties and concrete properties. The next chapter will discuss the results from field investigations of concrete structures visited to inspect for aggregate-related distress. Conclusions from the analysis performed in this chapter include the following:

- AIV testing showed the best correlation with both compressive strength and split cylinder strength.

- An increase in angularity increased the compressive and split cylinder strength when the Micro-Deval loss was less than 20%.

- An increase in the content of flat and elongated particles decreased the compressive and split cylinder strengths for materials that had over a 20% Micro-Deval loss.

- Comparing the complete mechanical properties (CoTE, modulus of elasticity, and split cylinder strength) provides a better explanation for thermal expansion cracking in pavements than just considering CoTE.

- The CoTE relationship between aggregate and concrete can be accurately determined if the volume of coarse aggregate in the mixture is known.

Chapter 10. Field Investigation

The survey results of TxDOT district personnel presented in Chapter 3 indicated that the current aggregate testing requirements prevent the majority of premature distress in concrete. However, of the isolated incidents of poor performance, the most probable causes of distress included coefficient of thermal expansion (CoTE)-related cracking and spalling in continuously reinforced concrete pavements (CRCP), popouts related to "dirty" aggregates, and alkali-silica reaction (ASR). As discussed in Chapter 3, distress related to ASR was not within the scope of this research project; however, this distress was the most reported issue when searching for field sites to visit. This chapter presents the findings from selected field inspections of aggregate-related issues.

10.1 Pavement Cracking

Pavement cracking and spalling are problems in CRCPs in Texas. This problem is most often associated with high CoTE aggregate such as river gravel and certain dolomite. Several cases of pavement cracking due to high CoTE aggregate were identified in this project. The desire for this research was to identify cases of field distress where the cause was unknown but likely aggregate-related. An exit ramp on Texas State Highway 183 South in Austin, Texas, was one location where the exact cause of cracking in the pavement was unknown; this pavement is approximately 15 years old. An investigation of this site revealed only one spall in the pavement; however, the spall was approximately 30 feet (10 meters) wide (Figure 10.1).

Figure 10.1: Pavement Cracking and Spalling on Texas 183

Inspection of the pavement indicated that limestone coarse aggregate and siliceous river sand was used in the pavement. Discussion with TxDOT personnel about the site resulted in

communication with one of the original field inspectors for the site. Information obtained in this discussion indicated that the site of the cracking was adjacent to a construction joint where the adjoining pavement had been placed weeks before. The cracked section was not placed by the slip-form paving machine because of the proximity to the hardened section; the former field inspector informed the researchers that the first 5 feet (1.5 meters) of this pavement were placed and finished by hand after sufficient distance was gained from the paving machine. Closer inspection of the road surface revealed a slight variance in color of this section when compared to the concrete placed by the slip-form paver. It is most likely that this section was overworked by the construction workers when it was placed.

10.2 Pavement Popouts

While popouts and other surface imperfections in pavements may seem to be an insignificant issue, the distress still requires attention and repair from transportation agencies. If the superficial surface problems are not corrected larger, more costly damage may result in time. An IH 35 frontage road near Amity Road near Belton, Texas, was one site visited to inspect surface imperfections in pavements (Figure 10.2).

Figure 10.2: Popout in Pavement Surface

Initial inspection of the site (constructed in 2012) revealed approximately 25 popouts larger than 0.75 inch (19 mm) in diameter on a 400-foot (120-meter) section of pavement. Several pieces of wood were also found imbedded into the pavement surface, shown in Figure 10.3.

Figure 10.3 Deleterious Material in Pavement Surface

The initial concern for this construction site was that the coarse aggregate used for construction had a magnesium sulfate soundness loss of 26%; the typical requirement for TxDOT is an 18% loss, but can be increased to 25% loss at the approval of the engineer of record (this value is used in areas where freezing and thawing damage is not likely to occur.) This was the only case where a structure was available for inspection with material known to have high magnesium sulfate loss that the researchers were able to view. Inspection of the larger popouts revealed that the opening at the pavement surface was smaller than the diameter of the void several inches into the pavement, shown in Figure 10.4.

Figure 10.4: Removing Loose Material from Popout

The decision was made to return to the site and remove cores from the pavement, intersecting the popouts to determine the size and possible cause. Deposits of clay were found approximately 1 inch (25 mm) below the surface extending to 3 inches (75 mm). The diameter of the larger deposits was approximately 6 inches (150 mm), as Figure 10.5 shows. These clay deposits found in the spalls were originally covered with a thin layer of concrete that eventually broke away.
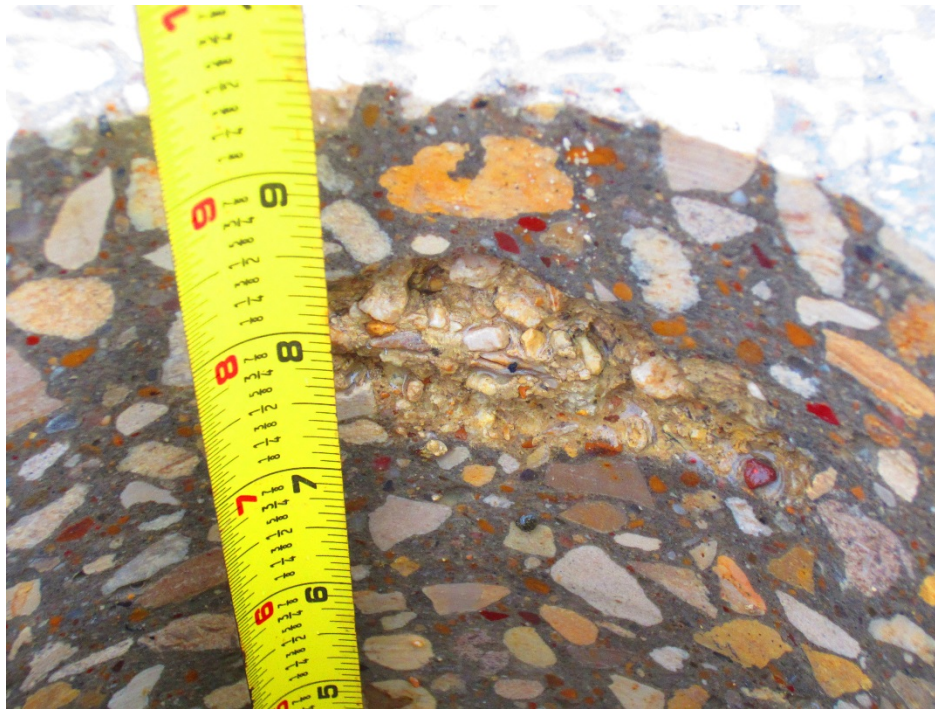
Figure 10.5: Clay Deposit in Pavement

Discussion with one of the TxDOT field inspectors present at the site revealed that the contractor responsible for construction was inexperienced with slip-form paving. The original quality of finish on the pavement was so poor that the surface required diamond polishing to provide a smooth surface. Evidence of surface unevenness is shown in Figure 10.6. A core was removed from the mortar-rich region shown in Figure 10.6; the core is shown in Figure 10.7. Several regions were visible in the pavement surface, indicating poor consolidation and placement of material; other regions indicated that excessive water was added to the surface for finishing.

Figure 10.6: Surface Texture Highlighting Exposed Aggregate Regions and Mortar Rich Region
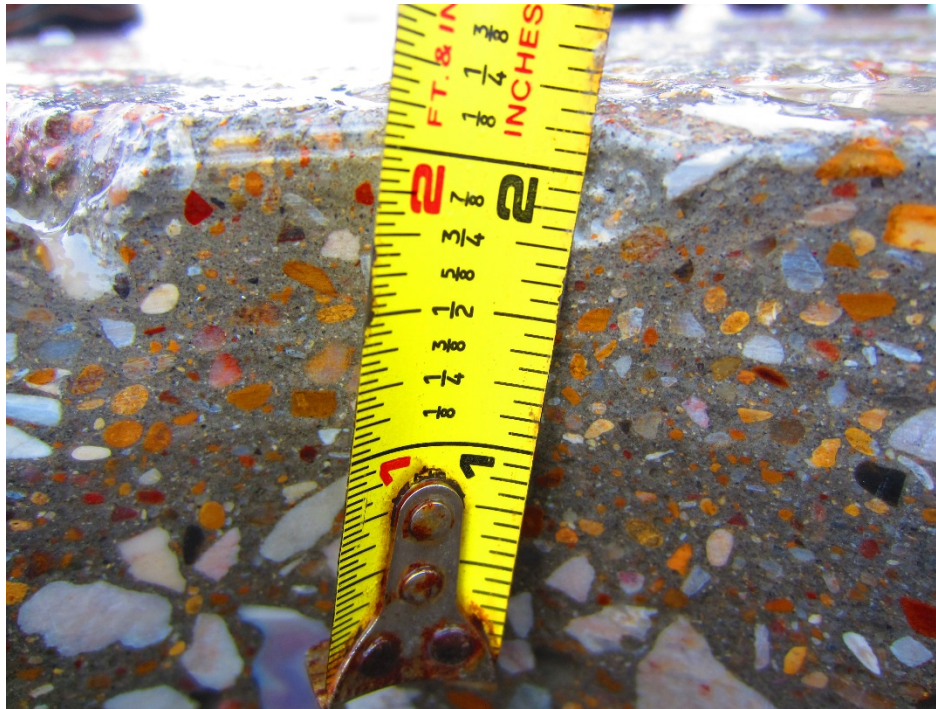
Figure 10.7: Excessive Mortar Content in Top Surface of Pavement

It was concluded that because of the size of the large clay discs found in the pavement, the clay could not have come from the original aggregate production; the clay discs were approximately four times larger than the maximum aggregate in the concrete. The origin of the

clay was most likely material that adhered to a bucket loader used to handle the material. Field inspectors noticed finishing crews forcing large "concrete" clumps below the pavement surface, and instructed them to remove and discard any of the clumps that were emptied from concrete mixing truck. It is likely that the main causes of distress at this site were due to improper material handling and poor construction practices.

10.3 Column Cracking

Column cracking is a distress that often results in concerns of compromised structural capacity. Possible non-materials causes of this distress include structural overload, vehicle impact, and foundation problems; possible materials-related issues include ASR, delayed ettringite formation (DEF), and thermal cracking. The interchange between State Highway 183 and Loop 1 in Austin, Texas, was identified as a site with column cracking, shown in Figure 10.8.

Figure 10.8: Column Cracking as Seen from Roadway

Closer inspection of the column revealed that the cracking seen was much less significant than the view from the roadway (Figure 10.9).

Figure 10.9: Close-up of Column Cracking

A close-up inspection of the columns revealed that the cracking visible from the roadway was actually cracking and peeling of the paint on the exterior of the column. Further communication with TxDOT Materials Division indicated that the structure was in the process of being instrumented to monitor for the possibility for ASR- and DEF-related expansion.

10.4 End of Service Life Materials Analysis

The IH 35 corridor is currently being expanded to allow for more lanes of traffic between Georgetown and Waco, Texas. New bridges are being constructed over IH 35 in order to accommodate the increased number of traffic lanes as well as increase the maximum permissible load height on IH 35. The bridges that are being removed, many of which date back to the original construction of IH 35, have performed to the design expectations for a 50-year-old structure.

10.4.1 Details of Structure

The bridge over IH 35 at Amity Road south of Belton, Texas, is one of the locations where the original bridge is being replaced to allow for the upgrade to the interstate, shown in Figure 10.10.

Figure 10.10: Left: Original Bridge over IH 35 at Amity Road; Right: Replacement Bridge

The last inspection record for the bridge was completed in 2011; at that time, the deck and superstructure were rated in "good condition" excluding some impact scraping damage to the soffits. Samples of the deck concrete and superstructure concrete were collected for determining the mechanical properties of the concrete, shown in Figure 10.11.

Figure 10.11: Concrete Samples Collected for Determining Mechanical Properties

10.4.2 Mechanical Properties

Cores were removed from the samples collected to determine the mechanical properties of the concrete in the Amity Road bridge. The purpose of performing this mechanical evaluation was to provide a comparison with the laboratory-cast concrete specimens. Two samples each were tested to determine the compressive strength, modulus of elasticity, split cylinder strength, and CoTE. The results from these tests are presented in Table 10.1.

Table 10.1: Mechanical Properties of Concrete from Amity Road Bridge

Test	Result
Compressive Strength	5340 psi
Modulus of Elasticity	5550 ksi
Split Cylinder Strength	435 psi
Coefficient of Thermal Expansion	4.04 με per °F

The mechanical testing of concrete from the Amity Road bridge has lower strengths than the laboratory concrete mixtures made with limestone river gravel presented in Chapter 8.

Compressive strength was approximately 15% lower than the laboratory mixtures; split cylinder strengths were approximately 30% lower. The modulus of elasticity and CoTE values were similar to the laboratory limestone river gravel concrete mixtures.

10.4.3 Petrographic Analysis

Concrete cores from the samples were also removed for petrographic analysis. The 50-year service life of the structure and minor distress listed in the 2011 bridge inspection report suggested that the concrete was not likely to be experiencing durability-related issues. Aggregate found in the concrete was a limestone river gravel similar in lithology to Aggregate #19 from Table 4.5. Uranyl acetate staining, described in the appendix of ASTM C856, was used to determine the presence of alkali-silica gel; a reaction occurs between the gel and uranyl acetate resulting in a bright green fluorescence under ultraviolet (UV) light. Figure 10.12 shows the prepared sample while exposed to UV light.
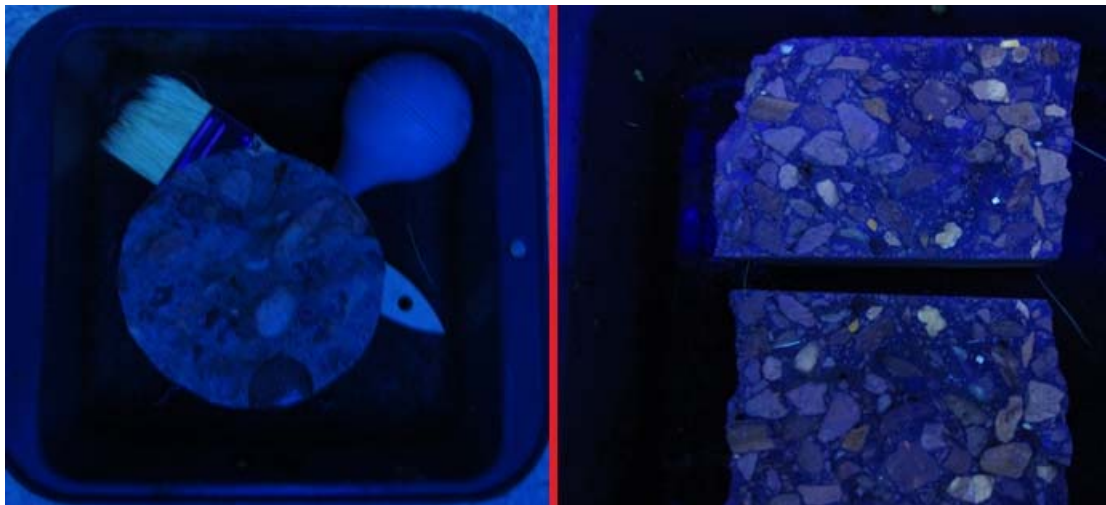
Figure 10.12: Left: Sample from Amity Bridge; Right: Sample of Concrete with ASR

Figure 10.12 shows the sample from the Amity Road Bridge on the left; no efflorescence is seen in the sample. The right image is of a typical concrete sample with ASR present.

Carbonation of concrete causes a reduction in pH that can lead to corrosion in the reinforcing steel; when this happens, significant cracking can occur and the structural capacity is decreased. The 2011 inspection noted no large cracks or conditions that would indicate a reduced structural capacity; this finding indicated that corrosion was unlikely. Phenolphthalein staining of concrete indicates regions where the pH has dropped below 9.5; at this pH corrosion of reinforcing steel is favorable (shown in Figure 10.13).

Figure 10.13: Phenolphthalein Staining of Amity Bridge Concrete

Figure 10.13 shows that carbonation of the concrete has progressed about 5/8 inch (15 mm) over the 50-year service life of the bridge; the concrete cover over the steel was measured to be at least 2 inches (50 mm).

The air void system of a concrete structure provides durability when exposed to freezing and thawing; this is of particular importance for bridges because environmental exposure allows ice to form more easily when compared to on-grade concrete. Air content of the Amity Road Bridge was determined using a Concrete International RapidAir 457 unit. This machine uses computer software to scan a polished section that has been colored black and treated with barium sulfate to fill the voids. The prepared sample is shown in Figure 10.14.
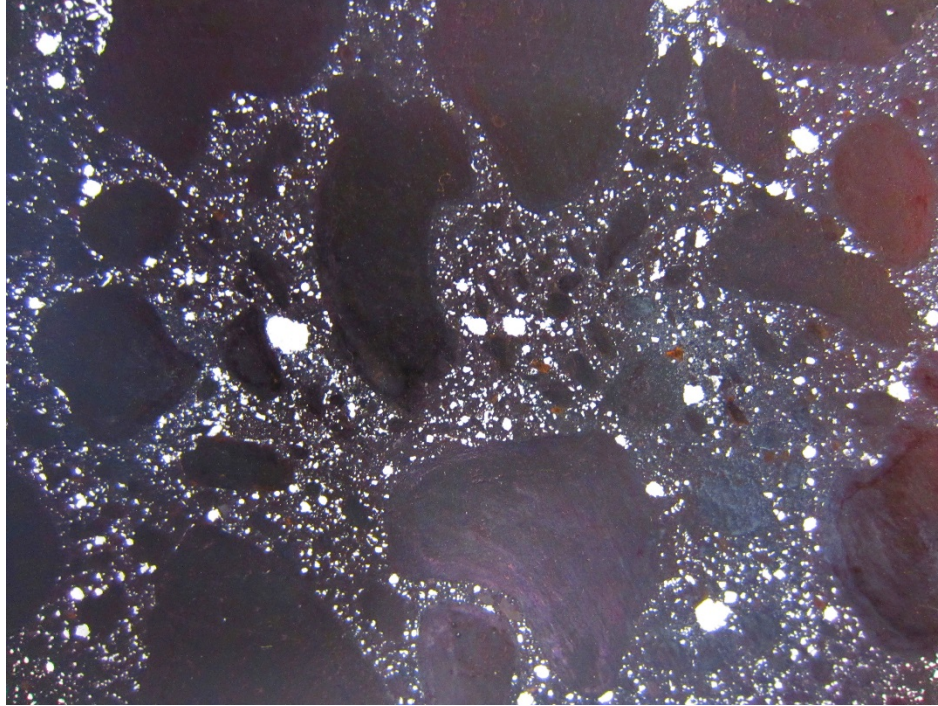
Figure 10.14: Amity Bridge Specimen Prepared for Air Content Determination

Test results from the RapidAir unit returned a value of 5.7% air content; this air content would provide adequate performance for freezing and thawing durability. However, larger air voids indicative of trapped bleed water were found beneath some of the coarse aggregate.

Permeability was also determined using the simplified version of ASTM C1202, the rapid chloride permeability test. An extrapolated charge of 1710 coulombs was calculated for the samples; Riding et al. (2008) reported that this value would be categorized in the lower end of moderate permeability.

10.5 Conclusions

This chapter presented results from inspections of field distress in concrete structures. Commentary on the distress mechanism and most probable cause was provided to establish a link between aggregate properties and concrete performance. Conclusions from the analysis performed in this chapter include the following:

- Very few aggregate-related problems were found in concrete used by TxDOT; this is most likely due to the conservative requirements used in screening aggregates.

- The most commonly reported issue with concrete was ASR; the current TxDOT aggregate specification does not implicitly state a limit for this reaction.

- A large portion of the sites visited for potential aggregate distress were most likely issues with construction; this suggests a need for more stringent field inspection criteria.

Chapter 11. Results and Analysis of Fine Aggregate Tests

11.1 Introduction

This chapter presents and analyzes the results of fine aggregate testing performed. The analysis consists of evaluating the result of each test based on mineralogy, finding the correlations between test methods, and comparing the results of the approved fine aggregates with the non-approved ones.

11.2 Uncompacted Void Test Results

The uncompacted void content test (ASTM C 1252) was performed on the 26 fine aggregates to evaluate the shape, texture, and angularity by comparing the packing densities. The uncompacted void content was determined according to the following methods: Method A, standard graded sample; Method B, individual size fraction; and Method C, as-received grading.

The results of the uncompacted void test using Methods A, B, and C are shown in Figure 11.1 and Table 11.1. Method B had the highest percentage of uncompacted void, while Method C had the lowest percentage of uncompacted void. The limestone, dolomite, and trap rock fine aggregates had the highest percentage of uncompacted void, whereas the river gravel and limestone river gravel sands had the lowest. It should be noted that an increase in void content indicates higher angularity, less sphericity, and rougher surface texture. Conversely, a decrease in void content indicates a rounded, smooth, and spherical surface.

Method A was found to be the most effective method since the sample used in this method can be obtained from the remaining size fractions after performing sieve analysis on each sieve of fine aggregate. Method B is time-consuming because the test method has to be conducted on each size fraction, which means a larger sample is required; however, this method provides more information about the shape and texture of each size fraction. Method C failed to evaluate the characteristics of the fine aggregate.

Table 11.1: Uncompacted Void Test Results Based on Mineralogy

Fine aggregate type	Method A	Method B	Method C
Limestone	46.25	50.99	42.13
Limestone River Gravel	38.89	44.24	36.60
River Gravel	40.64	44.28	38.76
Dolomite	46.71	51.46	41.35
Crushed River Gravel	41.52	44.78	41.77
Granite	47.49	51.35	43.63
Sandstone	46.95	51.46	40.08
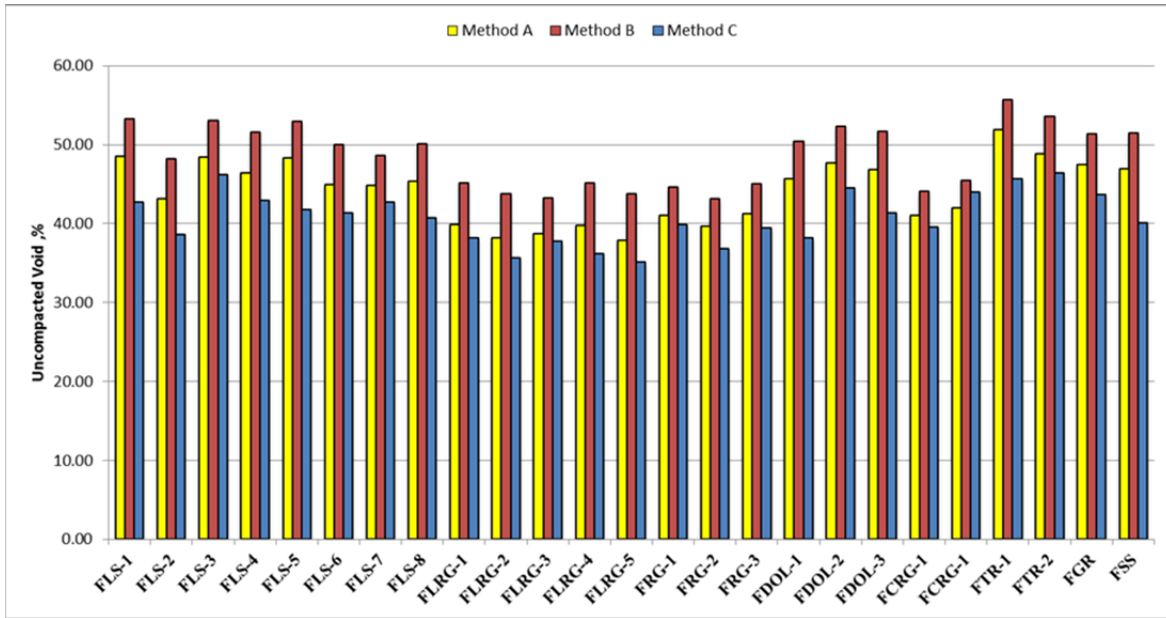
Figure 11.1: Uncompacted Void Test Results

11.3 Mortar Flow Test Results

The mortar flow test (ASTM C 1437) was performed on the 26 fine aggregates to evaluate the shape, texture, and angularity by comparing workability. The ASTM C 1437 was conducted both on the as-received sands and on the regraded sands. The mixture design for the mortar was based on a water-to-cement ratio of 0.485 and a sand-to-cement ratio of 2.75. The volumetric proportions for the mortar mixture are shown in Table 11.2; the grading requirement for making the mortars was chosen to meet ASTM C33, as shown in Table 11.3.

Table 11.2: The Mixture Proportions of Mortars

Cement, g	500
Sand, g	1375
Water, ml	242
Water-cement ratio	0.485

Table 11.3: The Grading Requirements for Fine Aggregate

Sieve	%Passing	%Retained
No. 4	100	0
No. 8	77	23
No. 16	54	23
No. 30	30	24
No. 50	14	16
No. 100	0	14

The results of the mortar flow test performed both on the as-received sands and on the regraded sands are shown in Figure 11.3. The regraded sands generally had a higher percentage of flow compared to the as-received sands. The flow in percent was determined by measuring the diameter of the mortar along the four lines marked on the tabletop; the diameter of the tabletop itself was 40 in.

The average values of flow in percent based on the mineralogy of the fine aggregates are shown in Figure 11.2. The river gravel and limestone river gravel sands had the highest percentage of flow both for the as-received sands and for regraded sands. However, the limestone and sandstone sands had the lowest percentage of the flow both for both categories. Thus, it can be said that the rounded, spherical, and smooth surfaces of the fine aggregates tend to have higher flow, whereas lower flow indicates higher angularity, less sphericity, and rougher surface texture.

The variations in the percentage of flow between the as-received and the regraded sands varied from 2 to 15%, as shown in Table 11.4. However, the difference was very large for the trap rock sand, because the trap rock fine aggregates had the highest average void content among all the fine aggregates.

Table 11.4: Mortar Flow Test Results Based on Mineralogy

Fine aggregate type	% As-received sand	% Regraded sand	% Difference
Limestone	91	100	11
Limestone River Gravel	139	156	13
River Gravel	140	160	14
Dolomite	128	138	8
Crushed River Gravel	129	145	13
Trap Rock	85	138	63
Granite	113	130	15
Sandstone	86	84	2
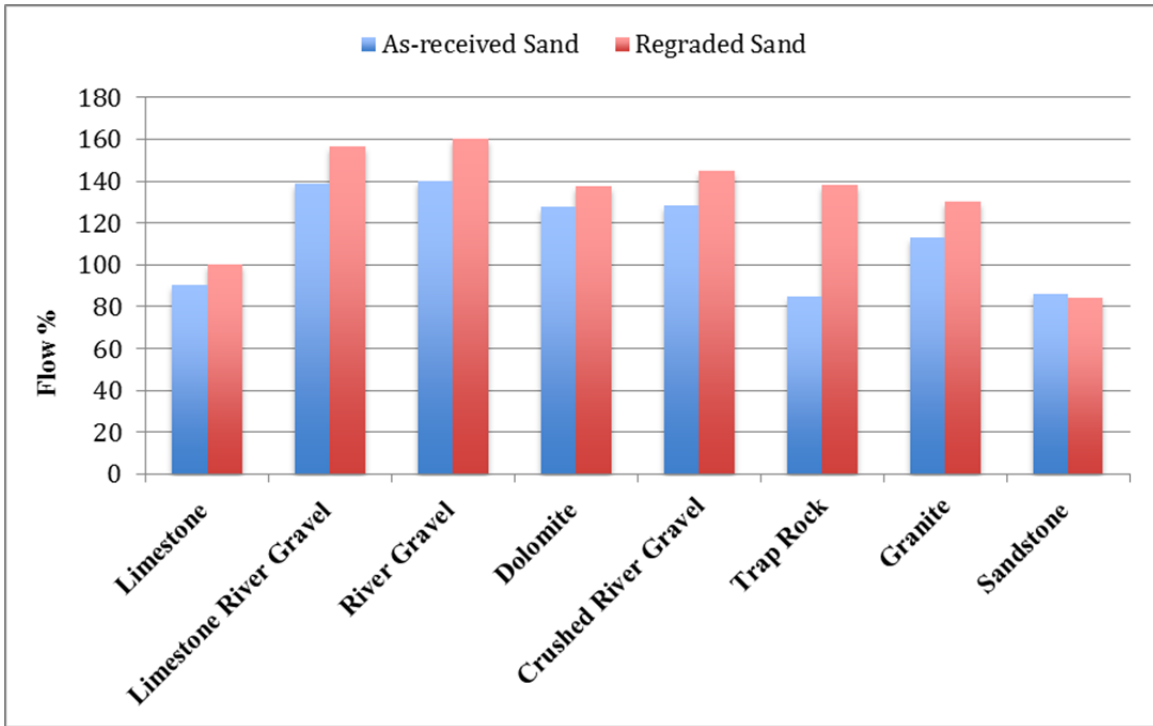
Figure 11.2: Mortar Flow Test Results Based on Mineralogy
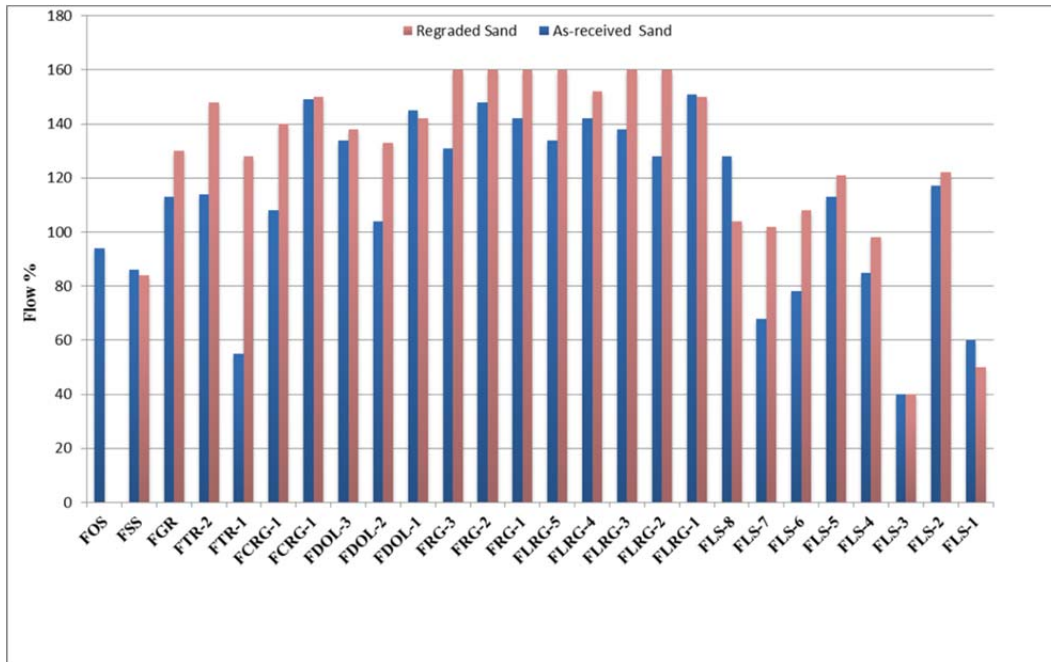
Figure 11.3: Mortar Flow Test Results for All Fine Aggregates

172

11.4 Mortar Compressive Strength Results

The test of compressive strength of mortars (ASTM C109/C109M) was performed on the 26 aggregates to evaluate the shape, texture, and angularity by comparing the compressive strength. The test method was conducted both on the as-received sands and on the graded standard sands. Tables 11.2 and 11.3 show the mixture proportions of mortars and the grading requirements for fine aggregate, respectively.

The results of the 7-day compressive strength of hydraulic cement mortars performed both on the as-received sands and on the regraded sands are shown in Figure 11.5. The regraded sands generally had higher compressive strength. The difference in the 7-day compressive strength between the as-received and the regraded sands varied between 2 and 13%, as shown in Table 11.5. However, the average compressive strength of mortars based on the mineralogy provided no information about the shape and angularity of the fine aggregates, as shown in Figure 11.4.

Table 11.5: Seven-Day Compressive Strength of Mortars Based on Mineralogy

Fine Aggregate Type	As-received sand (psi)	Regraded sand (psi)	% Difference
Limestone	5822	6103	5%
Limestone River Gravel	5636	6031	7%
River Gravel	5538	6214	12%
Dolomite	6249	6998	11%
Crushed River Gravel	5662	5649	0%
Trap Rock	7021	6864	2%
Granite	6668	5869	13%
Sandstone	8035	7858	2%
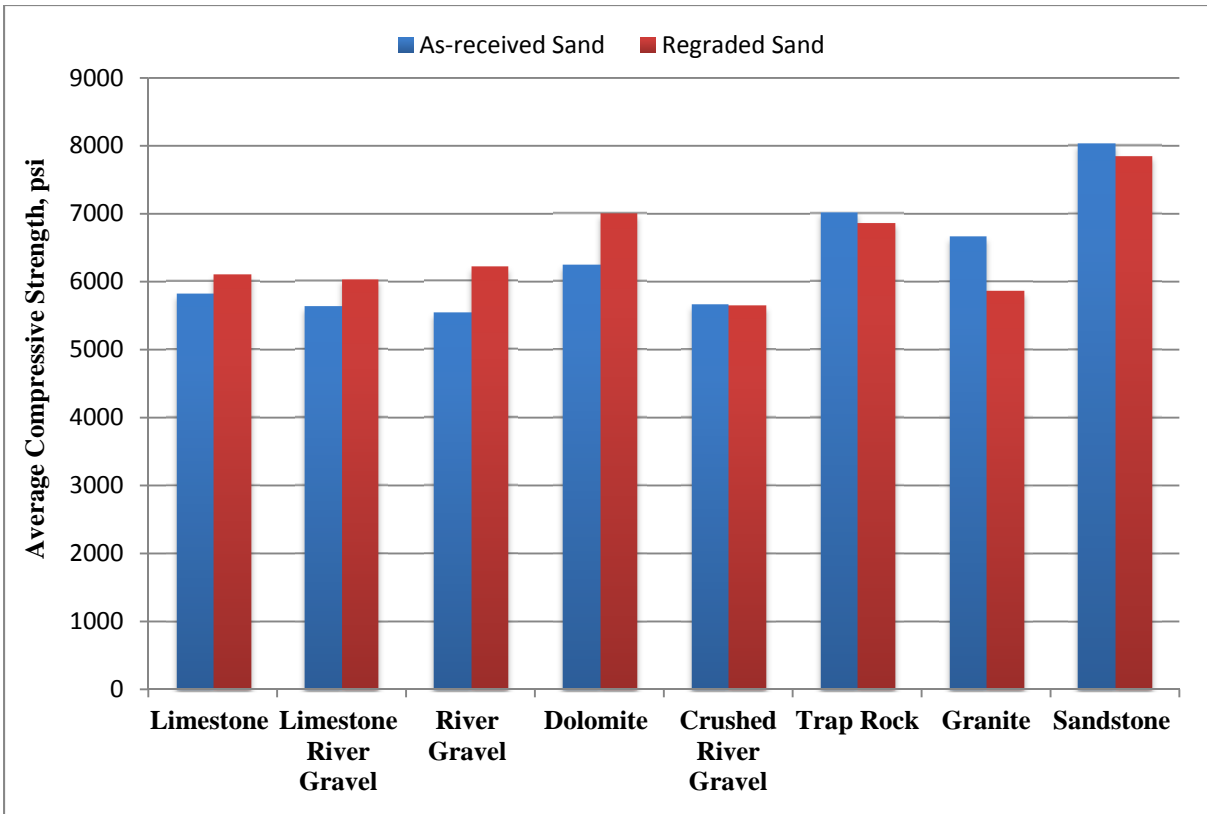
Figure 11.4: Seven-Day Compressive Strength of Mortars Based on Mineralogy
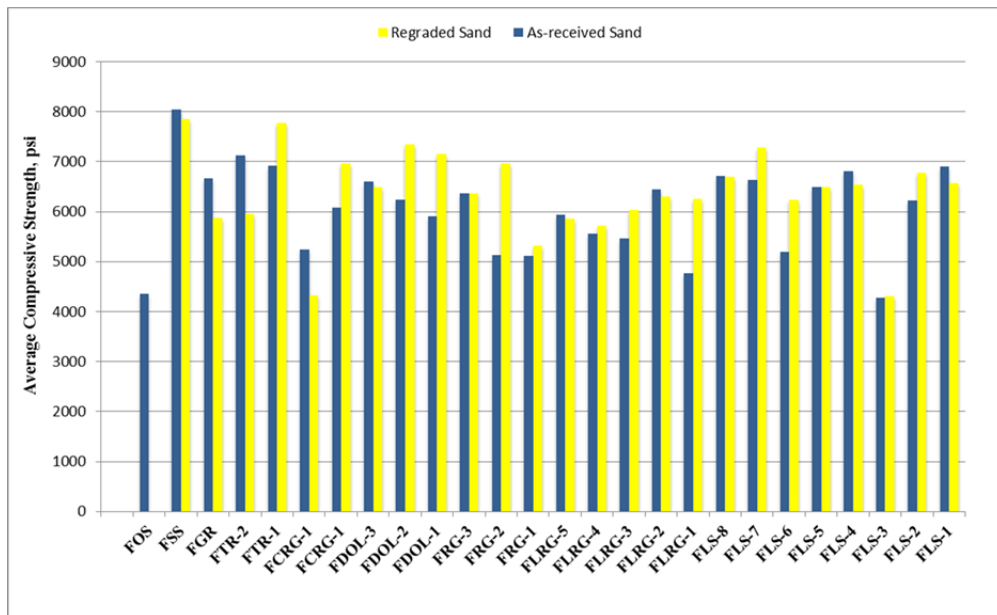
Figure 11.5: Seven-Day Compressive Strength of Mortars for All Fine Aggregates

11.5 AIMS Results

The characteristics of the 26 fine aggregates were evaluated using the AIMS, in accordance with AASHTO TP 81. The tested size fractions were obtained by sieving the fine aggregates. The form 2-D and angularity of the fine aggregate particles retained on No. 8, No. 16, No. 30, No. 50, No. 100, and No. 200 were evaluated before Micro-Deval.

The average form 2-D and gradient angularity for all size fractions combined was used as the basis for comparison. Table 11.6 shows the results of form 2-D and angularity based on mineralogy. The river gravel and limestone river gravel had the lowest form 2-D, and the same trend was also observed for the angularity. Thus, it can be concluded that rounded and spherical aggregate particle tend to have lower form 2-D and angularity. It should be emphasized the AIMS was not able to capture the trap rock aggregate particles since they were black.

Table 11.6: AIMS Form 2-D and Angularity Results Based on Mineralogy

Fine Aggregate Type	Form 2-D	Angularity
Limestone	7.10	2695.73
Limestone River Gravel	6.44	2351.92
River Gravel	6.61	2479.53
Dolomite	7.45	2889.77
Crushed River Gravel	6.76	2634.39
Granite	7.15	3304.64
Sandstone	7.15	3243.32

11.6 Camsizer Results

The characteristics of the 26 fine aggregates were evaluated using the Camsizer. A sample of 500 g of each as-received fine aggregate was analyzed to evaluate the sphericity and symmetry of the fine aggregates.

The average sphericity and symmetry for all size fractions combined was used as the basis for comparison. Table 11.7 shows the results of the average sphericity and symmetry based on mineralogy. The limestone river gravel, the river gravel, and the crushed river gravel had the highest level of sphericity, and the same trend was also observed for the symmetry. Thus, it can be concluded that rounded and spherical aggregate particles tend to have higher sphericity and symmetry.

Table 11.7: Camsizer Sphericity and Symmetry Results Based on Mineralogy

Fine Aggregate Type	Sphericity	Symmetry
Limestone	0.81	0.86
Limestone River Gravel	0.85	0.88
River Gravel	0.84	0.88
Dolomite	0.80	0.86
Crushed River Gravel	0.85	0.88
Trap Rock	0.81	0.86
Granite	0.79	0.86
Sandstone	0.79	0.85

11.7 Micro-Deval Test Results

The Micro-Deval test (ASTM D 7428) was performed on the 26 fine aggregate specimens to determine the resistance of the fine aggregates to abrasion in the presence of water and an abrasive charge.

The results of Micro-Deval loss for the fine aggregates are shown in Figure 11.6; as indicated, the limestone fine aggregates had the highest Micro-Deval loss. The variations in Micro-Deval loss between the fine aggregates ranged from 5 to 47%.

Table 11.8 shows the results of the average Micro-Deval loss based on mineralogy. The limestone fine aggregate had the highest Micro-Deval loss of 30.45%, while the river gravel fine aggregate had the lowest Micro-Deval loss of 7.73%.
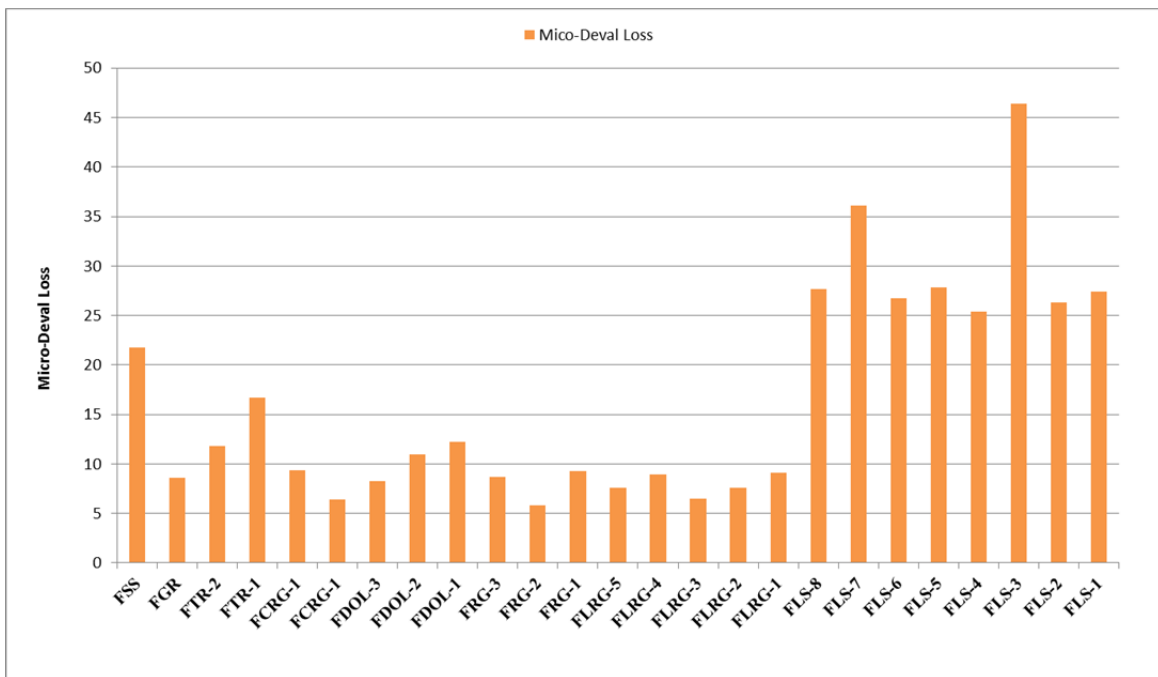
Figure 11.6 Micro-Deval Loss Results Based on Mineralogy

Table 11.8: Micro-Deval Results Based on Mineralogy

Fine Aggregate Type	Micro-Deval
Limestone	30.45
Limestone River Gravel	7.94
River Gravel	7.73
Dolomite	10.30
Crushed River Gravel	7.90
Granite	8.60
Sandstone	21.10

11.8 Flakiness Test Results

The flakiness test (MERO-034) was used to determine the amount of flaky particles in fine aggregate. The amount of flaky particles was used to assess the angularity of fine aggregates. The flakiness test results of the two size fractions No. 8 and No. 16 were determined.

The results of the flakiness test based on mineralogy are shown in Table 11.9. The limestone and dolomite fine aggregates had the highest level of flaky particles, whereas the river gravel fine aggregates had the lowest level of flaky particles. It can be inferred that rounded and spherical fine aggregate particles tend to have lower levels of flakiness particles, while higher levels of flakiness indicates higher angularity, less sphericity, and rougher surface texture.

Table 11.9: Flakiness Results Based on Mineralogy

Fine Aggregate Type	No. 8	No. 16
Limestone	25.88%	27.11%
Limestone River Gravel	19.20%	25.57%
River Gravel	7.67%	14.37%
Dolomite	28.01%	29.33%
Crushed River Gravel	8.50%	16.83%
Granite	29.20%	65.20%
Sandstone	14.40%	24.10%

11.9 Gradation Analysis Results

The gradation analysis of the 26 fine aggregates was evaluated in terms of percent retained using both the sieve analysis test (ASTM C 136) and the Camsizer. To compare the correlation between the two test methods, a 500-g sample of each fine aggregate was prepared. The same 500-g sample was used both for the sieve analysis test and for the Camsizer to reduce or eliminate the variation in results when using different samples for each test method.

The results of the percentage of the mass retained on each sieve (No. 8, No. 16, No. 30, No. 50, No. 100, and No. 200) for both test methods are shown in Figure 11.7. The results of both tests were approximately the same, with a correlation value R^2 of 0.92.
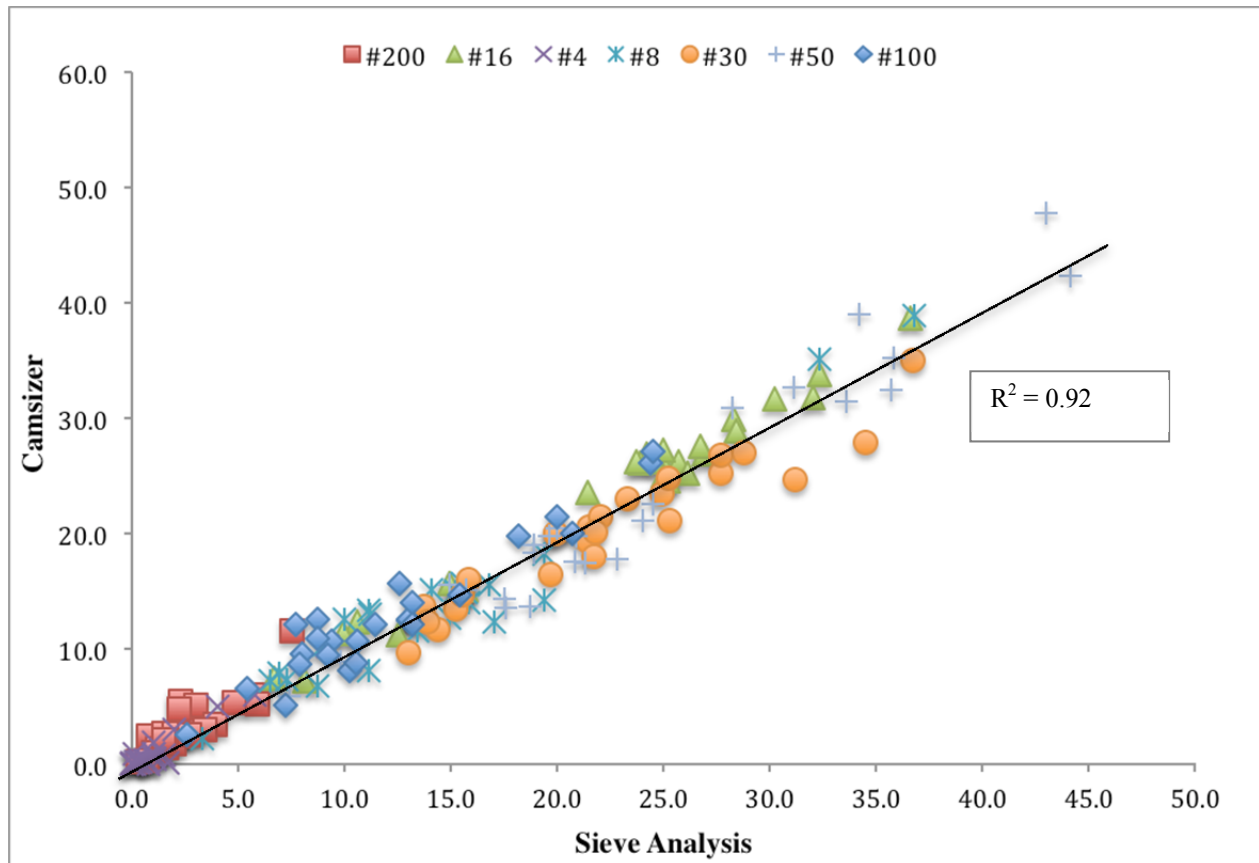
Figure 11.7: Comparison of Gradation Analysis Results from Camsizer and Sieve Analysis Test

The R^2 values for the percentage of the mass retained on each sieve (No. 8, No. 16, No. 30, No. 50, No. 100, and No. 200) using both test methods were 0.94, 0.93, 0.98, 0.92, 0.95, 0.92, and 0.75, respectively. The No. 200 sieve had the lowest R^2 value. There are two reasons for this. First, the percentage of the mass retained on No. 200 was in the range of 0.2 to 5%, which means a small change in the mass retained would have a significant impact on the *percentage* of the mass retained, unlike with the other sieves. Second, there is a possibility of losing finer materials when sieving. It is believed that the results of gradation analysis obtained by Camsizer are more accurate than those of the sieve analysis test.

11.9.1 The Effect of Size on Gradation Analysis

To investigate the effect of size on the result of gradation analysis, two different samples of each fine aggregate were tested using the Camsizer. The first sample was 20 to 30 g and the second sample was 500 g. The results showed that the size of the sample tested had a significant impact on the results of gradation analysis. The sieve analysis test results were used as the basis for comparison between the two sizes. The R^2 values between the Camsizer and sieve analysis

test were 0.48 for the smaller sample and 0.93 for the 500-g sample. It should be emphasized that the average time required to run the test was 2 to 3 minutes for the smaller sample and 28 to 35 minutes for the 500-g sample.

11.10 General Correlations

Laboratory test results were compared to find out whether trends exist between the different tests.

11.10.1 AIMS versus Flakiness Test

Figure 11.8 and Figure 11.9, respectively, depict the results of the flakiness test versus AIMS form 2-D for the fine aggregates retained on No. 8 and No. 16 (obtained by sieving). Little correlation was found between AIMS form 2-D and the flakiness test, especially with No. 8. The R^2 values for the fine aggregates retained on No. 8 and No. 16 were found to be 0.20 and 0.28, respectively.
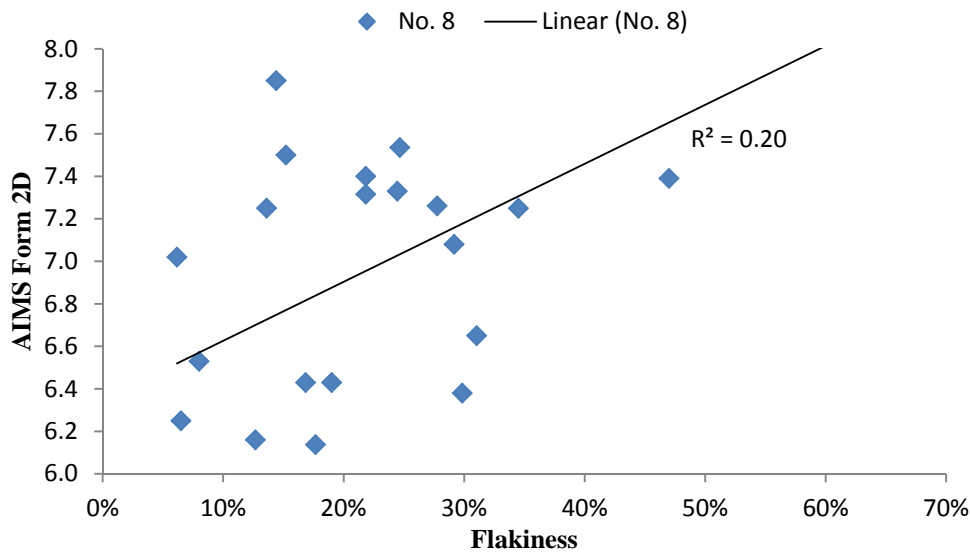
Figure 11.8: AIMS Form 2-D versus Flakiness (No. 8)
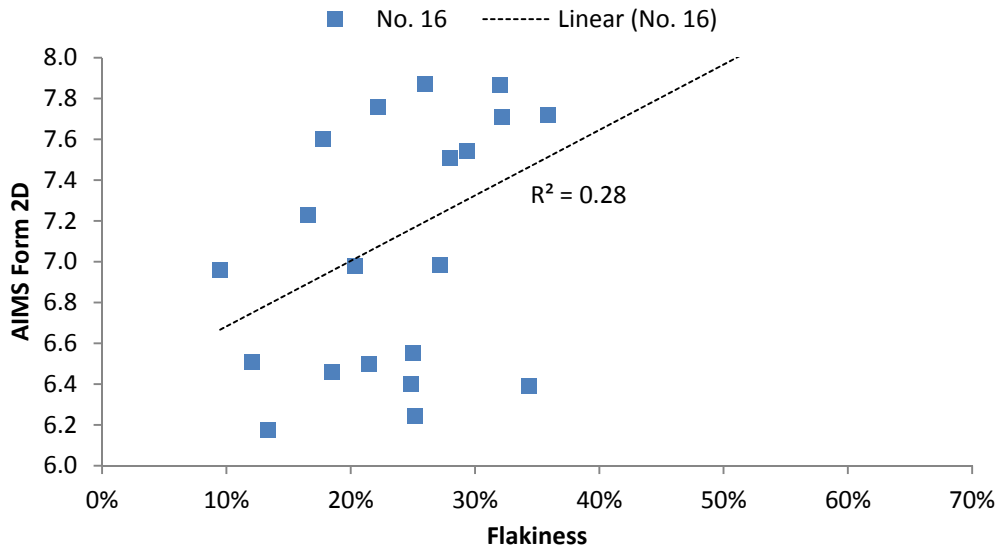
Figure 11.9: AIMS Form 2-D versus Flakiness (No. 16)

The results of the flakiness test versus the angularity for the two size fractions No. 8 and No. 16 are shown in Figure 11.10 and Figure 11.11. Almost no correlation appeared between AIMS angularity and the flakiness for the fine aggregates retained on No. 8. The R^2 values for the fine aggregates retained on No. 8 and No. 16 were 0.08 and 0.16, respectively. The flakiness results of the fine aggregates for sieve No. 16 thus gave a slightly higher R^2 value than that of No. 8.
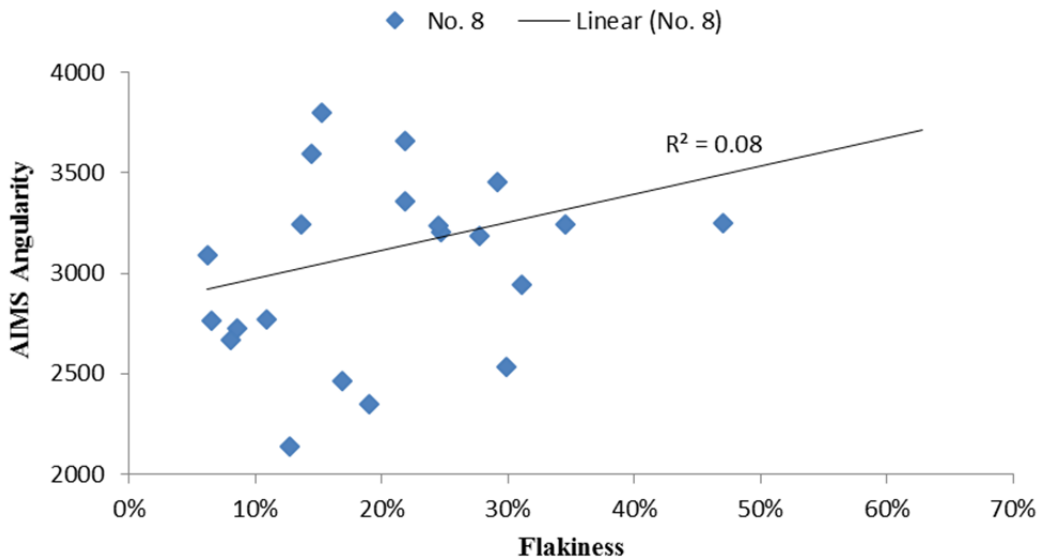
Figure 11.10: AIMS Angularity versus Flakiness (No. 8)
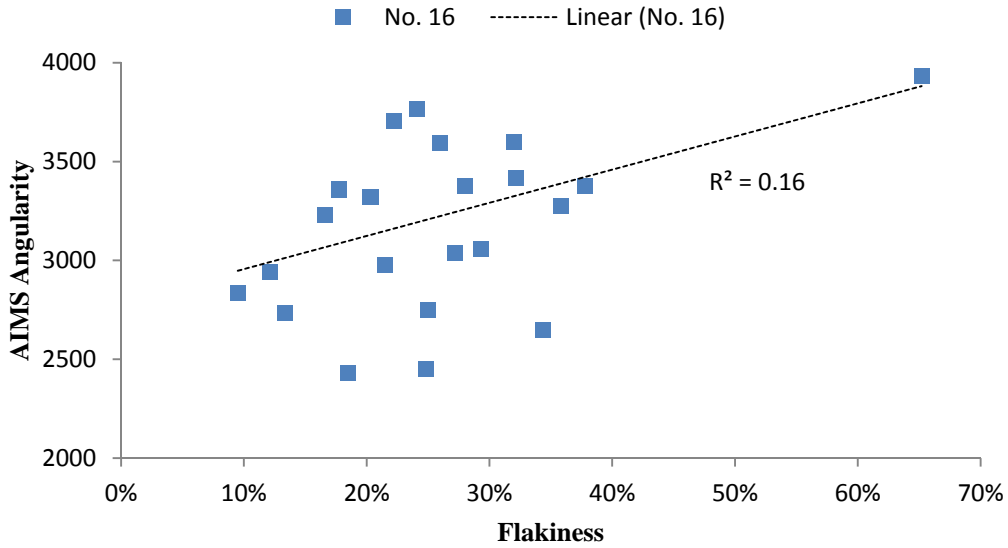
Figure 11.6: AIMS Angularity versus Flakiness (No. 16)

11.10.2 Camsizer versus Flakiness Test

The results of the flakiness test versus Camsizer sphericity for the two size fractions No. 8 and No. 16 are shown in Figure 11.12 and Figure 11.13, respectively. The two size fractions were obtained by sieving. The R^2 values for the fine aggregates retained on No. 8 and No. 16 were 0.34 and 0.43, respectively. Very little correlation was found between the results of Camsizer sphericity and the flakiness test for the No. 8 sieve, whereas the correlation increased to 0.43 for the No. 16 sieve.
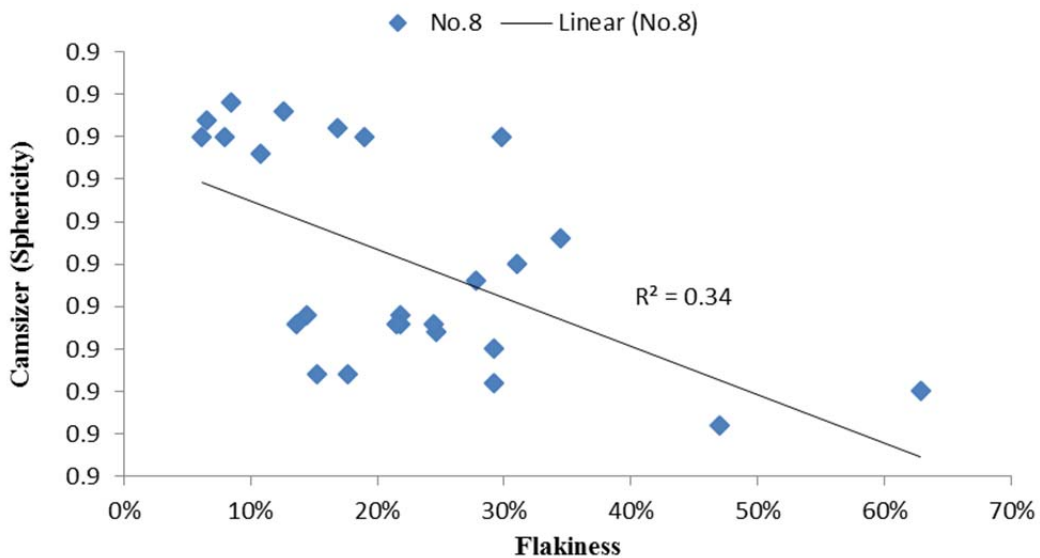
Figure 11.12: Camsizer Sphericity versus Flakiness (No. 8)

181
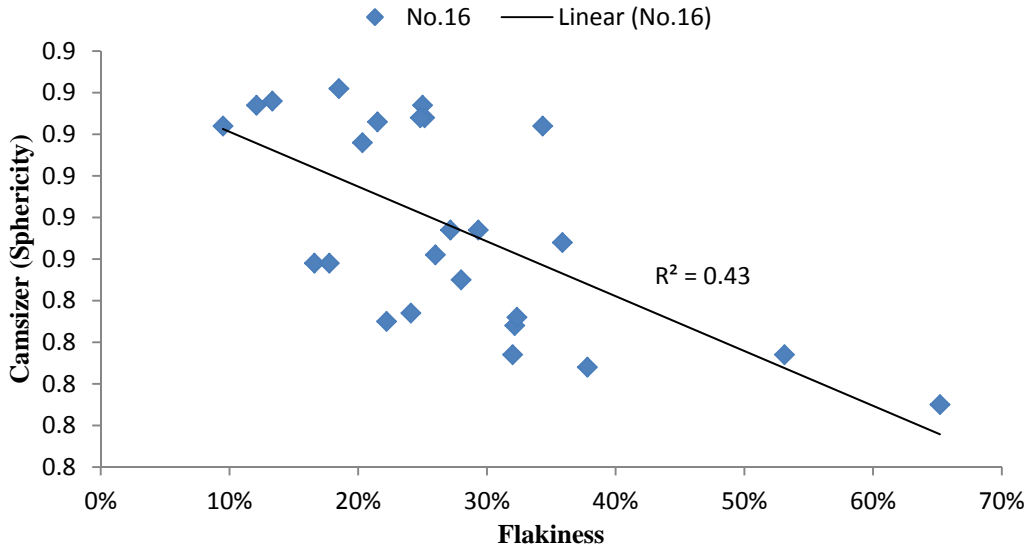
Figure 11.13: Camsizer Sphericity versus Flakiness (No. 16)

The results of the flakiness test versus Camsizer symmetry for the two size fractions No. 8 and No. 16 are shown in Figure 11.14 and Figure 11.15, respectively. The R^2 values for the fine aggregates retained on No. 8 and No. 16 were the same, 0.35.
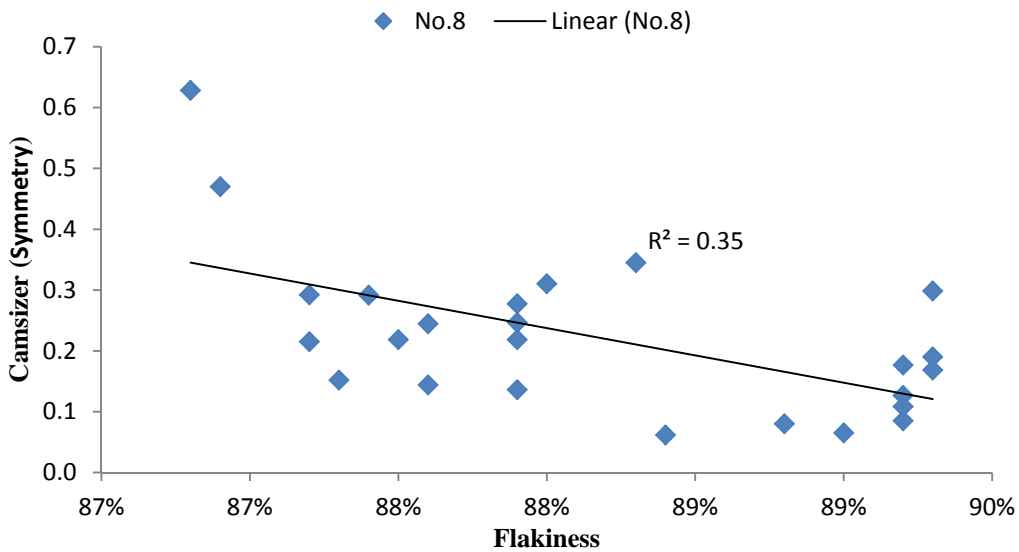
Figure 11.14: Camsizer Symmetry versus Flakiness (No. 8)
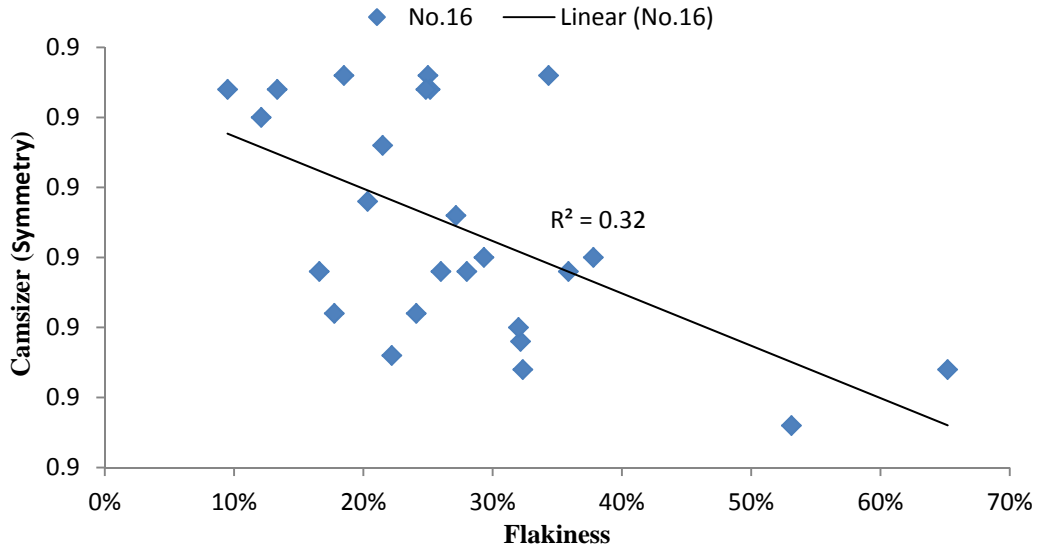
Figure 11.15: Camsizer Symmetry versus Flakiness (No. 16)

11.10.3 AIMS versus Uncompacted Void Test

The average form 2-D and angularity for all size fractions combined was used as the basis for comparison between the two tests. Table 11.10 shows the correlation between AIMS and uncompacted void test. Methods A and B correlated well with the AIMS form 2-D, whereas Method C had little correlation; the same trend was also observed with angularity, though with a lower R^2value.

Table 11.10: Correlation between AIMS and Uncompacted Void Test

	Method A	Method B	Method C
Form 2-D	0.66	0.66	0.29
Angularity	0.46	0.44	0.14

11.10.4 Camsizer versus Uncompacted Void Test

The average sphericity and symmetry for all size fractions combined was used as the basis for comparison between the two tests. Table 11.11 shows the correlation between the Camsizer and the uncompacted void test. Methods A and B correlated well with both sphericity and symmetry, whereas Method C had little correlation.

Table 11.11: Correlation between AIMS and Uncompacted Void Test

	Method A	Method B	Method C
Sphericity	0.64	0.67	0.26
Symmetry	0.60	0.66	0.20

11.10.5 AIMS versus Mortar Flow Test

The average form 2-D and angularity for all size fractions combined was used as the basis for comparison between the two tests. Table 11.12 shows the correlation between the AIMS and the mortar flow test. Almost no correlation was observed between the AIMS and the mortar flow test. The correlation tends to increase slightly with regraded sands.

Table 11.12: Correlation between AIMS and Mortar Flow Test

	As-received sand	Regraded sand
Form 2-D	0.10	0.19
Angularity	0.05	0.12

11.10.6 Camsizer versus Mortar Flow Test

The average sphericity and symmetry for all size fractions combined was used as the basis for comparison between the two tests. Table 11.13 shows the correlation between Camsizer and mortar flow test. Little correlation was observed between AIMS and mortar flow test. The correlation tends to increase with regraded sands.

Table 11.13: Correlation between AIMS and Mortar Flow Test

	As-received sand	Regraded sand
Sphericity	0.20	0.25
Symmetry	0.27	0.33

11.10.7 AIMS versus Compressive Strength of Mortars

The average form 2-D and angularity for all size fractions combined was used as the basis for comparison between the two tests. Table 11.14 shows the correlation between the AIMS and the compressive strength of mortars. Little correlation was observed between the AIMS and the compressive strength of mortars. The correlation tends to decrease slightly with regraded sands.

Table 11.14: Correlation between AIMS and Mortar Compressive Strength Test

	As-received sand	Regraded sand
Form 2-D	0.16	0.12
Angularity	0.25	0.08

11.10.8 Camsizer versus Compressive Strength of Mortars

The average sphericity and symmetry for all size fractions combined was used as the basis for comparison between the two tests. Table 11.15 shows the correlation between Camsizer

and compressive strength of mortars. Almost no correlation was observed between AIMS and compressive strength of mortars. The correlation tends to decrease with regraded sands.

Table 11.15: Correlation between AIMS and Mortar Compressive Strength Test

	As-received sand	**Regraded sand**
Sphericity	0.16	0.05
Symmetry	0.17	0.08

11.10.9 AIMS versus Camsizer

The results of the AIMS form 2-D versus Camsizer sphericity for the two size fractions No. 8 and No. 16 obtained by sieving are shown in Figure 11.16 and Figure 11.17, respectively. The results presented excellent correlations between the results of the Camsizer sphericity and the AIMS form 2-D for the two size fractions No. 8 and No. 16, with R^2 values of 0.89 and 0.87, respectively.
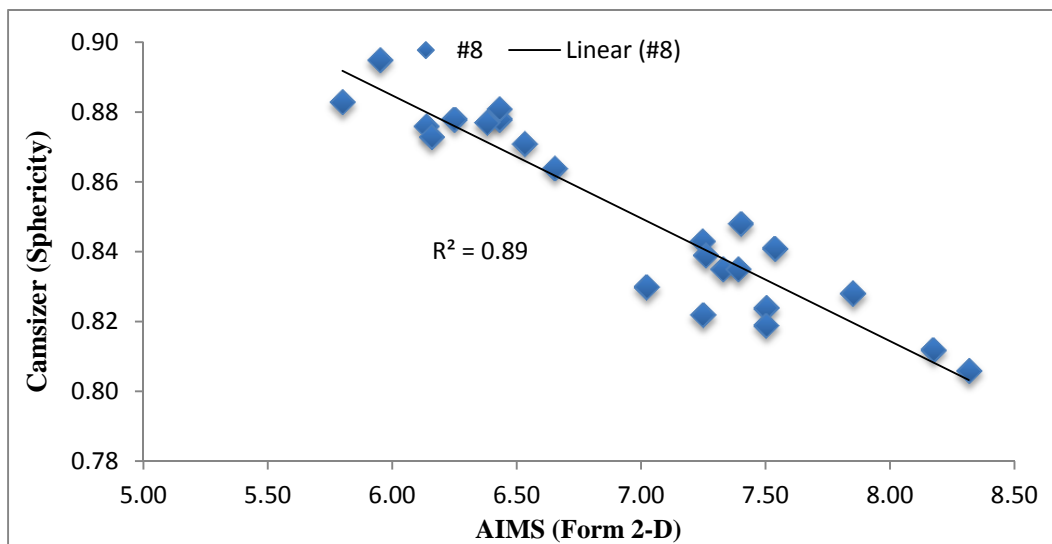
Figure 11.7: Camsizer Sphericity versus AIMS Form 2-D (No. 8)
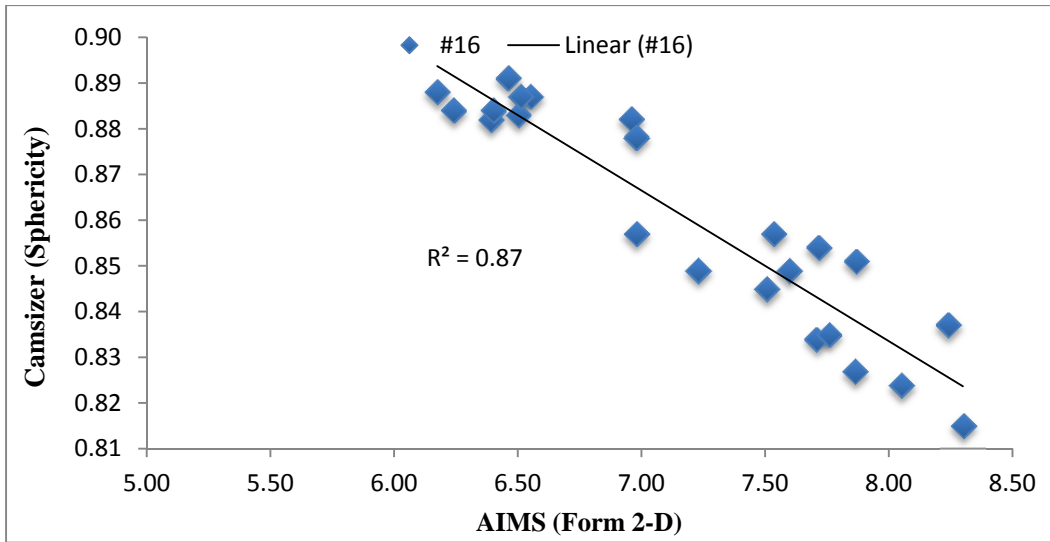
Figure 11.8: Camsizer Sphericity versus AIMS Form 2-D (No. 16)

The results of the AIMS angularity versus Camsizer symmetry are shown in Figure 11.17 and Figure 11.18, respectively. As illustrated, excellent correlations exist between the results of the Camsizer symmetry and the AIMS angularity for the two size fractions No. 8 and No. 16, with R^2 values of 0.83 and 0.82, respectively.
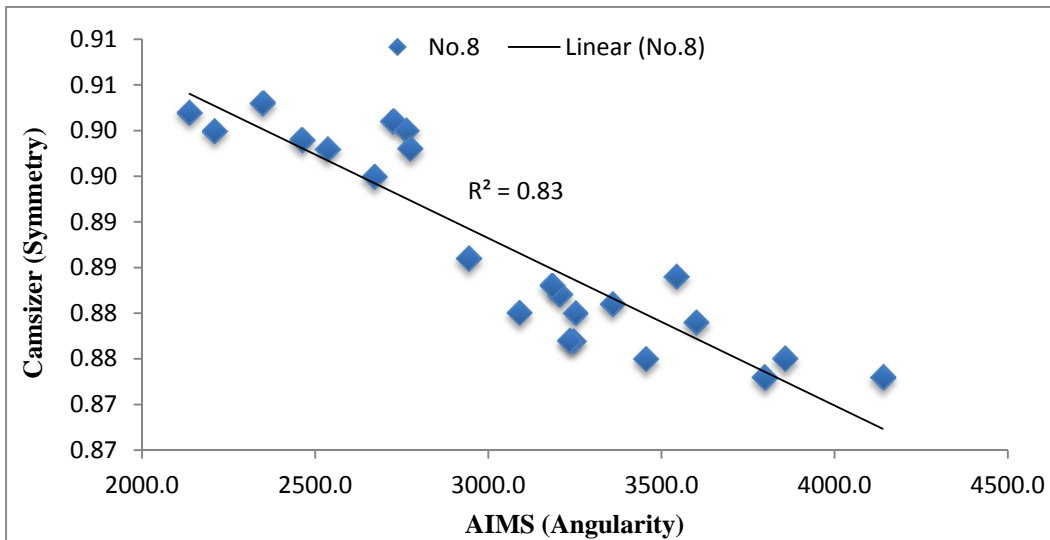
Figure 11.9: Camsizer Symmetry versus AIMS Form 2-D (No. 8)

186
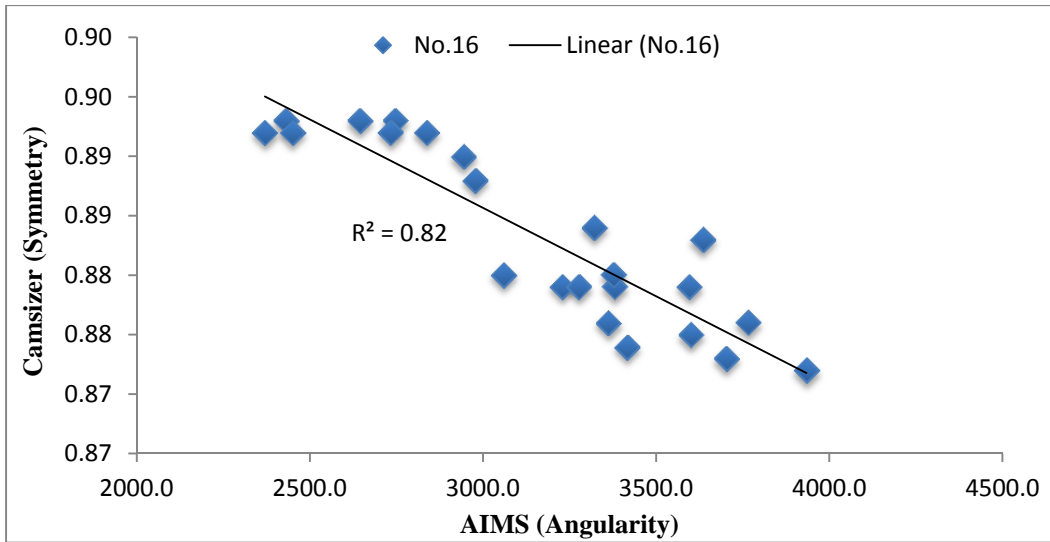
Figure 11.10: Camsizer Symmetry versus AIMS Angularity (No. 16)

11.10.10 Micro-Deval Test versus Mortar Flow Test

Figure 11.19 shows the relationship between the Micro-Deval test and the mortar flow test. The R^2 values between the Micro-Deval loss and the flow for the as-received sands and for the regraded sands were 0.59 and 0.77, respectively. It can be concluded that regraded sands having a flow percentage higher than or equal to 130 tend to have Micro-Deval loss of less than or equal to 12%. On the other hand, values of Micro-Deval loss greater than 20% were observed when the flow was below 110%, as shown in Figure 11.20.
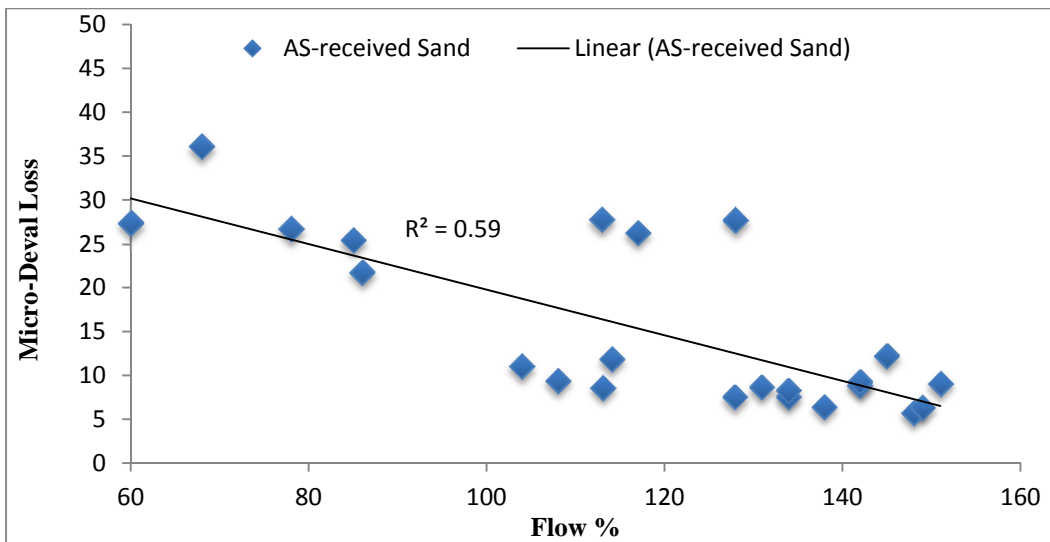
Figure 11.11 Micro-Deval Test versus Mortar Flow Test for the As-received Sands

187
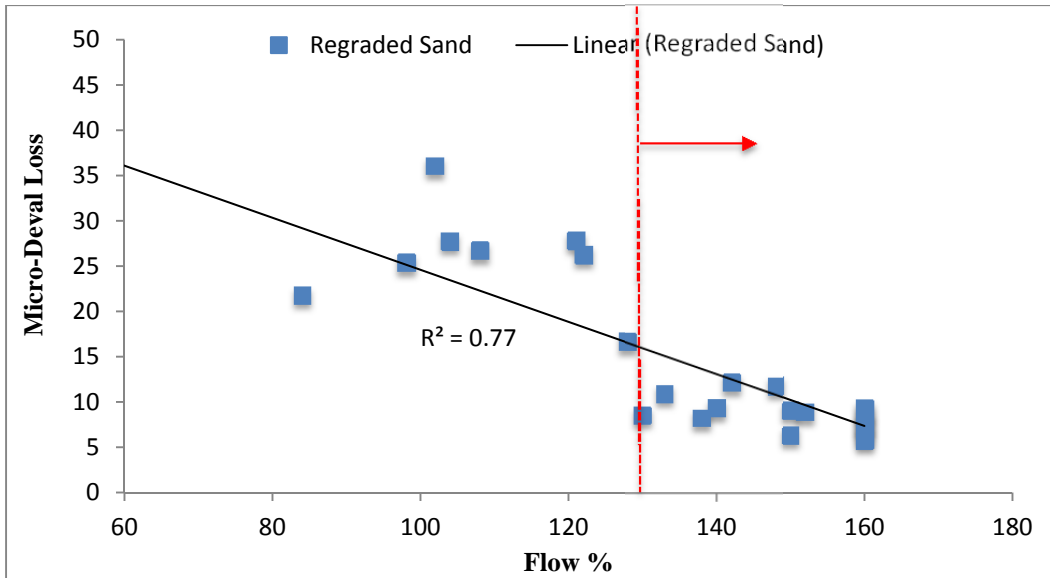
Figure 11.12 Micro-Deval Test versus Mortar Flow Test for the Regraded Sands

11.10.11 Micro-Deval Test versus AIMS

The Micro-Deval test had no correlation with the AIMS. The change in the results before and after the Micro-Deval for both form 2-D and angularity was not consistent. This means some fine aggregates had a higher value before the Micro-Deval—for both form 2-D and for angularity—than after, while other fine aggregates had a lower value.

11.10.12 Sand Equivalent Test versus Blue Methylene Test

The relative amount of harmful fine dust or clay-like particles in fine aggregates was evaluated using ASTM D 2419 (*Standard Test Method for Sand Equivalent Value of Soils and Fine Aggregate*) and ASTM C 837 (*Standard Test Method for Methylene Blue Index of Clay*). Figure 11.21 shows poor correlation between the two test methods, with an R^2 value of 0.34.
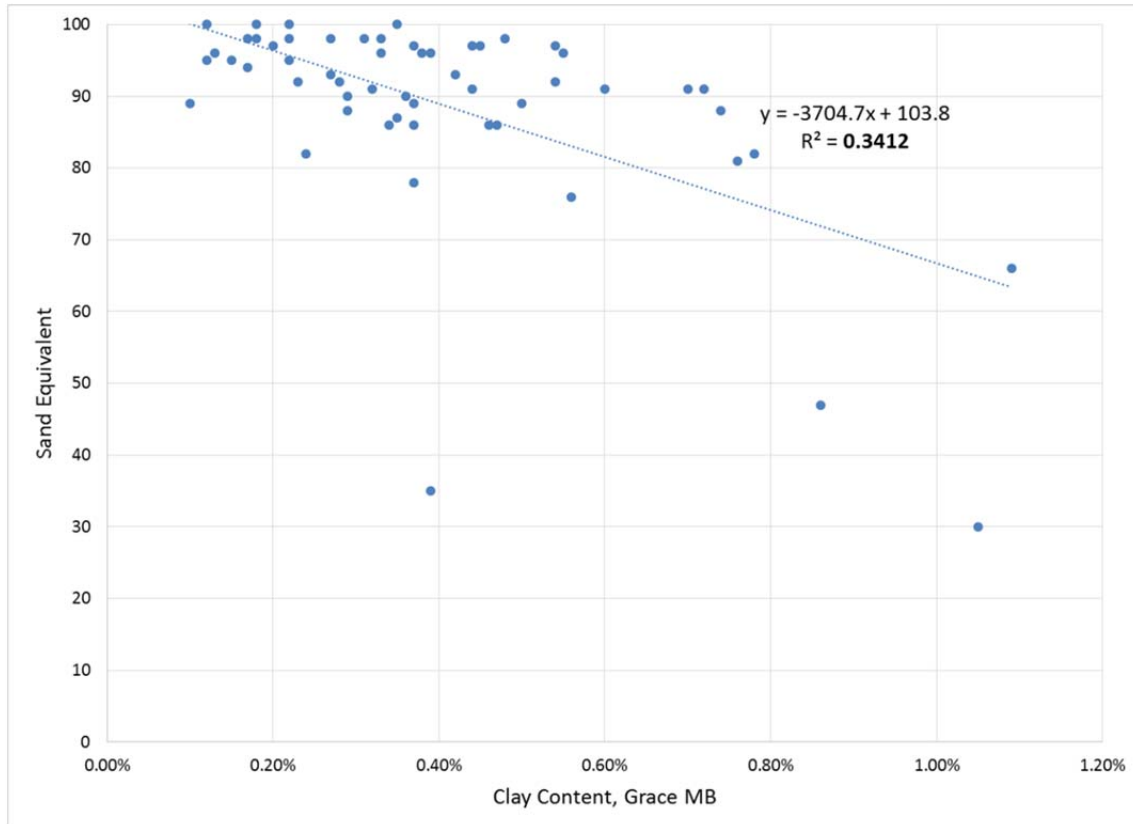
Figure 11.13 Sand Equivalent Test versus Blue Methylene Test

11.11 Comparison between Approved and Non-Approved Fine Aggregates

This section evaluates and compares the results of non-approved fine aggregates with the approved fine aggregates to see whether some non-approved fine aggregates can be successfully used. The following fine aggregates are classified as non-approved fine aggregates in accordance with TxDOT's specifications (ITEM 421): FLS-3, FLS-5, FLS-8, FTR-1, FTR-2, and FSS.

The TxDOT's specifications (ITEM 421) require that fine aggregates satisfy certain criteria when the following tests are conducted: a visual inspection test, the deleterious materials test (Tex-413-A), the organic impurities test (Tex-408-A), the acid insoluble test (Tex-612-J), the sieve analysis test (Tex-401-A), the sand equivalent test (Tex-203-F), and the fineness modulus test (Tex-402-A).

The non-approved fine aggregates had Micro-Deval loss values higher than 21%, except for FTR-1 and FTR-2. However, some of the approved fine aggregates had high Micro-Deval loss values. For instance, FLS-1 and FLS-5 had Micro-Deval loss values of 27% and 36%, respectively.

The results of the AIMS form 2-D and angularity differed little between the approved and non-approved fine aggregates. The AIMS was not able to evaluate FTR-1 and FTR-2 because they were black.

The Camsizer sphericity and symmetry results also differed little between the approved and non-approved fine aggregates.

189

Among all the non-approved fine aggregates, FLS-5, FLS-8, and FSS had values of uncompacted void similar to those of the approved fine aggregates. FTR-1 and FTR-2, however, had the highest uncompacted void content of all the approved and non-approved fine aggregates.

The non-approved fine aggregates generally had lower flow compared to the approved ones. The mortar flow was 84% for the as-received FSS and 86% for the regraded FSS. However, the compressive strength results were variable. This means that some of the non-approved fine aggregates had higher values on the compressive strength test, while other fine aggregates had a lower value compared to the approved fine aggregates.

FLS-3 had the highest absorption at 7.2%, while the other non-approved fine aggregates had absorption values similar to those of the approved fine aggregates. FTR-1 and FTR had the highest specific gravity: 3.08.

Chapter 12. Summary and Conclusions for Fine Aggregate

12.1 Summary

The objectives of this study were achieved by evaluating the characteristics of 26 fine aggregates (shape, angularity, and surface texture) using both direct and indirect test methods. Laboratory test results were compared to discover the trends between the different tests. The correlation value (R^2) between the different test methods helped identify which test methods could be recommended for use. The non-approved fine aggregates on TxDOT's list were analyzed and compared to those of the approved fine aggregates to see whether they could be successfully used.

12.2 Conclusion

The testing performed in this study evaluated the characteristics of fine aggregates (shape, angularity, and surface texture). Based on the results of this study, the following conclusions can be drawn:

1. The mortar flow test method was able to evaluate the characteristics of fine aggregates (shape and surface texture). The mortar flow test can be time-intensive if regraded sands are used. Interestingly, the flow of regraded sands can provide valuable information about the resistance of fine aggregate to. The mortar flow test for the regraded sands seems to correlate closely with the Micro-Deval test.

2. The compressive strength of mortars test did not yield any indication of the characteristics of a fine aggregate. However, higher compressive strength was generally observed for the regraded sands compared to the as-received sand.

3. The flakiness test provides little information about the characteristics of fine aggregate compared to other indirect test methods. The flakiness test did not correlate well with the AIMS and the Camsizer. Thus, it is not recommended for use.

4. The uncompacted void content test (Method A and Method B) was found to be the best indirect test for evaluating the characteristics of fine aggregates (shape and texture). Method C, however, failed to provide any indication of shape and texture. Method B's drawback is that it is more time-consuming, since the test is performed on three individual size fractions. In addition, the correlations between the results of Methods A and B with the results of the AIMS and the Camsizer were similar. Therefore, Method A can be used with confidence.

5. The AIMS is capable of measuring the characteristics of fine aggregate by evaluating form 2-D and angularity. However, the AIMS failed to capture the trap rock fine aggregate particles because the particles were black.

6. The Camsizer can evaluate the characteristics of fine aggregates by measuring sphericity and angularity, and it can also perform a gradation analysis of fine aggregate. However, the size of the sample was found to play an important role in obtaining accurate results.

7. The accuracy of the AIMS and the Camsizer was evaluated by comparing the results of each test. It was observed that excellent correlations exist between the two systems, even

though the mathematical formulas for evaluating the fine aggregate characteristics are not the same.

8. The Micro-Deval loss was significant for the limestone fine aggregates compared to that of other fine aggregates.

9. The Grace methylene blue test correlated poorly with the sand equivalent test. This raises questions and concerns between the method of determination between the Grace method and sand equivalent test.

10. The non-approved fine aggregates were compared with the approved fine aggregates. It was found that both FLS-5 and FLS-8 had good results—even better than the results of some of the approved fine aggregates. Thus, they can be successfully used.

12.3 Directions for Future Research

As stated previously, the mortar flow test (ASTM C 1437) indirectly evaluates the shape and texture of fine aggregates by comparing workability. The mortar flow test is based on fixed water-cement and fine aggregate-cement ratios of 0.485 and 2.75, respectively. The mortar flow test does not account for the absorption of fine aggregates. It would be interesting to see how much improvement in quantifying shape and texture of fine aggregates can be achieved when using different water-cement and fine aggregate-cement ratios and accounting for the absorption of fine aggregates.

The AIMS and the Camsizer are direct tests used to evaluate the characteristics of fine aggregate. More research is required to determine whether the AIMS and the Camsizer can measure the shape, angularity, and surface texture of fine aggregates crushed at different speeds and with different crushers. This would encourage the use of the AIMS and the Camsizer in practice as a form of quality control.

Chapter 13. Summary and Conclusions for Coarse Aggregate

13.1 Summary

The goal of this project was to evaluate test methods used for qualifying aggregate for use in PCC. This topic was investigated because of a need to better utilize the aggregate resources available in order to maintain the quality of construction while reducing material transportation cost. Aggregates were collected for testing from 58 sources representing a variety of lithologies and geographic regions. Current required TxDOT tests were performed on the collected aggregates as well as potential new tests. Concrete mixtures were cast for 24 of the aggregates collected to determine relationships between the mechanical properties of aggregate and concrete. Field inspections of structures were performed to determine the best possible requirements for future aggregate testing. This section provides a summary of different findings discussed in the document.

13.1.1 Notable Problems in Construction Due to Aggregate

A determination of current aggregate-related problems in concrete was discussed in Chapter 3; field inspections were also performed and discussed in Chapter 10. The observed distresses provided direction for testing and evaluation of material properties to better screen aggregate in the future. Key issues found in current construction suggest a need to directly address the alkali-silica reactivity and coefficient of thermal expansion (CoTE) potential for aggregates in future specifications. An improved inspection program and increased education of consequences for construction actions could also improve the future quality of construction projects.

13.1.2 Evaluation of Aggregate Impact on Concrete Properties

Concrete mixtures were cast with 24 of the 58 coarse aggregates collected for the project; 6 of the 24 materials did not meet current specifications for aggregates for use in concrete, as discussed in Chapter 9. Mechanical performance of the mixtures was tested to provide the compressive strength, modulus of elasticity, split cylinder strength, and flexural beam strength of the concrete. The concrete test results were then compared with aggregate test results to determine correlations between testing.

Aggregate impact value (AIV) test results showed the highest correlation with concrete strength data; the angularity and aspect ratio of an aggregate also showed correlation with concrete strengths. Combining the CoTE of a concrete mixture with the other mechanical concrete properties revealed a trend in the allowable thermal change to induce cracking that correlates with field observations.

13.1.3 Evaluation of Aggregate Test Methods

Aggregate samples were collected from 58 sources to evaluate test methods used for screening aggregate, as discussed in Chapter 7. Combining the Micro-Deval loss of an aggregate with the angularity change calculated with the AIMS 2.0 provided a basis to divide materials into groups based upon tendency to break and abrade. This data set was used when comparing the aggregate test results with concrete testing to filter the materials into the appropriate categories.

A high correlation was found between the LA abrasion results and AIV results; however, when comparing the test results with concrete data, the AIV test proved more closely related. Aggregate crushing value was also evaluated; poor correlation existed between this test and the other two.

Resistance to volume change was evaluated using magnesium sulfate soundness testing and unconfined freezing and thawing testing. Testing with unconfined freezing and thawing was determined to better simulate distress mechanisms seen in the field.

Aggregate shape characteristics were evaluated with the AIMS 2.0 system. Determination of angularity showed a high statistical probability in the precision of the measurements; however, the determination of texture and flat and elongated particles was much less statistically reliable for lithologies other than limestone.

13.1.4 Development of Automated AIV Test

Results obtained from use of a BS 812.112 AIV test apparatus showed the highest correlation between aggregate testing and mechanical concrete performance. However, the conventional test device required the test to be performed manually; this requirement increased the possibility of operator error as well as operator injury while performing the test. The AIV apparatus was successfully modified to run automatically without influencing the results from testing, as discussed in Section 7.2.2.

13.1.5 Development of Rapid Determination of CoTE Test

The evaluation of CoTE for concrete mixtures constructed for this project was both labor- and time-consuming. Development of a more rapid determination for the CoTE of a concrete mixture using cores removed from large aggregate resulted in a high correlation (R^2 =0.997). Error between this method and the theoretical determination of CoTE using the law of mixtures was less than 6% for the range of values tested, as discussed in Section 9.4.2.

However, this testing approach requires a uniform lithology of the material being tested; this requirement will exclude river gravels and similar materials from testing with this method. Further testing should be performed using mortars with differing CoTE values to evaluate the total applicability of the test method.

13.2 Conclusions

Concrete with mechanical properties in excess of design requirements can be easily produced with the aggregates tested that currently meet specification requirements. The use of aggregate that does not currently meet specification requirements can still result in a concrete mixture with adequate properties for certain construction applications.

Moderate correlations were found between the mechanical properties of aggregate and concrete. Theses correlations were used to select the most applicable test methods for qualifying aggregate; these test methods became the basis for recommendations for coarse aggregate testing.

Testing with the AIV apparatus provided the strongest correlation between aggregate performance and mechanical strength testing of concrete. However, test results from the conventional test apparatus could be influenced by operator execution. The AIV apparatus was successfully modified to eliminate potential variability from the operator.

A more rapid approach to determining the CoTE of an aggregate was investigated and determined to be feasible. However, the requirement that the aggregate being tested have uniform lithology is a major limitation of the approach.

The causes of distress for many of the field sites investigated were a combination of many factors. However, improved inspection during construction, combined with a better understanding by construction workers of the implications their actions could have for a construction project, could potentially reduce problems.

13.3 Significance of Findings

The results obtained in this study will provide a basis for concrete materials engineers to reevaluate the methods used for qualifying coarse aggregate for use in PCC. However, testing with the AIMS 2.0 device may not be the best method to evaluate all shape characteristics of an aggregate.

Incorporation of the recommended test methods could reduce the total time required and testing cost associated with aggregate qualification. The study demonstrated that aggregate that does not meet current specifications can be used in concrete applications where lower mechanical strengths are required. Use of these materials in select applications would result in a cost reduction and lower carbon footprint while maintaining the desired level of performance.

Appendix A: List of Attendees of June 2011 Aggregate Workshop

Organization	Name	Email
The University of Texas		
CTR	David Whitney	dpwhitney@mail.utexas.edu
CTR	Chris Clement	chris.clement@utexas.edu
CTR	Zack Stutts	zstutts@mail.utexas.edu
CTR	David Fowler	dwf@mail.utexas.edu
TxDOT		
CST Division	Michael Dawidczik	michael.dawidczik@txdot.gov
CST Division	Caroline Herrera	caroline.herrera@txdot.gov
CST Division	Lisa Lukefahr	elizabeth.lukefahr@txdot.gov
CST Division	Ryan Barborak	ryan.barborak@txdot.gov
Bridge Division	Graham Bettis	graham.bettis@dot.gov
Bridge Division	Kevin Pruski	kevin.pruski@txdot.gov
RTI	German Claros	german.claros@txdot.gov
District Personnel	Steve Swindell	steven.swindell@txdot.gov
District Personnel	Darlene Goehl	darlene.goehl@txdot.gov
District Personnel	Richard Willammee	richard.williammee@txdot.gov
District Personnel	Charles Chance	charles.chance@txdot.gov
District Personnel	Ron Johnston	ron.johnston@txdot.gov
Researchers		
Ontario MTO	Chris Rogers (Retired)	rogers.chris@rogers.com
Industry/Producers		
Jobe Materials	Martin Alerette	martin@jobeco.com
Vulcan	Harry Bush	bushh@vmcmail.com
Martin Marietta	Mike Carney	mike.carney@martinmarietta.com
Martin Marietta	Jason Ford	jason.ford@martinmarietta.com
Fordyce Materials	Matt Champion	matt@fordyceco.com
TACA	Richard Szecsy	rich.szecsy@tx-taca.org

Appendix B: Coarse Aggregate Property Sheets

Table B.1: Overview

Sample ID	Lithology	Source District	Sample ID	Lithology	Source District
1	Partly Crushed River Gravel	Yoakum	30	Limestone	San Antonio
2	Partly Crushed River Gravel	Yoakum	31	Limestone	Ft Worth
3	Partly Crushed River Gravel	Austin	32	Limestone	Lubbock
4	Partly Crushed River Gravel	Austin	33	Limestone	San Antonio
5	Partly Crushed River Gravel	Houston	34	Limestone	San Antonio
6	Partly Crushed River Gravel	Houston	35	Limestone	Austin
7	Partly Crushed River Gravel	Atlanta	36	Limestone	San Antonio
8	Partly Crushed River Gravel	Atlanta	37	Limestone	Abeline
9	Partly Crushed River Gravel	Atlanta	38	Limestone	Paris
10	Siliceous River Gravel	Austin	39	Limestone	Houston
11	Siliceous River Gravel	Austin	40	Limestone	San Antonio
12	Siliceous River Gravel	Dallas	41	Limestone	Austin
13	Siliceous River Gravel	Amarillo	42	Dolomite	Austin
14	Limestone River Gravel	El Paso	43	Dolomite	Austin
15	Limestone River Gravel	Lubbock	44	Dolomite	Paris
16	Limestone River Gravel	Waco	45	Dolomite	Paris
17	Limestone River Gravel	Waco	46	Dolomite	El Paso
18	Limestone River Gravel	Waco	47	Granite	El Paso
19	Limestone River Gravel	Waco	48	Granite	Paris
20	Limestone River Gravel	Amarillo	49	Granite	Childress
21	Limestone	Austin	50	Sand Stone	Austin
22	Limestone	Austin	51	Sand Stone	Paris
23	Limestone	Dallas	52	Sand Stone	Paris
24	Limestone	San Antonio	53	Sand Stone	Paris
25	Limestone	San Antonio	54	Trapp Rock	San Antonio
26	Limestone	Austin	55	Trapp Rock	San Antonio
27	Limestone	San Antonio	56	Rhyolite	Wichita Falls
28	Limestone	San Antonio	57	Rhyolite	Odessa
29	Limestone	Waco	58	Slate	Paris

Aggregate Identification Number:	1
Source District:	Yoakum
Lithology:	Partly Crushed River Gravel

Aggregate Test:	Method	Result
Specific Gravity	Tex 403-A	2.6
Absorption, %	Tex 403-A	0.7

Micro-Deval loss, %	Tex 461-A	3
Los Angeles Abrasion loss, %	Tex 410-A	15
Modified Aggregate Impact Value loss, %	Section 4.6	19.6
Modified Aggregate Crushing Value loss, %	Section 4.7	33.2

Magnesium Sulfate Soundness loss, %	Tex 411-A	1
Uncofined Freezing and Thawing loss, %	CSA 23.2-24A	9.3

Thermal Conduvity, w/(m^2 K)	Section 3.2.1.9	4.73

AIMS 2.0 Angularity	Section 3.2.1.8	2935
AIMS 2.0 Texture	Section 3.2.1.8	170
AIMS 2.0 Flat and Elongate % Over 4:1	Section 3.2.1.8	8
AIMS 2.0 Flat and Elongate % Over 5:1	Section 3.2.1.8	3
Direct Proportional Caliper Flat and Elongate % Over 4:1	Section 3.2.1.10	16
Direct Proportional Caliper Flat and Elongate % Over 5:1	Section 3.2.1.10	10

Concrete Test:	Method	Result
Compressive Strength, psi	ASTM C 39	6360
Flexure Beam Strength, psi	ASTM C 78	980
Split Cylinder Strength, psi	ASTM C 496	695
Modulus of Elasticity, ksi	ASTM C 469	7300
Coefficient of Thermal Expansion, $\mu\epsilon$ per °F	Tex 428-A	5.89

Aggregate Identification Number:		2
Source District:		Yoakum
Lithology:		Partly Crushed River Gravel

Aggregate Test:	Method	Result
Specific Gravity	Tex 403-A	2.6
Absorption, %	Tex 403-A	0.5
Micro-Deval loss, %	Tex 461-A	3.4
Los Angeles Abrasion loss, %	Tex 410-A	23
Modified Aggregate Impact Value loss, %	Section 4.6	22.9
Modified Aggregate Crushing Value loss, %	Section 4.7	35.8
Magnesium Sulfate Soundness loss, %	Tex 411-A	2
Uncofined Freezing and Thawing loss, %	CSA 23.2-24A	2.8
Thermal Conduvity, w/(m^2 K)	Section 3.2.1.9	NA
AIMS 2.0 Angularity	Section 3.2.1.8	3165
AIMS 2.0 Texture	Section 3.2.1.8	136
AIMS 2.0 Flat and Elongate % Over 4:1	Section 3.2.1.8	22
AIMS 2.0 Flat and Elongate % Over 5:1	Section 3.2.1.8	11
Direct Proportional Caliper Flat and Elongate % Over 4:1	Section 3.2.1.10	45
Direct Proportional Caliper Flat and Elongate % Over 5:1	Section 3.2.1.10	29

Concrete Test:	Method	Result
Compressive Strength, psi	ASTM C 39	NA
Flexure Beam Strength, psi	ASTM C 78	NA
Split Cylinder Strength, psi	ASTM C 496	NA
Modulus of Elasticity, ksi	ASTM C 469	NA
Coefficient of Thermal Expansion, $\mu\varepsilon$ per °F	Tex 428-A	NA

Aggregate Identification Number:		3
Source District:		Austin
Lithology:		Partly Crushed River Gravel

Aggregate Test:	Method	Result
Specific Gravity	Tex 403-A	2.63
Absorption, %	Tex 403-A	0.8

Micro-Deval loss, %	Tex 461-A	9.5
Los Angeles Abrasion loss, %	Tex 410-A	24
Modified Aggregate Impact Value loss, %	Section 4.6	26.4
Modified Aggregate Crushing Value loss, %	Section 4.7	44.3

Magnesium Sulfate Soundness loss, %	Tex 411-A	3
Uncofined Freezing and Thawing loss, %	CSA 23.2-24A	6.1

Thermal Conduvity, w/(m^2 K)	Section 3.2.1.9	NA

AIMS 2.0 Angularity	Section 3.2.1.8	2849
AIMS 2.0 Texture	Section 3.2.1.8	174
AIMS 2.0 Flat and Elongate % Over 4:1	Section 3.2.1.8	16
AIMS 2.0 Flat and Elongate % Over 5:1	Section 3.2.1.8	4
Direct Proportional Caliper Flat and Elongate % Over 4:1	Section 3.2.1.10	27
Direct Proportional Caliper Flat and Elongate % Over 5:1	Section 3.2.1.10	12

Concrete Test:	Method	Result
Compressive Strength, psi	ASTM C 39	NA
Flexure Beam Strength, psi	ASTM C 78	NA
Split Cylinder Strength, psi	ASTM C 496	NA
Modulus of Elasticity, ksi	ASTM C 469	NA
Coefficient of Thermal Expansion, με per °F	Tex 428-A	NA

Aggregate Identification Number:	4
Source District:	Austin
Lithology:	Partly Crushed River Gravel

Aggregate Test:	Method	Result
Specific Gravity	Tex 403-A	2.63
Absorption, %	Tex 403-A	0.9

Micro-Deval loss, %	Tex 461-A	8.4
Los Angeles Abrasion loss, %	Tex 410-A	25
Modified Aggregate Impact Value loss, %	Section 4.6	25.3
Modified Aggregate Crushing Value loss, %	Section 4.7	43.2

Magnesium Sulfate Soundness loss, %	Tex 411-A	3
Uncofined Freezing and Thawing loss, %	CSA 23.2-24A	14.5

Thermal Conduvity, w/(m^2 K)	Section 3.2.1.9	NA

AIMS 2.0 Angularity	Section 3.2.1.8	1938
AIMS 2.0 Texture	Section 3.2.1.8	168
AIMS 2.0 Flat and Elongate % Over 4:1	Section 3.2.1.8	7
AIMS 2.0 Flat and Elongate % Over 5:1	Section 3.2.1.8	3
Direct Proportional Caliper Flat and Elongate % Over 4:1	Section 3.2.1.10	20
Direct Proportional Caliper Flat and Elongate % Over 5:1	Section 3.2.1.10	12

Concrete Test:	Method	Result
Compressive Strength, psi	ASTM C 39	6450
Flexure Beam Strength, psi	ASTM C 78	915
Split Cylinder Strength, psi	ASTM C 496	660
Modulus of Elasticity, ksi	ASTM C 469	7100
Coefficient of Thermal Expansion, με per °F	Tex 428-A	4.12

Aggregate Identification Number:	5
Source District:	Houston
Lithology:	Partly Crushed River Gravel

Aggregate Test:	Method	Result
Specific Gravity	Tex 403-A	2.58
Absorption, %	Tex 403-A	0.9

Micro-Deval loss, %	Tex 461-A	2.1
Los Angeles Abrasion loss, %	Tex 410-A	17
Modified Aggregate Impact Value loss, %	Section 4.6	15.9
Modified Aggregate Crushing Value loss, %	Section 4.7	30

Magnesium Sulfate Soundness loss, %	Tex 411-A	3
Uncofined Freezing and Thawing loss, %	CSA 23.2-24A	4.7

Thermal Conduvity, w/(m^2 K)	Section 3.2.1.9	NA

AIMS 2.0 Angularity	Section 3.2.1.8	2010
AIMS 2.0 Texture	Section 3.2.1.8	195
AIMS 2.0 Flat and Elongate % Over 4:1	Section 3.2.1.8	4
AIMS 2.0 Flat and Elongate % Over 5:1	Section 3.2.1.8	0
Direct Proportional Caliper Flat and Elongate % Over 4:1	Section 3.2.1.10	6
Direct Proportional Caliper Flat and Elongate % Over 5:1	Section 3.2.1.10	4

Concrete Test:	Method	Result
Compressive Strength, psi	ASTM C 39	NA
Flexure Beam Strength, psi	ASTM C 78	NA
Split Cylinder Strength, psi	ASTM C 496	NA
Modulus of Elasticity, ksi	ASTM C 469	NA
Coefficient of Thermal Expansion, $\mu\varepsilon$ per °F	Tex 428-A	NA

Aggregate Identification Number:		6
Source District:		Houston
Lithology:		Partly Crushed River Gravel

Aggregate Test:	Method	Result
Specific Gravity	Tex 403-A	2.58
Absorption, %	Tex 403-A	0.7

Micro-Deval loss, %	Tex 461-A	4.9
Los Angeles Abrasion loss, %	Tex 410-A	22
Modified Aggregate Impact Value loss, %	Section 4.6	21.3
Modified Aggregate Crushing Value loss, %	Section 4.7	37

Magnesium Sulfate Soundness loss, %	Tex 411-A	1
Uncofined Freezing and Thawing loss, %	CSA 23.2-24A	1.2

Thermal Conduvity, w/(m^2 K)	Section 3.2.1.9	NA

AIMS 2.0 Angularity	Section 3.2.1.8	2763
AIMS 2.0 Texture	Section 3.2.1.8	148
AIMS 2.0 Flat and Elongate % Over 4:1	Section 3.2.1.8	NA
AIMS 2.0 Flat and Elongate % Over 5:1	Section 3.2.1.8	NA
Direct Proportional Caliper Flat and Elongate % Over 4:1	Section 3.2.1.10	NA
Direct Proportional Caliper Flat and Elongate % Over 5:1	Section 3.2.1.10	NA

Concrete Test:	Method	Result
Compressive Strength, psi	ASTM C 39	NA
Flexure Beam Strength, psi	ASTM C 78	NA
Split Cylinder Strength, psi	ASTM C 496	NA
Modulus of Elasticity, ksi	ASTM C 469	NA
Coefficient of Thermal Expansion, $\mu\varepsilon$ per °F	Tex 428-A	NA

Aggregate Identification Number:	7
Source District:	Atlanta
Lithology:	Partly Crushed River Gravel

Aggregate Test:	Method	Result
Specific Gravity	Tex 403-A	2.57
Absorption, %	Tex 403-A	1.1

Micro-Deval loss, %	Tex 461-A	4
Los Angeles Abrasion loss, %	Tex 410-A	24
Modified Aggregate Impact Value loss, %	Section 4.6	20.3
Modified Aggregate Crushing Value loss, %	Section 4.7	38

Magnesium Sulfate Soundness loss, %	Tex 411-A	6
Uncofined Freezing and Thawing loss, %	CSA 23.2-24A	4.9

Thermal Conduvity, w/(m^2 K)	Section 3.2.1.9	NA

AIMS 2.0 Angularity	Section 3.2.1.8	2000
AIMS 2.0 Texture	Section 3.2.1.8	116
AIMS 2.0 Flat and Elongate % Over 4:1	Section 3.2.1.8	NA
AIMS 2.0 Flat and Elongate % Over 5:1	Section 3.2.1.8	NA
Direct Proportional Caliper Flat and Elongate % Over 4:1	Section 3.2.1.10	NA
Direct Proportional Caliper Flat and Elongate % Over 5:1	Section 3.2.1.10	NA

Concrete Test:	Method	Result
Compressive Strength, psi	ASTM C 39	NA
Flexure Beam Strength, psi	ASTM C 78	NA
Split Cylinder Strength, psi	ASTM C 496	NA
Modulus of Elasticity, ksi	ASTM C 469	NA
Coefficient of Thermal Expansion, $\mu\varepsilon$ per °F	Tex 428-A	NA

Aggregate Identification Number:	8
Source District:	Atlanta
Lithology:	Partly Crushed River Gravel

Aggregate Test:	Method	Result
Specific Gravity	Tex 403-A	2.57
Absorption, %	Tex 403-A	1

Micro-Deval loss, %	Tex 461-A	7.4
Los Angeles Abrasion loss, %	Tex 410-A	20
Modified Aggregate Impact Value loss, %	Section 4.6	20
Modified Aggregate Crushing Value loss, %	Section 4.7	33

Magnesium Sulfate Soundness loss, %	Tex 411-A	6
Uncofined Freezing and Thawing loss, %	CSA 23.2-24A	2.3

Thermal Conduvity, w/(m^2 K)	Section 3.2.1.9	NA

AIMS 2.0 Angularity	Section 3.2.1.8	2230
AIMS 2.0 Texture	Section 3.2.1.8	173
AIMS 2.0 Flat and Elongate % Over 4:1	Section 3.2.1.8	7
AIMS 2.0 Flat and Elongate % Over 5:1	Section 3.2.1.8	3
Direct Proportional Caliper Flat and Elongate % Over 4:1	Section 3.2.1.10	8
Direct Proportional Caliper Flat and Elongate % Over 5:1	Section 3.2.1.10	4

Concrete Test:	Method	Result
Compressive Strength, psi	ASTM C 39	NA
Flexure Beam Strength, psi	ASTM C 78	NA
Split Cylinder Strength, psi	ASTM C 496	NA
Modulus of Elasticity, ksi	ASTM C 469	NA
Coefficient of Thermal Expansion, $\mu\varepsilon$ per °F	Tex 428-A	NA

Aggregate Identification Number:	9
Source District:	Atlanta
Lithology:	Partly Crushed River Gravel

Aggregate Test:	Method	Result
Specific Gravity	Tex 403-A	2.57
Absorption, %	Tex 403-A	1.1

Micro-Deval loss, %	Tex 461-A	4.2
Los Angeles Abrasion loss, %	Tex 410-A	25
Modified Aggregate Impact Value loss, %	Section 4.6	22.5
Modified Aggregate Crushing Value loss, %	Section 4.7	36.3

Magnesium Sulfate Soundness loss, %	Tex 411-A	7
Uncofined Freezing and Thawing loss, %	CSA 23.2-24A	7.6

Thermal Conduvity, w/(m^2 K)	Section 3.2.1.9	5.56

AIMS 2.0 Angularity	Section 3.2.1.8	2037
AIMS 2.0 Texture	Section 3.2.1.8	128
AIMS 2.0 Flat and Elongate % Over 4:1	Section 3.2.1.8	4
AIMS 2.0 Flat and Elongate % Over 5:1	Section 3.2.1.8	2
Direct Proportional Caliper Flat and Elongate % Over 4:1	Section 3.2.1.10	13
Direct Proportional Caliper Flat and Elongate % Over 5:1	Section 3.2.1.10	4

Concrete Test:	Method	Result
Compressive Strength, psi	ASTM C 39	6140
Flexure Beam Strength, psi	ASTM C 78	870
Split Cylinder Strength, psi	ASTM C 496	620
Modulus of Elasticity, ksi	ASTM C 469	6100
Coefficient of Thermal Expansion, με per °F	Tex 428-A	6.35

Aggregate Identification Number:	10
Source District:	Siliceous River Gravel
Lithology:	Austin

Aggregate Test:	Method	Result
Specific Gravity	Tex 403-A	2.6
Absorption, %	Tex 403-A	1.8

Micro-Deval loss, %	Tex 461-A	11.1
Los Angeles Abrasion loss, %	Tex 410-A	25
Modified Aggregate Impact Value loss, %	Section 4.6	26.1
Modified Aggregate Crushing Value loss, %	Section 4.7	43.1

Magnesium Sulfate Soundness loss, %	Tex 411-A	6
Uncofined Freezing and Thawing loss, %	CSA 23.2-24A	8.1

Thermal Conduvity, w/(m^2 K)	Section 3.2.1.9	4.64

AIMS 2.0 Angularity	Section 3.2.1.8	2154
AIMS 2.0 Texture	Section 3.2.1.8	179
AIMS 2.0 Flat and Elongate % Over 4:1	Section 3.2.1.8	4
AIMS 2.0 Flat and Elongate % Over 5:1	Section 3.2.1.8	1
Direct Proportional Caliper Flat and Elongate % Over 4:1	Section 3.2.1.10	15
Direct Proportional Caliper Flat and Elongate % Over 5:1	Section 3.2.1.10	7

Concrete Test:	Method	Result
Compressive Strength, psi	ASTM C 39	NA
Flexure Beam Strength, psi	ASTM C 78	NA
Split Cylinder Strength, psi	ASTM C 496	NA
Modulus of Elasticity, ksi	ASTM C 469	NA
Coefficient of Thermal Expansion, με per °F	Tex 428-A	NA

Aggregate Identification Number:	11
Source District:	Siliceous River Gravel
Lithology:	Austin

Aggregate Test:	Method	Result
Specific Gravity	Tex 403-A	2.63
Absorption, %	Tex 403-A	1

Micro-Deval loss, %	Tex 461-A	9.6
Los Angeles Abrasion loss, %	Tex 410-A	26
Modified Aggregate Impact Value loss, %	Section 4.6	26.4
Modified Aggregate Crushing Value loss, %	Section 4.7	41.9

Magnesium Sulfate Soundness loss, %	Tex 411-A	4
Uncofined Freezing and Thawing loss, %	CSA 23.2-24A	6

Thermal Conduvity, w/(m^2 K)	Section 3.2.1.9	4.36

AIMS 2.0 Angularity	Section 3.2.1.8	1613
AIMS 2.0 Texture	Section 3.2.1.8	137
AIMS 2.0 Flat and Elongate % Over 4:1	Section 3.2.1.8	10
AIMS 2.0 Flat and Elongate % Over 5:1	Section 3.2.1.8	1
Direct Proportional Caliper Flat and Elongate % Over 4:1	Section 3.2.1.10	24
Direct Proportional Caliper Flat and Elongate % Over 5:1	Section 3.2.1.10	12

Concrete Test:	Method	Result
Compressive Strength, psi	ASTM C 39	6720
Flexure Beam Strength, psi	ASTM C 78	830
Split Cylinder Strength, psi	ASTM C 496	620
Modulus of Elasticity, ksi	ASTM C 469	6900
Coefficient of Thermal Expansion, με per °F	Tex 428-A	4.48

Aggregate Identification Number:	11
Source District:	Siliceous River Gravel
Lithology:	Dallas

Aggregate Test:	Method	Result
Specific Gravity	Tex 403-A	2.68
Absorption, %	Tex 403-A	1.1
Micro-Deval loss, %	Tex 461-A	11.6
Los Angeles Abrasion loss, %	Tex 410-A	25
Modified Aggregate Impact Value loss, %	Section 4.6	29.4
Modified Aggregate Crushing Value loss, %	Section 4.7	44.6
Magnesium Sulfate Soundness loss, %	Tex 411-A	5
Uncofined Freezing and Thawing loss, %	CSA 23.2-24A	22.1
Thermal Conduvity, w/(m^2 K)	Section 3.2.1.9	NA
AIMS 2.0 Angularity	Section 3.2.1.8	1673
AIMS 2.0 Texture	Section 3.2.1.8	170
AIMS 2.0 Flat and Elongate % Over 4:1	Section 3.2.1.8	16
AIMS 2.0 Flat and Elongate % Over 5:1	Section 3.2.1.8	5
Direct Proportional Caliper Flat and Elongate % Over 4:1	Section 3.2.1.10	24
Direct Proportional Caliper Flat and Elongate % Over 5:1	Section 3.2.1.10	9

Concrete Test:	Method	Result
Compressive Strength, psi	ASTM C 39	NA
Flexure Beam Strength, psi	ASTM C 78	NA
Split Cylinder Strength, psi	ASTM C 496	NA
Modulus of Elasticity, ksi	ASTM C 469	NA
Coefficient of Thermal Expansion, με per °F	Tex 428-A	NA

Aggregate Identification Number:		13
Source District:		Siliceous River Gravel
Lithology:		Amarillo

Aggregate Test:	Method	Result
Specific Gravity	Tex 403-A	2.63
Absorption, %	Tex 403-A	0.9
Micro-Deval loss, %	Tex 461-A	10.4
Los Angeles Abrasion loss, %	Tex 410-A	29
Modified Aggregate Impact Value loss, %	Section 4.6	23.5
Modified Aggregate Crushing Value loss, %	Section 4.7	41
Magnesium Sulfate Soundness loss, %	Tex 411-A	7
Uncofined Freezing and Thawing loss, %	CSA 23.2-24A	6.6
Thermal Conduvity, w/(m^2 K)	Section 3.2.1.9	NA
AIMS 2.0 Angularity	Section 3.2.1.8	2164
AIMS 2.0 Texture	Section 3.2.1.8	265
AIMS 2.0 Flat and Elongate % Over 4:1	Section 3.2.1.8	NA
AIMS 2.0 Flat and Elongate % Over 5:1	Section 3.2.1.8	NA
Direct Proportional Caliper Flat and Elongate % Over 4:1	Section 3.2.1.10	NA
Direct Proportional Caliper Flat and Elongate % Over 5:1	Section 3.2.1.10	NA

Concrete Test:	Method	Result
Compressive Strength, psi	ASTM C 39	NA
Flexure Beam Strength, psi	ASTM C 78	NA
Split Cylinder Strength, psi	ASTM C 496	NA
Modulus of Elasticity, ksi	ASTM C 469	NA
Coefficient of Thermal Expansion, με per °F	Tex 428-A	NA

Aggregate Identification Number:	14
Source District:	Limestone River Gravel
Lithology:	El Paso

Aggregate Test:	Method	Result
Specific Gravity	Tex 403-A	2.57
Absorption, %	Tex 403-A	2.2
Micro-Deval loss, %	Tex 461-A	14.1
Los Angeles Abrasion loss, %	Tex 410-A	23
Modified Aggregate Impact Value loss, %	Section 4.6	22.3
Modified Aggregate Crushing Value loss, %	Section 4.7	39
Magnesium Sulfate Soundness loss, %	Tex 411-A	14
Uncofined Freezing and Thawing loss, %	CSA 23.2-24A	13.7
Thermal Conduvity, w/(m^2 K)	Section 3.2.1.9	3.13
AIMS 2.0 Angularity	Section 3.2.1.8	2654
AIMS 2.0 Texture	Section 3.2.1.8	229
AIMS 2.0 Flat and Elongate % Over 4:1	Section 3.2.1.8	10
AIMS 2.0 Flat and Elongate % Over 5:1	Section 3.2.1.8	4
Direct Proportional Caliper Flat and Elongate % Over 4:1	Section 3.2.1.10	21
Direct Proportional Caliper Flat and Elongate % Over 5:1	Section 3.2.1.10	12

Concrete Test:	Method	
Compressive Strength, psi	ASTM C 39	NA
Flexure Beam Strength, psi	ASTM C 78	NA
Split Cylinder Strength, psi	ASTM C 496	NA
Modulus of Elasticity, ksi	ASTM C 469	NA
Coefficient of Thermal Expansion, µε per °F	Tex 428-A	NA

Aggregate Identification Number:	15
Source District:	Limestone River Gravel
Lithology:	Lubbock

Aggregate Test:	Method	Result
Specific Gravity	Tex 403-A	2.62
Absorption, %	Tex 403-A	1.7

Micro-Deval loss, %	Tex 461-A	15.7
Los Angeles Abrasion loss, %	Tex 410-A	25
Modified Aggregate Impact Value loss, %	Section 4.6	22.3
Modified Aggregate Crushing Value loss, %	Section 4.7	38.6

Magnesium Sulfate Soundness loss, %	Tex 411-A	19
Uncofined Freezing and Thawing loss, %	CSA 23.2-24A	10.8

Thermal Conduvity, w/(m^2 K)	Section 3.2.1.9	5.38

AIMS 2.0 Angularity	Section 3.2.1.8	1763
AIMS 2.0 Texture	Section 3.2.1.8	223
AIMS 2.0 Flat and Elongate % Over 4:1	Section 3.2.1.8	4
AIMS 2.0 Flat and Elongate % Over 5:1	Section 3.2.1.8	1
Direct Proportional Caliper Flat and Elongate % Over 4:1	Section 3.2.1.10	19
Direct Proportional Caliper Flat and Elongate % Over 5:1	Section 3.2.1.10	12

Concrete Test:	Method	Result
Compressive Strength, psi	ASTM C 39	5950
Flexure Beam Strength, psi	ASTM C 78	800
Split Cylinder Strength, psi	ASTM C 496	635
Modulus of Elasticity, ksi	ASTM C 469	5900
Coefficient of Thermal Expansion, με per °F	Tex 428-A	5.06

Aggregate Identification Number:	16
Source District:	Limestone River Gravel
Lithology:	Waco

Aggregate Test:	Method	Result
Specific Gravity	Tex 403-A	2.61
Absorption, %	Tex 403-A	2.1

Micro-Deval loss, %	Tex 461-A	15.4
Los Angeles Abrasion loss, %	Tex 410-A	26
Modified Aggregate Impact Value loss, %	Section 4.6	25.4
Modified Aggregate Crushing Value loss, %	Section 4.7	44.1

Magnesium Sulfate Soundness loss, %	Tex 411-A	18
Uncofined Freezing and Thawing loss, %	CSA 23.2-24A	22.7

Thermal Conduvity, w/(m^2 K)	Section 3.2.1.9	3.14

AIMS 2.0 Angularity	Section 3.2.1.8	1751
AIMS 2.0 Texture	Section 3.2.1.8	150
AIMS 2.0 Flat and Elongate % Over 4:1	Section 3.2.1.8	2
AIMS 2.0 Flat and Elongate % Over 5:1	Section 3.2.1.8	1
Direct Proportional Caliper Flat and Elongate % Over 4:1	Section 3.2.1.10	26
Direct Proportional Caliper Flat and Elongate % Over 5:1	Section 3.2.1.10	12

Concrete Test:	Method	Result
Compressive Strength, psi	ASTM C 39	6340
Flexure Beam Strength, psi	ASTM C 78	785
Split Cylinder Strength, psi	ASTM C 496	685
Modulus of Elasticity, ksi	ASTM C 469	5950
Coefficient of Thermal Expansion, με per °F	Tex 428-A	4.23

Aggregate Identification Number:	17
Source District:	Limestone River Gravel
Lithology:	Waco

Aggregate Test:	Method	Result
Specific Gravity	Tex 403-A	2.6
Absorption, %	Tex 403-A	2.5

	Method	Result
Micro-Deval loss, %	Tex 461-A	16
Los Angeles Abrasion loss, %	Tex 410-A	30
Modified Aggregate Impact Value loss, %	Section 4.6	27.2
Modified Aggregate Crushing Value loss, %	Section 4.7	43.6

	Method	Result
Magnesium Sulfate Soundness loss, %	Tex 411-A	22
Uncofined Freezing and Thawing loss, %	CSA 23.2-24A	15

	Method	Result
Thermal Conduvity, w/(m^2 K)	Section 3.2.1.9	NA

	Method	Result
AIMS 2.0 Angularity	Section 3.2.1.8	1648
AIMS 2.0 Texture	Section 3.2.1.8	119
AIMS 2.0 Flat and Elongate % Over 4:1	Section 3.2.1.8	11
AIMS 2.0 Flat and Elongate % Over 5:1	Section 3.2.1.8	3
Direct Proportional Caliper Flat and Elongate % Over 4:1	Section 3.2.1.10	22
Direct Proportional Caliper Flat and Elongate % Over 5:1	Section 3.2.1.10	10

Concrete Test:	Method	Result
Compressive Strength, psi	ASTM C 39	NA
Flexure Beam Strength, psi	ASTM C 78	NA
Split Cylinder Strength, psi	ASTM C 496	NA
Modulus of Elasticity, ksi	ASTM C 469	NA
Coefficient of Thermal Expansion, $\mu\epsilon$ per °F	Tex 428-A	NA

Aggregate Identification Number:	18
Source District:	Limestone River Gravel
Lithology:	Waco

Aggregate Test:	Method	Result
Specific Gravity	Tex 403-A	2.63
Absorption, %	Tex 403-A	1.8
Micro-Deval loss, %	Tex 461-A	14.6
Los Angeles Abrasion loss, %	Tex 410-A	28
Modified Aggregate Impact Value loss, %	Section 4.6	25.6
Modified Aggregate Crushing Value loss, %	Section 4.7	42.5
Magnesium Sulfate Soundness loss, %	Tex 411-A	16
Uncofined Freezing and Thawing loss, %	CSA 23.2-24A	13.9
Thermal Conduvity, w/(m^2 K)	Section 3.2.1.9	NA
AIMS 2.0 Angularity	Section 3.2.1.8	1680
AIMS 2.0 Texture	Section 3.2.1.8	147
AIMS 2.0 Flat and Elongate % Over 4:1	Section 3.2.1.8	10
AIMS 2.0 Flat and Elongate % Over 5:1	Section 3.2.1.8	2
Direct Proportional Caliper Flat and Elongate % Over 4:1	Section 3.2.1.10	23
Direct Proportional Caliper Flat and Elongate % Over 5:1	Section 3.2.1.10	12

Concrete Test:	Method	Result
Compressive Strength, psi	ASTM C 39	NA
Flexure Beam Strength, psi	ASTM C 78	NA
Split Cylinder Strength, psi	ASTM C 496	NA
Modulus of Elasticity, ksi	ASTM C 469	NA
Coefficient of Thermal Expansion, με per °F	Tex 428-A	NA

Aggregate Identification Number:	19
Source District:	Limestone River Gravel
Lithology:	Waco

Aggregate Test:	Method	Result
Specific Gravity	Tex 403-A	2.6
Absorption, %	Tex 403-A	2

	Method	Result
Micro-Deval loss, %	Tex 461-A	19.2
Los Angeles Abrasion loss, %	Tex 410-A	28
Modified Aggregate Impact Value loss, %	Section 4.6	27.4
Modified Aggregate Crushing Value loss, %	Section 4.7	45.2

	Method	Result
Magnesium Sulfate Soundness loss, %	Tex 411-A	18
Uncofined Freezing and Thawing loss, %	CSA 23.2-24A	22.4

	Method	Result
Thermal Conduvity, w/(m^2 K)	Section 3.2.1.9	3.79

	Method	Result
AIMS 2.0 Angularity	Section 3.2.1.8	1890
AIMS 2.0 Texture	Section 3.2.1.8	188
AIMS 2.0 Flat and Elongate % Over 4:1	Section 3.2.1.8	6
AIMS 2.0 Flat and Elongate % Over 5:1	Section 3.2.1.8	2
Direct Proportional Caliper Flat and Elongate % Over 4:1	Section 3.2.1.10	20
Direct Proportional Caliper Flat and Elongate % Over 5:1	Section 3.2.1.10	11

Concrete Test:	Method	Result
Compressive Strength, psi	ASTM C 39	6470
Flexure Beam Strength, psi	ASTM C 78	845
Split Cylinder Strength, psi	ASTM C 496	660
Modulus of Elasticity, ksi	ASTM C 469	6550
Coefficient of Thermal Expansion, $\mu\varepsilon$ per °F	Tex 428-A	4.26

Aggregate Identification Number:	20
Source District:	Limestone River Gravel
Lithology:	Amarillo

Aggregate Test:	Method	Result
Specific Gravity	Tex 403-A	2.62
Absorption, %	Tex 403-A	1.2
Micro-Deval loss, %	Tex 461-A	16.3
Los Angeles Abrasion loss, %	Tex 410-A	27
Modified Aggregate Impact Value loss, %	Section 4.6	24.8
Modified Aggregate Crushing Value loss, %	Section 4.7	37.1
Magnesium Sulfate Soundness loss, %	Tex 411-A	12
Uncofined Freezing and Thawing loss, %	CSA 23.2-24A	3.7
Thermal Conduvity, w/(m^2 K)	Section 3.2.1.9	NA
AIMS 2.0 Angularity	Section 3.2.1.8	1780
AIMS 2.0 Texture	Section 3.2.1.8	219
AIMS 2.0 Flat and Elongate % Over 4:1	Section 3.2.1.8	NA
AIMS 2.0 Flat and Elongate % Over 5:1	Section 3.2.1.8	NA
Direct Proportional Caliper Flat and Elongate % Over 4:1	Section 3.2.1.10	NA
Direct Proportional Caliper Flat and Elongate % Over 5:1	Section 3.2.1.10	NA

Concrete Test:	Method	Result
Compressive Strength, psi	ASTM C 39	NA
Flexure Beam Strength, psi	ASTM C 78	NA
Split Cylinder Strength, psi	ASTM C 496	NA
Modulus of Elasticity, ksi	ASTM C 469	NA
Coefficient of Thermal Expansion, με per °F	Tex 428-A	NA

Aggregate Identification Number:	21
Source District:	Limestone
Lithology:	Austin

Aggregate Test:	Method	Result
Specific Gravity	Tex 403-A	2.53
Absorption, %	Tex 403-A	3.8

	Method	Result
Micro-Deval loss, %	Tex 461-A	27.3
Los Angeles Abrasion loss, %	Tex 410-A	32
Modified Aggregate Impact Value loss, %	Section 4.6	29.6
Modified Aggregate Crushing Value loss, %	Section 4.7	50.5

	Method	Result
Magnesium Sulfate Soundness loss, %	Tex 411-A	15
Uncofined Freezing and Thawing loss, %	CSA 23.2-24A	5.8

	Method	Result
Thermal Conduvity, w/(m^2 K)	Section 3.2.1.9	NA

	Method	Result
AIMS 2.0 Angularity	Section 3.2.1.8	2618
AIMS 2.0 Texture	Section 3.2.1.8	98
AIMS 2.0 Flat and Elongate % Over 4:1	Section 3.2.1.8	4
AIMS 2.0 Flat and Elongate % Over 5:1	Section 3.2.1.8	0
Direct Proportional Caliper Flat and Elongate % Over 4:1	Section 3.2.1.10	11
Direct Proportional Caliper Flat and Elongate % Over 5:1	Section 3.2.1.10	0

Concrete Test:	Method	Result
Compressive Strength, psi	ASTM C 39	NA
Flexure Beam Strength, psi	ASTM C 78	NA
Split Cylinder Strength, psi	ASTM C 496	NA
Modulus of Elasticity, ksi	ASTM C 469	NA
Coefficient of Thermal Expansion, $\mu\varepsilon$ per °F	Tex 428-A	NA

Aggregate Identification Number:	22
Source District:	Limestone
Lithology:	Austin

Aggregate Test:	Method	Result
Specific Gravity	Tex 403-A	2.52
Absorption, %	Tex 403-A	2.4

Micro-Deval loss, %	Tex 461-A	21.7
Los Angeles Abrasion loss, %	Tex 410-A	33
Modified Aggregate Impact Value loss, %	Section 4.6	31.5
Modified Aggregate Crushing Value loss, %	Section 4.7	51.2

Magnesium Sulfate Soundness loss, %	Tex 411-A	11
Uncofined Freezing and Thawing loss, %	CSA 23.2-24A	10.7

Thermal Conduvity, w/(m^2 K)	Section 3.2.1.9	NA

AIMS 2.0 Angularity	Section 3.2.1.8	2821
AIMS 2.0 Texture	Section 3.2.1.8	130
AIMS 2.0 Flat and Elongate % Over 4:1	Section 3.2.1.8	2
AIMS 2.0 Flat and Elongate % Over 5:1	Section 3.2.1.8	0
Direct Proportional Caliper Flat and Elongate % Over 4:1	Section 3.2.1.10	10
Direct Proportional Caliper Flat and Elongate % Over 5:1	Section 3.2.1.10	0

Concrete Test:	Method	Result
Compressive Strength, psi	ASTM C 39	NA
Flexure Beam Strength, psi	ASTM C 78	NA
Split Cylinder Strength, psi	ASTM C 496	NA
Modulus of Elasticity, ksi	ASTM C 469	NA
Coefficient of Thermal Expansion, με per °F	Tex 428-A	NA

221

Aggregate Identification Number:	23
Source District:	Limestone
Lithology:	Dallas

Aggregate Test:	Method	Result
Specific Gravity	Tex 403-A	2.66
Absorption, %	Tex 403-A	1.4
Micro-Deval loss, %	Tex 461-A	21.7
Los Angeles Abrasion loss, %	Tex 410-A	29
Modified Aggregate Impact Value loss, %	Section 4.6	25.8
Modified Aggregate Crushing Value loss, %	Section 4.7	43
Magnesium Sulfate Soundness loss, %	Tex 411-A	14
Uncofined Freezing and Thawing loss, %	CSA 23.2-24A	12.3
Thermal Conduvity, w/(m^2 K)	Section 3.2.1.9	NA
AIMS 2.0 Angularity	Section 3.2.1.8	2852
AIMS 2.0 Texture	Section 3.2.1.8	302
AIMS 2.0 Flat and Elongate % Over 4:1	Section 3.2.1.8	8
AIMS 2.0 Flat and Elongate % Over 5:1	Section 3.2.1.8	2
Direct Proportional Caliper Flat and Elongate % Over 4:1	Section 3.2.1.10	9
Direct Proportional Caliper Flat and Elongate % Over 5:1	Section 3.2.1.10	3

Concrete Test:	Method	Result
Compressive Strength, psi	ASTM C 39	NA
Flexure Beam Strength, psi	ASTM C 78	NA
Split Cylinder Strength, psi	ASTM C 496	NA
Modulus of Elasticity, ksi	ASTM C 469	NA
Coefficient of Thermal Expansion, με per °F	Tex 428-A	NA

Aggregate Identification Number:	24
Source District:	Limestone
Lithology:	San Antonio

Aggregate Test:	Method	Result
Specific Gravity	Tex 403-A	2.58
Absorption, %	Tex 403-A	2.1

Micro-Deval loss, %	Tex 461-A	21.9
Los Angeles Abrasion loss, %	Tex 410-A	27
Modified Aggregate Impact Value loss, %	Section 4.6	23.8
Modified Aggregate Crushing Value loss, %	Section 4.7	45.8

Magnesium Sulfate Soundness loss, %	Tex 411-A	10
Uncofined Freezing and Thawing loss, %	CSA 23.2-24A	2.4

Thermal Conduvity, w/(m^2 K)	Section 3.2.1.9	NA

AIMS 2.0 Angularity	Section 3.2.1.8	2834
AIMS 2.0 Texture	Section 3.2.1.8	136
AIMS 2.0 Flat and Elongate % Over 4:1	Section 3.2.1.8	1
AIMS 2.0 Flat and Elongate % Over 5:1	Section 3.2.1.8	0
Direct Proportional Caliper Flat and Elongate % Over 4:1	Section 3.2.1.10	7
Direct Proportional Caliper Flat and Elongate % Over 5:1	Section 3.2.1.10	1

Concrete Test:	Method	Result
Compressive Strength, psi	ASTM C 39	NA
Flexure Beam Strength, psi	ASTM C 78	NA
Split Cylinder Strength, psi	ASTM C 496	NA
Modulus of Elasticity, ksi	ASTM C 469	NA
Coefficient of Thermal Expansion, με per °F	Tex 428-A	NA

Aggregate Identification Number:	25
Source District:	Limestone
Lithology:	San Antonio

Aggregate Test:	Method	Result
Specific Gravity	Tex 403-A	2.57
Absorption, %	Tex 403-A	3

Micro-Deval loss, %	Tex 461-A	27.5
Los Angeles Abrasion loss, %	Tex 410-A	32
Modified Aggregate Impact Value loss, %	Section 4.6	29.2
Modified Aggregate Crushing Value loss, %	Section 4.7	45.2

Magnesium Sulfate Soundness loss, %	Tex 411-A	26
Uncofined Freezing and Thawing loss, %	CSA 23.2-24A	14.7

Thermal Conduvity, w/(m^2 K)	Section 3.2.1.9	3.4

AIMS 2.0 Angularity	Section 3.2.1.8	2433
AIMS 2.0 Texture	Section 3.2.1.8	89
AIMS 2.0 Flat and Elongate % Over 4:1	Section 3.2.1.8	4
AIMS 2.0 Flat and Elongate % Over 5:1	Section 3.2.1.8	1
Direct Proportional Caliper Flat and Elongate % Over 4:1	Section 3.2.1.10	9
Direct Proportional Caliper Flat and Elongate % Over 5:1	Section 3.2.1.10	3

Concrete Test:	Method	Result
Compressive Strength, psi	ASTM C 39	6650
Flexure Beam Strength, psi	ASTM C 78	770
Split Cylinder Strength, psi	ASTM C 496	625
Modulus of Elasticity, ksi	ASTM C 469	5300
Coefficient of Thermal Expansion, $\mu\varepsilon$ per °F	Tex 428-A	3.88

Aggregate Identification Number:		26
Source District:		Limestone
Lithology:		Austin

Aggregate Test:	Method	Result
Specific Gravity	Tex 403-A	2.55
Absorption, %	Tex 403-A	2.6
Micro-Deval loss, %	Tex 461-A	21.3
Los Angeles Abrasion loss, %	Tex 410-A	27
Modified Aggregate Impact Value loss, %	Section 4.6	28.6
Modified Aggregate Crushing Value loss, %	Section 4.7	48.7
Magnesium Sulfate Soundness loss, %	Tex 411-A	12
Uncofined Freezing and Thawing loss, %	CSA 23.2-24A	10.7
Thermal Conduvity, w/(m^2 K)	Section 3.2.1.9	NA
AIMS 2.0 Angularity	Section 3.2.1.8	2842
AIMS 2.0 Texture	Section 3.2.1.8	147
AIMS 2.0 Flat and Elongate % Over 4:1	Section 3.2.1.8	2
AIMS 2.0 Flat and Elongate % Over 5:1	Section 3.2.1.8	1
Direct Proportional Caliper Flat and Elongate % Over 4:1	Section 3.2.1.10	13
Direct Proportional Caliper Flat and Elongate % Over 5:1	Section 3.2.1.10	0

Concrete Test:	Method	Result
Compressive Strength, psi	ASTM C 39	NA
Flexure Beam Strength, psi	ASTM C 78	NA
Split Cylinder Strength, psi	ASTM C 496	NA
Modulus of Elasticity, ksi	ASTM C 469	NA
Coefficient of Thermal Expansion, $\mu\varepsilon$ per °F	Tex 428-A	NA

Aggregate Identification Number:	27
Source District:	Limestone
Lithology:	San Antonio

Aggregate Test:	Method	Result
Specific Gravity	Tex 403-A	2.57
Absorption, %	Tex 403-A	2
Micro-Deval loss, %	Tex 461-A	26.5
Los Angeles Abrasion loss, %	Tex 410-A	36
Modified Aggregate Impact Value loss, %	Section 4.6	31.9
Modified Aggregate Crushing Value loss, %	Section 4.7	51.4
Magnesium Sulfate Soundness loss, %	Tex 411-A	10
Uncofined Freezing and Thawing loss, %	CSA 23.2-24A	6.8
Thermal Conduvity, w/(m^2 K)	Section 3.2.1.9	3.14
AIMS 2.0 Angularity	Section 3.2.1.8	2650
AIMS 2.0 Texture	Section 3.2.1.8	113
AIMS 2.0 Flat and Elongate % Over 4:1	Section 3.2.1.8	3
AIMS 2.0 Flat and Elongate % Over 5:1	Section 3.2.1.8	0
Direct Proportional Caliper Flat and Elongate % Over 4:1	Section 3.2.1.10	11
Direct Proportional Caliper Flat and Elongate % Over 5:1	Section 3.2.1.10	4

Concrete Test:	Method	Result
Compressive Strength, psi	ASTM C 39	7540
Flexure Beam Strength, psi	ASTM C 78	825
Split Cylinder Strength, psi	ASTM C 496	695
Modulus of Elasticity, ksi	ASTM C 469	6500
Coefficient of Thermal Expansion, $\mu\epsilon$ per °F	Tex 428-A	3.49

Aggregate Identification Number:	28
Source District:	Limestone
Lithology:	San Antonio

Aggregate Test:	Method	Result
Specific Gravity	Tex 403-A	2.6
Absorption, %	Tex 403-A	2.1
Micro-Deval loss, %	Tex 461-A	21.4
Los Angeles Abrasion loss, %	Tex 410-A	30
Modified Aggregate Impact Value loss, %	Section 4.6	28.6
Modified Aggregate Crushing Value loss, %	Section 4.7	47.9
Magnesium Sulfate Soundness loss, %	Tex 411-A	20
Uncofined Freezing and Thawing loss, %	CSA 23.2-24A	15.2
Thermal Conduvity, w/(m^2 K)	Section 3.2.1.9	3.25
AIMS 2.0 Angularity	Section 3.2.1.8	2706
AIMS 2.0 Texture	Section 3.2.1.8	100
AIMS 2.0 Flat and Elongate % Over 4:1	Section 3.2.1.8	1
AIMS 2.0 Flat and Elongate % Over 5:1	Section 3.2.1.8	0
Direct Proportional Caliper Flat and Elongate % Over 4:1	Section 3.2.1.10	22
Direct Proportional Caliper Flat and Elongate % Over 5:1	Section 3.2.1.10	5

Concrete Test:	Method	Result
Compressive Strength, psi	ASTM C 39	NA
Flexure Beam Strength, psi	ASTM C 78	NA
Split Cylinder Strength, psi	ASTM C 496	NA
Modulus of Elasticity, ksi	ASTM C 469	NA
Coefficient of Thermal Expansion, με per °F	Tex 428-A	NA

227

Aggregate Identification Number:	29
Source District:	Limestone
Lithology:	Waco

Aggregate Test:	Method	Result
Specific Gravity	Tex 403-A	2.41
Absorption, %	Tex 403-A	7.6

Micro-Deval loss, %	Tex 461-A	50.1
Los Angeles Abrasion loss, %	Tex 410-A	50
Modified Aggregate Impact Value loss, %	Section 4.6	44.7
Modified Aggregate Crushing Value loss, %	Section 4.7	55.3

Magnesium Sulfate Soundness loss, %	Tex 411-A	49
Uncofined Freezing and Thawing loss, %	CSA 23.2-24A	9.5

Thermal Conduvity, w/(m^2 K)	Section 3.2.1.9	2.9

AIMS 2.0 Angularity	Section 3.2.1.8	2783
AIMS 2.0 Texture	Section 3.2.1.8	119
AIMS 2.0 Flat and Elongate % Over 4:1	Section 3.2.1.8	7
AIMS 2.0 Flat and Elongate % Over 5:1	Section 3.2.1.8	3
Direct Proportional Caliper Flat and Elongate % Over 4:1	Section 3.2.1.10	5
Direct Proportional Caliper Flat and Elongate % Over 5:1	Section 3.2.1.10	2

Concrete Test:	Method	Results
Compressive Strength, psi	ASTM C 39	4560
Flexure Beam Strength, psi	ASTM C 78	630
Split Cylinder Strength, psi	ASTM C 496	505
Modulus of Elasticity, ksi	ASTM C 469	4000
Coefficient of Thermal Expansion, $\mu\varepsilon$ per °F	Tex 428-A	3.97

Aggregate Identification Number:	30
Source District:	Limestone
Lithology:	San Antonio

Aggregate Test:	Method	Result
Specific Gravity	Tex 403-A	2.61
Absorption, %	Tex 403-A	2

Micro-Deval loss, %	Tex 461-A	18.9
Los Angeles Abrasion loss, %	Tex 410-A	29
Modified Aggregate Impact Value loss, %	Section 4.6	28.3
Modified Aggregate Crushing Value loss, %	Section 4.7	49

Magnesium Sulfate Soundness loss, %	Tex 411-A	18
Uncofined Freezing and Thawing loss, %	CSA 23.2-24A	13.5

Thermal Conduvity, w/(m^2 K)	Section 3.2.1.9	3.24

AIMS 2.0 Angularity	Section 3.2.1.8	2614
AIMS 2.0 Texture	Section 3.2.1.8	109
AIMS 2.0 Flat and Elongate % Over 4:1	Section 3.2.1.8	5
AIMS 2.0 Flat and Elongate % Over 5:1	Section 3.2.1.8	2
Direct Proportional Caliper Flat and Elongate % Over 4:1	Section 3.2.1.10	12
Direct Proportional Caliper Flat and Elongate % Over 5:1	Section 3.2.1.10	5

Concrete Test:	Method	Result
Compressive Strength, psi	ASTM C 39	6900
Flexure Beam Strength, psi	ASTM C 78	830
Split Cylinder Strength, psi	ASTM C 496	660
Modulus of Elasticity, ksi	ASTM C 469	6600
Coefficient of Thermal Expansion, με per °F	Tex 428-A	3.74

Aggregate Identification Number:		31
Source District:		Limestone
Lithology:		Ft Worth

Aggregate Test:	Method	Result
Specific Gravity	Tex 403-A	2.66
Absorption, %	Tex 403-A	1.4

Micro-Deval loss, %	Tex 461-A	15.1
Los Angeles Abrasion loss, %	Tex 410-A	26
Modified Aggregate Impact Value loss, %	Section 4.6	21.8
Modified Aggregate Crushing Value loss, %	Section 4.7	46

Magnesium Sulfate Soundness loss, %	Tex 411-A	11
Uncofined Freezing and Thawing loss, %	CSA 23.2-24A	14.4

Thermal Conduvity, w/(m^2 K)	Section 3.2.1.9	3.4

AIMS 2.0 Angularity	Section 3.2.1.8	2542
AIMS 2.0 Texture	Section 3.2.1.8	187
AIMS 2.0 Flat and Elongate % Over 4:1	Section 3.2.1.8	3
AIMS 2.0 Flat and Elongate % Over 5:1	Section 3.2.1.8	0
Direct Proportional Caliper Flat and Elongate % Over 4:1	Section 3.2.1.10	9
Direct Proportional Caliper Flat and Elongate % Over 5:1	Section 3.2.1.10	1

Concrete Test:	Method	Result
Compressive Strength, psi	ASTM C 39	NA
Flexure Beam Strength, psi	ASTM C 78	NA
Split Cylinder Strength, psi	ASTM C 496	NA
Modulus of Elasticity, ksi	ASTM C 469	NA
Coefficient of Thermal Expansion, με per °F	Tex 428-A	NA

Aggregate Identification Number:	32
Source District:	Limestone
Lithology:	Lubbock

Aggregate Test:	Method	Result
Specific Gravity	Tex 403-A	2.42
Absorption, %	Tex 403-A	3.1

Micro-Deval loss, %	Tex 461-A	12.3
Los Angeles Abrasion loss, %	Tex 410-A	23
Modified Aggregate Impact Value loss, %	Section 4.6	23.4
Modified Aggregate Crushing Value loss, %	Section 4.7	40.9

Magnesium Sulfate Soundness loss, %	Tex 411-A	14
Uncofined Freezing and Thawing loss, %	CSA 23.2-24A	33.2

Thermal Conduvity, w/(m^2 K)	Section 3.2.1.9	NA

AIMS 2.0 Angularity	Section 3.2.1.8	2848
AIMS 2.0 Texture	Section 3.2.1.8	110
AIMS 2.0 Flat and Elongate % Over 4:1	Section 3.2.1.8	1
AIMS 2.0 Flat and Elongate % Over 5:1	Section 3.2.1.8	0
Direct Proportional Caliper Flat and Elongate % Over 4:1	Section 3.2.1.10	4
Direct Proportional Caliper Flat and Elongate % Over 5:1	Section 3.2.1.10	1

Concrete Test:	Method	Result
Compressive Strength, psi	ASTM C 39	NA
Flexure Beam Strength, psi	ASTM C 78	NA
Split Cylinder Strength, psi	ASTM C 496	NA
Modulus of Elasticity, ksi	ASTM C 469	NA
Coefficient of Thermal Expansion, με per °F	Tex 428-A	NA

Aggregate Identification Number:		33
Source District:		Limestone
Lithology:		San Antonio

Aggregate Test:	Method	Result
Specific Gravity	Tex 403-A	2.6
Absorption, %	Tex 403-A	1.8
Micro-Deval loss, %	Tex 461-A	18.1
Los Angeles Abrasion loss, %	Tex 410-A	27
Modified Aggregate Impact Value loss, %	Section 4.6	24.4
Modified Aggregate Crushing Value loss, %	Section 4.7	48.2
Magnesium Sulfate Soundness loss, %	Tex 411-A	14
Uncofined Freezing and Thawing loss, %	CSA 23.2-24A	33.2
Thermal Conduvity, w/(m^2 K)	Section 3.2.1.9	NA
AIMS 2.0 Angularity	Section 3.2.1.8	2539
AIMS 2.0 Texture	Section 3.2.1.8	125
AIMS 2.0 Flat and Elongate % Over 4:1	Section 3.2.1.8	2
AIMS 2.0 Flat and Elongate % Over 5:1	Section 3.2.1.8	1
Direct Proportional Caliper Flat and Elongate % Over 4:1	Section 3.2.1.10	7
Direct Proportional Caliper Flat and Elongate % Over 5:1	Section 3.2.1.10	0

Concrete Test:	Method	Result
Compressive Strength, psi	ASTM C 39	NA
Flexure Beam Strength, psi	ASTM C 78	NA
Split Cylinder Strength, psi	ASTM C 496	NA
Modulus of Elasticity, ksi	ASTM C 469	NA
Coefficient of Thermal Expansion, με per °F	Tex 428-A	NA

Aggregate Identification Number:	34
Source District:	Limestone
Lithology:	San Antonio

Aggregate Test:	Method	Result
Specific Gravity	Tex 403-A	2.53
Absorption, %	Tex 403-A	2.1

Micro-Deval loss, %	Tex 461-A	25
Los Angeles Abrasion loss, %	Tex 410-A	32
Modified Aggregate Impact Value loss, %	Section 4.6	32.3
Modified Aggregate Crushing Value loss, %	Section 4.7	49.1

Magnesium Sulfate Soundness loss, %	Tex 411-A	10
Uncofined Freezing and Thawing loss, %	CSA 23.2-24A	8.2

Thermal Conduvity, w/(m^2 K)	Section 3.2.1.9	NA

AIMS 2.0 Angularity	Section 3.2.1.8	2608
AIMS 2.0 Texture	Section 3.2.1.8	147
AIMS 2.0 Flat and Elongate % Over 4:1	Section 3.2.1.8	4
AIMS 2.0 Flat and Elongate % Over 5:1	Section 3.2.1.8	0
Direct Proportional Caliper Flat and Elongate % Over 4:1	Section 3.2.1.10	12
Direct Proportional Caliper Flat and Elongate % Over 5:1	Section 3.2.1.10	4

Concrete Test:	Method	Result
Compressive Strength, psi	ASTM C 39	NA
Flexure Beam Strength, psi	ASTM C 78	NA
Split Cylinder Strength, psi	ASTM C 496	NA
Modulus of Elasticity, ksi	ASTM C 469	NA
Coefficient of Thermal Expansion, με per °F	Tex 428-A	NA

Aggregate Identification Number:	35
Source District:	Limestone
Lithology:	Austin

Aggregate Test:	Method	Result
Specific Gravity	Tex 403-A	2.55
Absorption, %	Tex 403-A	2.5

Micro-Deval loss, %	Tex 461-A	21.7
Los Angeles Abrasion loss, %	Tex 410-A	27
Modified Aggregate Impact Value loss, %	Section 4.6	27.9
Modified Aggregate Crushing Value loss, %	Section 4.7	44.6

Magnesium Sulfate Soundness loss, %	Tex 411-A	14
Uncofined Freezing and Thawing loss, %	CSA 23.2-24A	8.6

Thermal Conduvity, w/(m^2 K)	Section 3.2.1.9	NA

AIMS 2.0 Angularity	Section 3.2.1.8	2813
AIMS 2.0 Texture	Section 3.2.1.8	113
AIMS 2.0 Flat and Elongate % Over 4:1	Section 3.2.1.8	4
AIMS 2.0 Flat and Elongate % Over 5:1	Section 3.2.1.8	0
Direct Proportional Caliper Flat and Elongate % Over 4:1	Section 3.2.1.10	8
Direct Proportional Caliper Flat and Elongate % Over 5:1	Section 3.2.1.10	2

Concrete Test:	Method	Result
Compressive Strength, psi	ASTM C 39	NA
Flexure Beam Strength, psi	ASTM C 78	NA
Split Cylinder Strength, psi	ASTM C 496	NA
Modulus of Elasticity, ksi	ASTM C 469	NA
Coefficient of Thermal Expansion, με per °F	Tex 428-A	NA

Aggregate Identification Number:	36
Source District:	San Antonio
Lithology:	Limestone

Aggregate Test:	Method	Result
Specific Gravity	Tex 403-A	2.57
Absorption, %	Tex 403-A	2.5

	Method	Result
Micro-Deval loss, %	Tex 461-A	24.5
Los Angeles Abrasion loss, %	Tex 410-A	33
Modified Aggregate Impact Value loss, %	Section 4.6	32.5
Modified Aggregate Crushing Value loss, %	Section 4.7	49.6

	Method	Result
Magnesium Sulfate Soundness loss, %	Tex 411-A	11
Uncofined Freezing and Thawing loss, %	CSA 23.2-24A	4.8

	Method	Result
Thermal Conduvity, w/(m^2 K)	Section 3.2.1.9	NA

	Method	Result
AIMS 2.0 Angularity	Section 3.2.1.8	2827
AIMS 2.0 Texture	Section 3.2.1.8	134
AIMS 2.0 Flat and Elongate % Over 4:1	Section 3.2.1.8	3
AIMS 2.0 Flat and Elongate % Over 5:1	Section 3.2.1.8	1
Direct Proportional Caliper Flat and Elongate % Over 4:1	Section 3.2.1.10	6
Direct Proportional Caliper Flat and Elongate % Over 5:1	Section 3.2.1.10	2

Concrete Test:	Method	Result
Compressive Strength, psi	ASTM C 39	NA
Flexure Beam Strength, psi	ASTM C 78	NA
Split Cylinder Strength, psi	ASTM C 496	NA
Modulus of Elasticity, ksi	ASTM C 469	NA
Coefficient of Thermal Expansion, $\mu\varepsilon$ per °F	Tex 428-A	NA

Aggregate Identification Number:	37
Source District:	Abeline
Lithology:	Limestone

Aggregate Test:	Method	Result
Specific Gravity	Tex 403-A	2.45
Absorption, %	Tex 403-A	4.7

	Method	Result
Micro-Deval loss, %	Tex 461-A	44.6
Los Angeles Abrasion loss, %	Tex 410-A	33
Modified Aggregate Impact Value loss, %	Section 4.6	31
Modified Aggregate Crushing Value loss, %	Section 4.7	46.8

	Method	Result
Magnesium Sulfate Soundness loss, %	Tex 411-A	31
Uncofined Freezing and Thawing loss, %	CSA 23.2-24A	8.1

	Method	Result
Thermal Conduvity, w/(m^2 K)	Section 3.2.1.9	NA

	Method	Result
AIMS 2.0 Angularity	Section 3.2.1.8	2562
AIMS 2.0 Texture	Section 3.2.1.8	162
AIMS 2.0 Flat and Elongate % Over 4:1	Section 3.2.1.8	3
AIMS 2.0 Flat and Elongate % Over 5:1	Section 3.2.1.8	1
Direct Proportional Caliper Flat and Elongate % Over 4:1	Section 3.2.1.10	10
Direct Proportional Caliper Flat and Elongate % Over 5:1	Section 3.2.1.10	4

Concrete Test:	Method	Result
Compressive Strength, psi	ASTM C 39	6370
Flexure Beam Strength, psi	ASTM C 78	NA
Split Cylinder Strength, psi	ASTM C 496	615
Modulus of Elasticity, ksi	ASTM C 469	5050
Coefficient of Thermal Expansion, $\mu\varepsilon$ per °F	Tex 428-A	3.69

Aggregate Identification Number:	38
Source District:	Paris
Lithology:	Limestone

Aggregate Test:	Method	Result
Specific Gravity	Tex 403-A	2.4
Absorption, %	Tex 403-A	8.4

Micro-Deval loss, %	Tex 461-A	64.4
Los Angeles Abrasion loss, %	Tex 410-A	55
Modified Aggregate Impact Value loss, %	Section 4.6	47.1
Modified Aggregate Crushing Value loss, %	Section 4.7	50.8

Magnesium Sulfate Soundness loss, %	Tex 411-A	69
Uncofined Freezing and Thawing loss, %	CSA 23.2-24A	31.9

Thermal Conduvity, w/(m^2 K)	Section 3.2.1.9	NA

AIMS 2.0 Angularity	Section 3.2.1.8	2736
AIMS 2.0 Texture	Section 3.2.1.8	173
AIMS 2.0 Flat and Elongate % Over 4:1	Section 3.2.1.8	4
AIMS 2.0 Flat and Elongate % Over 5:1	Section 3.2.1.8	2
Direct Proportional Caliper Flat and Elongate % Over 4:1	Section 3.2.1.10	17
Direct Proportional Caliper Flat and Elongate % Over 5:1	Section 3.2.1.10	10

Concrete Test:	Method	Result
Compressive Strength, psi	ASTM C 39	4240
Flexure Beam Strength, psi	ASTM C 78	NA
Split Cylinder Strength, psi	ASTM C 496	480
Modulus of Elasticity, ksi	ASTM C 469	4150
Coefficient of Thermal Expansion, με per °F	Tex 428-A	3.78

237

Aggregate Identification Number:	39
Source District:	Mexico (Houston)
Lithology:	Limestone

Aggregate Test:	Method	Result
Specific Gravity	Tex 403-A	2.43
Absorption, %	Tex 403-A	4.9

	Method	Result
Micro-Deval loss, %	Tex 461-A	21.1
Los Angeles Abrasion loss, %	Tex 410-A	29
Modified Aggregate Impact Value loss, %	Section 4.6	30.6
Modified Aggregate Crushing Value loss, %	Section 4.7	50.7

	Method	Result
Magnesium Sulfate Soundness loss, %	Tex 411-A	7
Uncofined Freezing and Thawing loss, %	CSA 23.2-24A	5.4

	Method	Result
Thermal Conduvity, w/(m^2 K)	Section 3.2.1.9	NA

	Method	Result
AIMS 2.0 Angularity	Section 3.2.1.8	2942
AIMS 2.0 Texture	Section 3.2.1.8	99
AIMS 2.0 Flat and Elongate % Over 4:1	Section 3.2.1.8	1
AIMS 2.0 Flat and Elongate % Over 5:1	Section 3.2.1.8	1
Direct Proportional Caliper Flat and Elongate % Over 4:1	Section 3.2.1.10	7
Direct Proportional Caliper Flat and Elongate % Over 5:1	Section 3.2.1.10	4

Concrete Test:	Method	Result
Compressive Strength, psi	ASTM C 39	5850
Flexure Beam Strength, psi	ASTM C 78	NA
Split Cylinder Strength, psi	ASTM C 496	630
Modulus of Elasticity, ksi	ASTM C 469	5850
Coefficient of Thermal Expansion, $\mu\varepsilon$ per °F	Tex 428-A	3.21

Aggregate Identification Number:	40
Source District:	San Antonio
Lithology:	Limestone

Aggregate Test:	Method	Result
Specific Gravity	Tex 403-A	2.6
Absorption, %	Tex 403-A	1.4

	Method	Result
Micro-Deval loss, %	Tex 461-A	24
Los Angeles Abrasion loss, %	Tex 410-A	32
Modified Aggregate Impact Value loss, %	Section 4.6	29.4
Modified Aggregate Crushing Value loss, %	Section 4.7	47.8

	Method	Result
Magnesium Sulfate Soundness loss, %	Tex 411-A	12
Uncofined Freezing and Thawing loss, %	CSA 23.2-24A	4.8

	Method	Result
Thermal Conduvity, w/(m^2 K)	Section 3.2.1.9	NA

	Method	Result
AIMS 2.0 Angularity	Section 3.2.1.8	2902
AIMS 2.0 Texture	Section 3.2.1.8	116
AIMS 2.0 Flat and Elongate % Over 4:1	Section 3.2.1.8	2
AIMS 2.0 Flat and Elongate % Over 5:1	Section 3.2.1.8	0
Direct Proportional Caliper Flat and Elongate % Over 4:1	Section 3.2.1.10	10
Direct Proportional Caliper Flat and Elongate % Over 5:1	Section 3.2.1.10	4

Concrete Test:	Method	Result
Compressive Strength, psi	ASTM C 39	6320
Flexure Beam Strength, psi	ASTM C 78	NA
Split Cylinder Strength, psi	ASTM C 496	615
Modulus of Elasticity, ksi	ASTM C 469	6500
Coefficient of Thermal Expansion, µε per °F	Tex 428-A	3.56

239

Aggregate Identification Number:	41
Source District:	Austin
Lithology:	Limestone

Aggregate Test:	Method	Result
Specific Gravity	Tex 403-A	2.61
Absorption, %	Tex 403-A	1.9

Micro-Deval loss, %	Tex 461-A	17.8
Los Angeles Abrasion loss, %	Tex 410-A	27
Modified Aggregate Impact Value loss, %	Section 4.6	14.6
Modified Aggregate Crushing Value loss, %	Section 4.7	41.9

Magnesium Sulfate Soundness loss, %	Tex 411-A	11
Uncofined Freezing and Thawing loss, %	CSA 23.2-24A	12.6

Thermal Conduvity, w/(m^2 K)	Section 3.2.1.9	NA

AIMS 2.0 Angularity	Section 3.2.1.8	2324
AIMS 2.0 Texture	Section 3.2.1.8	125
AIMS 2.0 Flat and Elongate % Over 4:1	Section 3.2.1.8	13
AIMS 2.0 Flat and Elongate % Over 5:1	Section 3.2.1.8	8
Direct Proportional Caliper Flat and Elongate % Over 4:1	Section 3.2.1.10	24
Direct Proportional Caliper Flat and Elongate % Over 5:1	Section 3.2.1.10	15

Concrete Test:	Method	Result
Compressive Strength, psi	ASTM C 39	NA
Flexure Beam Strength, psi	ASTM C 78	NA
Split Cylinder Strength, psi	ASTM C 496	NA
Modulus of Elasticity, ksi	ASTM C 469	NA
Coefficient of Thermal Expansion, με per °F	Tex 428-A	NA

Aggregate Identification Number:	42
Source District:	Austin
Lithology:	Dolomite

Aggregate Test:	Method	Result
Specific Gravity	Tex 403-A	2.79
Absorption, %	Tex 403-A	0.6

Micro-Deval loss, %	Tex 461-A	9.2
Los Angeles Abrasion loss, %	Tex 410-A	20
Modified Aggregate Impact Value loss, %	Section 4.6	21.9
Modified Aggregate Crushing Value loss, %	Section 4.7	39.4

Magnesium Sulfate Soundness loss, %	Tex 411-A	2
Uncofined Freezing and Thawing loss, %	CSA 23.2-24A	6.6

Thermal Conduvity, w/(m^2 K)	Section 3.2.1.9	NA

AIMS 2.0 Angularity	Section 3.2.1.8	2822
AIMS 2.0 Texture	Section 3.2.1.8	145
AIMS 2.0 Flat and Elongate % Over 4:1	Section 3.2.1.8	7
AIMS 2.0 Flat and Elongate % Over 5:1	Section 3.2.1.8	1
Direct Proportional Caliper Flat and Elongate % Over 4:1	Section 3.2.1.10	12
Direct Proportional Caliper Flat and Elongate % Over 5:1	Section 3.2.1.10	0

Concrete Test:	Method	Results
Compressive Strength, psi	ASTM C 39	NA
Flexure Beam Strength, psi	ASTM C 78	NA
Split Cylinder Strength, psi	ASTM C 496	NA
Modulus of Elasticity, ksi	ASTM C 469	NA
Coefficient of Thermal Expansion, με per °F	Tex 428-A	NA

Aggregate Identification Number:	43
Source District:	Austin
Lithology:	Dolomite

Aggregate Test:	Method	Result
Specific Gravity	Tex 403-A	2.8
Absorption, %	Tex 403-A	0.6
Micro-Deval loss, %	Tex 461-A	10.4
Los Angeles Abrasion loss, %	Tex 410-A	26
Modified Aggregate Impact Value loss, %	Section 4.6	26.2
Modified Aggregate Crushing Value loss, %	Section 4.7	42.3
Magnesium Sulfate Soundness loss, %	Tex 411-A	4
Uncofined Freezing and Thawing loss, %	CSA 23.2-24A	13.7
Thermal Conduvity, w/(m^2 K)	Section 3.2.1.9	NA
AIMS 2.0 Angularity	Section 3.2.1.8	2396
AIMS 2.0 Texture	Section 3.2.1.8	154
AIMS 2.0 Flat and Elongate % Over 4:1	Section 3.2.1.8	3
AIMS 2.0 Flat and Elongate % Over 5:1	Section 3.2.1.8	0
Direct Proportional Caliper Flat and Elongate % Over 4:1	Section 3.2.1.10	23
Direct Proportional Caliper Flat and Elongate % Over 5:1	Section 3.2.1.10	0

Concrete Test:	Method	Result
Compressive Strength, psi	ASTM C 39	NA
Flexure Beam Strength, psi	ASTM C 78	NA
Split Cylinder Strength, psi	ASTM C 496	NA
Modulus of Elasticity, ksi	ASTM C 469	NA
Coefficient of Thermal Expansion, με per °F	Tex 428-A	NA

Aggregate Identification Number:	44
Source District:	Paris
Lithology:	Dolomite

Aggregate Test:	Method	Result
Specific Gravity	Tex 403-A	2.8
Absorption, %	Tex 403-A	0.5

Micro-Deval loss, %	Tex 461-A	12.6
Los Angeles Abrasion loss, %	Tex 410-A	28
Modified Aggregate Impact Value loss, %	Section 4.6	24.9
Modified Aggregate Crushing Value loss, %	Section 4.7	39.4

Magnesium Sulfate Soundness loss, %	Tex 411-A	2
Uncofined Freezing and Thawing loss, %	CSA 23.2-24A	5

Thermal Conduvity, w/(m^2 K)	Section 3.2.1.9	5.79

AIMS 2.0 Angularity	Section 3.2.1.8	3089
AIMS 2.0 Texture	Section 3.2.1.8	100
AIMS 2.0 Flat and Elongate % Over 4:1	Section 3.2.1.8	4
AIMS 2.0 Flat and Elongate % Over 5:1	Section 3.2.1.8	1
Direct Proportional Caliper Flat and Elongate % Over 4:1	Section 3.2.1.10	6
Direct Proportional Caliper Flat and Elongate % Over 5:1	Section 3.2.1.10	2

Concrete Test:	Method	Result
Compressive Strength, psi	ASTM C 39	7920
Flexure Beam Strength, psi	ASTM C 78	975
Split Cylinder Strength, psi	ASTM C 496	715
Modulus of Elasticity, ksi	ASTM C 469	7750
Coefficient of Thermal Expansion, με per °F	Tex 428-A	5.19

Aggregate Identification Number:	45
Source District:	Paris
Lithology:	Dolomite

Aggregate Test:	Method	Result
Specific Gravity	Tex 403-A	2.74
Absorption, %	Tex 403-A	1.4

	Method	Result
Micro-Deval loss, %	Tex 461-A	8.4
Los Angeles Abrasion loss, %	Tex 410-A	19
Modified Aggregate Impact Value loss, %	Section 4.6	25.8
Modified Aggregate Crushing Value loss, %	Section 4.7	41.3

	Method	Result
Magnesium Sulfate Soundness loss, %	Tex 411-A	10
Uncofined Freezing and Thawing loss, %	CSA 23.2-24A	24

	Method	Result
Thermal Conduvity, w/(m^2 K)	Section 3.2.1.9	4.29

	Method	Result
AIMS 2.0 Angularity	Section 3.2.1.8	2896
AIMS 2.0 Texture	Section 3.2.1.8	455
AIMS 2.0 Flat and Elongate % Over 4:1	Section 3.2.1.8	4
AIMS 2.0 Flat and Elongate % Over 5:1	Section 3.2.1.8	2
Direct Proportional Caliper Flat and Elongate % Over 4:1	Section 3.2.1.10	25
Direct Proportional Caliper Flat and Elongate % Over 5:1	Section 3.2.1.10	16

Concrete Test:	Method	Result
Compressive Strength, psi	ASTM C 39	7530
Flexure Beam Strength, psi	ASTM C 78	945
Split Cylinder Strength, psi	ASTM C 496	690
Modulus of Elasticity, ksi	ASTM C 469	7800
Coefficient of Thermal Expansion, $\mu\varepsilon$ per °F	Tex 428-A	5

Aggregate Identification Number:	46
Source District:	El Paso
Lithology:	Dolomite

Aggregate Test:	Method	Result
Specific Gravity	Tex 403-A	2.78
Absorption, %	Tex 403-A	0.9

Micro-Deval loss, %	Tex 461-A	9.7
Los Angeles Abrasion loss, %	Tex 410-A	20
Modified Aggregate Impact Value loss, %	Section 4.6	20.9
Modified Aggregate Crushing Value loss, %	Section 4.7	36.1

Magnesium Sulfate Soundness loss, %	Tex 411-A	4
Uncofined Freezing and Thawing loss, %	CSA 23.2-24A	10.2

Thermal Conduvity, w/(m^2 K)	Section 3.2.1.9	5.75

AIMS 2.0 Angularity	Section 3.2.1.8	2896
AIMS 2.0 Texture	Section 3.2.1.8	455
AIMS 2.0 Flat and Elongate % Over 4:1	Section 3.2.1.8	6
AIMS 2.0 Flat and Elongate % Over 5:1	Section 3.2.1.8	1
Direct Proportional Caliper Flat and Elongate % Over 4:1	Section 3.2.1.10	23
Direct Proportional Caliper Flat and Elongate % Over 5:1	Section 3.2.1.10	11

Concrete Test:	Method	Result
Compressive Strength, psi	ASTM C 39	7200
Flexure Beam Strength, psi	ASTM C 78	970
Split Cylinder Strength, psi	ASTM C 496	770
Modulus of Elasticity, ksi	ASTM C 469	7900
Coefficient of Thermal Expansion, με per °F	Tex 428-A	4.98

245

Aggregate Identification Number:	47
Source District:	El Paso
Lithology:	Granite

Aggregate Test:	Method	Result
Specific Gravity	Tex 403-A	2.6
Absorption, %	Tex 403-A	1.2

Micro-Deval loss, %	Tex 461-A	25.8
Los Angeles Abrasion loss, %	Tex 410-A	54
Modified Aggregate Impact Value loss, %	Section 4.6	44.6
Modified Aggregate Crushing Value loss, %	Section 4.7	55.1

Magnesium Sulfate Soundness loss, %	Tex 411-A	46
Uncofined Freezing and Thawing loss, %	CSA 23.2-24A	23

Thermal Conduvity, w/(m^2 K)	Section 3.2.1.9	2.96

AIMS 2.0 Angularity	Section 3.2.1.8	3779
AIMS 2.0 Texture	Section 3.2.1.8	313
AIMS 2.0 Flat and Elongate % Over 4:1	Section 3.2.1.8	2
AIMS 2.0 Flat and Elongate % Over 5:1	Section 3.2.1.8	0
Direct Proportional Caliper Flat and Elongate % Over 4:1	Section 3.2.1.10	6
Direct Proportional Caliper Flat and Elongate % Over 5:1	Section 3.2.1.10	2

Concrete Test:	Method	Result
Compressive Strength, psi	ASTM C 39	6230
Flexure Beam Strength, psi	ASTM C 78	665
Split Cylinder Strength, psi	ASTM C 496	575
Modulus of Elasticity, ksi	ASTM C 469	4350
Coefficient of Thermal Expansion, με per °F	Tex 428-A	4.67

Aggregate Identification Number:	48
Source District:	Paris
Lithology:	Granite

Aggregate Test:	Method	Result
Specific Gravity	Tex 403-A	2.67
Absorption, %	Tex 403-A	0.4

Micro-Deval loss, %	Tex 461-A	6
Los Angeles Abrasion loss, %	Tex 410-A	32
Modified Aggregate Impact Value loss, %	Section 4.6	31.5
Modified Aggregate Crushing Value loss, %	Section 4.7	45.2

Magnesium Sulfate Soundness loss, %	Tex 411-A	1
Uncofined Freezing and Thawing loss, %	CSA 23.2-24A	10.2

Thermal Conduvity, w/(m^2 K)	Section 3.2.1.9	NA

AIMS 2.0 Angularity	Section 3.2.1.8	3259
AIMS 2.0 Texture	Section 3.2.1.8	272
AIMS 2.0 Flat and Elongate % Over 4:1	Section 3.2.1.8	7
AIMS 2.0 Flat and Elongate % Over 5:1	Section 3.2.1.8	2
Direct Proportional Caliper Flat and Elongate % Over 4:1	Section 3.2.1.10	30
Direct Proportional Caliper Flat and Elongate % Over 5:1	Section 3.2.1.10	15

Concrete Test:	Method	Result
Compressive Strength, psi	ASTM C 39	NA
Flexure Beam Strength, psi	ASTM C 78	NA
Split Cylinder Strength, psi	ASTM C 496	NA
Modulus of Elasticity, ksi	ASTM C 469	NA
Coefficient of Thermal Expansion, με per °F	Tex 428-A	NA

Aggregate Identification Number:	49
Source District:	Childress
Lithology:	Granite

Aggregate Test:	Method	Result
Specific Gravity	Tex 403-A	2.63
Absorption, %	Tex 403-A	0.7

Micro-Deval loss, %	Tex 461-A	3.6
Los Angeles Abrasion loss, %	Tex 410-A	21
Modified Aggregate Impact Value loss, %	Section 4.6	22.2
Modified Aggregate Crushing Value loss, %	Section 4.7	38

Magnesium Sulfate Soundness loss, %	Tex 411-A	1
Uncofined Freezing and Thawing loss, %	CSA 23.2-24A	8.8

Thermal Conduvity, w/(m^2 K)	Section 3.2.1.9	NA

AIMS 2.0 Angularity	Section 3.2.1.8	3106
AIMS 2.0 Texture	Section 3.2.1.8	440
AIMS 2.0 Flat and Elongate % Over 4:1	Section 3.2.1.8	7
AIMS 2.0 Flat and Elongate % Over 5:1	Section 3.2.1.8	0
Direct Proportional Caliper Flat and Elongate % Over 4:1	Section 3.2.1.10	17
Direct Proportional Caliper Flat and Elongate % Over 5:1	Section 3.2.1.10	10

Concrete Test:	Method	Result
Compressive Strength, psi	ASTM C 39	NA
Flexure Beam Strength, psi	ASTM C 78	NA
Split Cylinder Strength, psi	ASTM C 496	NA
Modulus of Elasticity, ksi	ASTM C 469	NA
Coefficient of Thermal Expansion, με per °F	Tex 428-A	NA

Aggregate Identification Number:	50
Source District:	Austin
Lithology:	Sand Stone

Aggregate Test:	Method	Result
Specific Gravity	Tex 403-A	2.6
Absorption, %	Tex 403-A	1.3

Micro-Deval loss, %	Tex 461-A	12.7
Los Angeles Abrasion loss, %	Tex 410-A	17
Modified Aggregate Impact Value loss, %	Section 4.6	14.7
Modified Aggregate Crushing Value loss, %	Section 4.7	33.2

Magnesium Sulfate Soundness loss, %	Tex 411-A	6
Uncofined Freezing and Thawing loss, %	CSA 23.2-24A	6.1

Thermal Conduvity, w/(m^2 K)	Section 3.2.1.9	NA

AIMS 2.0 Angularity	Section 3.2.1.8	2501
AIMS 2.0 Texture	Section 3.2.1.8	287
AIMS 2.0 Flat and Elongate % Over 4:1	Section 3.2.1.8	6
AIMS 2.0 Flat and Elongate % Over 5:1	Section 3.2.1.8	2
Direct Proportional Caliper Flat and Elongate % Over 4:1	Section 3.2.1.10	16
Direct Proportional Caliper Flat and Elongate % Over 5:1	Section 3.2.1.10	0

Concrete Test:	Method	Result
Compressive Strength, psi	ASTM C 39	NA
Flexure Beam Strength, psi	ASTM C 78	NA
Split Cylinder Strength, psi	ASTM C 496	NA
Modulus of Elasticity, ksi	ASTM C 469	NA
Coefficient of Thermal Expansion, με per °F	Tex 428-A	NA

Aggregate Identification Number:	51
Source District:	Paris
Lithology:	Sand Stone

Aggregate Test:	Method	Result
Specific Gravity	Tex 403-A	2.53
Absorption, %	Tex 403-A	2.2

Micro-Deval loss, %	Tex 461-A	9.6
Los Angeles Abrasion loss, %	Tex 410-A	28
Modified Aggregate Impact Value loss, %	Section 4.6	24.7
Modified Aggregate Crushing Value loss, %	Section 4.7	37.2

Magnesium Sulfate Soundness loss, %	Tex 411-A	3
Uncofined Freezing and Thawing loss, %	CSA 23.2-24A	3.2

Thermal Conduvity, w/(m^2 K)	Section 3.2.1.9	5.66

AIMS 2.0 Angularity	Section 3.2.1.8	2521
AIMS 2.0 Texture	Section 3.2.1.8	142
AIMS 2.0 Flat and Elongate % Over 4:1	Section 3.2.1.8	6
AIMS 2.0 Flat and Elongate % Over 5:1	Section 3.2.1.8	3
Direct Proportional Caliper Flat and Elongate % Over 4:1	Section 3.2.1.10	16
Direct Proportional Caliper Flat and Elongate % Over 5:1	Section 3.2.1.10	11

Concrete Test:	Method	Result
Compressive Strength, psi	ASTM C 39	7620
Flexure Beam Strength, psi	ASTM C 78	820
Split Cylinder Strength, psi	ASTM C 496	700
Modulus of Elasticity, ksi	ASTM C 469	5650
Coefficient of Thermal Expansion, με per °F	Tex 428-A	5.84

Aggregate Identification Number:	52
Source District:	Paris
Lithology:	Sand Stone

Aggregate Test:	Method	Result
Specific Gravity	Tex 403-A	2.55
Absorption, %	Tex 403-A	2.7

Micro-Deval loss, %	Tex 461-A	13.5
Los Angeles Abrasion loss, %	Tex 410-A	35
Modified Aggregate Impact Value loss, %	Section 4.6	31.7
Modified Aggregate Crushing Value loss, %	Section 4.7	40.3

Magnesium Sulfate Soundness loss, %	Tex 411-A	17
Uncofined Freezing and Thawing loss, %	CSA 23.2-24A	12.9

Thermal Conduvity, w/(m^2 K)	Section 3.2.1.9	NA

AIMS 2.0 Angularity	Section 3.2.1.8	2857
AIMS 2.0 Texture	Section 3.2.1.8	175
AIMS 2.0 Flat and Elongate % Over 4:1	Section 3.2.1.8	19
AIMS 2.0 Flat and Elongate % Over 5:1	Section 3.2.1.8	4
Direct Proportional Caliper Flat and Elongate % Over 4:1	Section 3.2.1.10	32
Direct Proportional Caliper Flat and Elongate % Over 5:1	Section 3.2.1.10	23

Concrete Test:	Method	Result
Compressive Strength, psi	ASTM C 39	6090
Flexure Beam Strength, psi	ASTM C 78	NA
Split Cylinder Strength, psi	ASTM C 496	685
Modulus of Elasticity, ksi	ASTM C 469	4850
Coefficient of Thermal Expansion, $\mu\varepsilon$ per °F	Tex 428-A	5.35

Aggregate Identification Number:	53
Source District:	Paris
Lithology:	Sand Stone

Aggregate Test:	Method	Result
Specific Gravity	Tex 403-A	2.53
Absorption, %	Tex 403-A	2.2

	Method	Result
Micro-Deval loss, %	Tex 461-A	10.3
Los Angeles Abrasion loss, %	Tex 410-A	26
Modified Aggregate Impact Value loss, %	Section 4.6	22.1
Modified Aggregate Crushing Value loss, %	Section 4.7	37

	Method	Result
Magnesium Sulfate Soundness loss, %	Tex 411-A	11
Uncofined Freezing and Thawing loss, %	CSA 23.2-24A	17.8

	Method	Result
Thermal Conduvity, w/(m^2 K)	Section 3.2.1.9	NA

	Method	Result
AIMS 2.0 Angularity	Section 3.2.1.8	2950
AIMS 2.0 Texture	Section 3.2.1.8	110
AIMS 2.0 Flat and Elongate % Over 4:1	Section 3.2.1.8	NA
AIMS 2.0 Flat and Elongate % Over 5:1	Section 3.2.1.8	NA
Direct Proportional Caliper Flat and Elongate % Over 4:1	Section 3.2.1.10	NA
Direct Proportional Caliper Flat and Elongate % Over 5:1	Section 3.2.1.10	NA

Concrete Test:	Method	Result
Compressive Strength, psi	ASTM C 39	NA
Flexure Beam Strength, psi	ASTM C 78	NA
Split Cylinder Strength, psi	ASTM C 496	NA
Modulus of Elasticity, ksi	ASTM C 469	NA
Coefficient of Thermal Expansion, με per °F	Tex 428-A	NA

Aggregate Identification Number:	54
Source District:	San Antonio
Lithology:	Trapp Rock

Aggregate Test:	Method	Result
Specific Gravity	Tex 403-A	3.08
Absorption, %	Tex 403-A	0.6
Micro-Deval loss, %	Tex 461-A	14.8
Los Angeles Abrasion loss, %	Tex 410-A	9
Modified Aggregate Impact Value loss, %	Section 4.6	7.8
Modified Aggregate Crushing Value loss, %	Section 4.7	19.3
Magnesium Sulfate Soundness loss, %	Tex 411-A	5
Uncofined Freezing and Thawing loss, %	CSA 23.2-24A	7.6
Thermal Conduvity, w/(m^2 K)	Section 3.2.1.9	3.14
AIMS 2.0 Angularity	Section 3.2.1.8	2950
AIMS 2.0 Texture	Section 3.2.1.8	110
AIMS 2.0 Flat and Elongate % Over 4:1	Section 3.2.1.8	7
AIMS 2.0 Flat and Elongate % Over 5:1	Section 3.2.1.8	2
Direct Proportional Caliper Flat and Elongate % Over 4:1	Section 3.2.1.10	17
Direct Proportional Caliper Flat and Elongate % Over 5:1	Section 3.2.1.10	10

Concrete Test:	Method	Result
Compressive Strength, psi	ASTM C 39	6980
Flexure Beam Strength, psi	ASTM C 78	925
Split Cylinder Strength, psi	ASTM C 496	745
Modulus of Elasticity, ksi	ASTM C 469	7500
Coefficient of Thermal Expansion, με per °F	Tex 428-A	5.35

Aggregate Identification Number:	55
Source District:	San Antonio
Lithology:	Trapp Rock

Aggregate Test:	Method	Result
Specific Gravity	Tex 403-A	3.08
Absorption, %	Tex 403-A	0.8
Micro-Deval loss, %	Tex 461-A	9.3
Los Angeles Abrasion loss, %	Tex 410-A	8
Modified Aggregate Impact Value loss, %	Section 4.6	10.5
Modified Aggregate Crushing Value loss, %	Section 4.7	26.6
Magnesium Sulfate Soundness loss, %	Tex 411-A	2
Uncofined Freezing and Thawing loss, %	CSA 23.2-24A	5.5
Thermal Conduvity, w/(m^2 K)	Section 3.2.1.9	NA
AIMS 2.0 Angularity	Section 3.2.1.8	2826
AIMS 2.0 Texture	Section 3.2.1.8	106
AIMS 2.0 Flat and Elongate % Over 4:1	Section 3.2.1.8	4
AIMS 2.0 Flat and Elongate % Over 5:1	Section 3.2.1.8	1
Direct Proportional Caliper Flat and Elongate % Over 4:1	Section 3.2.1.10	27
Direct Proportional Caliper Flat and Elongate % Over 5:1	Section 3.2.1.10	14

Concrete Test:	Method	Result
Compressive Strength, psi	ASTM C 39	7490
Flexure Beam Strength, psi	ASTM C 78	990
Split Cylinder Strength, psi	ASTM C 496	790
Modulus of Elasticity, ksi	ASTM C 469	8100
Coefficient of Thermal Expansion, $\mu\varepsilon$ per °F	Tex 428-A	4.92

Aggregate Identification Number:	56
Source District:	Rhyolite
Lithology:	Wichita Falls

Aggregate Test:	Method	Result
Specific Gravity	Tex 403-A	2.68
Absorption, %	Tex 403-A	0.9

Micro-Deval loss, %	Tex 461-A	4.8
Los Angeles Abrasion loss, %	Tex 410-A	11
Modified Aggregate Impact Value loss, %	Section 4.6	11.5
Modified Aggregate Crushing Value loss, %	Section 4.7	28

Magnesium Sulfate Soundness loss, %	Tex 411-A	1
Uncofined Freezing and Thawing loss, %	CSA 23.2-24A	2.9

Thermal Conduvity, w/(m^2 K)	Section 3.2.1.9	NA

AIMS 2.0 Angularity	Section 3.2.1.8	3071
AIMS 2.0 Texture	Section 3.2.1.8	79
AIMS 2.0 Flat and Elongate % Over 4:1	Section 3.2.1.8	NA
AIMS 2.0 Flat and Elongate % Over 5:1	Section 3.2.1.8	NA
Direct Proportional Caliper Flat and Elongate % Over 4:1	Section 3.2.1.10	NA
Direct Proportional Caliper Flat and Elongate % Over 5:1	Section 3.2.1.10	NA

Concrete Test:	Method	Result
Compressive Strength, psi	ASTM C 39	NA
Flexure Beam Strength, psi	ASTM C 78	NA
Split Cylinder Strength, psi	ASTM C 496	NA
Modulus of Elasticity, ksi	ASTM C 469	NA
Coefficient of Thermal Expansion, με per °F	Tex 428-A	NA

Aggregate Identification Number:	57
Source District:	Rhyolite
Lithology:	Odessa

Aggregate Test:	Method	Result
Specific Gravity	Tex 403-A	2.51
Absorption, %	Tex 403-A	2.7

	Method	Result
Micro-Deval loss, %	Tex 461-A	7.4
Los Angeles Abrasion loss, %	Tex 410-A	17
Modified Aggregate Impact Value loss, %	Section 4.6	20.1
Modified Aggregate Crushing Value loss, %	Section 4.7	33.5

	Method	Result
Magnesium Sulfate Soundness loss, %	Tex 411-A	4
Uncofined Freezing and Thawing loss, %	CSA 23.2-24A	11

	Method	Result
Thermal Conduvity, w/(m^2 K)	Section 3.2.1.9	NA

	Method	Result
AIMS 2.0 Angularity	Section 3.2.1.8	2935
AIMS 2.0 Texture	Section 3.2.1.8	170
AIMS 2.0 Flat and Elongate % Over 4:1	Section 3.2.1.8	6
AIMS 2.0 Flat and Elongate % Over 5:1	Section 3.2.1.8	2
Direct Proportional Caliper Flat and Elongate % Over 4:1	Section 3.2.1.10	10
Direct Proportional Caliper Flat and Elongate % Over 5:1	Section 3.2.1.10	5

Concrete Test:	Method	Result
Compressive Strength, psi	ASTM C 39	6720
Flexure Beam Strength, psi	ASTM C 78	NA
Split Cylinder Strength, psi	ASTM C 496	670
Modulus of Elasticity, ksi	ASTM C 469	5450
Coefficient of Thermal Expansion, $\mu\varepsilon$ per °F	Tex 428-A	4.19

Aggregate Identification Number:		58
Source District:		Slate
Lithology:		Paris

Aggregate Test:	Method	Result
Specific Gravity	Tex 403-A	2.57
Absorption, %	Tex 403-A	1.2

Micro-Deval loss, %	Tex 461-A	8.4
Los Angeles Abrasion loss, %	Tex 410-A	17
Modified Aggregate Impact Value loss, %	Section 4.6	21.6
Modified Aggregate Crushing Value loss, %	Section 4.7	37

Magnesium Sulfate Soundness loss, %	Tex 411-A	1
Uncofined Freezing and Thawing loss, %	CSA 23.2-24A	12.1

Thermal Conduvity, w/(m^2 K)	Section 3.2.1.9	NA

AIMS 2.0 Angularity	Section 3.2.1.8	3098
AIMS 2.0 Texture	Section 3.2.1.8	121
AIMS 2.0 Flat and Elongate % Over 4:1	Section 3.2.1.8	NA
AIMS 2.0 Flat and Elongate % Over 5:1	Section 3.2.1.8	NA
Direct Proportional Caliper Flat and Elongate % Over 4:1	Section 3.2.1.10	NA
Direct Proportional Caliper Flat and Elongate % Over 5:1	Section 3.2.1.10	NA

Concrete Test:	Method	Result
Compressive Strength, psi	ASTM C 39	NA
Flexure Beam Strength, psi	ASTM C 78	NA
Split Cylinder Strength, psi	ASTM C 496	NA
Modulus of Elasticity, ksi	ASTM C 469	NA
Coefficient of Thermal Expansion, $\mu\varepsilon$ per °F	Tex 428-A	NA

Appendix C: Fine Aggregate Property Sheets

Table C.1: Physical Properties of Fine Aggregates

Designation	AIR %	SG	ABS %
FLS-1	4	2.56	2.4
FLS-2	4	2.54	3.3
FLS-3	4	2.41	7.2
FLS-4	4	2.58	2.1
FLS-5	1	2.63	1
FLS-6	4	2.58	2.1
FLS-7	5	2.6	2.2
FLS-8	8	2.64	1.8
FLRG-1	87	2.64	0.7
FLRG-2	79	2.62	1
FLRG-3	84	2.64	0.7
FLRG-4	76	2.62	1.7
FLRG-5	80	2.61	2.1
FRG-1	88	2.61	0.8
FRG-2	100	2.57	1.1
FRG-3	88	2.62	0.6
FDOL-1	4	2.8	0.5
FDOL-2	12	2.74	1.4
FDOL-3	21	2.81	0.5
FCRG-1	99	2.63	0.4
FCRG-1	92	2.63	0.6
FTR-1	83	3.08	0.6
FTR-2	89	3.08	0.8
FGR	96	2.67	0.4
FSS	63	2.62	0.8

Table C.2: Sand Equivalent Test Results

Designation	Sand Equivalents %
FLS-1	91
FLS-2	95
FLS-3	81
FLS-4	90
FLS-5	78
FLS-6	95
FLS-7	86
FLS-8	89
FLRG-1	98
FLRG-2	96
FLRG-3	97
FLRG-4	98
FLRG-5	98
FRG-1	100
FRG-2	100
FRG-3	100
FDOL-1	89
FDOL-2	98
FDOL-3	96
FCRG-1	100
FCRG-1	91
FTR-1	66
FTR-2	98
FGR	92
FSS	82

Table C.3: Blue Methylene Test Results

Designation	Blue Methylene %
FLS-1	0.32
FLS-2	0.22
FLS-3	0.76
FLS-4	0.29
FLS-5	0.37
FLS-6	0.12
FLS-7	0.46
FLS-8	0.5
FLRG-1	0.27
FLRG-2	0.38
FLRG-3	0.44
FLRG-4	0.31
FLRG-5	0.33
FRG-1	0.35
FRG-2	0.12
FRG-3	0.18
FDOL-1	0.1
FDOL-2	0.18
FDOL-3	0.13
FCRG-1	0.22
FCRG-1	0.44
FTR-1	1.09
FTR-2	0.17
FGR	0.23
FSS	0.24

Table C.4: Micro-Deval Test Results

Designation	Micro-Deval Loss %
FLS-1	27.4
FLS-2	26.3
FLS-3	46.4
FLS-4	25.4
FLS-5	27.8
FLS-6	26.7
FLS-7	36.1
FLS-8	27.7
FLRG-1	9.1
FLRG-2	7.6
FLRG-3	6.5
FLRG-4	8.9
FLRG-5	7.6
FRG-1	9.3
FRG-2	5.8
FRG-3	8.7
FDOL-1	12.2
FDOL-2	11
FDOL-3	8.3
FCRG-1	6.4
FCRG-1	9.4
FTR-1	16.7
FTR-2	11.8
FGR	8.6
FSS	21.8

Table C.5: Flakiness Test Results

Designation	No. 8	No. 16
FLS-1	13.6%	16.6%
FLS-2	24.7%	26.0%
FLS-3	34.5%	27.2%
FLS-4	24.5%	17.8%
FLS-5	29.2%	32.2%
FLS-6	31.0%	29.3%
FLS-7	27.8%	35.9%
FLS-8	21.8%	32.0%
FLRG-1	16.8%	25.0%
FLRG-2	17.7%	25.2%
FLRG-3	19.0%	18.5%
FLRG-4	29.8%	34.3%
FLRG-5	12.7%	24.8%
FRG-1	8.0%	21.5%
FRG-2	8.5%	9.5%
FRG-3	6.5%	12.1%
FDOL-1	21.8%	28.0%
FDOL-2	47.0%	37.8%
FDOL-3	15.2%	22.2%
FCRG-1	10.8%	13.3%
FCRG-1	6.2%	20.3%
FTR-1	21.5%	32.3%
FTR-2	62.8%	53.1%
FGR	29.2%	65.2%
FSS	14.4%	24.1%

Table C.6: Camsizer Sphericity Results

Designation	No. 8	No. 16	No. 30	No. 50	No. 100	No. 200	Average
FLS-1	0.81	0.85	0.87	0.72	0.76	0.84	0.81
FLS-2	0.80	0.84	0.87	0.74	0.78	0.84	0.81
FLS-3	0.82	0.87	0.88	0.74	0.78	0.84	0.82
FLS-4	0.81	0.84	0.87	0.74	0.77	0.84	0.81
FLS-5	0.78	0.84	0.86	0.67	0.74	0.83	0.79
FLS-6	0.84	0.86	0.88	0.73	0.77	0.84	0.82
FLS-7	0.81	0.85	0.88	0.77	0.79	0.85	0.83
FLS-8	0.80	0.85	0.87	0.73	0.77	0.83	0.81
FLRG-1	0.86	0.87	0.90	0.82	0.84	0.87	0.86
FLRG-2	0.86	0.89	0.85	0.74	0.78	0.84	0.83
FLRG-3	0.85	0.88	0.91	0.82	0.84	0.87	0.86
FLRG-4	0.87	0.87	0.89	0.82	0.84	0.86	0.86
FLRG-5	0.84	0.87	0.90	0.81	0.83	0.87	0.85
FRG-1	0.85	0.87	0.89	0.71	0.75	0.84	0.82
FRG-2	0.88	0.88	0.90	0.81	0.83	0.86	0.86
FRG-3	0.86	0.87	0.89	0.80	0.83	0.86	0.85
FDOL-1	0.79	0.85	0.87	0.71	0.75	0.83	0.80
FDOL-2	0.79	0.83	0.85	0.75	0.79	0.83	0.81
FDOL-3	0.79	0.84	0.85	0.74	0.78	0.84	0.81
FCRG-1	0.88	0.88	0.90	0.81	0.82	0.85	0.86
FCRG-1	0.83	0.87	0.90	0.81	0.83	0.87	0.85
FTR-1	0.79	0.84	0.88	0.74	0.76	0.83	0.81
FTR-2	0.81	0.82	0.84	0.76	0.80	0.84	0.81
FGR	0.78	0.83	0.85	0.72	0.75	0.81	0.79
FSS	0.81	0.84	0.87	0.71	0.70	0.81	0.79

Table C.7: Camsizer Symmetry Results

Designation	No. 8	No. 16	No. 30	No. 50	No. 100	No. 200	Average
FLS-1	0.87	0.88	0.87	0.84	0.83	0.86	0.86
FLS-2	0.87	0.88	0.87	0.86	0.85	0.86	0.86
FLS-3	0.88	0.89	0.87	0.85	0.85	0.86	0.87
FLS-4	0.87	0.88	0.87	0.86	0.86	0.85	0.86
FLS-5	0.87	0.88	0.86	0.84	0.84	0.84	0.86
FLS-6	0.88	0.88	0.87	0.84	0.84	0.86	0.86
FLS-7	0.88	0.88	0.87	0.87	0.86	0.86	0.87
FLS-8	0.87	0.88	0.87	0.85	0.85	0.85	0.86
FLRG-1	0.90	0.89	0.88	0.89	0.89	0.87	0.88
FLRG-2	0.87	0.87	0.86	0.86	0.86	0.86	0.86
FLRG-3	0.90	0.89	0.88	0.89	0.88	0.87	0.88
FLRG-4	0.90	0.89	0.88	0.89	0.88	0.87	0.88
FLRG-5	0.90	0.89	0.88	0.89	0.88	0.87	0.88
FRG-1	0.90	0.88	0.87	0.89	0.88	0.86	0.88
FRG-2	0.90	0.89	0.88	0.89	0.89	0.87	0.88
FRG-3	0.90	0.89	0.88	0.88	0.88	0.87	0.88
FDOL-1	0.87	0.88	0.87	0.84	0.83	0.85	0.86
FDOL-2	0.86	0.87	0.86	0.86	0.86	0.86	0.86
FDOL-3	0.87	0.87	0.86	0.86	0.86	0.86	0.86
FCRG-1	0.89	0.89	0.88	0.89	0.89	0.87	0.88
FCRG-1	0.90	0.88	0.87	0.89	0.88	0.87	0.88
FTR-1	0.87	0.88	0.87	0.86	0.84	0.85	0.86
FTR-2	0.87	0.87	0.86	0.87	0.87	0.86	0.86
FGR	0.87	0.87	0.86	0.86	0.85	0.85	0.86
FSS	0.87	0.88	0.87	0.85	0.81	0.84	0.85

Table C.8: Uncompacted Void Content Test Results

Designation	Method A	Method B	Method C
FLS-1	48.52	53.26	42.77
FLS-2	43.11	48.22	38.58
FLS-3	48.38	53.07	46.18
FLS-4	46.47	51.60	42.91
FLS-5	48.37	52.95	41.79
FLS-6	44.96	50.05	41.32
FLS-7	44.85	48.64	42.77
FLS-8	45.38	50.15	40.72
FLRG-1	39.85	45.11	38.22
FLRG-2	38.24	43.82	35.65
FLRG-3	38.71	43.28	37.77
FLRG-4	39.81	45.19	36.18
FLRG-5	37.85	43.81	35.17
FRG-1	41.00	44.61	39.92
FRG-2	39.69	43.15	36.85
FRG-3	41.22	45.06	39.50
FDOL-1	45.68	50.43	38.18
FDOL-2	47.66	52.27	44.53
FDOL-3	46.80	51.68	41.35
FCRG-1	41.06	44.14	39.54
FCRG-1	41.98	45.42	43.99
FTR-1	51.95	55.70	45.71
FTR-2	48.83	53.58	46.40
FGR	47.49	51.35	43.63
FSS	46.95	51.46	40.08

Table C.9: Mortar Flow Test Results of Fine Aggregates

Designation	As-received Grading	Standard Grading
FLS-1	60	50
FLS-2	117	122
FLS-3	76	98
FLS-4	85	98
FLS-5	113	121
FLS-6	78	108
FLS-7	68	102
FLS-8	128	104
FLRG-1	151	150
FLRG-2	128	160
FLRG-3	138	160
FLRG-4	142	152
FLRG-5	134	160
FRG-1	142	160
FRG-2	148	160
FRG-3	131	160
FDOL-1	145	142
FDOL-2	104	133
FDOL-3	134	138
FCRG-1	149	150
FCRG-1	108	140
FTR-1	55	128
FTR-2	114	148
FGR	113	130
FSS	86	84

Table C.10: Compressive strength Results of Fine Aggregates

Designation	As-received Grading (psi)	Standard Grading (psi)
FLS-1	6899	6566
FLS-2	6218	6779
FLS-3	1605	2223
FLS-4	6813	6546
FLS-5	6490	6487
FLS-6	5201	6236
FLS-7	6634	7281
FLS-8	6715	6705
FLRG-1	4768	6254
FLRG-2	6444	6297
FLRG-3	5458	6032
FLRG-4	5565	5721
FLRG-5	5943	5853
FRG-1	5123	5313
FRG-2	5123	6963
FRG-3	6367	6366
FDOL-1	5909	7155
FDOL-2	6243	7343
FDOL-3	6596	6496
FCRG-1	6078	6970
FCRG-1	5246	4328
FTR-1	6915	7778
FTR-2	7128	5950
FGR	6668	5869
FSS	8035	7858

Table C.11: Form 2-D Results (Before Micro-Deval)

Designation	No. 8	No. 16	No. 30	No. 50	No. 100	No. 200	Average
FLS-1	7.25	7.23	7.09	6.90	6.13	8.32	7.25
FLS-2	7.54	7.87	7.24	7.04	6.77	7.36	7.54
FLS-3	7.25	6.98	6.52	6.27	5.73	7.54	7.25
FLS-4	7.33	7.60	7.15	6.36	6.84	7.66	7.33
FLS-5	7.08	7.71	7.09	6.79	6.41	7.89	7.08
FLS-6	6.65	7.54	6.69	6.81	6.35	7.68	6.65
FLS-7	7.26	7.72	7.20	6.63	6.01	7.44	7.26
FLS-8	7.32	7.86	7.66	7.50	6.02	7.60	7.32
FLRG-1	6.43	6.55	6.15	6.14	5.99	7.62	6.43
FLRG-2	6.14	6.24	5.45	5.43	5.95	7.46	6.14
FLRG-3	6.43	6.46	6.02	5.72	6.51	7.87	6.43
FLRG-4	6.38	6.39	6.72	6.61	6.19	7.51	6.38
FLRG-5	6.16	6.40	5.90	5.95	6.31	8.00	6.16
FRG-1	6.53	6.50	6.45	6.21	6.54	7.79	6.53
FRG-2	5.80	6.96	6.70	5.70	5.94	7.88	5.80
FRG-3	6.25	6.51	6.24	6.22	6.26	8.41	6.25
FDOL-1	7.40	7.51	7.27	6.47	6.39	7.81	7.40
FDOL-2	7.39	8.05	8.00	7.58	6.63	7.67	7.39
FDOL-3	7.50	7.76	7.48	7.29	7.15	8.83	7.50
FCRG-1	5.95	6.18	6.02	6.17	6.56	8.28	5.95
FCRG-1	7.02	6.98	6.24	6.03	6.39	7.17	7.02
FTR-1	-	-	-	-	-	-	-
FTR-2	-	-	-	-	-	-	-
FGR	8.17	8.30	8.32	8.70	8.28	8.28	8.17
FSS	7.85	8.24	8.18	7.30	7.08	7.87	7.85

Table C.12: Form 2-D Results (After Micro-Deval)

Designation	No. 8	No. 16	No. 30	No. 50	No. 100	No. 200	Average
LS-1	7.25	7.23	7.09	6.90	6.13	8.32	7.25
LS-2	7.54	7.87	7.24	7.04	6.77	7.36	7.54
LS-3	7.25	6.98	6.52	6.27	5.73	7.54	7.25
LS-4	7.33	7.60	7.15	6.36	6.84	7.66	7.33
LS-5	7.08	7.71	7.09	6.79	6.41	7.89	7.08
LS-6	6.65	7.54	6.69	6.81	6.35	7.68	6.65
LS-7	7.26	7.72	7.20	6.63	6.01	7.44	7.26
LS-8	7.32	7.86	7.66	7.50	6.02	7.60	7.32
LRG-1	6.43	6.55	6.15	6.14	5.99	7.62	6.43
LRG-2	6.14	6.24	5.45	5.43	5.95	7.46	6.14
LRG-3	6.43	6.46	6.02	5.72	6.51	7.87	6.43
LRG-4	6.38	6.39	6.72	6.61	6.19	7.51	6.38
LRG-5	6.16	6.40	5.90	5.95	6.31	8.00	6.16
RG-1	6.53	6.50	6.45	6.21	6.54	7.79	6.53
RG-2	5.80	6.96	6.70	5.70	5.94	7.88	5.80
RG-3	6.25	6.51	6.24	6.22	6.26	8.41	6.25
DOL-1	7.40	7.51	7.27	6.47	6.39	7.81	7.40
DOL-2	7.39	8.05	8.00	7.58	6.63	7.67	7.39
DOL-3	7.50	7.76	7.48	7.29	7.15	8.83	7.50
CRG-1	5.95	6.18	6.02	6.17	6.56	8.28	5.95
CRG-1	7.02	6.98	6.24	6.03	6.39	7.17	7.02
TR-1	-	-	-	-	-	-	-
TR-2	-	-	-	-	-	-	-
GR	8.17	8.30	8.32	8.70	8.28	8.28	8.17
SS	7.85	8.24	8.18	7.30	7.08	7.87	7.85

270

Table C.13: Angularity Results (Before Micro-Deval)

Designation	No. 8	No. 16	No. 30	No. 50	No. 100	No. 200	Average
FLS-1	3245.8	3229.2	3243.6	3094.7	1916.9	1745.4	2745.9
FLS-2	3206.9	3595.9	3426.5	3253.5	2355.5	1495.7	2889.0
FLS-3	3241.8	3036.3	3113.9	2748.7	1948.2	1359.5	2574.7
FLS-4	3234.4	3360.0	3089.2	2745.9	2240.8	1379.4	2675.0
FLS-5	3453.5	3414.3	3320.5	2950.5	2218.1	1588.0	2824.2
FLS-6	2941.7	3060.0	2966.0	2503.1	1871.5	1500.5	2473.8
FLS-7	3184.6	3276.2	2969.9	2394.1	1833.7	1504.2	2527.1
FLS-8	3657.9	3600.6	3386.1	3394.0	1605.4	1493.0	2856.1
FLRG-1	2461.0	2747.2	2308.5	2260.8	1894.7	1587.5	2210.0
FLRG-2	4008.3	4370.1	2279.6	2859.4	1768.3	1455.0	2790.1
FLRG-3	2348.1	2429.9	2393.4	2205.0	2315.3	1792.4	2247.4
FLRG-4	2534.1	2646.1	2854.2	2604.3	2034.8	1686.3	2393.3
FLRG-5	2137.1	2448.8	2384.6	2100.6	1980.6	1661.7	2118.9
FRG-1	2670.6	2976.7	2886.9	2602.8	2410.8	1841.4	2564.9
FRG-2	2724.1	2836.5	2634.0	2189.3	1989.5	1747.6	2353.5
FRG-3	2762.1	2943.6	2770.3	2476.6	2159.5	2009.2	2520.2
FDOL-1	3357.7	3378.1	3353.1	2769.1	2273.1	1601.2	2788.7
FDOL-2	3251.6	3374.9	3286.5	2915.6	2138.7	1664.1	2771.9
FDOL-3	3799.4	3702.8	3580.5	3132.9	2404.0	2032.5	3108.7
FCRG-1	2773.0	2734.3	2626.4	2612.3	2336.7	2059.5	2523.7
FCRG-1	3090.1	3320.1	2443.1	2286.3	2075.3	1455.7	2445.1
FTR-1	-	-	-	-	-	-	-
FTR-2	-	-	-	-	-	-	-
FGR	4138.4	3933.9	3533.8	3322.2	2730.2	2169.2	3304.6
FSS	3598.3	3764.4	3874.2	3677.1	2769.0	1776.9	3243.3

Table C.14: Angularity Results (After Micro-Deval)

Designation	No. 8	No. 16	No. 30	No. 50	No. 100	No. 200	Average
FLS-1	2969.8	2987.3	3013.9	2601.9	1978.6	1660.9	2535.4
FLS-2	2816.4	2968.8	2931.5	2329.3	2142.7	1456.0	2440.8
FLS-3	2821.2	3256.5	2825.3	2584.5	2068.4	1394.3	2491.7
FLS-4	3076.3	3017.1	2884.4	2431.8	1880.7	1412.2	2450.4
FLS-5	3063.2	3072.6	2925.6	2538.2	2088.4	1532.1	2536.7
FLS-6	2804.5	2813.8	2726.7	2260.2	1950.4	1456.3	2335.3
FLS-7	3189.3	2982.3	2865.7	2558.6	1872.6	1604.9	2512.2
FLS-8	3645.9	3565.6	3027.0	2717.2	2286.6	1853.8	2849.3
FLRG-1	2381.1	2402.2	2375.0	2330.0	2226.4	1825.3	2256.7
FLRG-2	2337.5	2243.4	2279.6	2350.7	2026.1	1745.4	2163.8
FLRG-3	2188.2	2395.7	2349.5	2536.0	2485.4	1846.4	2300.2
FLRG-4	2637.4	2506.8	2890.0	2647.8	2497.4	1796.1	2495.9
FLRG-5	2221.0	2547.5	2331.6	2198.9	2245.6	1546.7	2181.9
FRG-1	2588.4	2884.3	2869.8	2680.4	2522.4	1650.8	2532.7
FRG-2	2598.4	2935.3	2660.7	2615.3	2503.1	1788.1	2516.8
FRG-3	2691.1	2723.2	2791.4	2597.9	2533.5	2093.0	2571.7
FDOL-1	3001.7	3146.0	3171.6	2646.3	2295.3	1817.0	2679.7
FDOL-2	3106.6	3101.4	2863.6	2563.2	2178.7	1766.6	2596.7
FDOL-3	3535.2	3610.7	3240.2	2909.1	2161.2	1933.7	2898.4
FCRG-1	2862.2	2814.0	2803.8	2581.8	2649.2	2172.9	2647.3
FCRG-1	3134.1	3016.7	2588.4	2716.0	2076.0	1678.8	2535.0
FTR-1	-	-	-	-	-	-	-
FTR-2	-	-	-	-	-	-	-
FGR	4101.9	3764.1	3459.2	3242.6	2817.3	2409.3	3299.1
FSS	3688.6	3736.6	3734.8	3471.6	2537.6	2196.9	3227.7

References

Alhozaimy, A. M. (1998). Correlation Between Materials Finer than No. 200 Sieve and Sand Equivalent tests for Natural and Crushed Stone Sands. *Cement, Concrete, and Aggregates*, 221-226.

American Association of State Highway and Transportation Officials. (2009). AASHTO T 327-09: Resistance of Coarse Aggregate to Degradation by Abrasion in the Micro-Deval Apparatus. Washington, D.C., United State of America: American Association of State Highway and Transportation Officials.

ASTM International. (2005, August). ASTM C 88-05: Soundness of Aggregates by Use of Sodium Sulfate or Magnesium Sulfate. West Conshohocken, Pennsylvania, United States of America: ASTM International.

ASTM International. (2006, August). ASTM C131-06: Resistance to Degradation of Small-Size Coarse Aggregate by Abrasion and Impact in the Los Angeles Machine. West Conshohocken, Pennsylvania, United States of America: ASTM International.

ASTM International. (2007, September). ASTM C 127-07: Density, Relative Density (Specific Gravity), and Absorption of Coarse Aggregate. West Conshohocken, Pennsylvania, United States of America: ASTM International.

ASTM International. (2008, March). ASTM D 7428-08: Resistance of Fine Aggregate to Degradation by Abrasion in the Micro-Deval Apparatus. West Conshohocken, Pennsylvania, United States of America: ASTM International.

ASTM International. (2009, July). ASTM D 2419-09: Sand Equivalent Value of Soils and Fine Aggregate. West Conshohocken, Pennsylvania, United States of America: ASTM International.

ASTM International. (2010, November). ASTM C 469: Static Modulus of Elasticity and Poisson's Ration of Concrete in Compression. West Conshohocken, Pennsylvania, United States of America: ASTM International.

ASTM International. (2010, September). ASTM C 78-10: Flexural Strength of Concrete (Using Simple Beam with Third-Point Loading). West Conshohocken, Pennsylvania, United States of America: ASTM International.

ASTM International. (2010, October). ASTM D 4791-10: Flat Particles, Elongated Particles, or Flat and Elongated Particles in Coarse Aggregate. West Conshohocken, Pennsylvania, United States of America: ASTM International.

ASTM International. (2012, February). ASTM C 39 / C 39M-12: Compressive Strength of Cylindrical Concrete Specimens. West Conshohocken, Pennsylvania, United States of America: ASTM International.

BSi. (1990, June). British Standard 812 Part 110: Methods for Determination of Aggregate Crushing Value. BSi.

BSi. (1995, August). BS 812 Part 112 - Methods for Determination of Aggregate Impact Value (AIV). BSi.

Carlson, J. D., Bhardwaj, R., Phelan, P. E., Kaloush, K. E., & Golden, J. S. (2010). Determining Thermal Conductivity of Paving Materials Using Cylindrical Sample Geometry. *Journal of Materials in Civil Engineering*, 186-195.

Cooley, L. A., & James, R. S. (2003). Micro-Deval Testing of Aggregates in the Southeast. *Transportation Research Record*, 73-79.

Cuelho, E., Mokwa, R., & Obert, K. (2007). *FHWA/MT-06-016/8117-27 Final Report - Comparative Analysis of Coarse Surfacing Aggregate Using Micro-Deval, LA Abrasion, and Sodium Sulfate Soundness Tests.* U.S. Department of Transportation Federal Highway Administration.

Dar Hao, C. (2010, November). Texas Experience with Micro-Deval Test. *Texas Department of Transportation Presentation*. Austin, Texas: Texas Department of Transportation.

Du, L., & Lukefahr, E. (2007). Coefficient of Thermal Expansion of Concrete with Different Coarse Aggregates. *15th Annual ICAR Symposium.* Austin, Texas: International Center for Aggregates Research.

Fisher, W. L., & Rodda, P. U. (1969, January). Edwards Formation (Lower Cretacous), Texas: Dolomitization in a Carbonate Platform System. *The American Association of Petroleum Geologists Bulletin (Vol. 53, No. 1)*, pp. 55-72.

Folliard, K., & Smith, K. (2002). *NCRHP 4-20C Final Report - Aggregate Tests for Portland Cement Concrete Pavements: State of the Knowledge.* National Cooperative Highway Research Program Transportation Research Board National Research Council.

Fowler, D., Allen, J., Lange, A., & Range, P. (2006). *ICAR 507-1F Final Report - The Prediction of Coarse Aggregate Performance by Micro-Deval and Soundness Related Aggregate Tests.* Austin, Texas: International Center for Aggretates Research.

Hardy, A., Abdelrahman, M., & Yazdani, S. (2010). Evaluation of Coarse Aggregate Quality with respect to Current Specifications for Pavement Mixtures. *Journal of Materials in Civil Engineering*, 110-119.

Hossain, M. S., Lane, D. S., & Schmidt, B. N. (2007). *Use of Micro-Deval Test for Assessing the Durability of Virginia Aggregates.* Charlottesville, Virginia: Virginia Transportation Research Council.

Hossain, M. S., Lane, D. S., & Schmidt, B. N. (2008). Results of Micro-Deval Test for Coarse Aggregates from Virginia Sources. *Transportation Research Record*, 1-10.

Hossain, M. S., Lane, D. S., & Schmidt, B. N. (2008). Use of the Micro-Deval Test for Assessing Fine Aggregate Durability. *Transportation Research Record*, 11-19.

Hudson, B. (2002). The Impact of Aggregate Quality on Concrete Performance. *10th Annual ICAR Symposium.* Austin, Texas: International Center for Aggregates Research.

Jayawickrama, P. W., Hossain, S., & Hoare, A. R. (2007). *Long-Term Research on Bituminous Coarse Aggregate: Use of Micro-Deval Test for Project Level Aggregate Quality Control.* College Station, Texas: Texas Transportation Institute.

Kahraman, S., & Fener, M. (2007). Predicting the Los Angeles Abrasion Loss of Rock Aggregates from the Uniaxial Compressive Strength. *Materials Letters*, 4861-4865.

Kazi, A., & Al-Mansour, Z. R. (1980). Influence of Geological Factors on Abrasion and Soundness Characteristics of Aggregates. *Engineering Geology*, 195-203.

Kiliç, A., Atiş, C. D., Teymen, A., Karahan, O., Özcan, F., Bilim, C., et al. (2008). The Influence of Aggregate Type on the Strength and Abrasion Resistance of High Strength Concrete. *Cement & Concrete Composites*, 290-296.

Koehler, E. P., Jeknavorian, A., Chun, B.-W., & Zhou, P. (2009, May 4-5). Ensuring Concrete Performance for Various Aggregates. *17th Annual ICAR Symposium.* Austin, Texas, United States: W.R. Grace & Co.

Koubaa, A., & Snyder, M. B. (1999). Development of a Test Protocol for Assessing Freeze-Thaw Resistance of Concrete Aggregates in Minnesota. *7th Annual ICAR Symposium.* Austin, Texas: International Center for Aggregates Research.

Lang, A. P., Range, P. H., Fowler, D. W., & Allen, J. J. (2007). Prediction of Coarse Aggregate Performance by Micro-Deval and Other Soundness, Strength, and Intrinsic Particle Property Tests. *Transportation Research Record: Journal of the Transportation Research Board*, 3-8.

Lewis Institute. (1921). Effects of Organic Impurities on Concrete. *Public Works* (pp. 425-426). Chicago, IL: American Society of Testing Materials.

Mahmoud, E., & Masad, E. (2007). Experimental Methods for the Evaluation of Aggregate Resistance to Polishing, Abrasion, and Breakage. *Journal of Civil Engineering Materials*, 977-985.

Mahmoud, E., Gates, L., Masad, E., Erdoğan, S., & Garboczi, E. (2010). Comprehensive Evaluation of AIMS Texture, Angularity, and Dimension Measurements. *Journal of Materials in Civil Engineering*, 369-379.

Masad, E. A. (2005). *Aggregate Imaging System (AIMS): Basics and Applications.* College Station, Texas: Texas Transportation Institute.

Mathis Instruments Ltd. (2012). Mathis TCi: Thermal Conductivity Analyzer. Pennsauken, New Jersey, United States of America: Setaram Instrumentation Technologies.

Muethel, R. (2007). *Research Report R-1494 - Graphical Analysis of Iowa Pore Index Test Results.* Lansing, Michigan: Michigan Department of Transportation Construction and Technology Division.

Mukhopadhyay, A. K., & Zollinger, D. G. (2009). Development of Dilatometer Test Method to Measure Coefficient of Thermal Expansion of Aggregates. *Journal of Materials in Civil Engineering*, 781-788.

Munoz, J. F., Gullerud, K. J., Cramer, S. M., Tejedor, I., & Anderson, M. A. (2010). Effects of Coarse Aggregate Coatings on Concrete Performance. *Journal of Materials in Civil Engineering*, 96-103.

Munoz, J. F., Tejedor, I., Anderson, M. A., & Cramer, S. M. (2005). *Report IPRF-01-G-002-01-4.2 - Effects of Coarse Aggregate Clay-Coatings on Concrete Performance.* Skokie, Illinois: Innovative Pavement Research Foundation.

Norvell, J., Stewart, J., Juenger, M., & Fowler, D. (2007). Effects of Clay and Clay-Sized Particles on Concrete. *15th Annual ICAR Symposium.* Austin, Texas: International Center for Aggregates Research.

Peapully, S., Zollinger, D. G., & McCullough, B. F. (1994). *Procedure for Classification of Coarse Aggregates Based on Properties Affecting Performance.* College Station, Texas: Texas Transportation Institute.

Rached, M. M. (2011). *Use of Manufactured Sands for Concrete Paving.* Austin, Texas: The University of Texas at Austin.

Rached, M., De Moya, M., & Fowler, D. (2009). *ICAR 401 Final Report - Utilizing Aggregates Characteristics to Minimize Cement Content in Portland Cement Concrete.* Austin, Texas: International Center for Aggregates Research.

Rangaraju, P. R., Edlinski, J., & Amirkhanian, S. (2005). *FHWA-SC-05-01 Summary Report - Evaluation of South Carolina Aggregate Durability Requirements.* Columbia, South Carolina: South Carolina Department of Transportation.

Rogers, C. (1998). Canadian Experience with Micro-Deval Test for Aggregates. *Engineering Geology Special Publications*, 139-147.

Rogers, C. A., & Senior, S. A. (1991). Laboratory Tests for Predicting Coarse Aggregate Performance in Ontario. *Transportation Research Record*, 97-105.

Rogers, C. A., Bailey, M. L., & Price, B. (1991). Micro-Deval Test for Evaluating the Quality of Fine Aggregate for Concrete and Asphalt. *Transportation Research Record*, 68-76.

Rogers, C., & Dziedziejko, T. (2007). Fine Aggregate Density Testing: What is the Right Way to Do It? *15th Annual ICAR Symposium.* Austin, Texas: International Center for Aggregates Research.

Rogers, C., & Gorman, B. (2008). A Flakiness Test for Fine Aggregate. *16th Annual ICAR Symposium.* Austin, Texas: International Center for Aggregates Research.

Texas Department of Transportation. (1999, August). Tex-403-A: Saturated Surface-Dry Specific Gravity and Absorption of Aggregates. Austin, Texas, United State of America: Texas Department of Transportation.

Texas Department of Transportation. (1999, August). Tex-408-A: Organic Impurities in Fine Aggregates for Concrete. Austin, Texas, United States of America: Texas Department of Transportation.

Texas Department of Transportation. (2000, June). Tex-612-J: Acid Insoluble Residue for Fine Aggregate. Austin, Texas, United States of America: Texas Department of Transportation.

Texas Department of Transportation. (2004, June 1). Standard Specifications for Construction and Maintenance of Highways, Streets, and Bridges. Austin, Texas: Texas Department of Transportation.

Texas Department of Transportation. (2004, October). Tex-411-A: Soundness of Aggregate Using Sodium Sulfate or Magnesium Sulfate. Austin, Texas, United States of America: Texas Department of Transportation.

Texas Department of Transportation. (2005, February). Tex-280-F: Determining Flat and Elongated Particles. Austin, Texas, United States of America: Texas Department of Transportation.

Texas Department of Transportation. (2005, July). Tex-461-A: Degradation of Coarse Aggregate by Micro-Deval Abrasion. Austin, Texas: Texas Department of Transportation.

Texas Department of Transportation. (2007, December). Tex-499-A: Test Procedure for Aggregate Quality Monitoring Program. Austin, Texas: Texas Department of Transportation.

Texas Department of Transportation. (2009, September). Tex-203-F: Test Procedure for Sand Equivalent Test. Austin, Texas: Texas Department of Transportation.

Texas Department of Transportation. (2011, June). Tex-428-A: Determining the Coefficient of Thermal Expansion of Concrete. Austin, Texas, United States of America: Texas Department of Transportation.

Texas Department of Transportation. (2012, February 2). Concrete Rated Source Quality Catalog. Texas: Texas Department of Transportation.

Ugur, I., Demirdag, S., & Yavuz, H. (2009). Effect of Rock Properties on the Los Angeles Abrasion and Impact Test Characteristics of the Aggregates. *Materials Characterization*, 90-96.

Villalobos, S., Lange, D. A., & Roesler, J. R. (2005). *Evaluation, Testing, and Comparison Between Crushed Manufactured Sand and Natural Sand.* Center of Excellence for Airport Technology.

W.R. Grace & Co. (2010, April). Grace Rapid Clay Test Kit: Step-by-Step Procedure. *Grace Custom Aggregate Solutiona*. Cambridge, Massachusetts, United States of America: W.R. Grace & Co.

Wang, L., Druta, C., & Lane, D. S. (2010). *VTRC 10-CR7 Final Report - Methods for Assessing the Polishing Characteristics of Coarse Aggregates for Use in Pavement Surface Layers.* Charlottesville, Virginia: Virginia Transportation Research Council.

Weyers, R. E., Williamson, G. S., Mokarem, D. W., Lane, D. S., & Cady, P. D. (2005). *WHRP 06-07 Final Report - Testing Methods to Determine Long Term Durability of Wisconsin Aggregate Resources.* Wisconsin Highway Research Program.

Won, M. (2001). Effects of Coarse Aggregate on Concrete Pavement Performance. *9th Annual ICAR Symposium.* Austin, Texas: International Center for Aggregates Research.

Wu, Y., Parker, F., & Kandhal, P. (1998). Aggregate Toughness/Abrasion Resistance and Durability/Soundness Tests Related to Asphalt Concrete Performance in Pavements. *Transportation Research Record*, 85-93.